The Influence of Selenium on Arsenic Hepatobiliary Transport

by

Janet Ruby Zhou

A thesis submitted in partial fulfillment of the requirements for the degree of

Doctor of Philosophy

Department of Laboratory Medicine and Pathology
University of Alberta

© Janet Ruby Zhou, 2022

Abstract

Chronic exposure to arsenic causes lung, skin, and bladder cancer in humans. Conservative estimates suggest at least 92-220 million people worldwide are exposed to arsenic through consumption of contaminated water. Unfortunately, removal of arsenic from contaminated water sources is not economically feasible. Selenium is an essential trace nutrient but is toxic in excess. Interestingly, arsenic and selenium are mutually protective. Simultaneous exposure to toxic doses of arsenic and selenium in laboratory animals result in reduced accumulation of both compounds through the formation and biliary excretion of the seleno-bis (*S*-glutathionyl) arsinium ion $[(GS)_2AsSe]^-$. Completed selenium-supplementation trials in arsenic-endemic regions have used various chemical species of selenium including selenite and selenomethionine. Methylselenocysteine has been shown to have anti-cancer effects *in vitro*. Despite completed selenium-supplementation trials, the influence of selenium on human arsenic hepatobiliary transport has not been studied using optimal human models. There is also likely a genetic component to susceptibility to arsenic-induced diseases as different outcomes between individuals with similar exposure histories are observed. In human hepatocytes, the ATP-binding cassette transporter, multidrug resistance protein 2 (MRP2, gene symbol *ABCC2*) is localized to the canalicular/apical membranes for biliary excretion of arsenic-glutathione conjugates, and the related multidrug resistance protein 4 (MRP4/*ABCC4*) is localized to the sinusoidal/basolateral membranes for arsenic transport into systemic circulation.

The objectives of this thesis were to: (i) investigate the influence of different selenium chemical forms on arsenic hepatobiliary transport, (ii) investigate the stimulatory effect of

methylselenocysteine on arsenic sinusoidal efflux, and lastly, (iii) investigate the effect of naturally occurring MRP2/*ABCC2* variants on arsenic transport.

Human HepaRG cells, a surrogate for primary human hepatocytes were established as a model for studying arsenic hepatobiliary transport. Arsenite + selenite and arsenite + selenide at different molar ratios revealed mutual toxicity antagonisms, with the latter being higher. Significant arsenic biliary excretion was detected with a biliary excretion index (BEI) of 14 ± 8%, which was stimulated to 32 ± 7% by selenide. Consistent with the formation and biliary efflux of $[(GS)_2AsSe]^-$, arsenite increased the BEI of selenide from 0% to 24 ± 5%. Arsenic biliary excretion was lost in the presence of selenite, selenomethionine, and methylselenocysteine. Sinusoidal arsenic efflux was stimulated by ~1.6-fold by methylselenocysteine, but unchanged by other selenium forms. Arsenic efflux across canalicular and sinusoidal membranes (± selenide) was temperature- and glutathione-dependent and inhibited by MK571, an MRP inhibitor.

Since MRP2/*ABCC2* and MRP4/*ABCC4* mediate biliary and sinusoidal efflux of arsenic, respectively, *ABCC2* and *ABCC4* were knocked down (individually) in HepaRG cells, resulting in barely detectable levels of MRP2 or MRP4. Experiments using *ABCC2*-knockdown HepaRG cells revealed that MRP2 accounted for all detectable biliary efflux of arsenic (± selenide). Similarly, arsenic sinusoidal efflux decreased by 27%, 57%, and 31% after glutathione depletion, temperature reduction and addition of MK571, respectively, which also resulted in a loss of methylselenocysteine stimulation. Further strategies were employed to determine if this process is MRP4-mediated. Arsenic sinusoidal efflux decreased by 35%, and methylselenocysteine-stimulated efflux was lost in the presence of ceefourin-1, an MRP4 inhibitor. Arsenic efflux from *ABCC4*-knockdown HepaRG cells decreased by 30%, and

methylselenocysteine-stimulated arsenic export was completely lost relative to control HepaRG cells with parental levels of MRP4. Overall, the chemical form of selenium and human MRP2 and MRP4 strongly influenced arsenic hepatobiliary transport.

Lastly, 13 naturally occurring MRP2 variants with a single nucleotide substitution resulting in an amino acid change were investigated for their influence on MRP2 level, plasma membrane localization, MRP2-enriched membrane vesicle transport of $As(GS)_3$ and $[(GS)_2AsSe]^-$, and cellular accumulation of arsenic ± selenium (selenide and selenite). The variants R412G-, V1188E-, C1515Y- and V1188E/C1515Y-MRP2 were similar to WT-MRP2 for protein levels, cell surface localization, and transport activity while S789F- and A1450T-MRP2 were undetected at the cell surface. $As(GS)_3$ transport activity of T1477M-MRP2 was 60% of WT-MRP2. R353H-, R1181L-, and P1291L-MRP2-enriched vesicles had $[(GS)_2AsSe]^-$ transport activity increased by 160%, 145% and 170%, respectively, compared to WT-MRP2. In contrast, V417I- and R1150H- had $[(GS)_2AsSe]^-$ transport that was 59% and 37%, respectively, of WT-MRP2. This thesis advances knowledge about the influence of selenium on human hepatic handling of arsenic and our understanding about inter-individual differences in arsenic transport pathways. Future studies could use our findings to help design efficacious selenium-supplementation trials and predict responses to selenium-supplementation.

Preface

Chapter 2 was published: as Janet R. Zhou, Gurnit Kaur, Yingze Ma, Denis Arutyunov, Xiufen Lu, X. Chris Le, and Elaine M. Leslie., Biliary Excretion of Arsenic by Human HepaRG Cells is Stimulated by Selenide and Mediated by the Multidrug Resistance Protein 2 (MRP2/ABCC2). *Biochem. Pharmacol*. 2021;193:114799 https://doi.org/10.1016/j.bcp.2021.114799

This project was led by Dr. Elaine M. Leslie, from the University of Alberta in collaboration with Dr. X. Chris Le. The author initiated all experiments with initial training from Dr. Gurnit Kaur, who also supported with a technical replicate for Fig 2.6A, ^{73}As-arsenite accumulation over 24 hr in HepaRG cells. Yingze Ma completed some technical replicates for Fig 2.2, by assisting with crude membrane preparations and immunoblotting for the detection of MRP2 and MRP4 in HepaRG cells. Yingze Ma also assisted with the cytotoxicity assays for Fig 2.4, cytotoxicity of selenium ± arsenite in HepaRG cells at different combinations of concentrations. Dr. Denis Arutyunov completed gene sequencing. Xiufen Lu performed the ICP-MS data acquisition and data analysis for Fig 2.9 under Dr. X. Chris Le's supervision.

The author designed the study with Dr. Elaine M. Leslie. The author wrote the first draft of the manuscript. Dr. Elaine M. Leslie provided extensive revisions on subsequent drafts and contributed substantially to the discussion contents. The method for section 2.3.11 was written by Xiufen Lu and Dr. X. Chris Le. All authors provided edits on the final draft.

For **Chapter 3, Sinusoidal Efflux of Human HepaRG cells is Stimulated by Methylselenocysteine and Mediated by the Multidrug Resistance Protein 4 (MRP4/*ABCC4*)**, all experiments were conducted by the author, with the exception of Fig 3.1C, which was

conducted by Dr. Gurnit Kaur. Primary hepatocytes used in Fig 3.1C were provided by Drs Norman Kneteman and Donna Douglas. This research project received ethics approval from the University of Alberta Research Ethics Board, Project Name "THE ROLE OF TRANSPORT PROTEINS IN TOXICOLOGY", protocol number 00001646, NOVEMBER 28, 2009.

For **Chapter 4: Naturally Occurring Variants of MRP2/*ABCC2* Differentially Modulate the Transport of Arsenic Triglutathione ($As(GS)_3$) and the seleno-bis (*S*-glutathionyl) arsinium ion $[(GS)_2AsSe]^-$**, Dr. Gurnit Kaur made the naturally occurring *ABCC2* variants by site-directed mutagenesis, ensured accuracy of the sequences by sending samples for sequencing, performed technical replicates of immunoblots of whole cell lysates and membrane vesicles, and the reverse mutagenesis for S789F- and A1450T-MRP2. The author performed all other experiments.

For **Appendix A: Determing the Species of Arsenic Transported by Human MRP4 Upon Sinusoidal Stimulation by Methylselenocysteine**, MRP4 cDNA was a kind gift from Dr. Dietrich Keppler. Xiufen Lu performed LC-ICP-MS data acquisition and analysis for arsenic speciation for Fig A1.3 under the supervision of Dr. X. Chris Le. The author performed all other experiments.

For **Appendix B: Further Characterization of Cellular Localization of Selected Naturally Occurring Variants of MRP2/*ABCC2* by Immunofluorescence Imaging**, the author performed all experiments.

Dedication

To the memory of my beloved grandmother.

She never had a formal education, but she was my first teacher, and continues to be an inspiration to me.

Acknowledgements

I would first like to give many (and more) thanks to my supervisor, Dr. Elaine Leslie for allowing me to pursue graduate studies in her laboratory. She has been an excellent mentor to me, both professionally and personally. Her office door was always open (literally) for assistance, and I enjoyed the few experiments we performed together. I think she is the only person I know of that would send me back my draft at 6 am. Most importantly, she has pushed me to learn and achieve so much more than I ever thought I could, and she is most definitely the best PhD supervisor that I have ever had.

I owe my supervisory committee members a lot of gratitude. I can always count on Drs. Monika Keelan and X. Chris Le for some enthusiastic encouragement. Dr. Monika Keelan has been extremely supportive throughout my undergraduate and graduate studies. I am very grateful for her mentorship, and our scientific and non-scientific discussions. Dr. X. Chris Le has enlightened me with his scientific guidance. I also relied heavily on his calming presence during my candidacy exam and presentations. I would also like to thank Drs. James Hammond and Robin Clugston for participating in my candidacy exam, as well as my external examiners, Drs. Lauren Aleksunes and Rene Jacobs for participating in my final exam.

My graduate coordinators Drs. Monika Keelan and Jelena Holovati have also been exceptional at giving me guidance as needed, and Cheryl Titus and was an amazing administrator. I have also been very lucky to have been supported by Diane, Jinghong, and Xiufen. I would like to thank Diane for her infinite willingness to help me, even when I needed selenide at 7 am, as well as the many happy laughs we shared. Jinghong has also been a

pleasure to work with and has always respected my requests for pink lab tape. Xiufen has been very generous with her time and knowledge.

I have been fortunate to have had good company in our ~182 sqft office (yes, we measured). I drank a lot of tea with Drs. Gurnit Kaur and Brayden Whitlock, who also humoured my germaphobe-ness. Gurnit was my big sister in our lab family. She enthusiastically taught me my first efflux experiment and how to grow the neediest cells ever, which has somehow led me to a whole thesis. Brayden showed me my first vesicle transport experiment and taught me how to count by 7 extremely well. I later reverted to counting by 5. I would also like to thank Serena for her friendliness and the cookies that I didn't think my waistline needed. I have also seen many undergraduate students come and go. Angela, Danielle, Yejun, Warda, Brooke, Naomi, Martin, Janaia: I hope you have learned as much from me as I have from you, and I appreciate all the laughs and food we shared. You have helped me become a better mentor. Martin also expanded my food palate and humoured the analogies I used when teaching.

My friends on the 7th floor of Med Sci as well as within the LMP department have also made my graduate student experience more social and enjoyable: Xiong, Midhat, Denis, Vladimir, Kris, Claire, Peter, Joye, and Teresa. Whether we shared reagents, taught each other, waited for the imaging room together, or kept each other company (even virtually) at our posters, you have improved my quality of life in some way. My other friends put up with me through this journey. They have patiently entertained my complaints and celebrated my success. Brian has an ability to lighten up my mood and is somehow always ready to hear about my work for the millionth time with an open ear, and I can always share food and laughs with Wing, Cindy, Maria, and members of my work families.

Tables of Contents

List of Tables

List of Figures

List of Abbreviations

ABC	ATP-binding cassette
AE1	Anion-exchanger 1
AMP	Adenosine monophosphate
ApoE	Apolipoprotein E
AQPs	Aquaglyceroporin channels
AQP9	Aquaglyceroporin 9
$As(GS)_3$	Arsenic triglutathione
As3MT	Arsenite methyltransferase
ATCC	American Type Culture Collection
ATP	Adenosine triphosphate
BCA	Bicinchoninic acid
BEI	Biliary excretion index
BSA	Bovine serum albumin
BSO	Buthionine sulfoximine
CDFDA	5(6)-Carboxy-2',7'-dichlorofluorescein diacetate
CHO	Chinese hamster ovary cells
DJS	Dubin-Johnson Syndrome
DMA^{III}	Dimethylarsinous acid
DMA^{V}	Dimethylarsinic acid
DMSO	Dimethyl sulfoxide

EDTA	Ethylenediaminetetraacetic acid
EGTA	Ethylene glycol-bis-(β-aminoethyl ether)-N,N,N’,N’-tetraacetic acid
EV	Empty vector
$E_2$17βG	Estradiol-17β-glucuronide
FBS	Fetal bovine serum
GSH	Glutathione
GS-MCB	Glutathione-monochlorobimane
$[(GS)_2AsSe]^-$	Seleno-bis (*S*-glutathionyl) arsinium ion
GS-MF	Glutathione-methylfluorescein
HBSS	Hanks’ balanced salt solution
HEPES	N-(2-Hydroxyethyl)piperazine-N’-(2-ethanesulfonic acid)
HPLC	High-performance liquid chromatography
HRP	Horse radish peroxidase
IARC	International Agency for Research on Cancer
ICP-MS	Inductively coupled plasma mass spectrometer
LDH	Lactate dehydrogenase
MeSeCys	Methylselenocysteine
$MgCl_2$	Magnesium chloride
MMA^{III}	Monomethylarsonous acid
MMA^{V}	Monomethylarsonic acid
MRPs	Multidrug Resistance Proteins
MSD	Membrane-spanning domain

NADPH	Nicotinamide adenine dinucleotide phosphate
$NaHCO_3$	Sodium bicarbonate
NBDs	Nucleotide binding domains
PBS	Phosphate buffered saline
PMSF	Phenylmethylsulfonyl fluoride
ppm	Parts per million
PVDF	Polyvinylidene fluoride
RBCs	Red blood cells
ROS	Reactive oxygen species
SAM	S-adenosyl-L-methionine
SCHH	Sandwich-cultured human hepatocytes
SeMet	Selenomethionine
SNPs	Single nucleotide polymorphisms
SUM_SYN_ANT	Summary metric value for synergy and antagonism
UMRR	University of Missouri Research Reactor

1. A Review of Arsenic, Selenium, and their Mutually Protective Relationship

1.1 Arsenic exposure

Arsenic naturally occurs in the Earth's crust, so contamination of water by natural geological processes is common [1–3]. Humans are exposed to arsenic primarily through consumption of contaminated drinking water, but arsenic exists ubiquitously in the environment so other routes of exposure are possible. Not only can arsenic be described as a natural contaminant, but it is also a proven human carcinogen, and somewhat paradoxically used as a therapeutic agent [1–4]. Some main sources of arsenic exposure are described below.

1.1.1 Sources and regulation of exposure

1.1.1.1 Arsenic exposure through consumption of drinking water and food

Conservative estimates suggest 92-220 million people worldwide are exposed to arsenic through contaminated drinking water [5]. To date, at least 108 countries are affected by arsenic contamination in groundwater exceeding the World Health Organization guideline of 10 µg/L (10 parts per billion) [6]. The majority of arsenic endemic areas include South Asian and South American countries [5,6]. Examples of severely affected countries include Bangladesh, India, China, Nepal, Cambodia, and Indonesia [5,6]. Developed countries such as Canada and USA also have arsenic contamination in groundwater but are not as severely affected, due to the availability of resources to avoid or treat drinking water [6].

Other than contaminated drinking water, ingestion of arsenic through food is another major source of exposure. Rice is a staple of many diets worldwide. Rice is a crop that is grown in a flooded field, unfortunately making it susceptible to arsenic contamination from irrigation water. Depending on the species of rice, where the rice is grown, and the irrigation water used, it accumulates inorganic arsenic at ~10-fold higher rate than other grains such as wheat and barley [7,8].

Since exposure to arsenic through food consumption may alarm many people, Health Canada has guidelines for maximum levels of arsenic in certain foods. For example, fish and edible bone meal are allowed to have maximum total arsenic levels of 3.5 and 1 parts per million (ppm), respectively [9]. Beverages, including fruit juices can only contain 0.1 ppm total arsenic, and water in sealed containers can have a maximum level of 0.01 ppm [9]. Brown rice and white rice have maximum inorganic arsenic levels of 0.35 and 0.2 ppm, respectively [9]. More recently, Health Canada has also added a guideline for maximum inorganic arsenic levels of 0.1 ppm in rice-based foods intended specifically for infants and young children [10].

1.1.1.2 Anthropogenic sources of exposure

Most anthropogenic sources of arsenic exposure involve industrial processes. For example, incineration of preserved wood products, manufacturing of glass, alloy, leather preservatives, and pigments involve the use of arsenic [11]. Arsenic was also commonly used in pesticides, insecticides, and fungicides [12]. Agent Blue was a commercial pesticide that contained cacodylic acid (dimethylarsinic acid (DMA^V)) as an active ingredient, and it was also heavily used in the Vietnam War to destroy enemies' crops [12,13]. However, its use was

deregulated in 2004 by the United States Environmental Protection Agency due to toxic side effects including headaches, dizziness, and vomiting [12].

1.1.2 Therapeutic uses of arsenic

Despite its harmful effects and regulations in place for exposure limits, arsenic has important medicinal applications. Arsenic was historically used to treat an array of diseases. For example, it was recommended for the treatment of malaria in the 1700s, and Fowler's solution containing 1% potassium arsenite was often used to treat remittent fevers, headaches, asthma, and psoriasis [4].

During the 1900s, particularly during the world wars, a common therapeutic use of arsenic was for treating parasitic infections caused by several species of *Trypanosoma,* as well as the bacterial infection syphilis [4]. Arsphenamine was given the trade name Salvarsan 606, and later Neosalvarsan when a more soluble compound was developed [4,14]. These drugs were effective but had toxic side effects when repeated doses were injected, including renal failure, optic neuritis, seizures, fevers, and rash [14]. Not only was preparation of the drugs difficult, but these drugs had to be stored in sealed vials under nitrogen gas to prevent oxidation [4]. Later, the use of arsphenamine to treat syphilis was replaced by penicillin [14,15].

Today, the melarsonyl potassium-containing drug, melarsoprol is still used in Africa as treatment for patients with *Trypanosoma brucei gambiense* trypanosomiasis. However, about 10% of patients develop a severe arsenical encephalopathy with a 50% mortality rate, so melarsoprol is only used in the late stages of the infection when no other treatment options are available [4].

Despite its carcinogenic effects, arsenic is also a chemotherapeutic agent. Arsenic trioxide was approved by the Food and Drug Administration in 2002 as a treatment for acute promyelocytic leukemia [16]. The pathogenicity of acute promyelocytic leukemia comes from the formation of a chimeric protein encoded by the *PML-RAR*α fusion gene caused by a translocation of chromosomes 15 and 17 [17,18]. Myeloid cell development is arrested at the promyelocytic stage, leading to an accumulation of abnormal promyelocytes in the bone marrow [17,18]. To alleviate this, arsenic trioxide promotes degradation of PML-RARα, which also promotes differentiation of promyelocytes [17]. When combined with all-trans retinoic acid-based regimens, the relapse rate is only 1-10%, making acute promyelocytic leukemia a curable disease [19].

1.1.3 Symptoms of arsenic exposure

Acute poisoning occurs most commonly through ingestion of insecticides or pesticides as well as attempted suicide or murder [20–22]. Initial symptoms of acute arsenic poisoning are quite ambiguous and involve the gastrointestinal system. These symptoms include nausea, vomiting, abdominal pain, excessive salivation, and watery diarrhea [20]. Other signs include acute psychosis, skin rashes, and seizures [20]. The systemic shock caused by acute arsenic poisoning eventually leads to massive fluid loss causing reduced blood volume and circulatory collapse [20]. Hematological abnormalities, including intravascular hemolysis leading to hemoglobinuria, intravascular coagulation, and bone marrow depression leading to severe pancytopenia, can occur [20,23]. Renal failure and respiratory failure have also been observed [20,24].

Symptoms and signs of chronic arsenic exposure vary between individuals [20]. Individuals chronically exposed to arsenic can exhibit dermatological signs such as hyperpigmentation [20,25]. Brown dark spots with a raindrop appearance as well as solar and palmer keratosis are often observed [25]. Arsenic has also been shown to cause basal cell carcinoma and Bowen's disease [3,20,26]. Distinct keratin-rich areas forming white horizontal lines in the finger and toenails called Mee's lines may also develop [20]. Hepatomegaly and cirrhosis were observed in people living in West Bengal with chronic exposure to arsenic for >15 years [26,27]. Blackfoot disease, a peripheral vascular disease has been observed in exposed Taiwanese populations [28]. Other long-term effects include cardiovascular, neurological, and renal symptoms [20,26,27]. Cancer also results from chronic exposure and will be discussed further below.

1.2 Arsenic toxicokinetics

1.2.1 Bioavailability

The bioavailability of arsenic varies depending on the source of the arsenic and solubility of the species. For example, the bioavailability of soluble forms of arsenic can be as high as 90% when ingested through drinking water [29]. However, the bioavailability can be as low as 10%, especially when it is in soil or house dust [30]. The pH of the arsenic-containing matrix as well as a person's diet, and other factors discussed below can also influence the bioavailability of arsenic.

1.2.2 Arsenic uptake

Arsenic is naturally found in the environment in the inorganic forms, arsenate and arsenite. At pH 7, arsenate (pKa ~2.3, 6.8 and 11.3) exists predominantly as $H_2AsO_4^-$ and $HAsO_4^{2-}$

and exhibits similar physicochemical properties as inorganic phosphate [31,32]. Arsenate undergoes cellular uptake by sodium-dependent phosphate transporters such as the Na^+/P_i cotransporter type II (gene name *SLC34A2*) [31,32].

As for arsenite, it exists as $As(OH)_3$ at pH 7 (pKa ~9.2) and due to its neutral charge, uptake into cells can occur through aquaglyceroporin channels (AQPs) [33–35]. Evidence also suggests that facilitated glucose transporters (GLUTs) can allow passage of arsenite into cells. Rat GLUT1 (*SLC2A1*) overexpressed in yeast and *Xenopus laevis* oocytes increased arsenite accumulation, suggesting that GLUT1 plays a role in arsenite uptake [34]. GLUT1 is found at high levels in human red blood cells (RBCs) [36]. In a study by Kaur et al. [37], GLUT1 contribution to arsenite uptake by human RBCs was investigated using BAY-876, a highly selective competitive GLUT1 inhibitor [38]. There was unexpectedly no inhibition of arsenite uptake by human RBCs in the presence of BAY-876, even at concentrations 50 000 times greater than the IC_{50} reported for glucose uptake [38]. In a study by Calatayud et al. [39], knockdown of the glucose transporter GLUT5 (*SLC2A5*) reduced arsenite accumulation by ~60%, so they concluded that GLUT5 is involved in arsenite uptake. However, the knockdown studies using siRNA lacked appropriate controls, including a non-target control [39]. Further characterization of uptake by heterologously expressed GLUT5 in transport assays could be helpful in future studies [39].

There are few studies suggesting members of the organic anion transporting polypeptides (OATP1B1/*SLCO1B1* and OATP2B1/*SLCO2B1*) may also be involved in the uptake of arsenite and arsenate [40,41]. In HEK293T cells transfected with OATP1B1, there was increased accumulation of arsenite and arsenate compared to empty vector [41]. Knockdown of

SLCO2B1 in Caco-2 cells using siRNA reduced arsenite accumulation by 70% [39]. More extensive evidence using transport assays are required to support these studies.

Studies using *Xenopus laevis* oocytes have also suggested that methylated species of arsenic, present in blood after formation in the liver can permeate cells through AQP9 and GLUT1 [33,42].

1.2.3 Cellular metabolism of arsenic

There are a few proposed pathways for inorganic arsenic methylation. The Challenger pathway, also known as the classical pathway, proposes that arsenate is reduced to arsenite, which is then methylated to form monomethylarsonic acid (MMA^{V}), monomethylarsonous acid (MMA^{III}), dimethylarsinic acid (DMA^{V}), dimethylarsinous acid (DMA^{III}), trimethylarsine oxide (TMA^{V}), and trimethylarsine (TMA^{III}) [43,44]. Methylation is mainly catalyzed by arsenite methyltransferase (As3MT), which uses S-adenosyl-L-methionine (SAM) as a methyl donor [43,44]. The Challenger Pathway is outlined in **Fig 1.1.**

Arsenic forms glutathione (GSH) conjugates with arsenite and methylated arsenicals. Arsenite, MMA^{III} and DMA^{III} can form $As(GS)_3$, $MMA(GS)_2$, and DMA(GS), respectively in the presence of excess GSH [45,46]. However, identification of these conjugates in biological samples have been limited by their short half-lives at physiological pH. $As(GS)_3$ and $MMA(GS)_2$ have been isolated in biological samples such as rat bile and urine of mice that were deficient in gamma glutamyl transpeptidase, which normally catabolizes GSH and GSH conjugates [45,46]. Even though DMA(GS) should be the most chemically stable arsenic-GSH conjugate with the longest half-life (23-37 minutes at physiological pH) relative to $As(GS)_3$ and $MMA(GS)_2$ (both less

than 6 minutes at physiological pH), it has never been isolated in a biological sample [47]. The reason for this is unclear but may imply that DMA(GS) is not formed *in vivo*.

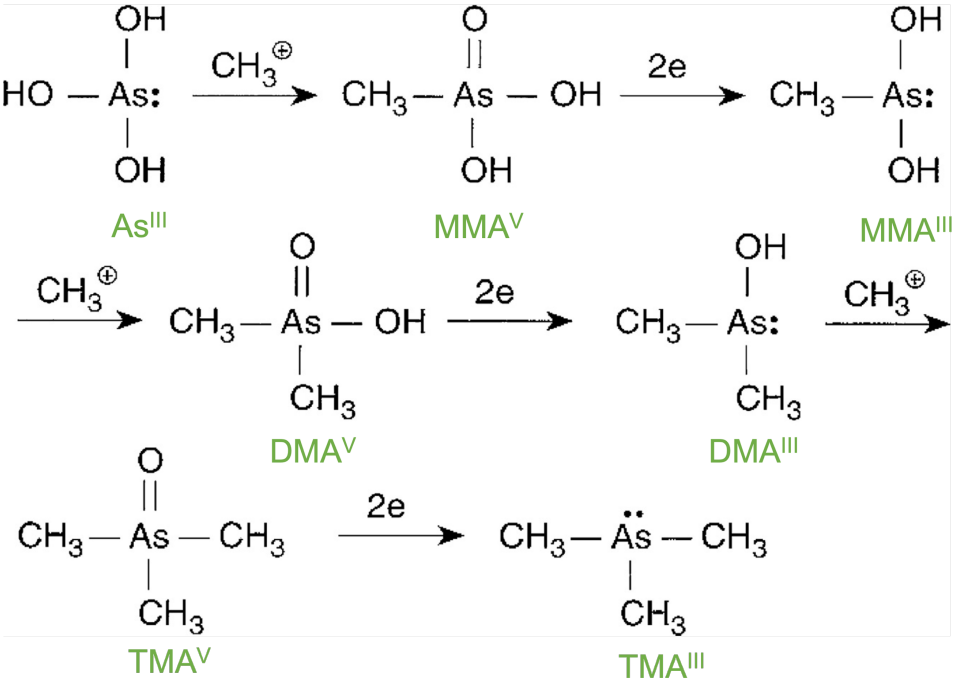

Figure 1.1: The Challenger Pathway for arsenic methylation. Modified from [43], with permission. As^{III}, arsenite; MMA^{V}, monomethylarsinic acid; MMA^{III}, monomethylarsonous acid; DMA^{V}, dimethylarsinic acid; DMA^{III}, dimethylarsinous acid; TMA^{V}, trimethylarsine oxide; TMA^{III}, trimethylarsine

1.2.4 The ATP-Binding Cassette Transporter superfamily

In humans, there are 48 ATP-binding cassette (ABC) proteins that are organized into seven subfamilies (A-G) based on their relative level of sequence homology [48–50]. ABC transporters collectively have broad substrate specificities and are responsible for the active transport of many compounds ranging from phospholipids, peptides, amino acids, and various drugs [51–54].

1.2.4.1 ABC subfamily C

The ABC subfamily C (ABCC) consists of 12 functional members that are localized to the plasma membrane of cells. The 12 functional members include transporters that are involved in

primary active transport of their substrates, a channel, as well as channel regulatory proteins that are ATP-dependent [52,53]. The cystic fibrosis transmembrane conductance regulator (CFTR/*ABCC7*) is an ATP-dependent chloride channel. There are also two sulfonylurea receptors (SUR1/*ABCC8*, and SUR2/*ABCC9*), as well as nine so-called multidrug resistance proteins which are all thought to be transporters: MRP1/*ABCC1*, MRP2/*ABCC2*, MRP3/*ABCC3*, MRP4/*ABCC4*, MRP5/*ABCC5*, MRP6/*ABCC6*, MRP7/*ABCC10*, and MRP8/*ABCC11*. MRP9/*ABCC12* does not transport substrates typical of MRPs but evidence from human patients as well as *ABCC12*-null zerba fish and *ABCC12*-deficient mice suggest it is involved in neonatal cholestasis [54,55]. A pseudogene (*ABCC13*) was identified but does not encode for a functional protein [56].

The ABC subfamily C transporters can be classified as having short or long structures. The short transporters are ABCC4, 5, 11 and 12. These ABC subfamily C transporters contain the typical mammalian ABC structure, consisting of two polytopic membrane-spanning domains (MSD) each with six transmembrane helices, and two cytosolic nucleotide binding domains (NBDs). The long ABC subfamily C transporters include ABCC1, 2, 3, 6 and 10 and are distinguished from the short ABC subfamily C proteins by a third MSD (MSD0) that is comprised of five transmembrane helices. The function of MSD0 is not fully understood for the ABC subfamily C transporters [50,57]. However, for non-transporter members of ABC subfamily C that are of the “long-form”, SUR1 and SUR2, MSD0 associates with the potassium channel Kir6.2 to form a large ion channel called the K_{ATP} channel [58,59]. The coupling of the MSD0 of SUR1 or 2 with Kir6.2 enhanced the trafficking of Kir6.2 to the plasma membrane and increased its sensitivity to ATP.

The Walker A and B motifs are highly conserved regions of the NBDs that are common amongst all ATP-binding proteins [60]. The Walker A motif is characterized as having the sequence: GXXGXGK(S/T), where X is any amino acid [60]. Walker B is characterized by φφφφD, where φ is any hydrophobic amino acid [60]. The conserved aspartic acid chelates the magnesium ion that is bound to nucleotide [61]. A glutamate residue following the aspartate facilitates the nucleophilic attack of ATP by water [61]. Another highly conserved signature motif, unique to ABC proteins, is the C-motif (LSGGQ), which is located between the Walker A and B motifs [62]. The glycine residues in this motif are involved in nucleotide binding [62,63]. For substrate binding from the cytosol and release into extracellular space to occur, the NBDs of the ABC transport proteins dimerize to allow for binding of two ATP molecules between the Walker A motif of one NBD and the C-motif of the other NBD [57,64]. Bundles of transmembrane helices within the two MSDs alternate between an inward and outward facing conformation powered by ATP hydrolysis [53,63–65]. MRP1/*ABCC1*, MRP2/*ABCC2* and MRP4/*ABCC4* are discussed further below because they are established transporters of arsenic metabolites. Other MRPs (MRP3, 5 and 6) are also present in the liver, but no transport of $As(GS)_3$ was detected using plasma membrane-enriched vesicles expressing these MRPs [77, Swanlund, Whitlock, and Leslie, unpublished]. Furthermore, no resistance to As^{III}, As^{V}, MMA^{III}, MMA^{V}, DMA^{III}, or DMA^{V} was found in stable HEK293 cells expressing human MRP3 or MRP5 [77].

1.2.4.1.1 Multidrug Resistance Protein 1

MRP1 is important for cellular protection against arsenic due to its expression in many cells and tissues in the body. It also has an ability to efflux many structurally diverse chemotherapeutic agents, rendering tumour cells multidrug resistant [66,67]. MRP1 also has ability to efflux many physiological molecules including conjugates of GSH such as leukotriene C_4, as well as conjugates of glucuronide, or sulfate [67]. Many unconjugated organic anions are also transported by MRP1 [67]. MRP1 is expressed in most tissues throughout the body, with relatively high levels in the lungs, testes, kidneys, blood-brain barrier, small/large intestine, placenta, skeletal muscle, and skin [49,50,68,69]. However, MRP1 levels are undetectable in healthy human hepatocytes [67,69]. In polarized epithelium, MRP1 localizes to the basolateral surface [69].

In vitro studies using MRP1-enriched vesicles prepared from the doxorubicin selected H69AR, and the stable and/or transiently MRP1 expressing HEK293 and HeLa cells have demonstrated that MRP1 transports $As(GS)_3$, $MMA(GS)_2$, and DMA^V [70–73].

1.2.4.1.2 Multidrug Resistance Protein 2

Although MRP2 has a similar substrate specificity as MRP1, MRP2 is the only ABC subfamily C transporter localized to the canalicular surface of hepatocytes. Some examples of physiological substrates include GSH and estradiol conjugates, leukotrienes, bilirubin glucuronides, and conjugated bile salts [74].

In rats, Mrp2 is responsible for most (>98%) of arsenic export into bile in the form of $As(GS)_3$ and $MMA(GS)_2$ [46]. In human hepatocytes, levels of MRP2 were upregulated by arsenite [75]. *In vitro* studies using plasma membrane enriched vesicles expressing human

MRP2 demonstrated that human MRP2 is a transporter of $As(GS)_3$ and $[(GS)_2AsSe]^-$ [46,76]. There is also preliminary data suggesting that human MRP2 transports $MMA(GS)_2$ *in vitro* [77]. Studies presented in this thesis (Chapter 2) also show that arsenic biliary excretion from human hepatocytes is mediated by MRP2.

1.2.4.1.3 Multidrug Resistance Protein 4

MRP4 is localized to the sinusoidal surface of hepatocytes as well as apical surface of renal proximal tubular cells, making it optimally situated for urinary elimination of hepatic arsenic metabolites [78]. Similar to MRP1 and 2, MRP4 has a diverse array of substrates. Some endogenous substrates include prostaglandin E_2, cyclic AMP, as well as GSH and glucuronide conjugates [50,79]. Human MRP4 has been shown previously to transport DMA^V and $MMA(GS)_2$ in *in vitro* studies using plasma membrane enriched vesicles [80].

1.2.5 Arsenic excretion

For biliary excretion, MRP2 is the only MRP located at the canalicular surface of hepatocytes that can transport arsenic-GSH conjugates into bile [46]. However, not all arsenic-GSH conjugates are stable at biliary pH, so they dissociate and undergo enterohepatic cycling through the intestine and back to the liver in the portal circulation. When in the liver, arsenic can also undergo sinusoidal excretion, enter the systemic circulation, and eventually undergo urinary elimination [81]. Most ingested arsenic is eliminated through the urine (60-80%) [82]. In human urine, the speciation profile is variable and ranges typically from 10-30% inorganic arsenic, 10-20% monomethylated species, and 60-80% dimethylated species [82–84].

1.3 Arsenic-induced diseases

1.3.1 Cancer

Arsenic is classified by the International Agency for Research on Cancer (IARC) as a human group I (proven) carcinogen [3]. There is sufficient evidence in support of arsenic causing skin cancer, particularly squamous cell carcinoma (both *in situ* and invasive), as well as basal cell carcinoma [3]. Arsenic also causes bladder cancer, particularly affecting the transitional urothelium, as well as lung cancer [3]. For multiple reasons it is difficult to define the exact cancer-causing mechanism of arsenic, including the fact that arsenic metabolism yields many arsenic metabolites with different degrees of toxicity. Arsenic likely causes cancer through a combination of many different mechanisms, and not all of which are understood.

1.3.1.1 General mechanisms of toxicity

Arsenate is very similar to phosphate, so phosphate mimicry is a way by which arsenate exerts its toxic effects. Arsenate competes against phosphate for cellular uptake, and eventually leads to inhibition of phosphorylation reactions and uncoupling of ATP production [85]. Arsenite has a high affinity for thiols, so it can bind to free sulfhydryl groups of proteins, including enzymes, leading to their inactivation [86].

Arsenic metabolism also generates reactive oxygen species (ROS). This occurs when trivalent arsenic species are oxidized to pentavalent forms and two electrons are generated, which results in hydrogen peroxide formation. Hydroxyl radicals are formed, leading to oxidative stress and damage to DNA, lipids, and proteins [87,88]. Arsenic-induced ROS can aberrantly activate signaling pathways that result in various diseases [87,89]. Cellular redox status is also affected during methylation because arsenic depletes the cell's antioxidant

reserves by consuming GSH through the formation of arsenic-GSH conjugates [70,90]. The depletion of the cell's antioxidant capacity further leads to oxidative damage [88].

1.3.1.2 Mechanisms of carcinogenesis

Although the genotoxic mechanism of arsenic is not very well understood, some examples of genotoxic effects of arsenic include sister chromatid exchanges, aneuploidies, DNA strand breaks, chromosomal aberrations, as well as micronuclei formation [91,92]. Furthermore, arsenic can interfere with DNA repair by covalently binding with DNA repair enzymes such as DNA polymerase, rendering it inactive [91,93]. Arsenite can also target key players involved in base and nucleotide excision repair pathways, which are important when DNA lesions occur [94]. Other mechanisms by which arsenic can cause cancer include affecting cellular pathways involved in apoptosis, those involved in elevated cell proliferation, cell cycle checkpoints and more [94].

Arsenic also causes epigenetic modifications including alteration of DNA methylation. Arsenic metabolism involves the use of SAM as the methyl donor, but SAM is also a methyl donor of DNA methylation [43,95]. When SAM gets depleted, hypomethylation occurs, resulting in altered methylation patterns and consequently results in the upregulation of oncogenes or downregulation of tumour suppressor genes [91,96]. Other examples of epigenetic modifications that arsenic induces include histone modifications and microRNAs [94,97,98].

1.3.2 Other arsenic-induced diseases

Arsenic has been associated with inducing immunosuppression, which leads to increased susceptibility to severe infections including sepsis [99]. Arsenic exposure has also

been associated with the impairment of the development of the thymus and spleen in infants, which are important lymphoid organs for proper immunity [100].

Exposure to arsenic has also been associated with Type II diabetes. An increased prevalence of Type II diabetes has been observed in arsenic-endemic areas relative to low-arsenic exposure areas [101]. The mechanism for arsenic-induced diabetes is not well understood, but *in vivo* animal studies suggest that arsenic impairs insulin-dependent glucose uptake, and/or glucose-stimulated insulin secretion [101].

Arsenic exposure also has been associated with cardiovascular disease, particularly atherosclerosis [102,103]. Arsenic induces endothelial dysfunction, which leads to inflammation. Platelets aggregate in endothelium leading to loss of vasodilation [103]. Most studies of arsenic-induced atherosclerosis have been done in apolipoprotein E (ApoE) deficient mice [102,103]. In these mice, As3MT and methylated trivalent arsenic species were proatherogenic [102]. Interestingly, atherosclerosis was not observed in mice deficient in both ApoE and As3MT, suggesting that methylated forms of arsenic are responsible for inducing atherosclerosis [102].

Since arsenic induces oxidative stress and oxidative stress impacts many pathways in the body, it is very possible that arsenic exposure will be associated with many more diseases. More studies need to be completed to elucidate the various mechanisms by which arsenic may induce disease.

1.3.3 Differences in susceptibility to arsenic-induced diseases

1.3.3.1 Diet

Exposure to arsenic through food varies between ethnicities due to cultural differences in diets. Rice is a staple food in many diets, especially in Asia. Studies have found that those on gluten-free diets had elevated arsenic levels in the blood and urine compared to non-gluten-free diet controls, and this could be associated with increased rice consumption [104]. Children may also be more susceptible to arsenic exposure due to higher consumption per kilogram body weight in foods containing rice or rice products that are marketed towards children [8]. During arsenic methylation, SAM and GSH are consumed. The production of SAM is influenced by nutrients such as folate, vitamin B12, betaine, choline, creatine, and riboflavin [105]. Nutrition differences can possibly influence arsenic metabolism and therefore susceptibility to arsenic-induced diseases.

1.3.3.2 Differences in arsenic methylation

1.3.3.2.1 Polymorphisms in metabolism

Arsenic methylation capacity differs between individuals, and this has been associated with genetic variations in *As3MT*. In Bangladesh, genetic variants of *As3MT* were found to be a strong predictor of arsenic methylation capacity [106,107]. Single nucleotide polymorphisms (SNPs) of *As3MT* have also been associated with altered proportions of arsenic metabolites found in urine relative to what is normally expected in healthy individuals [108,109]. *As3MT* SNPs have also been associated with adverse arsenic-related health problems such as diabetes, skin cancer, and skin lesions [107,110].

1.3.3.2.2 Animal differences in methylation

While most evidence for arsenic carcinogenicity comes from epidemiological studies of exposed human populations, some animal models have been utilized [44,111–117]. However, the arsenic toxicokinetics are different in animals other than humans. For carcinogenicity in rodents, exposures to arsenic need to be 100-200 times higher in drinking water to achieve similar levels of arsenic in human blood [113]. At best, arsenic is a poor carcinogen in rodent models.

Different animals also have varying capacities for methylating arsenic. For example, marmoset and tamarin monkeys, chimpanzees and guinea pigs do not methylate arsenic [118–120]. Drobna et al. [44] examined differences in arsenic methylation in human, rat, mouse, rabbit, dog, and rhesus monkey primary cultured hepatocytes. They specifically looked at As3MT expression and GSH concentration in the hepatocytes [44]. Hepatocytes from rat, macaque, and dog were considered fast methylators, and had greater ability to methylate arsenic than did rabbit, mouse, and human [44]. As3MT protein levels were higher in hepatocytes from the high methylator group relative to the low methylator group [44]. Interestingly, there was highest degree of homology between human and macaque *As3MT* sequences yet the rate and pattern of arsenic metabolism from the two species were markedly different [44]. Due to species differences in arsenic methylation and toxicokinetics, it is in our best interest to use human models to address questions about human arsenic metabolism.

1.3.3.3 Genetic variation in arsenic efflux pathways

The ability of cells to efflux arsenic can modulate toxicity and this is known to be mediated by MRPs. Therefore, SNPs in *ABCC*s involved in arsenic efflux can potentially affect

susceptibility to arsenic-induced diseases. Many SNPs in *ABCC1*, *ABCC2*, and *ABCC4* have been identified but still await characterization for arsenic transport. Banerjee et al. [121] previously characterized the localization and transport of eight *ABCC4* SNPs. The SNPs resulting in the mutant proteins MRP4-V776I and -C956S were not localized to the plasma membrane and MRP4-K304N had a reduced capability of transporting $MMA(GS)_2$ and DMA^V relative to MRP4-WT [121]. Individuals with these SNPs could have reduced ability to eliminate hepatic arsenic metabolites via urine. In contrast, individuals with SNPs that have an enhanced ability to efflux arsenic may have an increased ability for urinary elimination of hepatic arsenic metabolites. For example, MRP4-C171G and -Y556C had higher transport activity of $MMA(GS)_2$ and DMA^V, respectively, compared to MRP4-WT [121]. Therefore, genetic variations in *ABCC4* (and possibly *ABCC1* and *ABCC2)* can potentially contribute to inter-individual differences in susceptibility to arsenic-induced diseases.

1.3.3.3.1 Dubin-Johnson Syndrome

Dubin-Johnson syndrome (DJS) is a rare autosomal recessive condition characterized by a lack of functionally active MRP2 protein [122–125]. Patients with DJS often have conjugated hyperbilirubinemia caused by an impaired ability to efflux bilirubin glucuronide [122–125]. Despite having conjugated hyperbilirubinemia, patients with DJS are generally asymptomatic under normal conditions and no treatment is typically needed [125,126]. No signs of hepatic injury are typically observed [126]. Although this disease is quite benign and people with DJS have a normal life expectancy, it is still important to diagnose those with DJS to aid in the differential diagnosis of similar conditions causing conjugated hyperbilirubinemia, such as rotor syndrome, intrahepatic cholestasis, and others [126]. Since those with DJS lack functionally

active MRP2 protein, their hepatocytes likely have an impaired ability to excrete arsenic into bile.

1.4 Selenium: an essential trace element

Selenium is an essential trace nutrient with many important biological functions. The recommended daily intake is 55 μg/day, but selenium is toxic in excess with a tolerable upper intake level of 400 μg/day [127]. Most of our selenium intake is dietary. Some main dietary sources of selenium include bread and cereals, meat, eggs, and dairy products [128,129]. Garlic, onion, mushrooms, broccoli, and brazil nuts can also be rich in selenium, depending on the soil they have been grown in [128,129].

Selenium mainly exerts its biological functions through selenoproteins. Since selenium has very similar physicochemical properties as sulfur, it can substitute for sulfur to form seleno-amino acids [128,130,131]. Selenium can be incorporated into proteins as the 21st amino acid, selenocysteine by a co-translational mechanism [128,130,131]. Selenoprotein synthesis involves the insertion of a selenocysteine residue at the UGA codon, which is normally read as a stop codon [128,140,149]. A unique tRNA is required for the synthesis of selenocysteine and incorporation into proteins [128,140,149]. So far, 25 selenoproteins have been identified in humans, although not all have been functionally characterized. Some important selenoproteins with essential roles include glutathione peroxidases, thioredoxin reductases, and iodothyronine deiodinases [128,132–135].

Although selenium is required in small quantities, deficiencies still exist. Selenium deficiencies are especially prevalent in areas where there are low amounts of selenium in the soil [136]. Keshan disease was first discovered as a juvenile cardiomyopathy in China that

predominantly affected women and children [137]. Another disease associated with selenium deficiency is Kashin-Beck disease, which is prevalent in Tibet, parts of China, Siberia, and North Korea [137]. This disease is characterized as a chronic osteochondropathy with joint necrosis [137]. Fortunately, supplementation with sodium selenite tablets have been effective at preventing the development of these diseases [136]. Myxedematous endemic cretinism, a disease of thyroid atrophy that may also result in mental retardation is prevalent in central Africa, where iodine and selenium deficient regions overlap [136].

In contrast, diseases of selenium toxicity, known as selenosis also exist. The signs and symptoms associated with selenosis are quite ambiguous. Some examples include hair loss, blotchy white spots on the nails, garlic odour in the breath, gastrointestinal issues, fatigue, neurological damage, and irritability [138].

1.4.1 Selenium toxicokinetics

1.4.1.1 Selenium absorption

In general, ~80% of dietary selenium is absorbed, but this depends on the type of food consumed. Selenium is absorbed differently depending on its chemical species [139]. Selenomethionine, selenocysteine, selenite and selenate are the predominant dietary forms, depending on the food source, and are readily absorbed [140].

Selenomethionine uptake occurs by intestinal amino acid transporters and enters the methionine pool where it can get randomly inserted into proteins in place of methionine depending on its concentration relative to methionine [140,141].

Selenate is absorbed across the gastrointestinal tract through the paracellular pathway [128,142]. Once absorbed, it gets reduced to selenite in the blood [128]. Selenite exists

predominantly as $HSeO_3^-$ at physiological pH and has pKa values of 2.6 and 8.3 [143]. The uptake of selenite is mediated by the chloride/bicarbonate anion exchanger 1 in red blood cells (RBCs) [37,143]. Uptake of selenite also occurs in the intestine transcellularly and paracellularly, but the proteins involved in uptake are not well understood [128,144]. Aquaglyceroporin 9 has also been shown to transport selenite at acidic pH when overexpressed in *Xenopus laevis* oocytes [145]. The zinc transport protein, ZIP8 (*SLC39A8*) may also be involved in selenite uptake and this has been shown to be zinc and bicarbonate-dependent [146]. However, human RBCs, which are thought to express ZIP8 had no detectable zinc or bicarbonate dependence of selenite uptake [37,147].

1.4.1.2 Selenium metabolism

Selenium is mainly metabolized in the liver [128,148]. Once taken up, selenium can be metabolized to selenide, and undergo selenoprotein synthesis [128,140,149]. Selenomethioine has high bioavailability and low toxicity and proteins act as a selenomethionine store until protein degradation occurs [128,140,149]. The production and metabolism of selenomethionine is not regulated, as translational machinery cannot distinguish between selenomethionine and methionine [128,140,149].

Methylselenocysteine can form methylselenol upon cleavage of the cysteine group [128,140,149]. Methylselenol has been reported as a key metabolite in the anti-cancer effect of methylselenocysteine [149]. The main metabolic intermediate is selenide, which can be formed from selenomethionine, selenocysteine and inorganic selenium species through the transulfuration pathway, as outlined in **Fig 1.2** [128,140,149]. If needed, selenide is used for the synthesis of more selenoproteins.

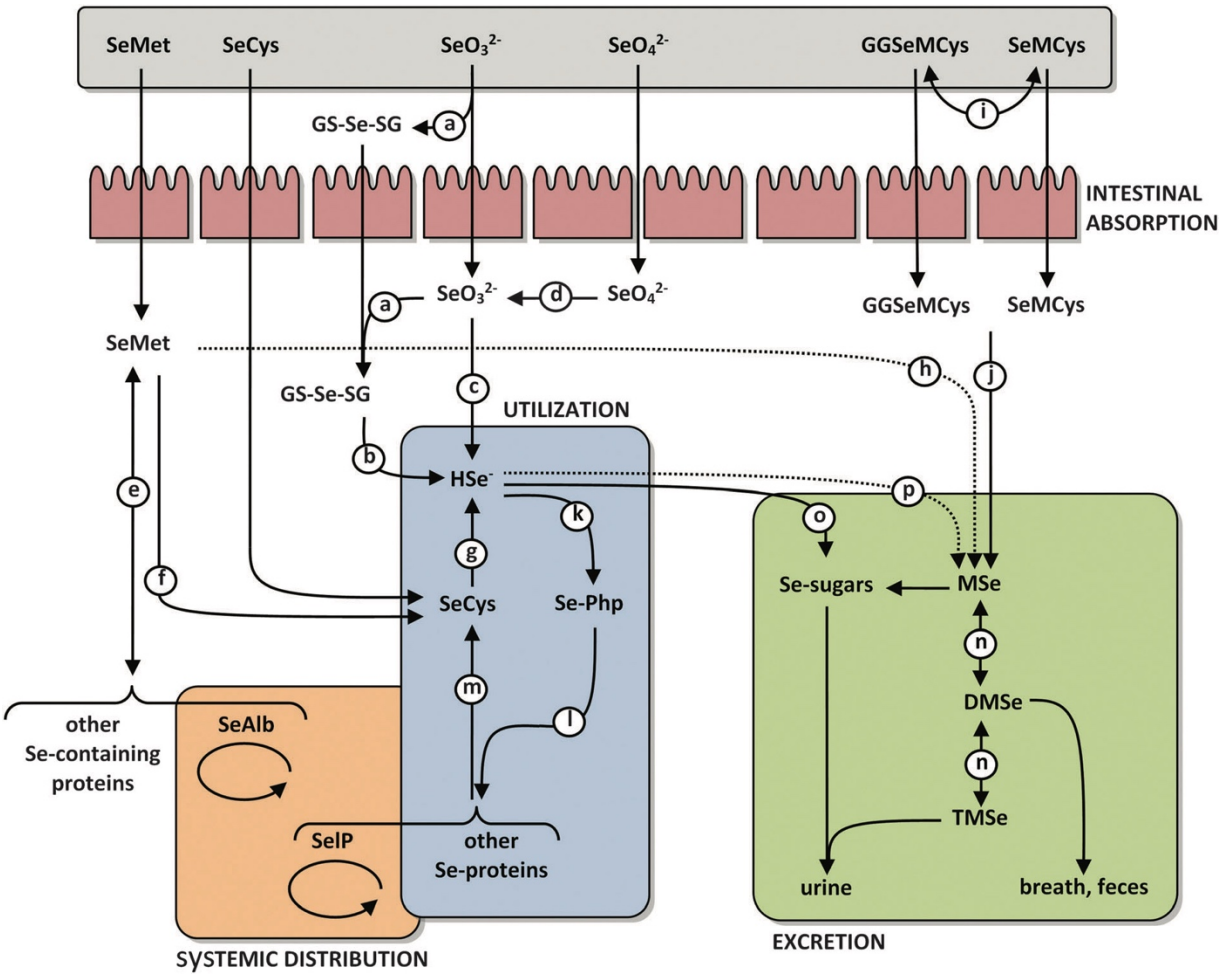

Figure 1.2: Selenium metabolic pathways in mammals. Taken from [128], with permission. SeMet, selenomethionine; SeCys, selenocysteine; SeO_3^{2-}, selenate; SeO_4^{2-}, selenite; GGSeMCys, gamma-glutamyl-Se-methylselenocysteine; SeMCys, Se-methylselenocysteine; GS-Se-SG, selenodiglutathione; HSe^-, hydrogen selenide; SeAlb, selenium-albumin; SelP, selenoprotein P; Se-Php, selenophosphate; MSe, methylselenide; DMSe, dimethylselenide; TMSe, trimethylselenide, Se-sugars, selenosugars

1.4.1.3 Selenium elimination

The route of excretion depends on the selenium status of the individual, as well as the starting selenium species [128]. The routes of excretion either involve methylation or the formation of selenosugars [128,140,149]. The methylation pathway produces less toxic methylated metabolites [128,140,149]. Methylation of selenium is achieved through

methyltransferases, using SAM as a donor and forms hydrogen selenide and its methylated metabolites, dimethyl selenide, which is volatile and eliminated across the lungs [128,140,149]. Selenium can also be eliminated through urine in the form trimethylselenomium and is thought to be a main product of selenium metabolism [128,140,149]. However, trimethylselenomium was only found as a trace metabolite in urine relative to selenosugars in cancer patients who received high doses of selenomethionine [150]. Selenide can also be converted to selenosugars such as SeMethyl-*N*-acetyl-galactosamine for urinary elimination. Other forms of selenium-sugar conjugates have also been detected in urine [128]. However, the formation of dimethyl selenide is thought to be more kinetically favored than trimethylselenide [128].

1.5 Arsenic and selenium interactions

Arsenic and selenium have similar chemical properties but have very different biological effects. Interestingly, these two compounds have a mutually protective relationship. The interactions between arsenic and selenium are discussed below.

1.5.1 Mutual detoxification in animals

The mutually protective relationship between arsenic and selenium was first investigated in animals when drinking water containing arsenic protected rats against selenium induced liver damage [151]. In a study by Moxon [151], seleniferous grains fed to adult rats prevented symptoms of selenium-induced injury in a dose-dependent manner. Rats given 5 ppm of arsenite in drinking water had full protection against liver damage, whereas only partial protection was observed when rats were given 2.5 ppm of arsenite [151]. Later on, Levander and Baumann [152] injected arsenic and selenium into adult rats at subacutely toxic doses. Arsenic promoted selenium elimination into the gut and decreased the amount of selenium in

the carcass, blood, and expired air. Consistent with this finding, selenite stimulated gastrointestinal excretion of arsenic. Arsenic also significantly increased the amount of selenium excreted into rat bile, and this was observed over a wide range of doses. Levander and Baumann [152] concluded that arsenic and selenium enhance biliary elimination of each other. Findings from these early experiments provided the basis for many future studies.

1.5.2 The seleno-bis (S-glutathionyl) arsinium ion

The seleno-bis (*S*-glutathionyl) arsinium ion, $[(GS)_2AsSe]^-$ was first identified as $[(RS)_2AsSe]^-$ in the bile of rabbits that were co-injected with arsenite and selenite [153]. In this conjugate, R was thought to be a low molecular weight thiol, but the sulfur donor could not be identified due to limitations with X-ray absorption spectroscopy. Nonetheless, Gailer et al. [153] revealed that the conjugate contained equimolar amounts of arsenic and selenium. In a later study, Gailer et al. [154] treated rabbits with selenite and arsenite and analyzed bile samples by size-exclusion chromatography. Results from this study suggested that GSH is the sulfur donor and demonstrated that $[(GS)_2AsSe]^-$ can form *in vivo*.

Ponomarenko et al. [155] also demonstrated that $[(GS)_2AsSe]^-$ forms *in vivo*. In hamsters that were dually dosed with arsenite and selenite, co-localization of these two compounds were visually apparent throughout the whole body, with an especially high degree of co-localization in the liver [155]. After equimolar dosing, there was >92% of arsenic and selenium in the liver, and almost all of arsenic and selenium in the gallbladder was present as $[(GS)_2AsSe]^-$ [155]. This study provides more evidence for the formation of $[(GS)_2AsSe]^-$ *in vivo* and its role in biliary elimination of arsenic and selenium.

Carew and Leslie [76] showed that $[(GS)_2AsSe]^-$ and $As(GS)_3$ are transported by human MRP2 using plasma membrane enriched vesicles. Human MRP2 transported $[(GS)_2AsSe]^-$ and $As(GS)_3$ with relatively high affinities [76]. More importantly, arsenite transport in the presence or absence of selenite was only detected when GSH was present, suggesting that GSH is required [76]. Ophthalmic acid, which is structurally similar to GSH but contains a methyl group in place of the thiol group, thus unable to form a conjugate, was used as a functional substitute for GSH to determine if a conjugate was formed, or whether GSH co-transport was occurring [76]. There was no arsenite transport observed in the presence of ophthalmic acid, suggesting that conjugation to GSH is required for transport [76]. Overall, this study demonstrates that these conjugates can be transported *in vitro* by human MRP2. Although $As(GS)_3$ can be transported by human MRP2, $As(GS)_3$ is not stable at biliary pH (pH ~8) and dissociates to arsenite and glutathione in bile and then undergoes enterohepatic circulation. During enterohepatic circulation, some arsenic likely gets transported from the liver to sinusoidal blood for urinary elimination. However, $[(GS)_2AsSe]^-$ is stable at alkaline biliary pH, enabling fecal elimination [49,154].

1.5.3 Selenium and arsenic sequestration in red blood cells

The sequestration of $[(GS)_2AsSe]^-$ in RBCs is thought to be another mechanism by which arsenic and selenium are mutually protective [37,156,157]. When Palmer et al. [157] co-injected rats with arsenite and ^{75}Se-selenite and measured the distribution of ^{75}Se-selenium in whole blood, there was greater accumulation of ^{75}Se-selenium in rats co-injected with arsenite and selenite than for selenite alone. These findings were later corroborated by Csanaky and Gregus [156] when arsenic distribution was followed, rats co-injected with selenite and arsenite

had increased levels of arsenic in blood compared to arsenite alone. In rabbit RBC lysate, ~70% of arsenite and selenite were converted to $[(GS)_2AsSe]^-$ within two minutes [158]. Interestingly, RBC membrane ghosts prepared from human RBCs had no ATP-dependent transport of $[(GS)_2AsSe]^-$ [76], providing evidence for the sequestration of this conjugate.

Kaur et al. [37] characterized arsenite and selenite uptake by human RBCs. Uptake of selenite in human RBCs was demonstrated to be mediated by the anion-exchanger 1 (AE1 or Band 3, gene *SLC4A1*), and accumulation of selenite was increased by arsenite. Arsenite uptake was temperature-dependent, partly reduced by aquaglyceroporin 3 inhibitors and did not reach saturation. Near-edge X-ray absorption spectroscopy revealed the formation of $[(GS)_2AsSe]^-$ in human RBCs after exposure to arsenite and selenite. Furthermore, insignificant RBC toxicity was observed for selenite and arsenite individually or in combination at up to 30 µM, suggesting that at dietary and environmental exposures, arsenite, selenite, and $[(GS)_2AsSe]^-$ is not harmful to RBCs.

Overall, the sequestration of arsenic and selenium in human RBCs is thought to decrease the amount of distributed arsenic and selenium, diminishing their toxic effects in susceptible tissues, and preventing (or alleviating) arsenic-induced diseases.

1.5.4 Selenium competes for arsenic methylation

As previously discussed, both arsenic and selenium undergo methylation. GSH is required for both arsenic and selenium methylation. For arsenic, GSH is involved in the reduction of pentavalent to trivalent species [135,159]. In selenium metabolism, selenate and selenite are reduced by GSH to selenodiglutathione, which is metabolized to hydrogen selenide by GSH reductase [160,161].

Styblo and Thomas [111] studied the effect of selenite on the cellular retention, methylation, and cytotoxicity of arsenite in primary rat hepatocytes in conventional culture. They found that concurrent exposure to arsenite and selenite inhibited methylation and/or significantly increased cellular retention of arsenite in the cells [111]. The ratio of DMA:MMA was decreased, suggesting that selenite inhibited arsenic methylation [111]. In a later study, Walton et al. [162] examined the effect of sodium selenite, as well as mono-, di- and trimethylated selenium compounds on arsenite methylation using a purified recombinant form of rat As3MT. This study evaluated methylation of arsenite using an *in vitro* methylation assay alongside primary rat and human hepatocytes. In the methylation assay and cultured primary hepatocytes, selenite was the most potent methylation inhibitor of arsenite, suggesting that selenite is directly responsible for inhibition of arsenite methylation rather than its metabolites [162]. While selenium and arsenic are methylated by different enzymes it is thought that these compounds compete for available SAM and this leads to reduced methylation [43,163].

1.5.5 Selenium protects against oxidative DNA damage

Arsenic produces oxidative damage through the formation of excess reactive oxygen species such as superoxide anions and hydroxyl radicals [133,134,164]. In *in vitro* studies where cells are treated with arsenite, an increase in ROS are observed, as well as an upregulation of oxidative-stress related genes [132,164]. The release of liver enzymes typically used to evaluate hepatic function (alkaline phosphatase, alanine transaminase and aspartate transaminase) were also elevated in primary rat hepatocytes after treatment with arsenic [134]. However, these studies found that genes upregulated when under oxidative stress were decreased in cells treated with arsenite and selenite compared to when cells are only treated with arsenite

[132,164]. Furthermore, selenoproteins that exert antioxidant effects such as glutathione peroxidase and thioredoxin reductase were increased [132,164]. It is likely that the interaction between arsenite and selenite led to the formation of $[(GS)_2AsSe]^-$ and prevented free radical formation through sequestration, and selenoproteins with antioxidant properties played a protective role.

1.5.6 Selenium-supplementation trials

There are many arsenic-endemic regions worldwide where people are exposed to arsenic through drinking water [5]. Although cessation of arsenic exposure should be a priority, removal of arsenic from water is not easily achieved, is expensive, and these struggles are compounded by the poor socio-economic status of many populations affected [165]. Furthermore, humans are thought to remain susceptible to arsenic-induced diseases decades following cessation of exposure [166,167].

In multiple arsenic-endemic regions, there have been selenium-supplementation trials where participants have been given selenium in multiple chemical forms. Some trials have used selenium-enriched yeast or lentils comprised predominantly of selenomethionine but contain hundreds of additional selenium species, and there is likely variability between batches [168–170]. Purified selenomethionine in pill form has also been utilized as a supplement [170]. Selenite, which is rapidly converted to selenide in the presence of glutathione within cells [171] has also been used in supplementation trials [172,173]. Methylselenocysteine is another selenium compound that has been shown to have anti-cancer effects *in vitro* [149].

Yang et al. [174] conducted a small population study consisting of 186 people who had been exposed to arsenic through drinking water in Inner Mongolia. Participants from 19 villages were

given either selenized yeast or placebo tablets. Doses administered were varied to avoid any adverse health effects resulting from a continuous dose of 200 μg/day of selenium. Hair and blood samples were taken every 3 months for the 14-month study and arsenic concentrations in these samples decreased throughout the trial in the selenium-supplemented group relative to the placebo group. Skin lesions also improved throughout the study.

Verret et al. [175] performed a randomized, double-blind placebo-controlled trial in a population in Bangladesh. L-selenomethionine (200 μg/day) in pill form was given to the participants. The outcomes were measured using urine and blood samples, as well as examination of skin lesions. Participants had a significant decrease in urinary arsenic, which would be consistent with arsenic biliary elimination. Although there were trends in skin lesion improvement in the L-selenomethionine group, they were not statistically different from controls.

Smits et al. [176] performed a randomized, double-blind, placebo-control pilot study in Bangladesh. Participants in the control group were given lentils containing 1.5 μg selenium/day, whereas those in the treatment group were given lentils containing the recommended daily allowance of 55 μg selenium/day. Measurements taken included blood, urine, stool, and hair. The group supplemented with selenium-enriched lentils had 1.3-fold higher urinary arsenic excretion, especially DMA after 6 months, compared to the control group. The increased urinary elimination of DMA was not expected because it is not consistent with increased biliary elimination through the formation of $[(GS)_2AsSe]^-$.

Alauddin et al. [173] conducted a small study consisting of five arsenicosis patients from Bangladesh. Participants lived in a clinic where meals were provided, and food was prepared

from arsenic-contaminated drinking water from their homes. On the sixth day, participants were given drinking water containing selenium (^{77}Sodium selenite, 800 µg) or placebo (drinking water without selenite). Urine and feces were collected alongside food samples provided to the participants at each meal for analysis. The main findings of this study suggested fecal arsenic elimination increased after ingestion of selenium, which is consistent with the notion that selenium supplementation promotes arsenic and selenium elimination through the formation of $[(GS)_2AsSe]^-$ and excretion in bile.

Despite these ongoing selenium-supplementation trials, it is unclear which chemical form of selenium is most efficacious as it is difficult to compare outcomes of the studies due to differences in study design. The actual mechanism and interactions between arsenic and selenium are also not very well understood. Overall, there is a knowledge gap in how selenium influences the handling of arsenic by the human body, especially by the human liver. Furthermore, nothing is known regarding the best chemical form of selenium to supplement with.

1.6 Models of transport

In order to explore the influence of selenium on arsenic transport by human cells, several models were used in this thesis. The advantages and limitations of these models are discussed below.

1.6.1 Human hepatocyte models

Primary human hepatocytes are the gold standard for studying hepatic transport pathways. When primary human hepatocytes are cultured between two layers of collagen, they are known as sandwich-cultured human hepatocytes (SCHH) [177]. SCHH retain important

features of hepatocytes in liver, including formation of intact canalicular networks, and correct apical and basolateral localization of hepatic plasma membrane proteins [178–180]. However, primary human hepatocytes have disadvantages in that they are not readily available, are prohibitively expensive to purchase, and donor-to-donor variability makes it difficult to optimize assay conditions and draw definitive conclusions.

Immortalized liver cell lines are useful for studies where little variability between experiments is desired, such as when establishing/optimizing conditions rather than for investigating genetic variability. The immortalized HepaRG cells were initially isolated from a hepatitis C positive female hepatocarcinoma patient [181–183]. These cells differentiate into both cholangiocyte-like and hepatocyte-like cells, and the hepatocytes polarize appropriately and form canalicular networks [181–183]. HepaRG cells also maintain expression of hepatocyte transport proteins that are correctly localized [181–183]. The unique features of HepaRG cells make them an excellent surrogate in place of primary human hepatocytes for studying polarized transport of arsenic and selenium. Challenges of using this model include a lengthy proliferation and differentiation in culture time, and the 1:1 ratio of cholangiocyte-like and hepatocyte-like cells does not accurately reflect what is found *in vivo* (on a cellular basis the liver is ~70% hepatocytes and ~3% cholangiocytes). However, these limitations are preferred over using non-human models that have previously been used to study arsenic and selenium interactions [44,111].

Although HepG2 cells are an immortalized human liver cell line, they are not ideal because they do not form canalicular networks or polarize like HepaRG cells [184]. The protein

levels of membrane transporters and metabolic enzymes also differ between HepG2 cells and human hepatocytes [184].

Upcyte hepatocytes have comparable features to human hepatocytes [185]. They form canalicular networks, have similar metabolic profiles to human hepatocytes and retain conjugating enzyme activities [185]. However, they are prohibitively expensive to culture and maintain, and have limited number of passages [185]. Similar to primary human hepatocytes, they are not suitable for optimizing conditions as they originate from different donors [185].

Animal hepatocyte models, including rat hepatocytes could also be used to study arsenic and selenium interactions. As discussed above, there are differences in metabolism and likely transport between human and rat hepatocytes that are not desired for studying handling of arsenic and selenium by human liver [186]. Previous studies with arsenic and selenium were performed using primary rat hepatocytes cultured in a non-sandwich configuration [44,111]. Thus, these studies used primary rat hepatocytes that lacked canalicular networks and polarized transport of compounds.

1.6.2 Transfected immortalized cells

Transfected immortalized cells offer the advantage of allowing the study of transport characteristics of a specific protein of interest [187]. Depending on the cell line, they are generally more cost-effective to culture and maintain, making them suitable for large-scale experiments. They can also be used to generate stable cell lines, as well as for transient overexpression of proteins [187]. Some limitations include lack of polarization in some cell lines (HEK293T), low transfection efficiency (LLC-PK1, HepaRG, HepG2), and possibly some cell line-

specific differences in protein level, post-translational modifications, localization, and transport activity.

1.6.2.1 Whole cell accumulation assays

Whole cell accumulation assays are simple to perform and allow for the study of uptake or accumulation of substrates over time using cells expressing the protein of interest [188]. The cells are pre-incubated with substrate to allow for accumulation, then the cells are washed and lysed, and then the lysate is collected for quantification of accumulated substrate [188]. However, results may be confounded by endogenous levels of uptake or efflux transporters found in the cell line chosen. The assay may also be limited by transfection efficiency.

1.6.2.2 Vesicular transport assays

Transport assays using plasma membrane enriched vesicles (**Fig 1.3**) allow for the study of substrates in an isolated system where the protein of interest is highly expressed [178]. Utilization of plasma membrane enriched vesicles to study MRP1, 2, and 4 transport are particularly beneficial because these are ATP-dependent unidirectional transporters. Inside-out vesicles have the ATP-binding site and substrate binding sites facing outward [189,190]. Therefore, in the presence of ATP, the substrates are transported into the vesicles and are trapped, allowing for quantification. The need for prior accumulation of substrate before studying efflux is also eliminated, which helps reduce variability of results due to uptake of the substrate and allows for the use of precise concentrations of substrate to allow for kinetic parameter determination. This model can also be adapted to study various proteins and their substrates. The challenge of using this model is that vesicle preparation steps are labour intensive and costly, and vesicular transport assays are an artificial system.

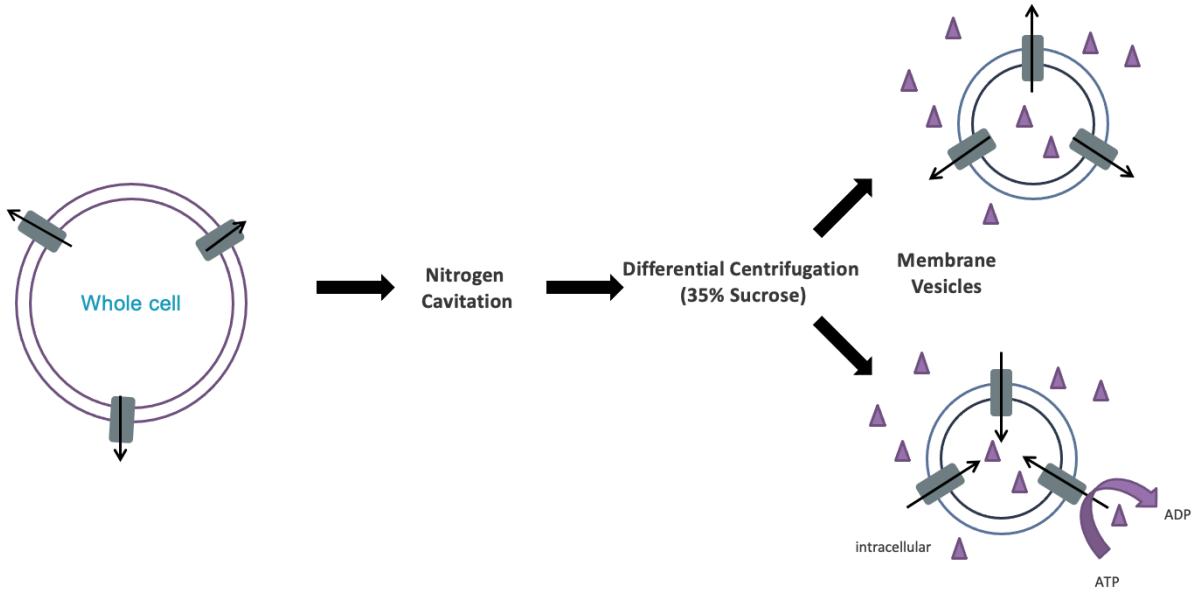

Figure 1.3: **Preparation of plasma membrane enriched vesicles.**

1.7 Objectives, hypothesis, and rationale

Although there are ongoing and completed selenium supplementation trials to alleviate symptoms related to chronic arsenic exposure, there are gaps in foundational knowledge that may be useful for designing more efficacious supplementation trials [168,172,174–176,191]. Animal studies have demonstrated that the mutually protective relationship between arsenic and selenium is likely predominantly through the formation and biliary excretion of $[(GS)_2AsSe]^-$ [152,155,158,192,193]. Furthermore, sequestration of this conjugate in RBCs likely plays a protective role [37,156,157]. However, the handling of arsenic and selenium by the human liver is poorly understood and has not been well studied in relevant human models. Many forms of selenium are utilized in supplementation trials; however, it is unclear which form is most efficacious. Additionally, there is likely a genetic component to susceptibility to arsenic-induced disease as different outcomes are observed in populations with similar diet, socioeconomic

status, and arsenic exposure histories [194]. This thesis explores the influence of different selenium chemical forms on the hepatobiliary transport of arsenite. Biliary excretion of arsenic in the presence and absence of selenium was found to be dependent on MRP2, leading us to investigate how naturally occurring human MRP2 variants influence selenium independent and dependent arsenic transport. Hepatic sinusoidal efflux of arsenic was also found to be stimulated by MeSeCys, so we sought to further characterize the role of MRP4 in this process. The following are my objectives:

1.7.1 Objective 1: To investigate the influence of different selenium chemical forms on arsenic hepatobiliary transport

The overall hypothesis for this objective was that selenium will increase biliary excretion of arsenic, and this process is mediated by MRP2. To begin this objective, studies to establish the HepaRG cell line as a model for studying arsenic hepatobiliary transport were designed and performed. Then the influence of selenium on arsenic hepatobiliary transport was studied with established conditions, with the selenium forms summarized in **Fig 1.4**. Finally, *ABCC2*-knockdown HepaRG cells were generated to further characterize arsenic hepatobiliary transport.

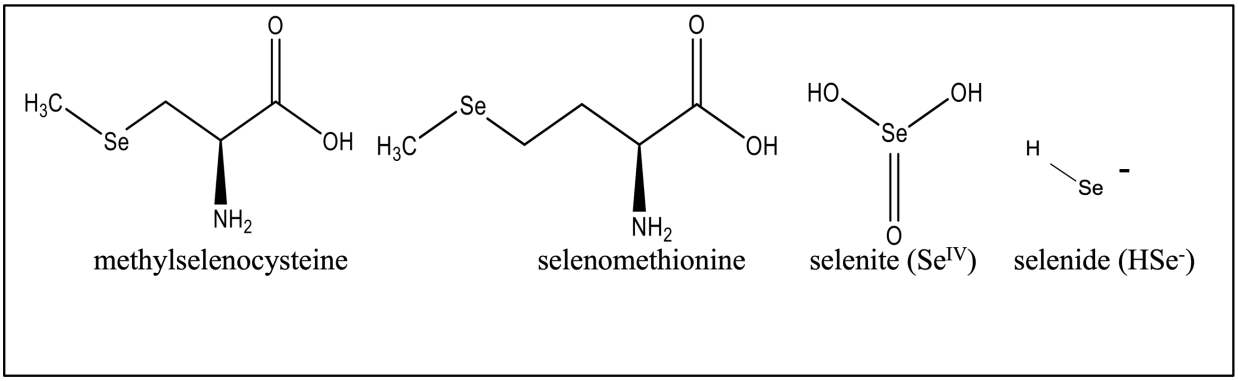

Fig 1.4: Structures of selenium-containing compounds studied in Chapters 2 and 3

1.7.2 Objective 2: To investigate the stimulatory effect of methylselenocysteine on arsenic sinusoidal efflux

During the studies in Objective 1, the novel observation that methylselenocysteine (MeSeCys) stimulated the sinusoidal efflux of arsenic was made. This led to the hypothesis that arsenic sinusoidal transport by MRP4 is stimulated by MeSeCys. To investigate this hypothesis, arsenic sinusoidal efflux in the presence of MeSeCys in HepaRG cells was measured under various conditions to determine if the process is MRP4-mediated. Then, *ABCC4*-knockdown HepaRG cells were generated to further characterize sinusoidal efflux of arsenic in the presence of MeSeCys. All of these data are included in Chapter 3. Preliminary data to supplement this work are included in Appendix A, which includes using plasma membrane enriched vesicles to measure ATP-dependent transport of arsenic by MRP4 in the presence of MeSeCys to give some more insight into the mechanism of stimulation of sinusoidal efflux. In addition, the species of arsenic in culture media of HepaRG cells with and without *ABCC4*-knockdown in the presence and absence of MeSeCys was investigated.

1.7.3 Objective 3: To investigate the effect of naturally occurring MRP2/ABCC2 variants on arsenic transport

In Chapter 2, I demonstrated that selenide, the biologically active form of selenium stimulates arsenic biliary excretion. My MRP2-knockdown studies provided strong evidence that arsenic hepatobiliary transport is MRP2-mediated. To build upon this foundational knowledge, I explored the effect of selected naturally occurring MRP2 variants on arsenic transport and sought to determine if different MRP2 variants have an altered capability of transporting arsenic glutathione conjugates (structures summarized in **Fig 1.5**). Protein levels and cellular localization of the variants were characterized using several methods. Various

methods to determine if the variants have an altered capability of transporting arsenic and selenium were also employed. The findings from this chapter may provide some foundational knowledge as to why some people are more susceptible to arsenic-induced diseases, and why selenium supplementation may not be as beneficial to some people compared to others. Preliminary data are included in Appendix B to help further characterize cellular localization of MRP2 variants in a polarized cell line.

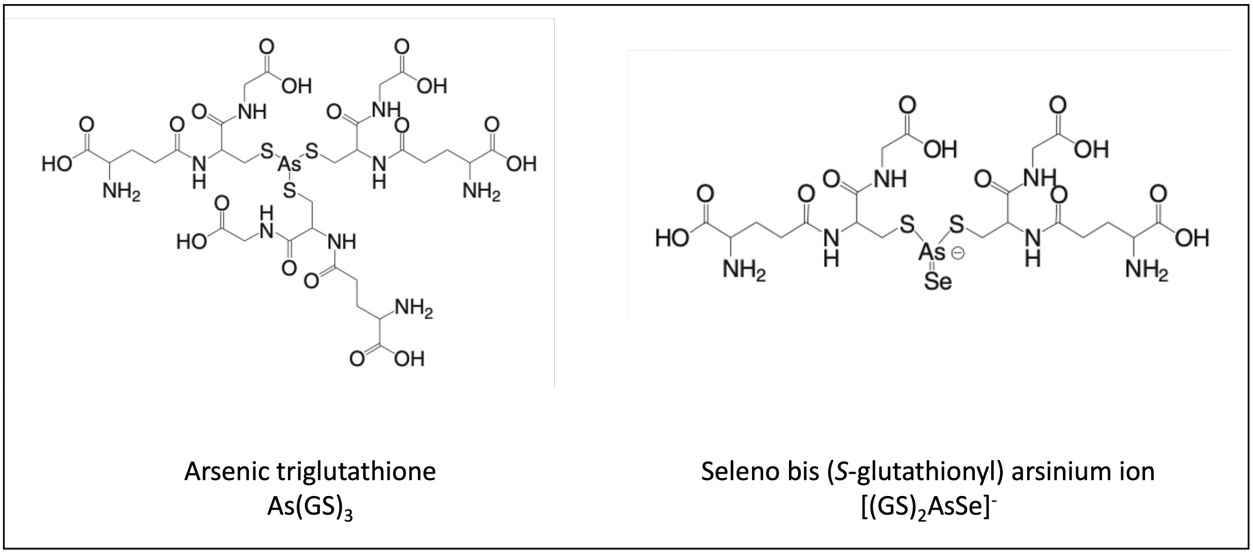

Fig 1.5: Structures of arsenic-glutathione conjugates studied in Chapter 4. Modified from [49], with permission.

1.8 References

[1] H. Masuda, Arsenic cycling in the Earth's crust and hydrosphere: interaction between naturally occurring arsenic and human activities, Progress in Earth and Planetary Science. 5 (2018) 1–11. https://doi.org/10.1186/S40645-018-0224-3/TABLES/1.

[2] N.R.C. (US) C. on M. and B.E. of E. Pollutants, Distribution of Arsenic in the Environment, (1977). https://www.ncbi.nlm.nih.gov/books/NBK231016/ (accessed December 6, 2021).

[3] IARC, A review of human carcinogens – Part C: metals, arsenic, dusts, and fibres., 2012.

[4] S. Gibaud, G. Jaouen, Arsenic-Based Drugs: From Fowler's Solution to Modern Anticancer Chemotherapy, in: 2010: pp. 1–20. https://doi.org/10.1007/978-3-642-13185-1_1.

[5] J. Podgorski, M. Berg, Global threat of arsenic in groundwater, Science. 368 (2020) 845 LP – 850. https://doi.org/10.1126/science.aba1510.

[6] E. Shaji, M. Santosh, K.V. Sarath, P. Prakash, V. Deepchand, B.V. Divya, Arsenic contamination of groundwater: A global synopsis with focus on the Indian Peninsula, Geoscience Frontiers. 12 (2021) 101079. https://doi.org/10.1016/j.gsf.2020.08.015.

[7] J.F. Ma, N. Yamaji, N. Mitani, X.-Y. Xu, Y.-H. Su, S.P. McGrath, F.-J. Zhao, Transporters of arsenite in rice and their role in arsenic accumulation in rice grain, Proceedings of the National Academy of Sciences. 105 (2008) 9931–9935. https://doi.org/10.1073/PNAS.0802361105.

[8] M.A. Davis, A.J. Signes-Pastor, M. Argos, F. Slaughter, C. Pendergrast, T. Punshon, A. Gossai, H. Ahsan, M.R. Karagas, Assessment of human dietary exposure to arsenic through rice, Science of The Total Environment. 586 (2017) 1237–1244. https://doi.org/10.1016/j.scitotenv.2017.02.119.

[9] Government of Canada, List of contaminants and other adulterating substances in foods, Https://Www.Canada.ca/En/Health-Canada/Services/Food-Nutrition/Food-Safety/Chemical-Contaminants/Contaminants-Adulterating-Substances-Foods.Html. (2020).

[10] Government of Canada, Health Canada's Proposal to Add a Maximum Level for Inorganic Arsenic in Rice-based Foods Intended Specifically for Infants and Young Children, Https://Www.Canada.ca/En/Health-Canada/Services/Food-Nutrition/Public-Involvement-Partnerships/Proposal-Add-Maximum-Level-Inorganic-Arsenic-Rice-Based-Foods/Document.Html. (2021).

[11] J.-Y. Chung, S.-D. Yu, Y.-S. Hong, Environmental source of arsenic exposure, Journal of Preventive Medicine and Public Health = Yebang Uihakhoe Chi. 47 (2014) 253–257. https://doi.org/10.3961/jpmph.14.036.

[12] V. Bencko, F.Y.L. Foong, The history of arsenical pesticides and health risks related to the use of Agent Blue, Ann Agric Environ Med. 24 (2017) 312–316. https://doi.org/10.26444/AAEM/74715.

[13] K.R. Olson, L. Cihacek, The Fate of Agent Blue, the Arsenic Based Herbicide, Used in South Vietnam during the Vietnam War, Open Journal of Soil Science. 10 (2020) 518–577. https://doi.org/10.4236/OJSS.2020.1011027.

[14] K.A. Sepkowitz, One Hundred Years of Salvarsan, New England Journal of Medicine. 365 (2011) 291–293. https://doi.org/10.1056/NEJMp1105345.

[15] J. Parascandola, History of Salvarsan (Arsphenamine), in: ELS, Wiley, 2001. https://doi.org/10.1038/npg.els.0003622.

[16] L. Falchi, S. Verstovsek, F. Ravandi-Kashani, H.M. Kantarjian, The evolution of arsenic in the treatment of acute promyelocytic leukemia and other myeloid neoplasms: Moving toward an effective oral, outpatient therapy, Cancer. 122 (2016) 1160–1168. https://doi.org/10.1002/cncr.29852.

[17] K. Davison, K.K. Mann, W.H. Miller, Arsenic trioxide: Mechanisms of action, Seminars in Hematology. 39 (2002) 3–7. https://doi.org/10.1053/shem.2002.33610.

[18] A.R. Mistry, E.W. Pedersen, E. Solomon, D. Grimwade, The molecular pathogenesis of acute promyelocytic leukaemia: implications for the clinical management of the disease, Blood Reviews. 17 (2003) 71–97. https://doi.org/10.1016/S0268-960X(02)00075-9.

[19] S. Gong, H. Wang, H. Zhang, W. Liu, X. Zhang, C. Zhao, Real-world data on the dose-related effect of arsenic trioxide in the relapse of acute promyelocytic leukemia, Molecular and Clinical Oncology. 13 (2020) 1–1. https://doi.org/10.3892/mco.2020.2161.

[20] R.N. Ratnaike, Acute and chronic arsenic toxicity, Postgraduate Medical Journal. 79 (2003) 391–396. https://doi.org/10.1136/PMJ.79.933.391.

[21] E. Logemann, B. Krützfeldt, S. Pollak, [Suicidal administration of elemental arsenic]., Archiv Fur Kriminologie. 185 (1990) 80–8.

[22] M. Ghariani, M.L. Adrien, M. Raucoules, J. Bayle, Y. Jacomet, D. Grimaud, Intoxication suraiguë à l'arsenic, Annales Françaises d'Anesthésie et de Réanimation. 10 (1991) 304–307. https://doi.org/10.1016/S0750-7658(05)80838-X.

[23] B.B. Lerman, N. Ali, D. Green, Megaloblastic, dyserythropoietic anemia following arsenic ingestion, Ann Clin Lab Sci. 10 (1980) 515–517. https://pubmed.ncbi.nlm.nih.gov/7447393/ (accessed December 6, 2021).

[24] C. Greenberg, S. Davies, T. McGowan, A. Schorer, C. Drage, Acute respiratory failure following severe arsenic poisoning, Chest. 76 (1979) 596–598. https://doi.org/10.1378/CHEST.76.5.596.

[25] A.H. Smith, A.P. Arroyo, D.N. Guha Mazumder, M.J. Kosnett, A.L. Hernandez, M. Beeris, M.M. Smith, L.E. Moore, Arsenic-induced skin lesions among Atacameño people in Northern Chile despite good nutrition and centuries of exposure, Environ Health Perspect. 108 (2000) 617–620. https://doi.org/10.1289/EHP.00108617.

[26] C.O. Abernathy, Y.P. Liu, D. Longfellow, H.V. Aposhian, B. Beck, B. Fowler, R. Goyer, R. Menzer, T. Rossman, C. Thompson, M. Waalkes, Arsenic: health effects, mechanisms of actions, and research issues, Environ Health Perspect. 107 (1999) 593–597. https://doi.org/10.1289/EHP.99107593.

[27] D.N. Guha Mazumder, Effect of chronic intake of arsenic-contaminated water on liver, Toxicology and Applied Pharmacology. 206 (2005) 169–175. https://doi.org/10.1016/j.taap.2004.08.025.

[28] C.H. Tseng, Blackfoot disease and arsenic: a never-ending story, J Environ Sci Health C Environ Carcinog Ecotoxicol Rev. 23 (2005) 55–74. https://doi.org/10.1081/GNC-200051860.

[29] D. Caussy, Case studies of the impact of understanding bioavailability: arsenic, Ecotoxicology and Environmental Safety. 56 (2003) 164–173. https://doi.org/10.1016/S0147-6513(03)00059-9.

[30] G. Freeman, Bioavailability of Arsenic in Soil and House Dust Impacted by Smelter Activities Following Oral Administration in Cynomolgus Monkeys, Fundamental and Applied Toxicology. 28 (1995) 215–222. https://doi.org/10.1006/FAAT.1995.1162.

[31] R. Villa-Bellosta, S. V, Arsenate transport by sodium/phosphate cotransporter type IIb, Toxicology and Applied Pharmacology. 247 (2010) 36–40.

[32] R. Villa-Bellosta, V. Sorribas, Role of rat sodium/phosphate cotransporters in the cell membrane transport of arsenate, Toxicology and Applied Pharmacology. 232 (2008) 125–134. https://doi.org/10.1016/j.taap.2008.05.026.

[33] Z. Liu, M.A. Sanchez, X. Jiang, E. Boles, S.M. Landfear, B.P. Rosen, Mammalian glucose permease GLUT1 facilitates transport of arsenic trioxide and methylarsonous acid, Biochemical and Biophysical Research Communications. 351 (2006) 424–430. https://doi.org/10.1016/J.BBRC.2006.10.054.

[34] Z. Liu, E. Boles, B.P. Rosen, Arsenic Trioxide Uptake by Hexose Permeases in Saccharomyces cerevisiae, Journal of Biological Chemistry. 279 (2004) 17312–17318. https://doi.org/10.1074/JBC.M314006200.

[35] T.C. Lee, I.C. Ho, W.J. Lu, J.D. Huang, Enhanced Expression of Multidrug resistance-associated Protein 2 and Reduced Expression of Aquaglyceroporin 3 in an Arsenic-resistant Human Cell Line, Journal of Biological Chemistry. 281 (2006) 18401–18407. https://doi.org/10.1074/JBC.M601266200.

[36] M. Mueckler, B. Thorens, The SLC2 (GLUT) family of membrane transporters, Molecular Aspects of Medicine. 34 (2013) 121–138. https://doi.org/10.1016/J.MAM.2012.07.001.

[37] G. Kaur, W. Javed, O. Ponomarenko, K. Shekh, D.P. Swanlund, J.R. Zhou, K.L. Summers, A. Casini, M.N. Wenzel, J.R. Casey, E. Cordat, I.J. Pickering, G.N. George, E.M. Leslie, Human red blood cell uptake and sequestration of arsenite and selenite: Evidence of seleno-bis(S-glutathionyl) arsinium ion formation in human cells, Biochemical Pharmacology. 180 (2020) 114141. https://doi.org/https://doi.org/10.1016/j.bcp.2020.114141.

[38] H. Siebeneicher, A. Cleve, H. Rehwinkel, R. Neuhaus, I. Heisler, T. Müller, M. Bauser, B. Buchmann, Identification and Optimization of the First Highly Selective GLUT1 Inhibitor BAY-876, ChemMedChem. 11 (2016) 2261–2271. https://doi.org/10.1002/CMDC.201600276.

[39] M. Calatayud, J.A. Barrios, D. Vélez, V. Devesa, In Vitro Study of Transporters Involved in Intestinal Absorption of Inorganic Arsenic, Chemical Research in Toxicology. 25 (2012) 446–453. https://doi.org/10.1021/TX200491F.

[40] M. Calatayud, M. Vázquez, V. Devesa, D. Vélez, In Vitro Study of Intestinal Transport of Inorganic and Methylated Arsenic Species by Caco-2/HT29-MTX Cocultures, Chemical Research in Toxicology. 25 (2012) 2654–2662. https://doi.org/10.1021/TX300295N.

[41] W.J. Lu, I. Tamai, J.I. Nezu, M.L. Lai, J.D. Huang, Organic anion transporting polypeptide-C mediates arsenic uptake in HEK-293 cells, Journal of Biomedical Science 2006 13:4. 13 (2006) 525–533. https://doi.org/10.1007/S11373-006-9071-0.

[42] Z. Liu, J. Shen, J.M. Carbrey, R. Mukhopadhyay, P. Agre, B.P. Rosen, Arsenite transport by mammalian aquaglyceroporins AQP7 and AQP9, Proc Natl Acad Sci U S A. 99 (2002) 6053–6058. https://doi.org/10.1073/PNAS.092131899.

[43] W.R. Cullen, Chemical mechanism of arsenic biomethylation, Chemical Research in Toxicology. 27 (2014) 457–461. https://doi.org/10.1021/tx400441h.

[44] Z. Drobná, F.S. Walton, A.W. Harmon, D.J. Thomas, M. Stýblo, Interspecies differences in metabolism of arsenic by cultured primary hepatocytes, Toxicology and Applied Pharmacology. 245 (2010) 47–56. https://doi.org/10.1016/j.taap.2010.01.015.

[45] S. v. Kala, G. Kala, C.I. Prater, A.C. Sartorelli, M.W. Lieberman, Formation and Urinary Excretion of Arsenic Triglutathione and Methylarsenic Diglutathione, Chemical Research in Toxicology. 17 (2004) 243–249.

[46] S. v. Kala, M.W. Neely, G. Kala, C.I. Prater, D.W. Atwood, J.S. Rice, M.W. Lieberman, The MRP2/cMOAT transporter and arsenic-glutathione complex formation are required for biliary excretion of arsenic, Journal of Biological Chemistry. 275 (2000) 33404–33408.

[47] L. Yehiayan, M. Pattabiraman, K. Kavallieratos, X. Wang, L.H. Boise, Y. Cai, Speciation, formation, stability and analytical challenges of human arsenic metabolites, Journal of Analytical Atomic Spectrometry. 24 (2009) 1397–1405. https://doi.org/10.1039/B910943A.

[48] K. Moitra, M. Dean, Evolution of ABC transporters by gene duplication and their role in human disease, Biol Chem. 392 (2011) 29–37. https://doi.org/10.1515/BC.2011.006.

[49] E.M. Leslie, Arsenic-glutathione conjugate transport by the human multidrug resistance proteins (MRPs/ABCCs), Journal of Inorganic Biochemistry. 108 (2012) 141–149. https://doi.org/10.1016/j.jinorgbio.2011.11.009.

[50] B.D. Whitlock, E.M. Leslie, Efflux transporters in anti-cancer drug resistance: Molecular and functional identification and characterization of multidrug resistance proteins (MRPs/ABCCs), in: Drug Efflux Pumps in Cancer Resistance Pathways: From Molecular Recognition and Characterization to Possible Inhibition Strategies in Chemotherapy, 2020: pp. 31–65. https://doi.org/10.1016/b978-0-12-816434-1.00002-4.

[51] I. Klein, B. Sarkadi, A. Váradi, An inventory of the human ABC proteins, Biochim Biophys Acta. 1461 (1999) 237–262. https://doi.org/10.1016/S0005-2736(99)00161-3.

[52] Z. Chen, T. Shi, L. Zhang, P. Zhu, M. Deng, C. Huang, T. Hu, L. Jiang, J. Li, Mammalian drug efflux transporters of the ATP binding cassette (ABC) family in multidrug resistance: A review of the past decade, Cancer Letters. 370 (2016) 153–164. https://doi.org/10.1016/J.CANLET.2015.10.010.

[53] P.M. Jones, A.M. George, A reciprocating twin-channel model for ABC transporters, Quarterly Reviews of Biophysics. 47 (2014) 189–220. https://doi.org/10.1017/S0033583514000031.

[54] N. Ono, I. van der Heijden, G.L. Scheffer, K. van de Wetering, E. van Deemter, M. de Haas, A. Boerke, B.M. Gadella, D.G. de Rooij, J.J. Neefjes, T.A.M. Groothuis, L. Oomen, L. Brocks, T. Ishikawa, P. Borst, Multidrug resistance-associated protein 9 (ABCC12) is present in mouse and boar sperm., The Biochemical Journal. 406 (2007) 31–40. https://doi.org/10.1042/BJ20070292.

[55] D.H. Pham, R. Kudira, L. Xu, C.A. Valencia, J.L. Ellis, T. Shi, K.J. Evason, I. Osuji, N. Matuschek, L. Pfuhler, M. Mullen, S.K. Mohanty, A. Husami, L.N. Bull, K. Zhang, S. Wali, C. Yin, A. Miethke, Deleterious Variants in ABCC12 are Detected in Idiopathic Chronic Cholestasis and Cause Intrahepatic Bile Duct Loss in Model Organisms, Gastroenterology. 161 (2021) 287-300.e16. https://doi.org/10.1053/J.GASTRO.2021.03.026.

[56] T. Annilo, M. Dean, Degeneration of an ATP-binding cassette transporter gene, ABCC13, in different mammalian lineages, Genomics. 84 (2004) 34–46. https://doi.org/10.1016/J.YGENO.2004.02.010.

[57] Z.L. Johnson, J. Chen, Structural Basis of Substrate Recognition by the Multidrug Resistance Protein MRP1, Cell. 168 (2017) 1075-1085.e9. https://doi.org/10.1016/j.cell.2017.01.041.

[58] K.W. Chan, H. Zhang, D.E. Logothetis, N-terminal transmembrane domain of the SUR controls trafficking and gating of Kir6 channel subunits, The EMBO Journal. 22 (2003) 3833. https://doi.org/10.1093/EMBOJ/CDG376.

[59] N. Inagaki, T. Gonoi, J.P. Clement IV, C.Z. Wang, L. Aguilar-Bryan, J. Bryan, S. Seino, A family of sulfonylurea receptors determines the pharmacological properties of ATP-sensitive K+ channels, Neuron. 16 (1996) 1011–1017. https://doi.org/10.1016/S0896-6273(00)80124-5.

[60] C. Oswald, I.B. Holland, L. Schmitt, The motor domains of ABC-transporters. What can structures tell us?, Naunyn Schmiedebergs Arch Pharmacol. 372 (2006) 385–399. https://doi.org/10.1007/S00210-005-0031-4.

[61] C.R. Zito, E. Antony, J.F. Hunt, D.B. Oliver, M.M. Hingorani, Role of a conserved glutamate residue in the Escherichia coli SecA ATPase mechanism, Journal of Biological Chemistry. 280 (2005) 14611–14619. https://doi.org/10.1074/JBC.M414224200/ATTACHMENT/1FB8B7CD-2BAE-4369-A14A-8FBDF61EDAFC/MMC1.PDF.

[62] Z. Szentpétery, A. Kern, K. Liliom, B. Sarkadi, A. Váradi, É. Bakos, The Role of the Conserved Glycines of ATP-binding Cassette Signature Motifs of MRP1 in the Communication between the Substrate-binding Site and the Catalytic Centers *, Journal of Biological Chemistry. 279 (2004) 41670–41678. https://doi.org/10.1074/JBC.M406484200.

[63] P.C. Smith, N. Karpowich, L. Millen, J.E. Moody, J. Rosen, P.J. Thomas, J.F. Hunt, ATP binding to the motor domain from an ABC transporter drives formation of a nucleotide sandwich dimer, Mol Cell. 10 (2002) 139–149. https://doi.org/10.1016/S1097-2765(02)00576-2.

[64] Z.L. Johnson, J. Chen, ATP Binding Enables Substrate Release from Multidrug Resistance Protein 1, Cell. 172 (2018) 81–89. https://doi.org/10.1016/j.cell.2017.12.005.

[65] V. Materna, H. Lage, Homozygous mutation Arg768Trp in the ABC-transporter encoding gene MRP2/cMOAT/ABCC2 causes Dubin-Johnson syndrome in a Caucasian patient, Journal of Human Genetics 2003 48:9. 48 (2003) 484–486. https://doi.org/10.1007/s10038-003-0057-8.

[66] S.P.C. Cole, K.E. Sparks, K. Fraser, D.W. Loe, C.E. Grant, G.M. Wilson, R.G. Deeley, Pharmacological Characterization of Multidrug Resistant MRP-transfected Human Tumor Cells, Cancer Research. 54 (1994).

[67] S.P.C. Cole, Targeting Multidrug Resistance Protein 1 (MRP1, ABCC1): Past, Present, and Future, Http://Dx.Doi.Org/10.1146/Annurev-Pharmtox-011613-135959. 54 (2014) 95–117. https://doi.org/10.1146/ANNUREV-PHARMTOX-011613-135959.

[68] S.P.C. Cole, Multidrug Resistance Protein 1 (MRP1 , ABCC1), a " Multitasking " ATP-binding Cassette (ABC), The Journal of Biological Chemistry. 289 (2014) 30880–30888. https://doi.org/10.1074/jbc.R114.609248.

[69] R.G. Deeley, C. Westlake, S.P.C. Cole, Transmembrane transport of endo- and xenobiotics by mammalian ATP-binding cassette multidrug resistance proteins, Physiological Reviews. 86 (2006) 849–899. https://doi.org/10.1152/PHYSREV.00035.2005/ASSET/IMAGES/LARGE/Z9J003062405001 0.JPEG.

[70] E.M. Leslie, A. Haimeur, M.P. Waalkes, Arsenic transport by the human multidrug resistance protein 1 (MRP1/ABCC1): Evidence that a tri-glutathione conjugate is required, Journal of Biological Chemistry. 279 (2004) 32700–32708. https://doi.org/10.1074/jbc.M404912200.

[71] M.W. Carew, H. Naranmandura, C.B. Shukalek, X.C. Le, E.M. Leslie, Monomethylarsenic diglutathione transport by the human multidrug resistance protein 1 (MRP1/ABCC1), Drug Metabolism and Disposition. 39 (2011) 2298–304. https://doi.org/10.1124/dmd.111.041673.

[72] M. Banerjee, G. Kaur, Brayden.D. Whitlock, M.W. Carew, X.C. Le, E.M. Leslie, Multidrug Resistance Protein 1 (MRP1/ABCC1)-Mediated Cellular Protection and Transport of

Methylated Arsenic Metabolites Differs between Human Cell Lines, Drug Metabolism and Disposition. 46 (2018) 1096–1105.

[73] C.B. Shukalek, D.P. Swanlund, R.K. Rousseau, K.E. Weigl, V. Marensi, S.P.C. Cole, E.M. Leslie, Arsenic Triglutathione [As (GS) 3] Transport by Multidrug Resistance Protein 1 (MRP1 / ABCC1) Is Selectively Modified by Phosphorylation of Tyr920 / Ser921 and Glycosylation of Asn19 / Asn23 s, Molecular Pharmacology. 90 (2016) 127–139.

[74] G. Jedlitschky, U. Hoffmann, H.K. Kroemer, Structure and function of the MRP2 (ABCC2) protein and its role in drug disposition, Expert Opin Drug Metab Toxicol. 2 (2006) 351–366. https://doi.org/10.1517/17425255.2.3.351.

[75] B.A. Roggenbeck, M.W. Carew, G.J. Charrois, D.N. Douglas, N.M. Kneteman, X. Lu, X. Chris Le, E.M. Leslie, Characterization of arsenic hepatobiliary transport using sandwich-cultured human hepatocytes, Toxicological Sciences. 145 (2015) 307–320. https://doi.org/10.1093/toxsci/kfv051.

[76] M.W. Carew, E.M. Leslie, Selenium-dependent and -independent transport of arsenic by the human multidrug resistance protein 2 (MRP2/ABCC2): Implications for the mutual detoxification of arsenic and selenium, Carcinogenesis. 31 (2010) 1450–1455.

[77] B.A. Roggenbeck, Hepatobiliary Transport of Arsenic, University of Alberta, 2016.

[78] F.G.M. Russel, J.B. Koenderink, R. Masereeuw, Multidrug resistance protein 4 (MRP4/ABCC4): a versatile efflux transporter for drugs and signalling molecules, Trends Pharmacol Sci. 29 (2008) 200–207. https://doi.org/10.1016/J.TIPS.2008.01.006.

[79] J. Wen, J. Luo, W. Huang, J. Tang, H. Zhou, W. Zhang, The Pharmacological and Physiological Role of Multidrug-Resistant Protein 4, J Pharmacol Exp Ther. 354 (2015) 358–375. https://doi.org/10.1124/JPET.115.225656.

[80] M. Banerjee, M.W. Carew, B.A. Roggenbeck, B.D. Whitlock, H. Naranmandura, X.C. Le, E.M. Leslie, A Novel Pathway for Arsenic Elimination: Human Multidrug Resistance Protein 4 (MRP4/ABCC4) Mediates Cellular Export of Dimethylarsinic Acid (DMAV) and the Diglutathione Conjugate of Monomethylarsonous Acid (MMAIII), Molecular Pharmacology. 86 (2014) 168–179.

[81] C.G. Dietrich, R. Ottenhoff, D.R. de Waart, R.P.J. Oude Elferink, Role of MRP2 and GSH in intrahepatic cycling of toxins, Toxicology. 167 (2001) 73–81. https://doi.org/https://doi.org/10.1016/S0300-483X(01)00459-0.

[82] M. Vahter, Variation in Human Metabolism of Arsenic, Arsenic Exposure and Health Effects III. (1999) 267–279. https://doi.org/10.1016/B978-008043648-7/50031-5.

[83] B.K. Mandal, Y. Ogra, K.T. Suzuki, Identification of Dimethylarsinous and Monomethylarsonous Acids in Human Urine of the Arsenic-Affected Areas in West Bengal, India, Chemical Research in Toxicology. 14 (2001) 371–378. https://doi.org/10.1021/TX000246H.

[84] X.C. Le, X. Lu, M. Ma, W.R. Cullen, H. v. Aposhian, B. Zheng, Speciation of Key Arsenic Metabolic Intermediates in Human Urine, Analytical Chemistry. 72 (2000) 5172–5177. https://doi.org/10.1021/AC000527U.

[85] M.F. Hughes, Arsenic toxicity and potential mechanisms of action, Toxicol Lett. 133 (2002) 1–16. https://doi.org/10.1016/S0378-4274(02)00084-X.

[86] S. Shen, X.F. Li, W.R. Cullen, M. Weinfeld, X.C. Le, Arsenic binding to proteins, Chemical Reviews. 113 (2013) 7769–7792. https://doi.org/10.1021/CR300015C/SUPPL_FILE/CR300015C_SI_001.PDF.

[87] H. Shi, X. Shi, K.J. Liu, Oxidative mechanism of arsenic toxicity and carcinogenesis, Mol Cell Biochem. 255 (2004) 67–78. https://doi.org/10.1023/B:MCBI.0000007262.26044.E8.

[88] L. Li, F. Chen, Oxidative stress, epigenetics, and cancer stem cells in arsenic carcinogenesis and prevention, Curr Pharmacol Rep. 2 (2016) 57. https://doi.org/10.1007/S40495-016-0049-Y.

[89] M. Valko, D. Leibfritz, J. Moncol, M.T.D. Cronin, M. Mazur, J. Telser, Free radicals and antioxidants in normal physiological functions and human disease, Int J Biochem Cell Biol. 39 (2007) 44–84. https://doi.org/10.1016/J.BIOCEL.2006.07.001.

[90] K. Rehman, H. Naranmandura, Arsenic metabolism and thioarsenicals, Metallomics. 4 (2012). https://doi.org/10.1039/c2mt00181k.

[91] E. Bustaffa, A. Stoccoro, F. Bianchi, L. Migliore, Genotoxic and epigenetic mechanisms in arsenic carcinogenicity, Arch Toxicol. 88 (2014) 1043–1067. https://doi.org/10.1007/S00204-014-1233-7.

[92] T.W. Gebel, Genotoxicity of arsenical compounds, Int J Hyg Environ Health. 203 (2001) 249–262. https://doi.org/10.1078/S1438-4639(04)70036-X.

[93] P. Mandal, Molecular insight of arsenic-induced carcinogenesis and its prevention, Naunyn Schmiedebergs Arch Pharmacol. 390 (2017) 443–455. https://doi.org/10.1007/S00210-017-1351-X.

[94] L.M. Tam, N.E. Price, Y. Wang, Molecular Mechanisms of Arsenic-Induced Disruption of DNA Repair, Chem Res Toxicol. 33 (2020) 709. https://doi.org/10.1021/ACS.CHEMRESTOX.9B00464.

[95] K.E. Pelch, E.J. Tokar, B.A. Merrick, M.P. Waalkes, Differential DNA methylation profile of key genes in malignant prostate epithelial cells transformed by inorganic arsenic or cadmium, Toxicol Appl Pharmacol. 286 (2015) 159–167. https://doi.org/10.1016/J.TAAP.2015.04.011.

[96] G. Lu, H. Xu, D. Chang, Z. Wu, X. Yao, S. Zhang, Z. Li, J. Bai, Q. Cai, W. Zhang, Arsenic exposure is associated with DNA hypermethylation of the tumor suppressor gene p16, J Occup Med Toxicol. 9 (2014). https://doi.org/10.1186/S12995-014-0042-5.

[97] B. Chen, J. Liu, Q. Chang, K. Beezhold, Y. Lu, F. Chen, JNK and STAT3 signaling pathways converge on Akt-mediated phosphorylation of EZH2 in bronchial epithelial cells induced by arsenic, Cell Cycle. 12 (2013) 112. https://doi.org/10.4161/CC.23030.

[98] L. Cantone, F. Nordio, L. Hou, P. Apostoli, M. Bonzini, L. Tarantini, L. Angelici, V. Bollati, A. Zanobetti, J. Schwartz, P.A. Bertazzi, A. Baccarelli, Inhalable Metal-Rich Air Particles and Histone H3K4 Dimethylation and H3K9 Acetylation in a Cross-sectional Study of Steel Workers, Environmental Health Perspectives. 119 (2011) 964. https://doi.org/10.1289/EHP.1002955.

[99] R. Gera, V. Singh, S. Mitra, A.K. Sharma, A. Singh, A. Dasgupta, D. Singh, M. Kumar, P. Jagdale, S. Patnaik, D. Ghosh, Arsenic exposure impels CD4 commitment in thymus and

suppress T cell cytokine secretion by increasing regulatory T cells, Scientific Reports 2017 7:1. 7 (2017) 1–13. https://doi.org/10.1038/s41598-017-07271-z.

[100] X. Duan, S. Gao, J. Li, L. Wu, Y. Zhang, W. Li, L. Zhao, J. Chen, S. Yang, G. Sun, B. Li, Acute arsenic exposure induces inflammatory responses and CD4 + T cell subpopulations differentiation in spleen and thymus with the involvement of MAPK, NF-kB, and Nrf2, Mol Immunol. 81 (2017) 160–172. https://doi.org/10.1016/J.MOLIMM.2016.12.005.

[101] C.F. Huang, Y.W. Chen, C.Y. Yang, K.S. Tsai, R. sen Yang, S.H. Liu, Arsenic and diabetes: current perspectives, Kaohsiung J Med Sci. 27 (2011) 402–410. https://doi.org/10.1016/J.KJMS.2011.05.008.

[102] L.F. Negro Silva, M. Lemaire, C.A. Lemarié, D. Plourde, A.M. Bolt, C. Chiavatti, D.S. Bohle, V. Slavkovich, J.H. Graziano, S. Lehoux, K.K. Mann, Effects of inorganic arsenic, methylated arsenicals, and arsenobetaine on atherosclerosis in the apoE-/- mouse model and the role of as3mt-mediated methylation, Environmental Health Perspectives. 125 (2017). https://doi.org/10.1289/EHP806.

[103] P.P. Simeonova, M.I. Luster, Arsenic and atherosclerosis, Toxicol Appl Pharmacol. 198 (2004) 444–449. https://doi.org/10.1016/J.TAAP.2003.10.018.

[104] C.M. Bulka, M.A. Davis, M.R. Karagas, H. Ahsan, M. Argos, The Unintended Consequences of a Gluten-Free Diet, Epidemiology. 28 (2017) e24. https://doi.org/10.1097/EDE.0000000000000640.

[105] R. Saxena, A.K. Bozack, M. v Gamble, Nutritional Influences on One-Carbon Metabolism: Effects on Arsenic Methylation and Toxicity., Annu Rev Nutr. (2018) 1–29. https://doi.org/10.1146/annurev-nutr-082117-051757.

[106] R.J. Jansen, M. Argos, L. Tong, J. Li, M. Rakibuz-Zaman, M.T. Islam, V. Slavkovich, A. Ahmed, A. Navas-Acien, F. Parvez, Y. Chen, M. v. Gamble, J.H. Graziano, B.L. Pierce, H. Ahsan, Determinants and Consequences of Arsenic Metabolism Efficiency among 4,794 Individuals: Demographics, Lifestyle, Genetics, and Toxicity, Cancer Epidemiology and Prevention Biomarkers. 25 (2016) 381–390. https://doi.org/10.1158/1055-9965.EPI-15-0718.

[107] J. Gao, L. Tong, M. Argos, M.S. Bryan, A. Ahmed, M. Rakibuz-Zaman, M.G. Kibriya, F. Jasmine, V. Slavkovich, J.H. Graziano, H. Ahsan, B.L. Pierce, The Genetic Architecture of Arsenic Metabolism Efficiency:A SNP-Based Heritability Study of Bangladeshi Adults, Environ Health Perspect. 123 (2015) 985–992. https://doi.org/10.1289/EHP.1408909.

[108] K. Engström, M. Vahter, S.J. Mlakar, G. Concha, B. Nermell, R. Raqib, A. Cardozo, K. Broberg, Polymorphisms in Arsenic(+III Oxidation State) Methyltransferase (AS3MT) Predict Gene Expression of AS3MT as Well as Arsenic Metabolism, Environmental Health Perspectives. 119 (2011) 182. https://doi.org/10.1289/EHP.1002471.

[109] T. Agusa, H. Iwata, J. Fujihara, T. Kunito, H. Takeshita, T.B. Minh, P.T.K. Trang, P.H. Viet, S. Tanabe, Genetic polymorphisms in AS3MT and arsenic metabolism in residents of the Red River Delta, Vietnam, Toxicol Appl Pharmacol. 236 (2009) 131–141. https://doi.org/10.1016/J.TAAP.2009.01.015.

[110] Z. Drobná, L.M. del Razo, G.G. García-Vargas, L.C. Sánchez-Peña, A. Barrera-Hernández, M. Stýblo, D. Loomis, Environmental exposure to arsenic, AS3MT polymorphism and prevalence of diabetes in Mexico, J Expo Sci Environ Epidemiol. 23 (2013) 151. https://doi.org/10.1038/JES.2012.103.

[111] M. Styblo, D.J. Thomas, Selenium modifies the metabolism and toxicity of arsenic in primary rat hepatocytes, Toxicology and Applied Pharmacology. 172 (2001) 52–61.

[112] M.P. Waalkes, J. Liu, J.M. Ward, B.A. Diwan, Animal models for arsenic carcinogenesis : inorganic arsenic is a transplacental carcinogen in mice, Toxicology and Applied Pharmacology. 198 (2004) 377–384. https://doi.org/10.1016/j.taap.2003.10.028.

[113] E.J. Tokar, L. Benbrahim-tallaa, J.M. Ward, R. Lunn, R.L. Sams, M.P. Waalkes, Cancer in Experimental Animals Exposed to Arsenic and Arsenic Compounds, 40 (2011) 912–927. https://doi.org/10.3109/10408444.2010.506641.Cancer.

[114] M.P. Waalkes, W. Qu, E.J. Tokar, G.E. Kissling, D. Dixon, Lung tumors in mice induced by “whole-life” inorganic arsenic exposure at human-relevant doses, Arch Toxicol. 88 (2014) 1619–1629. https://doi.org/10.1007/S00204-014-1305-8.

[115] K. Shao, Z. Zhou, P. Xun, S.M. Cohen, Bayesian benchmark dose analysis for inorganic arsenic in drinking water associated with bladder and lung cancer using epidemiological data, Toxicology. 455 (2021) 152752. https://doi.org/10.1016/J.TOX.2021.152752.

[116] S.M. Cohen, L.L. Arnold, B.D. Beck, A.S. Lewis, M. Eldan, Evaluation of the carcinogenicity of inorganic arsenic, Crit Rev Toxicol. 43 (2013) 711–752. https://doi.org/10.3109/10408444.2013.827152.

[117] M. Krishnamohan, L. Qi, P.K.S. Lam, M.R. Moore, J.C. Ng, Urinary arsenic and porphyrin profile in C57BL/6J mice chronically exposed to monomethylarsonous acid (MMAIII) for two years, Toxicology and Applied Pharmacology. 224 (2007) 89–97. https://doi.org/10.1016/J.TAAP.2007.04.020.

[118] M. Vahter, E. Marafante, Reduction and binding of arsenate in marmoset monkeys., Archives of Toxicology. 57 (1985) 119–124.

[119] M. Vahter, R. Couch, B. Nermell, J. Nilsson, Lack of methylation of inorganic arsenic in the chimpanzee., Toxicology and Applied Pharmacology. 133 (1995) 262–268.

[120] S. Healy, R. Zakharyan, H. Aposhian, Enzymatic methylation of arsenic compounds: IV. In vitro and in vivo deficiency of the methylation of arsenite and monomethylarsonic acid in the guinea pig., Mutation Research - Genetic Toxicology and Environmental Mutagenesis. 386 (1997) 229–239.

[121] M. Banerjee, V. Marensi, G. Conseil, X.C. Le, S.P.C. Cole, E.M. Leslie, Polymorphic variants of MRP4/ABCC4 differentially modulate the transport of methylated arsenic metabolites and physiological organic anions, Biochemical Pharmacology. 120 (2016) 72–82.

[122] V. Keitel, A.T. Nies, M. Brom, J. Hummel-Eisenbeiss, H. Spring, D. Keppler, A common Dubin-Johnson syndrome mutation impairs protein maturation and transport activity of MRP2 (ABCC2)., Am J Physiol Gastrointest Liver Physiol. 284 (2003) G165-74. https://doi.org/10.1152/ajpgi.00362.2002.

[123] R. Mor-Cohen, A. Zivelin, N. Rosenberg, M. Shani, S. Muallem, U. Seligsohn, Identification and Functional Analysis of Two Novel Mutations in the Multidrug Resistance Protein 2 Gene in Israeli Patients with Dubin-Johnson Syndrome, Journal of Biological Chemistry. 276 (2001) 36923–36930. https://doi.org/10.1074/jbc.M105047200.

[124] K. Jemnitz, K. Heredi-Szabo, J. Janossy, E. Ioja, L. Vereczkey, P. Krajcsi, ABCC2/Abcc2: a multispecific transporter with dominant excretory functions, Http://Dx.Doi.Org/10.3109/03602530903491741. 42 (2010) 402–436. https://doi.org/10.3109/03602530903491741.

[125] M. Wada, S. Toh, K. Taniguchi, T. Nakamura, T. Uchiumi, K. Kohno, I. Yoshida, A. Kimura, S. Sakisaka, Y. Adachi, M. Kuwano, Mutations in the canilicular multispecific organic anion transporter (cMOAT) gene, a novel ABC transporter, in patients with hyperbilirubinemia II/Dubin-Johnson syndrome, Hum Mol Genet. 7 (1998) 203–207. https://doi.org/10.1093/HMG/7.2.203.

[126] Z.J. Talaga, P.N. Vaidya, Dubin Johnson Syndrome, StatPearls. (2021). https://www.ncbi.nlm.nih.gov/books/NBK536994/ (accessed December 13, 2021).

[127] Institute of Medicine (US) Panel on Dietary Antioxidants and Related Compounds, Dietary Reference Intakes for Vitamin C, Vitamin E, Selenium, and Carotenoids, Washington, 2000.

[128] M. Roman, P. Jitaru, C. Barbante, Selenium biochemistry and its role for human health, Metallomics. 6 (2014) 25–54. https://doi.org/10.1039/C3MT00185G.

[129] M.P. Rayman, Food-chain selenium and human health: emphasis on intake, British Journal of Nutrition. 100 (2008) 254–268. https://doi.org/10.1017/S0007114508939830.

[130] L.V. Papp, J. Lu, A. Holmgren, K.K. Khanna, From Selenium to Selenoproteins: Synthesis, Identity, and Their Role in Human Health, Antioxidants & Redox Signaling. 9 (2007) 775–806. https://doi.org/10.1089/ars.2007.1528.

[131] G. v. Kryukov, S. Castellano, S. v. Novoselov, A. v. Lobanov, O. Zehtab, R. Guigó, V.N. Gladyshev, Characterization of Mammalian Selenoproteomes, Science (1979). 300 (2003) 1439–1443. https://doi.org/10.1126/science.1083516.

[132] Z. Xu, Z. Wang, J. Li, C. Chen, P. Zhang, L. Dong, J. Chen, Q. Chen, X. Zhang, Z. Wang, Protective effects of selenium on oxidative damage and oxidative stress related gene expression in rat liver under chronic poisoning of arsenic, Food and Chemical Toxicology. 58 (2013) 1–7. https://doi.org/10.1016/j.fct.2013.03.048.

[133] T.G. Rossman, A.N. Uddin, Selenium prevents spontaneous and arsenite-induced mutagenesis, International Congress Series. 1275 (2004) 173–179. https://doi.org/10.1016/j.ics.2004.09.038.

[134] M. Messarah, F. Klibet, A. Boumendjel, C. Abdennour, N. Bouzerna, M.S. Boulakoud, A. el Feki, Hepatoprotective role and antioxidant capacity of selenium on arsenic-induced liver injury in rats, Experimental and Toxicologic Pathology. 64 (2012) 167–174. https://doi.org/10.1016/j.etp.2010.08.002.

[135] B. Németi, M.E. Anderson, Z. Gregus, Glutathione synthetase promotes the reduction of arsenate via arsenolysis of glutathione, Biochimie. 94 (2012) 1327–1333. https://doi.org/10.1016/j.biochi.2012.02.033.

[136] S. Kurokawa, M.J. Berry, Selenium. Role of the essential metalloid in health, Metal Ions in Life Sciences. 13 (2013) 499–534.

[137] G. Li, F. Wang, D. Kang, C. Li, Keshan disease: An endemic cardiomyopathy in China, Human Pathology. 16 (1985) 602–609. https://doi.org/10.1016/S0046-8177(85)80110-6.

[138] J.K. Wrobel, R. Power, M. Toborek, Biological activity of selenium: Revisited, IUBMB Life. 68 (2016) 97–105. https://doi.org/10.1002/iub.1466.

[139] M. Navarro-Alarcon, C. Cabrera-Vique, Selenium in food and the human body: A review, Science of The Total Environment. 400 (2008) 115–141. https://doi.org/10.1016/j.scitotenv.2008.06.024.

[140] R.F. Burk, K.E. Hill, Regulation of Selenium Metabolism and Transport, Annual Review of Nutrition. 35 (2015). https://doi.org/10.1146/annurev-nutr-071714-034250.

[141] K. McConnell, G. Cho, Active transport of L-selenomethionine in the intestine, American Journal of Physiology-Legacy Content. 213 (1967) 150–156. https://doi.org/10.1152/ajplegacy.1967.213.1.150.

[142] B. Gammelgaard, L.H. Rasmussen, C. Gabel-Jensen, B. Steffansen, Estimating intestinal absorption of inorganic and organic selenium compounds by in vitro flux and biotransformation studies in Caco-2 cells and ICP-MS detection, Biol Trace Elem Res. 145 (2012) 248–256. https://doi.org/10.1007/S12011-011-9174-Y.

[143] K.T. Suzuki, Y. Shiobara, M. Itoh, M. Ohmichi, Selective uptake of selenite by red blood cells, in: Analyst, 1998. https://doi.org/10.1039/a706230c.

[144] Y. Shiobara, K.T. Suzuki, Binding of selenium (administered as selenite) to albumin after efflux from red blood cells, Journal of Chromatography B: Biomedical Applications. 710 (1998). https://doi.org/10.1016/S0378-4347(98)00142-X.

[145] X. Geng, J. McDermott, J. Lundgren, L. Liu, K.-J. Tsai, J. Shen, Z. Liu, Role of AQP9 in transport of monomethyselenic acid and selenite, BioMetals. 30 (2017) 747–755. https://doi.org/10.1007/s10534-017-0042-x.

[146] J.R. McDermott, X. Geng, L. Jiang, M. Gálvez-Peralta, F. Chen, D.W. Nebert, Z. Liu, Zinc- and bicarbonate-dependent ZIP8 transporter mediates selenite uptake, Oncotarget. 7 (2016) 35327–35340. https://doi.org/10.18632/oncotarget.9205.

[147] M.S. Ryu, G.J. Guthrie, A.B. Maki, T.B. Aydemir, R.J. Cousins, Proteomic analysis shows the upregulation of erythrocyte dematin in zinc-restricted human subjects, The American Journal of Clinical Nutrition. 95 (2012) 1096–1102. https://doi.org/10.3945/AJCN.111.032862.

[148] Y. Suzuki, Y. Hashiura, K. Matsumura, T. Matsukawa, A. Shinohara, N. Furuta, Dynamic pathways of selenium metabolism and excretion in mice under different selenium nutritional statuses, Metallomics. 2 (2010) 126–132. https://doi.org/10.1039/B915816B.

[149] C.M. Weekley, H.H. Harris, Which form is that? the importance of selenium speciation and metabolism in the prevention and treatment of disease, Chemical Society Reviews. 42 (2013) 8870–8894. https://doi.org/10.1039/c3cs60272a.

[150] D. Kuehnelt, D. Juresa, K.A. Francesconi, M. Fakih, M.E. Reid, Selenium metabolites in urine of cancer patients receiving L-selenomethionine at high doses, Toxicol Appl Pharmacol. 220 (2007) 211–215. https://doi.org/10.1016/J.TAAP.2007.01.005.

[151] A.L. Moxon, The effect of arsenic on the toxicity of seleniferous grains, Science (1979). 88 (1938) 81. https://doi.org/10.1126/science.88.2273.81.

[152] O.A. Levander, C.A. Baumann, Selenium metabolism. VI. Effect of arsenic on the excretion of selenium in the bile, Toxicology and Applied Pharmacology. (1966) 106–115. https://doi.org/10.1016/0041-008X(66)90035-4.

[153] J. Gailer, G.N. George, I.J. Pickering, R.C. Prince, S.C. Ringwald, J.E. Pemberton, R.S. Glass, H.S. Younis, D.W. DeYoung, H.V. Aposhian, A metabolic link between arsenite and selenite: The seleno-bis(S- glutathionyl) arsinium ion, J Am Chem Soc. (2000).

[154] J. Gailer, S. Madden, M.F. Burke, M.B. Denton, H. v Aposhian, Simultaneous multielement-specific detection of a novel glutathione–arsenic–selenium ion [(GS)2AsSe]− by ICP AES after micellar size- exclusion chromatography, Applied Organometallic Chemistry. 14 (2000) 355–363. https://doi.org/https://doi.org/10.1002/1099-0739(200007)14:7<355::AID-AOC8>3.0.CO;2-0.

[155] O. Ponomarenko, P.F. la Porte, S.P. Singh, G. Langan, D.E.B. Fleming, J.E. Spallholz, M. Alauddin, H. Ahsan, S. Ahmed, J. Gailer, G.N. George, I.J. Pickering, Selenium-mediated arsenic excretion in mammals: A synchrotron-based study of whole-body distribution and tissue-specific chemistry, Metallomics. 9 (2017) 1585–1595.

[156] I. Csanaky, Z. Gregus, Effect of selenite on the disposition of arsenate and arsenite in rats, Toxicology. 186 (2003) 33–50. https://doi.org/https://doi.org/10.1016/S0300-483X(02)00604-2.

[157] I.S. Palmer, C.W. Bonhorst, Selenium Poisoning, Modification of Selenite Metabolism by Arsenite, Journal of Agricultural and Food Chemistry. 5 (1957) 928–930. https://doi.org/10.1021/jf60082a004.

[158] S.A. Manley, G.N. George, I.J. Pickering, R.S. Glass, E.J. Prenner, R. Yamdagni, Q. Wu, J. Gailer, The Seleno Bis(S-glutathionyl) Arsinium Ion Is Assembled in Erythrocyte Lysate, Chemical Research in Toxicology. 19 (2006) 601–607. https://doi.org/10.1021/tx0503505.

[159] D.J. Thomas, Unraveling Arsenic—Glutathione Connections, Toxicological Sciences. 107 (2009) 309–311. https://doi.org/10.1093/toxsci/kfn257.

[160] I. Zwolak, H. Zaporowska, Selenium interactions and toxicity: A review, Cell Biology and Toxicology. (2012) 31–46. https://doi.org/10.1007/s10565-011-9203-9.

[161] H.E. Ganther, Reduction of the selenotrisulfide derivative of glutathione to a persulfide analog by gluthathione reductase, Biochemistry. 10 (1971) 4089–4098. https://doi.org/10.1021/bi00798a013.

[162] F.S. Walton, S.B. Waters, S.L. Jolley, E.L. LeCluyse, D.J. Thomas, M. Styblo, Selenium compounds modulate the activity of recombinant rat AsIII-methyltransferase and the methylation of arsenite by rat and human hepatocytes, Chemical Research in Toxicology. 16 (2003) 261–265.

[163] Y. Fukumoto, H. Yamada, K. Matsuhashi, W. Okada, Y.K. Tanaka, N. Suzuki, Y. Ogra, Production of a Urinary Selenium Metabolite, Trimethylselenonium, by Thiopurine S-Methyltransferase and Indolethylamine N-Methyltransferase, Chemical Research in Toxicology. 33 (2020) 2467–2474. https://doi.org/10.1021/ACS.CHEMRESTOX.0C00254/SUPPL_FILE/TX0C00254_SI_001.PDF .

[164] S.X. Liu, M. Athar, I. Lippai, C. Waldren, T.K. Hei, Induction of oxyradicals by arsenic: Implication for mechanism of genotoxicity, Proceedings of the National Academy of Sciences. 98 (2001) 1643–1648. https://doi.org/10.1073/pnas.98.4.1643.

[165] S.A. Joya, G. Mostofa, J. Yousuf, A. Islam, A. Elahi, G. Mahiuddin, M. Rahman, Q. Quamruzzaman, R. Wilson, One solution to the arsenic problem: a return to surface (improved dug) wells., J Health Popul Nutr. 24 (2006) 363–75.

[166] E.M. Hall, J. Acevedo, F.G. López, S. Cortés, C. Ferreccio, A.H. Smith, C.M. Steinmaus, Hypertension among adults exposed to drinking water arsenic in Northern Chile, Environmental Research. 153 (2017). https://doi.org/10.1016/j.envres.2016.11.016.

[167] C.M. Steinmaus, C. Ferreccio, J.A. Romo, Y. Yuan, S. Cortes, G. Marshall, L.E. Moore, J.R. Balmes, J. Liaw, T. Golden, A.H. Smith, Drinking water arsenic in northern chile: High cancer risks 40 years after exposure cessation, Cancer Epidemiology Biomarkers and Prevention. 22 (2013). https://doi.org/10.1158/1055-9965.EPI-12-1190.

[168] S. Sah, A. Vandenberg, J. Smits, Treating chronic arsenic toxicity with high selenium lentil diets, Toxicology and Applied Pharmacology. 272 (2013) 256–2662. https://doi.org/10.1016/j.taap.2013.06.008.

[169] Y.F. Li, W. Xiaoyan, W. Liming, L. Bai, G. Yuxi, C. Chunying, Direct quantitative speciation of selenium in selenium-enriched yeast and yeast-based products by X-ray absorption

spectroscopy confirmed by HPLC-ICP-MS, Journal of Analytical Atomic Spectrometry. 25 (2010) 426–430. https://doi.org/10.1039/B921570K.

[170] D. Thavarajah, A. Vandenberg, G.N. George, I.J. Pickering, Chemical form of selenium in naturally selenium-rich lentils (Lens culinaris L.) from Saskatchewan, Journal of Agricultural and Food Chemistry. 55 (2007) 7337–7341. https://doi.org/10.1021/jf070681i.

[171] A. Tarze, M. Dauplais, I. Grigoras, M. Lazard, N.T. Ha-Duong, F. Barbier, S. Blanquet, P. Plateau, Extracellular production of hydrogen selenide accounts for thiol-assisted toxicity of selenite against Saccharomyces cerevisiae, Journal of Biological Chemistry. 282 (2007) 8759–8767. https://doi.org/10.1074/jbc.M610078200.

[172] NCT01442727, Selenium in the Treatment of Arsenic Toxicity and Cancers, 2011.

[173] M. Alauddin, R. Cekovic, S. Alauddin, L. Bolevic, S. Saha, J.E. Spallholz, P.F. Laporte, S. Ahmed, H. Ahsan, J. Gailer, O. Ponomarenko, I.J. Pickering, S.P. Singh, G.N. George, Pharmacodynamic study of the selenium-mediated arsenic excretion in arsenicosis patients in Bangladesh, Environmental Arsenic in a ChangingWorld - 7th International Congress and Exhibition Arsenic in the Environment, 2018. 2 (2018) 391–394. https://doi.org/10.1201/9781351046633-152.

[174] L. Yang, W. Wang, S. Hou, P.J. Peterson, W.P. Williams, Effects of selenium supplementation on arsenism: An intervention trial in inner Mongolia, Environmental Geochemistry and Health. 24 (2002) 359–374.

[175] W.J. Verret, Y. Chen, A. Ahmed, T. Islam, F. Parvez, M.G. Kibriya, J.H. Graziano, H. Ahsan, A randomized, double-blind placebo-controlled trial evaluating the effects of vitamin E and selenium on arsenic-induced skin lesions in Bangladesh, Journal of Occupational and Environmental Medicine. 47 (2005) 1026–1035.

[176] J.E. Smits, R.M. Krohn, E. Akhtar, S.K. Hore, M. Yunus, A. Vandenberg, R. Raqib, Food as medicine: Selenium enriched lentils offer relief against chronic arsenic poisoning in Bangladesh, Environmental Research. 176 (2019). https://doi.org/10.1016/j.envres.2019.108561.

[177] B. Swift, N.D. Pfeifer, K.L.R. Brouwer, Sandwich-cultured hepatocytes: An in vitro model to evaluate hepatobiliary transporter-based drug interactions and hepatotoxicity, Drug Metabolism Reviews. 42 (2010) 446–471. https://doi.org/10.3109/03602530903491881.

[178] K.L.R. Brouwer, D. Keppler, K.A. Hoffmaster, D.A.J. Bow, Y. Cheng, Y. Lai, J.E. Palm, B. Stieger, R. Evers, In Vitro Methods to Support Transporter Evaluation in Drug Discovery and Development, Clinical Pharmacology & Therapeutics. 94 (2013). https://doi.org/10.1038/clpt.2013.81.

[179] P. Zhang, X. Tian, P. Chandra, K.L.R. Brouwer, Role of Glycosylation in Trafficking of Mrp2 in Sandwich-Cultured Rat Hepatocytes, Molecular Pharmacology. 67 (2005). https://doi.org/10.1124/mol.104.004481.

[180] G. Ghibellini, L.S. Vasist, E.M. Leslie, W.D. Heizer, R.J. Kowalsky, B.F. Calvo, K.L.R. Brouwer, In vitro-in vivo correlation of hepatobiliary drug clearance in humans, Clinical Pharmacology and Therapeutics. 81 (2007). https://doi.org/10.1038/sj.clpt.6100059.

[181] M.-J. Marion, O. Hantz, D. Durantel, The HepaRG Cell Line: Biological Properties and Relevance as a Tool for Cell Biology, Drug Metabolism, and Virology Studies, in: 2010. https://doi.org/10.1007/978-1-60761-688-7_13.

[182] P. Bachour-El Azzi, A. Sharanek, A. Burban, R. Li, R. le Guével, Z. Abdel-Razzak, B. Stieger, C. Guguen-Guillouzo, A. Guillouzo, Comparative localization and functional activity of the main hepatobiliary transporters in HepaRG cells and primary human hepatocytes, Toxicological Sciences. 145 (2015) 157–168. https://doi.org/10.1093/toxsci/kfv041.

[183] M. le Vee, E. Jigorel, D. Glaise, P. Gripon, C. Guguen-Guillouzo, O. Fardel, Functional expression of sinusoidal and canalicular hepatic drug transporters in the differentiated human hepatoma HepaRG cell line, European Journal of Pharmaceutical Sciences. 28 (2006) 109–117. https://doi.org/10.1016/j.ejps.2006.01.004.

[184] J.R. Wiśniewski, A. Vildhede, A. Norén, P. Artursson, In-depth quantitative analysis and comparison of the human hepatocyte and hepatoma cell line HepG2 proteomes, J Proteomics. 136 (2016) 234–247. https://doi.org/10.1016/J.JPROT.2016.01.016.

[185] P.D. Petrov, M.L. Fernández-Murga, M. López-Riera, M.J. Goméz-Lechón, J. v. Castell, R. Jover, Predicting drug-induced cholestasis: preclinical models, Expert Opinion on Drug

Metabolism and Toxicology. 14 (2018) 721–738. https://doi.org/10.1080/17425255.2018.1487399.

[186] B. Whitlock, Arsenic Cellular Handling by Human Multidrug Resistance Protein 1 (MRP1/ABCC1) and MRP4 (ABCC4), 2021.

[187] T.K. Kim, J.H. Eberwine, Mammalian cell transfection: the present and the future, Analytical and Bioanalytical Chemistry. 397 (2010) 3173. https://doi.org/10.1007/S00216-010-3821-6.

[188] T. Bansal, M. Jaggi, R.K. Khar, S. Talegaonkar, Emerging significance of flavonoids as P-glycoprotein inhibitors in cancer chemotherapy., Journal of Pharmacy & Pharmaceutical Sciences : A Publication of the Canadian Society for Pharmaceutical Sciences, Societe Canadienne Des Sciences Pharmaceutiques. 12 (2009) 46–78. https://doi.org/10.18433/j3rc77.

[189] D.W. Loe, K.C. Almquist, R.G. Deeley, S.P.C. Cole, Multidrug Resistance Protein (MRP)-mediated Transport of Leukotriene C4 and Chemotherapeutic Agents in Membrane Vesicles, Journal of Biological Chemistry. 271 (1996). https://doi.org/10.1074/jbc.271.16.9675.

[190] D.W. Loe, K.C. Almquist, S.P.C. Cole, R.G. Deeley, ATP-dependent 17β-Estradiol 17-(β-D-Glucuronide) Transport by Multidrug Resistance Protein (MRP), Journal of Biological Chemistry. 271 (1996). https://doi.org/10.1074/jbc.271.16.9683.

[191] R.M. Krohn, R. Raqib, E. Akhtar, A. Vandenberg, J.E.G. Smits, A high-selenium lentil dietary intervention in Bangladesh to counteract arsenic toxicity: Study protocol for a randomized controlled trial, Trials. 17 (2016). https://doi.org/10.1186/s13063-016-1344-y.

[192] J. Gailer, G.N. George, I.J. Pickering, R.C. Prince, H.S. Younis, J.J. Winzerling, Biliary excretion of [(GS)2AsSe]- after intravenous injection of rabbits with arsenite and selenate, Chemical Research in Toxicology. 15 (2002) 1466–1471. https://doi.org/10.1021/tx025538s.

[193] G.N. George, J. Gailer, O. Ponomarenko, P.F. la Porte, K. Strait, M. Alauddin, H. Ahsan, S. Ahmed, J. Spallholz, I.J. Pickering, Observation of the seleno bis-(S-glutathionyl) arsinium

anion in rat bile, Journal of Inorganic Biochemistry. 158 (2016) 24–29. https://doi.org/https://doi.org/10.1016/j.jinorgbio.2016.01.022.

[194] P. Ghosh, A. Basu, J. Mahata, S. Basu, M. Sengupta, J.K. Das, A. Mukherjee, A.K. Sarkar, L. Mondal, K. Ray, A.K. Giri, Cytogenetic damage and genetic variants in the individuals susceptible to arsenic-induced cancer through drinking water, International Journal of Cancer. 118 (2006) 2470–2478. https://doi.org/10.1002/ijc.21640.

2. Biliary Excretion of Arsenic by Human HepaRG Cells is Stimulated by Selenide and Mediated by the Multidrug Resistance Protein 2 (MRP2/ABCC2)*

* A version of this thesis chapter has been published: Janet R. Zhou, Gurnit Kaur, Yingze Ma, Denis Arutyunov, Xiufen Lu, X. Chris Le, and Elaine M. Leslie., Biliary Excretion of Arsenic by Human HepaRG Cells is Stimulated by Selenide and Mediated by the Multidrug Resistance Protein 2 (MRP2/ABCC2). *Biochem. Pharmacol*. 2021;193:114799 https://doi.org/10.1016/j.bcp.2021.114799

2.1 Introduction

Inorganic arsenic is classified as a Group I (proven) human carcinogen by the International Agency for Research on Cancer [1]. Chronic arsenic exposure causes lung, skin, and bladder cancer, and is associated with a myriad of other adverse health outcomes including other cancers (kidney, liver, and prostate), and cardiovascular disease [1,2]. Humans remain susceptible to arsenic-induced diseases for decades following cessation of chronic exposure [3]. Conservative estimates suggest that 92-220 million people worldwide are exposed to arsenic at levels exceeding the World Health Organization guideline of 10 µg/L through contaminated drinking water [4,5], making it a major global public health concern.

Arsenic is naturally found in the environment in the inorganic forms arsenate and arsenite. Cellular uptake of arsenate (a mixture of predominantly $H_2AsO_4^-$ and $HAsO_4^{2-}$ at pH 7) is mediated by sodium-dependent phosphate transporters such as the Na^+/P_i cotransporter type IIb (gene symbol, *SLC34A2*) [6,7]. Arsenite ($As(OH)_3$ at pH 7) uptake can occur through aquaglyceroporins (AQPs) and facilitative glucose transporters (GLUTs/*SLC2A*s) [8]. After uptake, arsenic methylation can occur, catalyzed by a series of oxidative methylation reactions by arsenic (+3 oxidation state) methyltransferase (As3MT), which results in the formation of monomethylarsonic acid (MMA^V), monomethylarsonous acid (MMA^{III}), dimethylarsinic acid (DMA^V) and dimethylarsinous acid (DMA^{III}) [9,10]. Arsenite, MMA^{III} and DMA^{III} can form glutathione conjugates [($As(GS)_3$), $MMA(GS)_2$ and DMA(GS)], but only $As(GS)_3$ and $MMA(GS)_2$ have been detected in biological samples [11,12]. In the liver, ATP-binding cassette (ABC) transporters multidrug resistance proteins 2 (MRP2/*ABCC2*) and MRP4 (*ABCC4*) are thought to be important for canalicular and sinusoidal efflux, respectively, of arsenic metabolites [13–15].

Furthermore, sandwich cultured primary human hepatocytes (SCHH) exhibit hepatobiliary transport of arsenic with characteristics consistent with MRP4- and MRP2-mediated sinusoidal and canalicular transport, respectively [14].

Selenium is an essential trace nutrient that is an important component of many antioxidants and other enzymes with important biological functions [16]. Selenium has a recommended dietary allowance of 55 μg/day, but is toxic in excess with an upper tolerable limit of 400 μg/day [17]. Interestingly, a mutually protective relationship between arsenic and selenium has been observed. A molecular basis for mutual detoxification is the formation and biliary excretion of the seleno-bis (*S*-glutathionyl) arsinium ion ($[(GS)_2AsSe]^-$), which was first detected in the bile of rabbits co-injected with arsenite and selenite, and has also been found in rats and hamsters [18–21]. When these lab animals were given toxic doses of arsenite and selenite, the ability of these compounds to induce liver damage was reduced, relative to when dosed individually [18–20,22,23]. Furthermore, skin lesions, a hallmark symptom of chronic arsenic exposure have been observed at a higher frequency in selenium-deficient than selenium-replete people [24]. In addition to the biliary excretion of $[(GS)_2AsSe]^-$, this conjugate is formed and sequestered in laboratory animal and human red blood cells, slowing and/or preventing the distribution of arsenic and selenium to tissues [13,25–29].

In arsenic-endemic regions, there have been selenium-supplementation trials where participants are given selenium-enriched yeast or lentils comprised predominantly of selenomethionine (SeMet) [30–34]. Purified SeMet has also been given [35]. Methylselenocysteine (MeSeCys) is another selenium compound shown to have anti-cancer effects *in vitro* [36]. Selenite, which is rapidly converted to selenide in the presence of

glutathione within cells [37], has also been used in selenium-supplementation trials [38,39]. Despite these trials, little is understood about the influence of selenium on human hepatic handling of arsenic. Furthermore, the impact of the chemical species of selenium on the efficacy of supplementation is unknown.

When arsenic hepatobiliary transport was studied using the SCHH model, biliary excretion of arsenic only occurred in 36% of preparations, due to donor-to-donor variability [14]. The mutually protective relationship between arsenic and selenium was recently studied in human HepG2 cells, and it was found that selenide was more protective than selenite [40]. Several studies have shown that selenide is taken up by cells more efficiently than selenite, potentially allowing for more mutual protection to occur [40–42]. However, HepG2 cells in monolayer culture do not form canalicular networks and are not a suitable model for exploring polarized transport [43]. The immortalized human HepaRG cells differentiate into hepatocyte and cholangiocyte-like cells, form extensive canalicular networks, and are considered an excellent surrogate for primary human hepatocytes without donor-to-donor variability. The objectives of this study were to first establish the HepaRG cell line as a model of arsenic hepatobiliary transport and then to utilize them to study the influence of various chemical forms of selenium on arsenic biliary excretion. Our overall hypothesis was that selenium would stimulate biliary excretion of arsenic[†].

[†] Project was led by Dr. Elaine M. Leslie in collaboration with Dr. X. Chris Le at the University of Alberta

2.2 Materials and Methods[‡]

2.2.1 Chemicals and Reagents

^{73}As-arsenate (> 5.6 Ci/mg) was purchased from Los Alamos Meson Production Facility (Los Alamos, NM). ^{75}Se-selenite (0.296 Ci/mg) was obtained from the University of Missouri Research Reactor (MURR, Columbia, MO)[§]. ^{3}H(G)-Taurocholic acid (5.0 Ci/mmol) was purchased from PerkinElmer Life and Analytical Sciences (Woodbridge, ON). Sodium selenite, sodium(meta) arsenite, MeSeCys, bovine serum albumin (BSA), reduced glutathione (GSH), poly-L-lysine solution, William's E media, dimethyl sulfoxide (DMSO), hydrocortisone 21-hemisucccinate sodium salt, fetal bovine serum (FBS), sodium taurocholate, standard Hanks' balanced salt solution (HBSS), Ca^{2+}/Mg^{2+}-free HBSS, MK571, oltipraz, buthionine sulfoximine (BSO), sodium bicarbonate ($NaHCO_3$), 5(6)-Carboxy-2',7'-dichlorofluorescein (CDF) diacetate, ethylene glycol-bis-(β-aminoethyl ether)-N,N,N',N'-tetraacetic acid (EGTA), Immobilon Crescendo Western HRP substrate, and puromycin dihydrochloride were purchased from MilliporeSigma (Oakville, ON, Canada). The MISSION® shRNA plasmid DNA glycerol stocks of TRC2 pLKO.5-puro empty vector control plasmid, pLKO.5-puro non-mammalian shRNA control plasmid (non-target), and *ABCC2* KD clones targeting the coding sequence of *ABCC2* TRCN#0000059307 (NM_000392.1-624s1c1) (9307) and TRCN#0000289640 (NM_000392.1-4097s1c1) (9640) were also purchased from Millipore Sigma (Oakville, ON, Canada). Sodium selenide was purchased from Alfa Aesar (Ward Hill, MA). Triton X-100 was purchased from Fisher Scientific (Fair Lawn, NJ). GlutaMAX supplement, human recombinant insulin and

[‡] Janet R. Zhou initiated all experiments with training from Dr. Gurnit Kaur

[§] The isotopes (^{73}As and ^{75}Se) used in this research were supplied by the United States Department of Energy Office of Science by the Isotope Program in the Office of Nuclear Physics.

Pierce™ bicinchoninic acid (BCA) protein assay reagent were purchased from Thermo Scientific (Rockford, IL). SeMet was purchased from BioVision (Miltipas, CA). The cytotoxicity detection kit (LDH) and X-tremeGENE9 transfection reagent were purchased from Roche, Applied Sciences (Indianapolis, IN). The tetrazolium based CellTiter96® Aqueous Non-Radioactive Cell Proliferation Assay was purchased from Promega (Madison, MI).

2.2.2 Antibodies

The MRP2 specific mouse monoclonal antibody (M_2I-4) was purchased from EMD Millipore (Billerica, MA). The MRP4 specific rat monoclonal antibody (M_4I-10) was purchased from Abcam Inc. (Cambridge, MA). The Na^+/K^+-ATPase mouse monoclonal (H-3/SC-48345) was purchased from Santa Cruz Biotechnology (Dallas, TX). The IgG (H+L) cross-adsorbed goat anti-mouse and anti-rat HRP conjugated polyclonal secondary antibodies were purchased from ThermoFisher Scientific (Waltham, MA).

2.2.3 Preparation of reagents

Arsenite, selenite, SeMet, MeSeCys, and sodium taurocholate were freshly prepared for all experiments by dissolving in sterile phosphate buffered saline (PBS) before serial dilutions of each compound in growth media for immediate use. Solutions containing selenide in the form Na_2Se were prepared by weighing Na_2Se under nitrogen gas, and then immediately dissolving in 33 mg/mL BSA in degassed PBS, followed by serial dilutions in growth media for immediate use.

^{73}As-arsenite was reduced from ^{73}As-arsenate with metabisulfite-thiosulfate reducing agent, as previously described [44]. ^{75}Se-selenide was reduced from ^{75}Se-selenite by incubating ^{75}Se-selenite with GSH at a molar ratio of at least 1:550 at room temperature for 20 min, as previously described [42]. Stock solutions of oltipraz, CDFDA and MK571 were prepared in

DMSO prior to preparation of final desired concentration in growth media, with a maximum final 0.5% DMSO.

2.2.4 HepaRG cell culture

HepaRG cells were obtained from Biopredic International at passage 12 (St Gregoire, France). A working bank in liquid N_2 was then established according to the instructions provided by Biopredic International[¤]. For all experiments, HepaRG cells were used between passages 15-18. HepaRG cells were first seeded from frozen vials at a density of $2x10^6$ cells/T-75 flasks and maintained in growth media comprised of Williams' E medium supplemented with 10% fetal bovine serum, 5 µg/ml human recombinant insulin, 50 µM hydrocortisone hemisuccinate, and 200 mM Glutamax™, as established previously [45]. After 2 weeks, HepaRG cells were seeded into 6, 24, or 96-well plates, or T-25 flasks at densities of 200 000, 55 000, 9 000, or 500 000 cells/well or flask, respectively. HepaRG cells were maintained in growth media for 2 weeks, then differentiated by including 0.75% dimethylsulfoxide (DMSO) in growth media for 2 days, followed by 1.5% DMSO for 12 to 40 days. All experiments were performed up to 4 weeks following the end of the 2-week differentiation period, as previously described [46]. HepaRG cells were maintained at 37°C in a humidified incubator with 95% air/5% CO_2 with media changes every 2-3 days.

[¤] Dr. Christiane Guguen-Guillouzo, Dr. Philippe Gripon, Dr. Christian Trepo, and Biopredic International© are thanked for supplying the undifferentiated cryopreserved HepaRG cells. Diane Swanlund is thanked for providing outstanding technical assistance and establishing the HepaRG cell line working bank.

2.2.5 Efflux Studies

Fully differentiated HepaRG cells in 24-well plates were incubated in fresh growth media containing [^{3}H(G)]-taurocholate (1 µM, 100 nCi) for 20 min. B-CLEAR® technology (BioIVT) was used to determine the canalicular vs sinusoidal efflux of taurocholate, thus, cells were washed twice with either standard ice-cold HBSS, or Ca^{2+}/Mg^{2+}-free HBSS (with 1 mM EGTA), then 0.5 mL of 37°C standard HBSS or Ca^{2+}/Mg^{2+}-free HBSS was added to each well. Under the Ca^{2+}-containing condition (standard HBSS), tight junctions remain intact, allowing only sinusoidal efflux. Under the Ca^{2+}/Mg^{2+}-free condition, the tight junctions that seal the canalicular networks are disrupted and allow for both sinusoidal and canalicular efflux [47]. Plates were incubated at 37°C and at indicated time points, 50 µL of buffer was removed and placed in a scintillation vial. After the last time point, HepaRG cells were washed twice with their respective ice-cold HBSS buffers and lysed in 250 µL 0.5% Triton X-100. [^{3}H(G)]-taurocholate in 50 µL of efflux buffer was quantified using liquid scintillation counting with the PerkinElmer MicroBeta^{2} liquid scintillation counter. Efflux activity was normalized to total protein levels of cell lysates, determined using a BCA assay.

Arsenic efflux was evaluated in the same manner as described for taurocholate efflux, except HepaRG cells were treated with growth media containing ^{73}As-arsenite (1 µM, 100 nCi/well) ± Se (1 µM as selenide, selenite, SeMet or MeSeCys) for 1 hr prior to measuring efflux across sinusoidal and canalicular membranes. To determine the influence of GSH on arsenic efflux, HepaRG cells were treated with the GSH synthesis inhibitor, BSO (500 µM) for 48 hr prior to and during efflux experiments. Total GSH levels in untreated and BSO-treated HepaRG cells were quantified as previously described [48], and corrected to protein levels determined using

a BCA assay. To determine the influence of the general MRP-inhibitor MK571 (100 µM) on arsenic efflux, HepaRG cells were treated with MK571 for 30 min prior to initiation and during efflux. To determine if biliary excretion of arsenic was temperature-dependent, efflux was completed with HepaRG cells on ice for the duration of the assay.

Selenium efflux was evaluated in the same way as arsenic, except HepaRG cells were treated with growth media containing ^{75}Se-selenite (1 µM, 100 nCi/well) ± arsenite, or ^{75}Se-selenide (1 µM, 100 nCi/well) ± arsenite (1 µM) prior to measuring efflux across sinusoidal and canalicular membranes and ^{75}Se radioactivity was quantified with the Packard Cobra II gamma counter.

To determine the extent of biliary excretion of taurocholate, arsenic, and selenium, a biliary excretion index (BEI) was calculated, as described [47], with the following formula:

$$\text{Biliary Excretion Index (\%)} = \frac{\text{Efflux}_{\text{Canalicular + Sinsuoidal}} - \text{Efflux}_{\text{Sinusoidal}}}{\text{Efflux}_{\text{Canalicular + Sinusoidal}}} \text{ x } 100$$

After efflux, the release of lactate dehydrogenase (LDH) from cells was quantified using the Cytotoxicity Detection Kit (Roche, Mississauga ON), as previously described [14,49]. Efflux data with >5% LDH release at the 10 min time point was considered unacceptable and omitted. This prevented the inclusion of data from cellular leakage instead of efflux.

2.2.6 Fluorescence microscopy[ø]

HepaRG cells were seeded on poly-L-lysine coated glass coverslips in 6-well plates, grown and differentiated as described above. HepaRG cells were then either untreated, treated

[ø] Drs. Vladmir Rancic and Klaus Ballanyi are thanked for providing assistance with the Olympus IX81 fluorescence microscope. Midhat Rizvi and Dr. Emmanuelle Cordat are thanked for providing assistance with the Olympus BX51 fluorescence microscope.

with 1 µM arsenite, or 1 µM Se (selenide, selenite, SeMet, or MeSeCys) ± 1 µM arsenite in growth media (lacking DMSO) for 24 hr. CDF accumulation in cells and canalicular networks were then determined as described [50,51]. Briefly, cells were washed three times in 1 mL ice-cold standard HBSS and treated with 5(6)-carboxy-2',7'-dichlorofluorescein diacetate (CDFDA, 2 µM) in standard HBSS for 10 min at 37°C. The influence of MK571 on CDF accumulation was evaluated by incubating with MK571 (100 µM) and CDFDA (2 µM) for 30 min at 37°C. HepaRG cells were washed three times with 1 mL ice-cold standard HBSS and imaged using a fluorescence microscope (Olympus, IX81 or Olympus BX51, Olympus Canada, Richmond Hill, Ontario).

2.2.7 Evaluation of *ABCC2*, *ABCC4* and *As3MT* gene expression

RNA was isolated from HepaRG cells, and a randomly primed cDNA library was generated as previously described [52]. Primers, specific to regions including the coding sequence and adjacent to the coding sequences, were used to amplify *ABCC2, ABCC4* and *As3MT*. An agarose gel (1%) was used to evaluate for the presence of PCR products. Sanger DNA sequencing of purified PCR products was performed by the Molecular Biology Service Unit (Dept. Biological Sciences, University of Alberta) and also by The Applied Genomics Core (Faculty of Medicine and Dentistry, University of Alberta)[℘].

2.2.8 Crude membrane preparation and immunoblotting [τ]

HepaRG cells were grown in T-25 flasks and differentiated as described above. Cells were then either untreated, treated with 0.5 µM or 1 µM arsenite, 1 µM Se (selenide, selenite

---

℘ Dr. Denis Arutyunov completed the gene sequencing.

τ Yingze Ma assisted with technical replicates for crude membrane preparation and immunoblotting.

SeMet, or MeSeCys) in the presence or absence of 1 µM arsenite, or 50 µM oltipraz in DMSO-free growth media for 48 hr. Crude membranes were prepared as previously described [53], and 10 µg protein subjected to SDS-PAGE (6%) and transferred to a polyvinylidene fluoride (PVDF) membrane. Immunoblotting of the PVDF membrane was performed using the MRP2-specific monoclonal mouse antibody M_2I-4 (1:1000) and the MRP4-specific monoclonal rat antibody M_4I-10 (1:2000). A Na^+/K^+-ATPase monoclonal mouse antibody (H-3) (1:30 000) was used to detect the Na^+/K^+-ATPase as a sample loading control. Secondary anti-rat (1:5000) and anti-mouse antibodies (1:10 000) were HRP-conjugated (1:10 000). All antibodies were prepared in 4% skim milk. Membranes were imaged using ChemiDoc™ (BioRad) after addition of Immobilon Crescendo Western HRP substrate. Relative protein levels of MRP2 and MRP4 were quantified using ImageJ software normalized against the Na^+/K^+-ATPase signal. Levels of MRP2 and MRP4 were reported relative to untreated HepaRG cells.

2.2.9 Cytotoxicity studies

HepaRG cells were seeded into 96-well plates, maintained, and differentiated as described above. Fully differentiated HepaRG cells were then treated with growth media containing arsenite and Se compounds (selenide, selenite, SeMet or MeSeCys) individually, or together at equimolar concentrations (1-3000 µM) in quadruplicate for 48 hr. Cell viability was determined using the tetrazolium-salt based CellTiter96® Aqueous Non-Radioactive Cell Proliferation Assay from Promega (Madison, MI). EC_{50} values were determined using the sigmoidal dose response fit (GraphPad Prism 8).

To assess toxicity of different arsenic and selenium concentration combinations, HepaRG cells were treated with growth media containing arsenite and Se compounds (selenide

or selenite) (1 – 3000 µM) in triplicate[¶]. This resulted in each concentration of arsenite being paired with every concentration of Se, resulting in 81 different treatment combinations over nine different concentrations. Cytotoxicity data were analyzed using the Combenefit software [54] as previously described [40]. In brief, the Loewe, Bliss and Highest Single Agent mathematical models were used to analyze cytotoxicity data. The synergistic and antagonist effect of arsenite and Se were quantified using a summary metric value for synergy and antagonism (SUM_SYN_ANT), with a negative value suggesting antagonism of toxicity and a positive value suggesting synergy of toxicity.

2.2.10 Selenium and arsenic accumulation studies[ɜ]

HepaRG cells were seeded in 24-well plates, grown, and differentiated as described above. Fully differentiated HepaRG cells were then treated with growth media containing ^{73}As-arsenite (1 µM, 100 nCi/well), ^{75}Se-selenite (1 µM, 100 nCi/well) or ^{75}Se-selenide (1 µM, 100 nCi/well). Cells were then washed three times with 500 µL ice cold PBS and lysed in 250 µL 0.5% Triton X-100 at the indicated time points. Lysate (125 µL) was transferred into scintillation vials for ^{73}As-arsenic and ^{75}Se-selenide/selenite accumulation quantification. Accumulation of ^{73}As-arsenite was measured with the PerkinElmer MicroBeta^2 liquid scintillation counter, and accumulation of ^{75}Se-selenide/selenite was measured with the Packard Cobra II gamma counter. A BCA assay was performed to normalize accumulation to total protein concentration for each sample.

[¶] Yingze Ma assisted with these cytotoxicity assays
[ɜ] Dr. Gurnit Kaur assisted with a technical replicate

2.2.11 High-performance liquid chromatography-inductively coupled plasma mass spectrometry analysis of arsenic methylation in HepaRG cells [Ψ]

Fully differentiated HepaRG cells in 6-well plates were treated with growth media (no DMSO) containing 1 µM Se (selenite or selenide) ± 1 µM arsenite for 24 hr. After 24 hr, this media was collected and stored at -80°C until analysis. The HepaRG cells were washed three times with ice cold growth media and then 37°C growth media was added. The plates were incubated for 1 hr, allowing efflux of arsenic metabolites to occur. After 1 hr, the efflux media was collected and immediately placed at -80°C until analysis.

An Agilent 1100 series high-performance liquid chromatography (HPLC) system, consisting of a pump, degasser, autosampler, column temperature control, and reverse-phased C_{18} column (ODS-3, 150 mm x 4.6 mm, 3 µM particle size; Phenomenex, Torrance, CA), was used for separation of arsenicals. The column was equilibrated with the mobile phase, consisting of 5 mM tetrabutylammonium, 5% methanol, and 3 mM malonic acid (pH 5.85), for at least 0.5 hr before sample injection. The flow rate of the mobile phase was 1.2 ml/min. The injection volume of samples and standards was 50 µL. The column temperature was maintained at 50°C. The effluent from the HPLC column was directly introduced into the nebulizer of a 7500ce inductively coupled plasma mass spectrometer (ICP-MS) (Agilent Technologies, Japan) using a PEEK tubing. The collision cell of the ICP-MS instrument was operated in helium mode. Helium at a flow rate of 3.5 ml/min was introduced to the octopole reaction cell to reduce isobaric and polyatomic interferences. The ICP was operated at a radio-frequency power of 1550 W, and the flow rate of argon carrier gas was 0.9-1.0 L/min. Arsenic was monitored at *m/z*

[Ψ] Xiufen Lu and Dr. X. Chris Le performed the ICP-MS data acquisition and analysis

75. Chromatograms from HPLC separation with ICP-MS detection were recorded and analyzed using the ChemStation software (Agilent Technologies, Santa Clara, CA). Peak areas from the analysis of samples were calibrated against those of arsenic standards to obtain concentrations of individual arsenic species in the samples. Certified reference material #18 "Human Urine" was used for quality control. The measured concentrations were in good agreement with the certified values.

2.2.12 shRNA knockdown of *ABCC2* in HepaRG cells

HepaRG cells were seeded into 6-well plates at 2 x 10^5 cells/well and transfected with shRNA targeting the MRP2 gene *ABCC2* (1 µg) with DNA:XtremeGENE 9 (3 µl) as per manufacturer's instructions. HepaRG cells were also separately transfected with the empty vector (EV), PLKO.5-puro and non-target (pLKO.5-puro non-mammalian shRNA) as negative controls. Cells were selected 72 hr post-transfection and maintained as described above, with the addition of 2 µg/ml puromycin. After the two-weeks of selection (corresponding to the usual proliferation phase), cells were trypsinized and seeded in appropriate plates at the appropriate cell density for proliferation/differentiation for characterization by immunoblot, fluorescence microscopy and efflux studies, as described above. Cells were maintained in media containing 2µg/ml puromycin except this was reduced to 1 µg/ml during the differentiation period and experiments.

2.2.13 Whole cell lysate preparations of MRP2 knockdown HepaRG cells

Fully differentiated parental HepaRG cells, as well as HepaRG cells expressing empty vector, non-target or *ABCC2*-targeted shRNA maintained in 6-well plates were lysed in 100 µL of

0.5% Triton X-100 containing protease inhibitors. Protein concentrations were determined using a BCA assay.

2.2.14 Selection of arsenic and selenium concentrations for experiments

Chronic arsenic exposure in humans has been reported to result in blood total arsenic levels of 0.01-0.8 µM, generally with means of 10-100 nM in those exposed to 10-100 µg/L of arsenic in water [24]. Mean blood total selenium levels can range from ~1.6-4 µM depending on population and diet [24]. Therefore, the concentration of 1 µM was selected for all experiments, with the exception of cytotoxicity studies, where higher concentrations were used in order to achieve accurate EC_{50} values.

2.2.15 Data analysis and statistics

For efflux studies, a BEI was calculated if there was a significant difference between canalicular and sinusoidal efflux for each condition (determined with a Student's t-test). A Student's t-test was used to determine if there was significant difference between BEI values. A one-way ANOVA followed by Dunnett's post hoc test was used to determine if there were statistical differences in densitometry data. An alpha value of <0.05 was used to define significance.

Cytotoxicity assays were analyzed using the GraphPad Prism 8 software and EC_{50} values were determined using the sigmoidal dose response fit. Significant differences between EC_{50} values were determined using a one-way ANOVA followed by Tukey's post hoc test. Data from cytotoxicity assays comparing combinations of concentrations of arsenic and selenium were analyzed using the Combenefit software and synergy distribution plots were determined using the Lowe additivity synergy model [54]. Significant differences in selenium accumulation time

courses were determined using linear regression. To determine if there was a difference between GSH levels in untreated HepaRG cells and BSO-treated HepaRG cells, a Student's t-test was used.

2.3 Results

2.3.1 Taurocholate and CDF undergo biliary excretion by HepaRG cells

In order to ensure that HepaRG cells were functioning properly under the conditions used in our laboratory, several control experiments were completed. The bile acid taurocholate undergoes extensive biliary excretion [46], and is commonly used to assess the formation and integrity of canalicular networks. In the presence of calcium, tight junctions that seal canalicular networks remain fully intact, allowing for measurement of efflux across the sinusoidal membranes of hepatocytes. When calcium is removed, the tight junctions are disrupted, allowing for measurement of efflux across canalicular and sinusoidal membranes [47]. Therefore, a significant difference in these conditions suggest there is biliary excretion of the substrate. As expected, significantly greater efflux of taurocholate across the canalicular plus sinusoidal membranes, compared to the sinusoidal membranes alone was observed, with a BEI of 27 ± 7% **(Fig 2.1A)**, which is similar to findings from other studies using this cell line [46,55].

Fully differentiated HepaRG cells were treated with the diacetate form of CDF **(Fig 2.1B)** as a positive control for both canalicular network formation and MRP2 function. CDF is transported by MRP2 into the canalicular networks [51] and can be visualized with fluorescence microscopy. CDF was accumulated within canalicular networks, suggesting that canalicular networks have formed and MRP2 was functional **(Fig 2.1B)**. Treatment with MK571, an LTD_4 receptor

antagonist and general MRP inhibitor [56], resulted in a loss of CDF accumulation in the canalicular networks **(Fig 2.1C)**, consistent with findings from other studies [14,46,56]

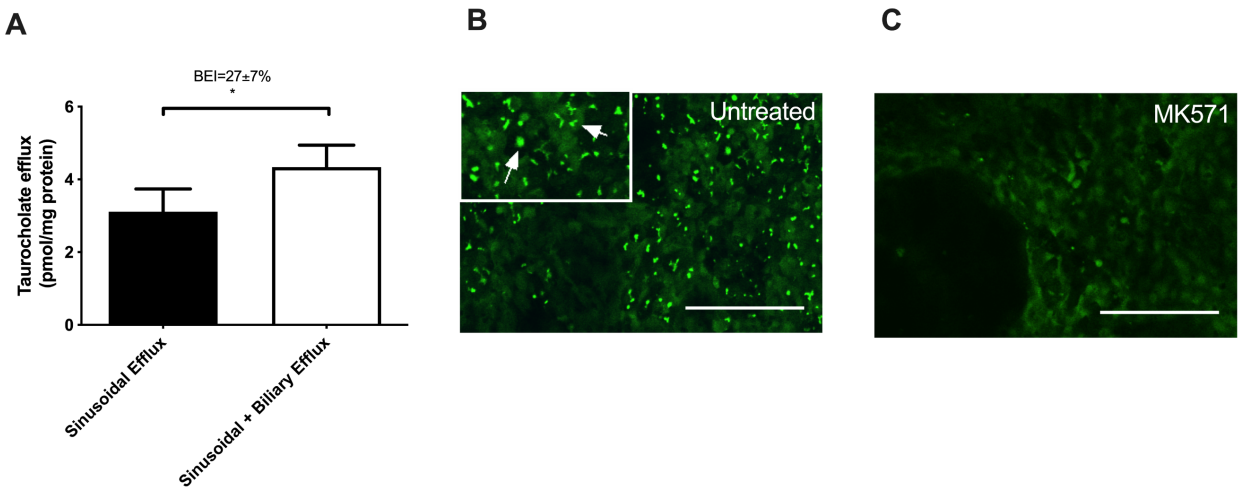

Figure 2.1: Characterization of canalicular network formation and integrity through the measurement of taurocholate biliary excretion and CDF accumulation. (A) HepaRG cells were treated with media containing ^{3}H(G)-Taurocholic acid (1 µM, 100 nCi) for 20 min. Incubation media was washed off and replaced with standard HBSS (closed bar) or Ca^{2+}/Mg^{2+}-free HBSS (with 1 mM EGTA) (open bar) at 37℃ and taurocholate efflux was measured at a 10 min time point. Bars represent means ± SD of five independent experiments. The significant difference between sinusoidal and sinusoidal and canalicular efflux is indicated with * $P < 0.05$ (Student's t-test) **(B and C)** cells were treated with the diacetate form of CDF (2 µM) at 37℃ for 10 min. CDF accumulation in canalicular networks was viewed with a fluorescence microscope and is indicated with arrows in (**B inset**, 200X magnification). **(C)** Cells were treated as in **(B)** but in the presence of MK571 (100 µM). **(B)** and **(C)** are at 100X magnification and scale bars represent 100 µm.

2.3.2 *ABCC2, ABCC4* and *As3MT* are expressed in HepaRG cells

MRP2, MRP4 and As3MT are important for arsenic hepatobiliary transport and metabolism, so it was determined if the genes that encode for these proteins are expressed in HepaRG cells. RNA was isolated from the cells and a randomly primed cDNA library was generated. Primers were designed to amplify *ABCC2, ABCC4* and *As3MT*, and PCR products were detected on a 1% agarose gel. Results showed that *ABCC2, ABCC4* and *As3MT* are expressed in HepaRG cells. Sequencing of the genes revealed the presence of previously reported heterozygous *ABCC2* (NM_000392) single nucleotide polymorphisms -24C>T, 1249G>A (V417I), and 3972C>T (I1324I)

(consistent with Biopredic International Certificate of Analysis). *ABCC4* (NM_005845.4) and *As3MT* (NM_020682.4) sequences were consistent with their respective reference sequences.

2.3.3 Arsenic increases MRP2 and MRP4 protein levels in HepaRG cells

To investigate whether MRP2 and MRP4 were found at the protein level in HepaRG cells, crude membrane preparations and immunoblots were completed. MRP2 and MRP4 were both detected in untreated HepaRG cells **(Fig 2.2).** MRP2 levels were significantly increased by 2.6-fold after a 48 hr treatment with 0.5 µM arsenite as well as 1 µM arsenite **(Fig 2.2A and C).** MRP4 levels were significantly increased by 2-fold after a 48 hr treatment with 1 µM arsenite **(Fig 2.2B and D).** No significant increases in MRP2 or MRP4 level were observed after treatment of cells with selenite, selenide, or either of these selenium compounds in combination with arsenite **(Fig 2.2).** Oltipraz is an Nrf2 activator and has been shown to upregulate expression of MRP2 and MRP4 in human hepatocytes [14,57,58]. As expected, a 48 hr treatment with 50 µM oltipraz resulted in a 5.7-fold increase in MRP2 levels but surprisingly, no significant increase in MRP4 levels **(Fig 2.2C and D).** The 5'UTR remains to be sequenced for *ABCC4* (NM_005845.4), therefore it is possible that a single nucleotide polymorphism exists in this region that would prevent upregulation of Nrf2 by Oltipraz. Previous studies performed by our laboratory using SCHH have resulted in increased MRP4 levels after treatment with Oltipraz [14]. Perhaps a wider range of exposure times and concentrations of Oltipraz could be tested in the future as well.

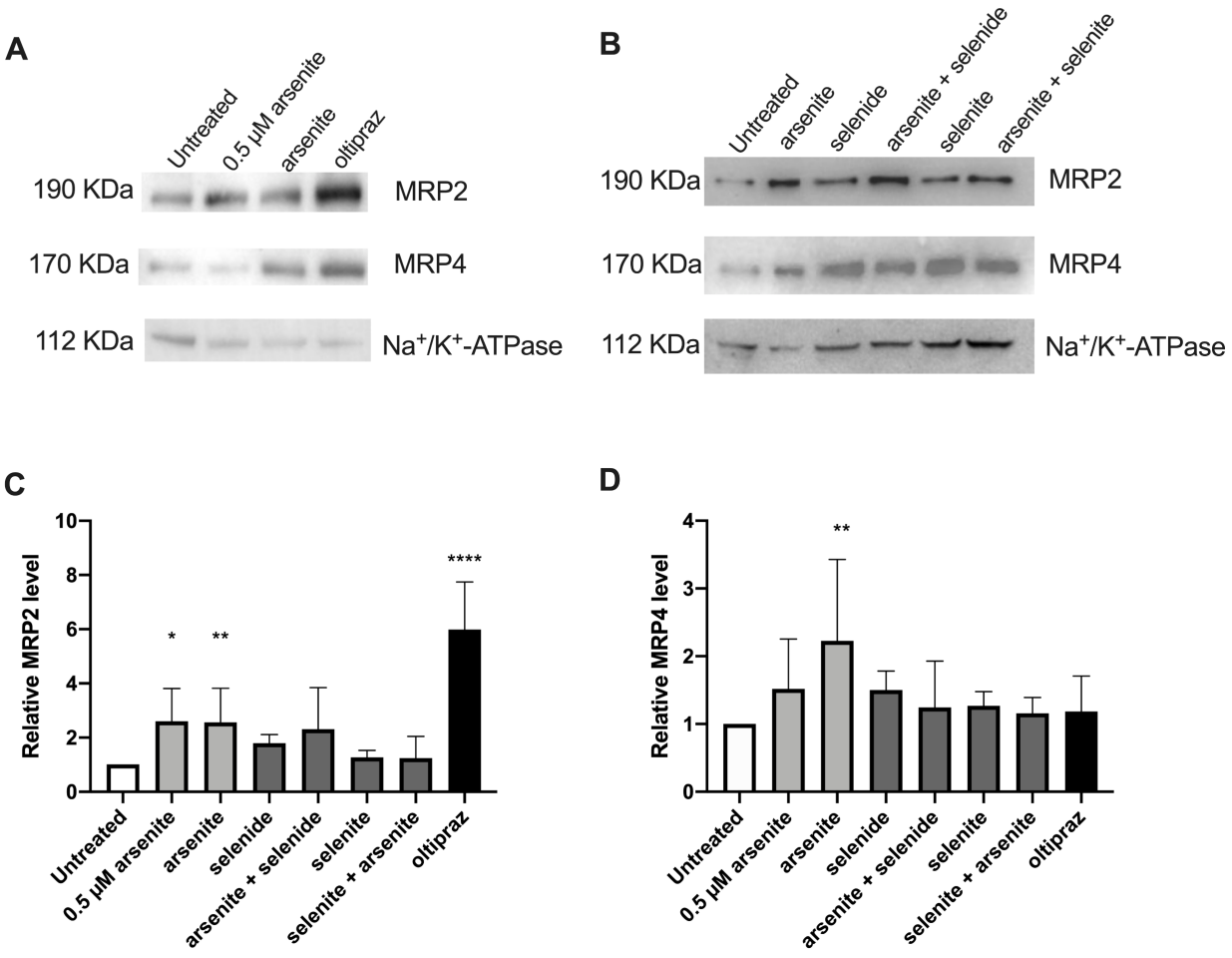

Figure 2.2: MRP2 and MRP4 proteins are detected in HepaRG cell crude membrane preparations. HepaRG cells were untreated, treated with arsenite, selenide or selenite ± arsenite, or oltipraz for 48 hr. All arsenic and selenium compounds were used at a concentration of 1 µM unless otherwise indicated, and oltipraz was used at 50 µM. Crude membranes were prepared and then subjected to SDS-PAGE (6%) and transferred to a PVDF membrane. Immunoblotting was performed using the MRP2-specific mouse monoclonal antibody M_2I-4 (1:1000) or the MRP4-specific rat monoclonal antibody M_4I-10 (1:2000). The Na^+/K^+-ATPase mouse monoclonal antibody H-3 (1:30 000) was used as a loading control. Secondary antibodies labeled with horseradish peroxidase and a chemiluminescent substrate were added to enable visualization of signals. **(A)** and **(B)** are representative figures. Densitometry data (analyzed with ImageJ) show relative levels of MRP2 **(C)** and MRP4 **(D)** in comparison to untreated HepaRGs. The mean ± SD of at least three independent experiments is shown. Significant differences are indicated with * $P < 0.05$, ** < 0.01, and **** $P < 0.0001$ (One-way ANOVA followed by Dunnett's post-hoc test).

2.3.4 Determination of EC_{50} values for selenium (selenide, selenite, SeMet and MeSeCys) and arsenite in HepaRG cells

The toxicity of arsenite, selenide, selenite, SeMet and MeSeCys were evaluated individually and in combination using a tetrazolium-salt based cytotoxicity assay.

2.3.4.1 Equimolar arsenite and selenium concentrations

Concentration versus cytotoxicity curves for arsenite and selenium (selenide, selenite, SeMet and MeSeCys) individually and in combination at equimolar concentrations are shown in **Fig 2.3A-D**. Half effective concentration (EC_{50}) values were determined for independent experiments using the sigmoidal dose response fit (GraphPad Prism 8) and mean values are summarized in **Table 2.1**. There was unexpectedly no mutual protection between arsenite and selenide as the EC_{50} value was higher for arsenite than with selenide alone, and selenide plus arsenite **(Fig 2.3A).** The EC_{50} value for arsenite plus selenite was less than those of arsenite and selenite individually, suggesting no mutual protection between these compounds, under these conditions **(Fig 2.3B and Table 2.1).** SeMet and MeSeCys had no detectable toxicity with EC_{50} values of greater than 3000 μM **(Table 1 and Fig 2.3C and 3D).** When HepaRG cells were treated in combination with arsenite and these selenium-containing amino acids, no shift in EC_{50} compared to arsenite alone was detected **(Table 2.1 and Fig 2.3C and D).**

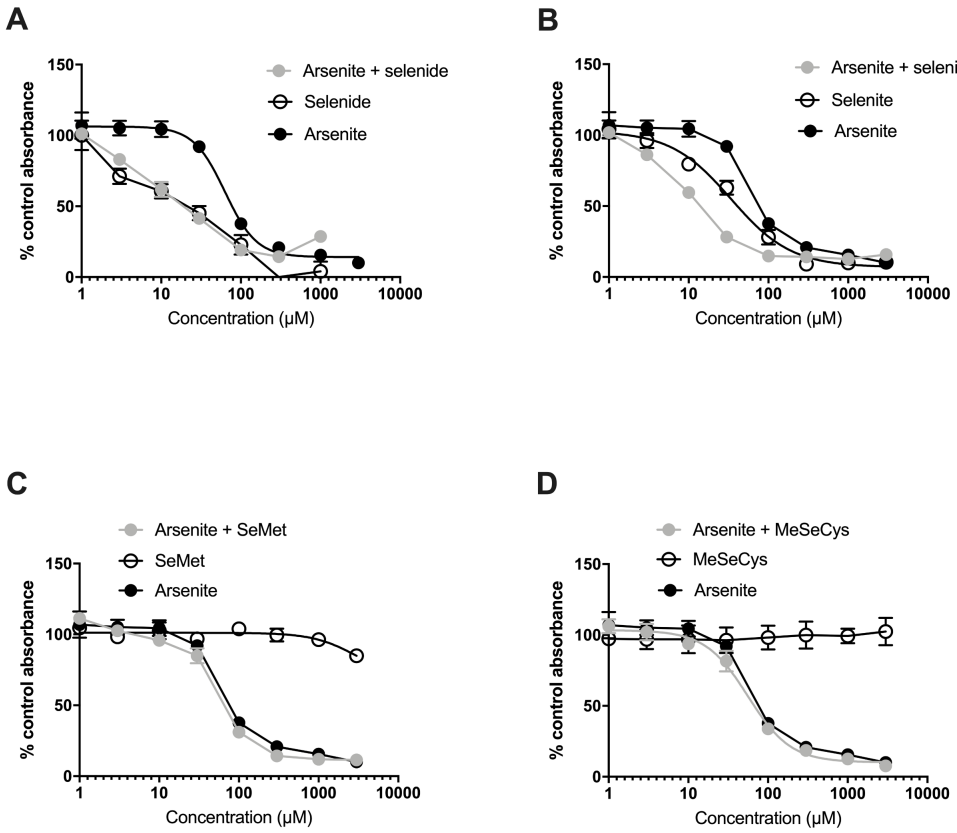

Figure 2.3: **Cytotoxicity of selenium ± arsenite in HepaRG cells at equimolar concentrations. Cells were treated with arsenite and selenium.** (**(A)** selenide, **(B)** selenite, **(C),** SeMet, **(D)**MeSeCys) individually (1-3000 μM) or together at equimolar concentrations for 48 hr. Cell viability was determined using a tetrazolium salt-based cytotoxicity assay. Data points represent mean determinations ± S.D. from at least three independent experiments. EC_{50} values were determined for individual experiments using the sigmoidal dose response fit (GraphPad Prism 8) and are summarized in **Table 2.1.**

Table 2.1: EC_{50} values for arsenite, selenide, selenite, methylselenocysteine, selenomethionine individually and in equimolar concentration arsenite/selenium combinations.

Arsenic/Selenium Species	EC_{50} ± SD (μM)[a]
Arsenite	64 ± 12
Selenide	5 ± 1 ****
Selenite	42 ± 6 **
Methylselenocysteine	>3000 ****
Selenomethionine	>3000 ****
Arsenite + selenide	8 ± 3 ****
Arsenite + selenite	15 ± 9 ****
Arsenite + methylselenocysteine	57 ± 17
Arsenite + selenomethionine	52 ± 15

[a]EC50 values were calculated from at least three independent experiments as described in Figure 2.3
** P < 0.01
**** P < 0.0001 compared with arsenite (analysis of variance followed by a Tukey's post hoc test)

2.3.4.2 Arsenite with selenide displayed a higher level of toxicity antagonism than arsenite with selenite

HepaRG cells were treated with arsenite plus selenite or arsenite plus selenide over nine concentrations, resulting in 81 concentration combinations, which were analyzed using the Combenefit software [54].

Statistically significant antagonism was observed with 1 µM arsenite with 30 µM selenite, as well as 3 µM arsenite with 10, 30 and 100 µM selenite **(Fig 2.4Ai and 2.4Aii).** The antagonism of toxicity between selenite and arsenite was strongest at 3 µM arsenite with 30 µM selenite.

Between selenide and arsenite, statistically significant antagonism was observed between 3 µM selenide with 1 and 3 µM arsenite **(Fig 2.4Bi and 2.4Bii).** Other statistically significant antagonistic combinations included 30 µM selenide with 3 µM arsenite as well as 100 µM selenide with 1 and 3 µM arsenite.

The antagonism of toxicity displayed between arsenite and selenide were at lower concentrations more relevant to environmental and dietary exposures than between arsenite and selenite. The overall summary metric values for synergy and antagonism (SUM_SYN_ANT) for arsenite in combination with selenite and arsenite in combination with selenide were -239 and -323, respectively, suggesting a stronger antagonistic relationship between selenide and arsenite compared to selenite and arsenite.

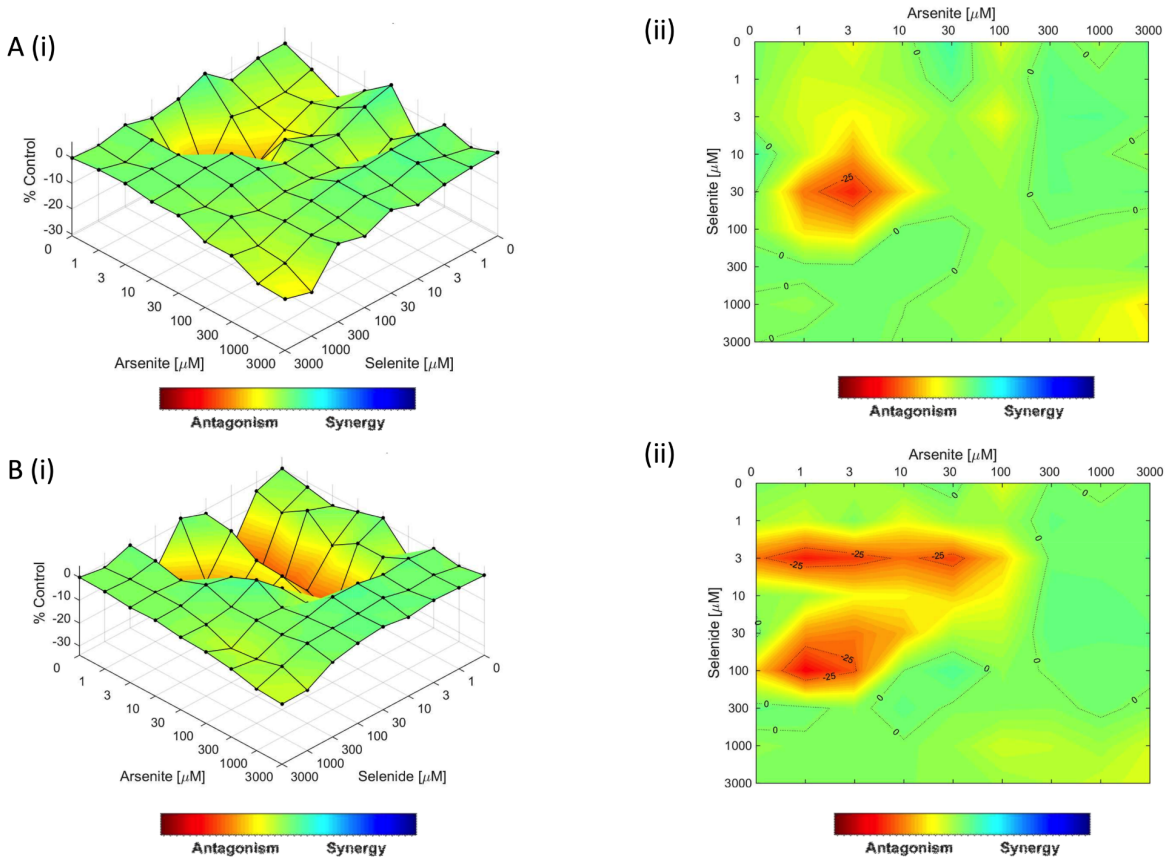

Figure 2.4: Cytotoxicity of selenium ± arsenite in HepaRG cells at different combinations of concentrations. Cells were treated with **(A)** arsenite and selenite or **(B)** arsenite and selenide at indicated concentration combinations for 48 hr. Cell viability was determined using a tetrazolium salt-based cytotoxicity assay. Data used in analyses were means of at least five independent experiments. Synergy distribution contour **(Ai & Bi)** and matrix **(Aii & Bii)** plots were obtained using the Loewe additive synergy model [54].

2.3.5 HepaRG cells treated with selenium (selenide, selenite, SeMet or MeSeCys) and/or arsenite retained CDF in canalicular networks

Fully differentiated HepaRG cells were treated with 1 µM arsenite, or 1 µM Se (selenide, selenite, SeMet, and MeSeCys) ± 1 µM arsenite for 24 hr prior to assessment of CDF accumulation. Canalicular networks retained CDF after treatment with arsenite and selenium compounds individually or combination **(Fig 2.5A-J),** suggesting that these compounds do not disrupt the integrity of canalicular networks at the concentrations used in transport assays.

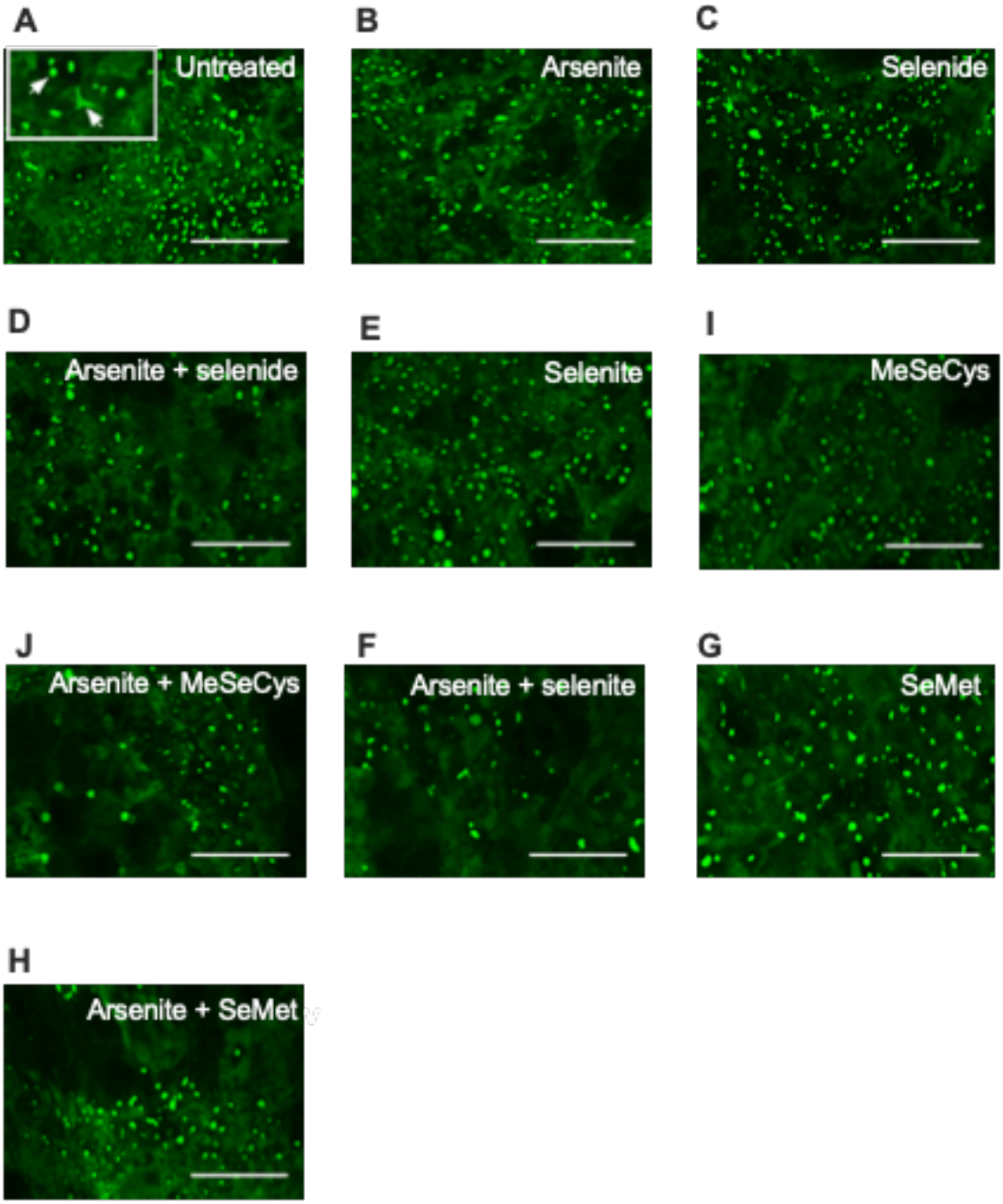

Figure 2.5: CDF accumulation within canalicular networks of HepaRG cells in the presence of arsenite and/or selenium compounds. HepaRG cells were either **(A)** untreated or treated with 1 µM of **(B)** arsenite, **(C)** selenide**, (E)** selenite**, (G)** SeMet**, (I)** MeSeCys or the selenium compounds with **(D, F, H & J)** arsenite for 24 hr. Cells were washed and treated with the diacetate form of CDF (2 µM) at 37°C for 10 min. CDF accumulation in canalicular networks was viewed with a fluorescence microscope and is indicated with arrows in (**A inset**, 200X magnification). Images shown are at 100X magnification and scale bars represent 100 µm.

2.3.6 Accumulation of arsenic and selenium (selenite and selenide) in HepaRG cells over time

Accumulation of 1 µM ^{73}As-arsenite, ^{75}Se-selenide and ^{75}Se-selenite by HepaRG cells was measured over time. Arsenite and Se data are expressed as a % arsenite accumulation and % selenide accumulation at a 24 hr time point. At 1 hr, accumulation of ^{73}As-arsenite began to plateau, with an average accumulation of 481 ± 17 pmol/mg protein at 24 hr**. (Fig 2.6A)**. The accumulation of ^{75}Se-selenium was linear over time, with significantly greater accumulation of ^{75}Se-selenide than ^{75}Se-selenite (range of 1.6 to 5.5-fold higher) **(Fig 2.6B).** At 24 hr, the average accumulation values for ^{75}Se-selenide and ^{75}Se-selenite were 108 ± 27 pmol/mg protein and 68 ± 9 pmol/mg protein, respectively.

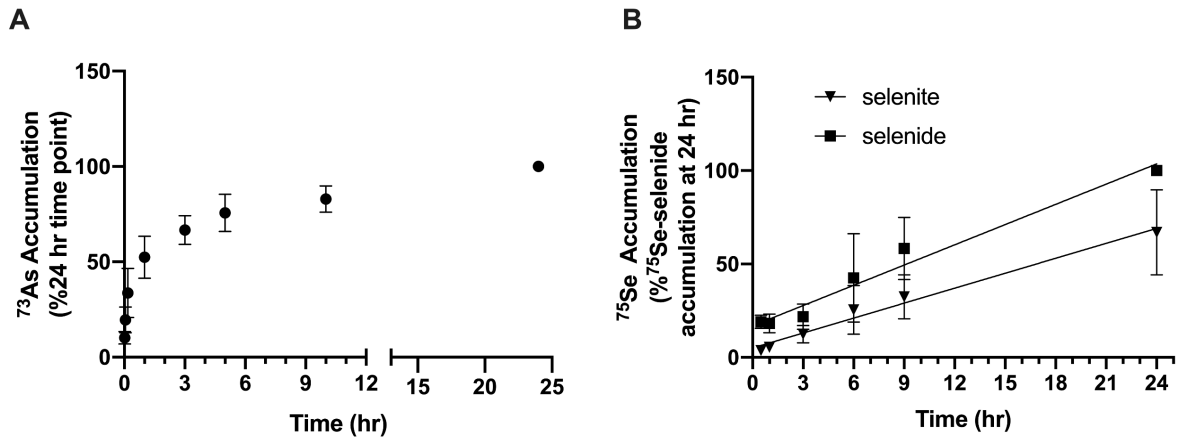

Figure 2.6: Time courses of arsenite and selenium accumulation over 24 hr in HepaRG cells. HepaRG cells were treated with media containing ^{73}As-arsenite (1 µM, 100 nCi) or ^{75}Se-selenite/^{75}Se-selenide (1 µM, 100 nCi). Then cells were washed and lysed in 0.5% Triton X-100 at indicated time points. **(A)** ^{73}As-arsenite accumulation was quantified by beta liquid scintillation counting and **(B)** ^{75}Se-selenite/^{75}Se-selenide accumulation was quantified by gamma scintillation counting. Symbols represent the mean ± SD of four independent experiments. Significance was determined using a linear regression analysis (P = 0.003)

2.3.7 Selenide increased biliary excretion of arsenic from HepaRG cells, and arsenite increased biliary excretion of selenium.

SCHHs are considered the gold standard model for studying hepatobiliary transport. Previous studies showed donor to donor variability in arsenic biliary excretion, making it difficult to reliably optimize conditions to characterize this process [14,59]. HepaRG cells originated from a single donor [45], eliminating this variability, potentially making them a suitable surrogate for SCHHs for studying hepatobiliary transport of arsenic. Fully differentiated HepaRG cells were treated with ^{73}As-arsenite (1 µM, 100 nCi). ^{73}As-arsenic efflux was measured across canalicular and sinusoidal membranes. Export of ^{73}As-arsenic was detected across both the sinusoidal alone and canalicular + sinusoidal surfaces and expressed as a % of arsenic alone effluxed across the sinusoidal surface (activity of 7.3 ± 2 pmol/mg protein at 10 min). Export of ^{73}As-arsenic across the sinusoidal + canalicular surface was significantly higher than across the sinusoidal surface alone with a BEI of 14 ± 8% **(Fig 2.7A).**

Since there was biliary excretion of arsenic from HepaRG cells, the influence of selenium on arsenic hepatobiliary transport was studied in the same manner described for measuring arsenic biliary excretion, but ^{73}As-arsenite (1 µM, 100 nCi) was added in the presence and absence of selenium (1 µM selenide, selenite, SeMet and MeSeCys) for an hour. In the presence of selenide, the BEI for arsenic increased by 2.3-fold to 32 ± 7% **(Fig 2.7A)**, suggesting greater canalicular efflux of arsenic in the presence of selenide. In the presence of selenite and SeMet, biliary excretion of arsenic was lost. Biliary excretion was also lost in the presence of MeSeCys, but interestingly, a 1.6-fold increase in sinusoidal efflux relative to the minus Se control was observed.

Export of ^{75}Se-selenite was measured across the sinusoidal membrane and sinusoidal + canalicular membrane and expressed as a % of ^{75}Se-selenite + arsenite effluxed across the sinusoidal surface (activity of 1.8 ± 1 pmol/mg protein at 10 min) **(Fig 2.7B).** No difference in selenite efflux was detected between the sinusoidal and sinusoidal + canalicular surfaces **(Fig 2.7B),** suggesting ^{75}Se-selenite did not undergo biliary excretion. The presence of arsenite had no effect on sinusoidal or canalicular export of ^{75}Se-selenite **(Fig 2.7B).**

Export of ^{75}Se-selenide was measured across the sinusoidal membrane and sinusoidal + canalicular membrane and expressed as a % of ^{75}Se-selenide + arsenite effluxed across the sinusoidal surface (activity of 1.7 ± 0.5 pmol/mg protein at 10 min) **(Fig 2.7C).** No difference in selenide efflux was detected between the sinusoidal and sinusoidal + canalicular surfaces **(Fig 2.7C)**, suggesting ^{75}Se-selenide did not undergo biliary excretion. In the presence of arsenite, there was significant biliary excretion of selenide with a BEI of 24 ± 5% **(Fig 2.7C).**

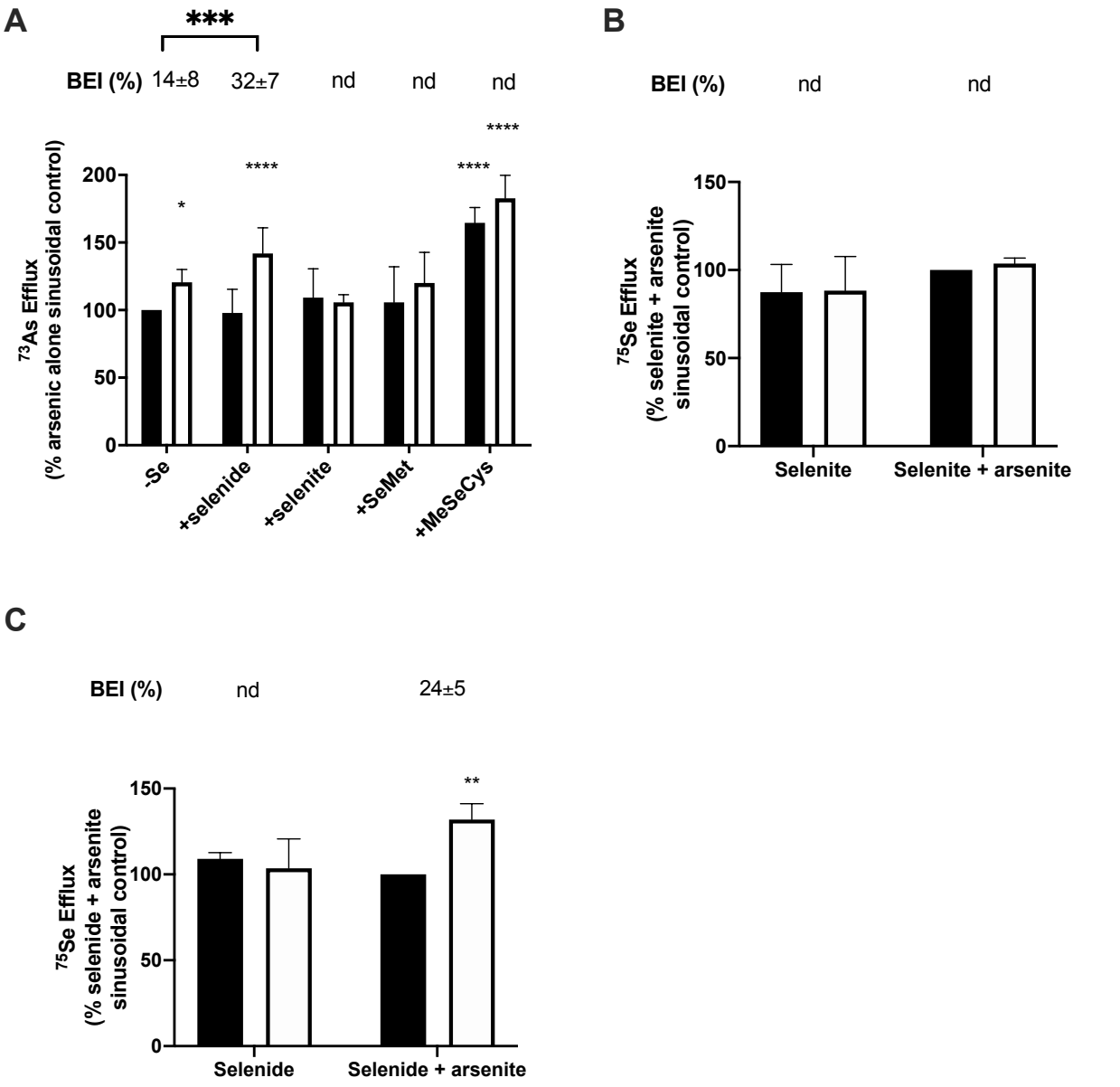

Figure 2.7: The effect of selenium on arsenic hepatobiliary transport in HepaRG cells. (A) HepaRG cells were treated with media containing ^{73}As-arsenite (1 µM, 100 nCi) ± Se (selenide, selenite, SeMet, or MeSeCys, 1 µM) for 1 hr. Incubation media was replaced with standard HBSS or Ca^{2+}/Mg^{2+}-free HBSS (with 1 mM EGTA) at 37℃ and arsenic efflux was measured. Black bars represent means ± SD of sinusoidal efflux and white bars represent means ± SD of sinusoidal plus biliary efflux from at least three independent experiments. BEI values were only calculated if sinusoidal plus biliary efflux at a 10 min time point was significantly higher than sinusoidal efflux alone ($P < 0.05$, Student's t test), and significant differences in BEIs are indicated with *** $P < 0.001$. Conditions where biliary excretion was not detected are indicated with ND. Conditions that are significantly different than the %arsenic alone sinusoidal control are indicated with * $P < 0.05$, or **** $P < 0.0001$ (One-way ANOVA followed by a Tukey's post hoc test). **(B)** Efflux of ^{75}Se-selenite efflux alone (1 µM, 100 nCi) and in the presence of arsenite (1 µM)**,** as well as **(C)** ^{75}Se-selenide alone (1 µM, 100 nCi) and in the presence of arsenite (1 µM) were evaluated in the same manner as for ^{73}As-arsenite with data represented in the same manner.

2.3.8 Evaluation of arsenite efflux with and without selenide from HepaRG cells after GSH-depletion, MRP inhibition, and temperature reduction.

^{73}As-arsenite export was measured under various conditions in the presence and absence of selenide and expressed as a % of untreated arsenite alone sinusoidal export (activity of 5.1 ± 1.7 pmol/mg protein at 10 min) **(Fig 2.8Ai & ii).** The BEI for arsenic alone was 14 ± 3%, which was stimulated by selenide to 29 ± 3% **(Fig 2.8Ai & ii).**

2.3.8.1 Arsenic hepatobiliary transport is GSH-dependent

Previously, we and others have shown that biliary and sinusoidal excretion of arsenic is GSH-dependent [11,14,60]. Therefore, GSH-dependence of arsenic hepatobiliary transport in HepaRG cells was evaluated. First, HepaRG cells were treated with BSO (500 µM) for 48 hr and GSH levels were found to be 70% lower in BSO-treated than untreated HepaRG cells **(Fig 2.8B)**. Treatment with BSO also resulted in a loss of biliary excretion of arsenic when measured by itself **(Fig 2.8Ai)** or in the presence of selenide **(Fig 2.8Aii).** Sinusoidal efflux of arsenic alone **(Fig 2.8Ai)** and in the presence of selenide **(Fig 2.8BAi)** both decreased 42% in BSO-treated HepaRG cells compared to minus BSO **(Fig 2.8Bi).** Sinusoidal + canalicular efflux of arsenic alone and in the presence of selenide decreased by 39% and 45% respectively in BSO-treated HepaRG cells compared to minus BSO **(Fig 2.8Aii).** These data show that both sinusoidal and canalicular efflux of arsenic with and without selenide are reduced upon GSH depletion, consistent with transport being MRP-mediated and with previous observations in the SCHH model [14].

2.3.8.2 Biliary excretion of arsenic is inhibited by MK571

To determine if MK571 inhibited arsenic efflux from HepaRG cells, cells were treated with MK571 (100 µM) for 30 min prior to initiation and for the duration of efflux. Treatment with MK571 resulted in a 30% decrease in arsenic efflux across sinusoidal membranes in the

absence of selenide, and a 16% decrease in the presence of selenide **(Fig 2.8Ai & ii).** There was a 30% and 25% decrease in arsenic efflux across sinusoidal + canalicular membranes in the absence and presence of selenide, respectively **(Fig 2.8Ai & ii),** consistent with a loss of arsenic biliary excretion. The loss in arsenic biliary excretion after treatment with MK571 suggest that arsenic hepatobiliary transport is MRP-mediated. We previously observed similar findings using the SCHH model [14].

2.3.8.3 Arsenic hepatobiliary transport is temperature sensitive

To further characterize arsenic hepatobiliary transport, temperature dependence of arsenic export alone and in the presence of selenide was evaluated at 4°C, compared to 37°C. There was a 73% decrease in sinusoidal efflux at 4°C for arsenic efflux alone and in the presence of selenide **(Fig 2.8Ai & ii).** There was a 73% decrease in sinusoidal plus canalicular efflux in both conditions, and biliary excretion of arsenic was lost at 4°C. The temperature sensitivity suggests that arsenic sinusoidal and canalicular efflux processes are predominantly transporter mediated.

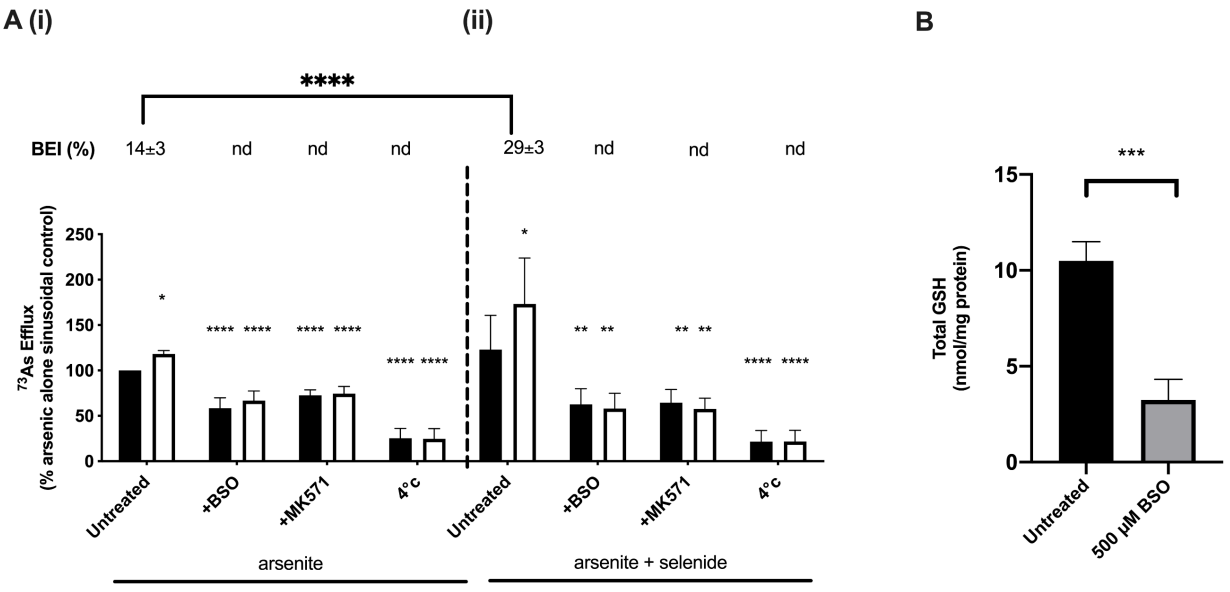

Figure 2.8: The effect of BSO, MK571 and temperature on arsenic hepatobiliary efflux in the absence and presence of selenide. (A) Efflux of ^{73}As-arsenic alone **(i)** and **(ii)** in the presence of selenide was re-evaluated after 48 hr pre-treatment of cells with BSO (500 µM), 30 min treatment with MK571 (100 µM) before and during efflux, and at 4°C using ice cold buffers. Black bars represent the mean ± SD of sinusoidal efflux and white bars represent means ± SD of sinusoidal plus biliary efflux from at least five independent experiments. BEI values were only calculated if sinusoidal plus biliary efflux was significantly higher than sinusoidal efflux alone ($P < 0.05$, Student's t test). Conditions that are significantly different than the % arsenic alone sinusoidal control are indicated with * $P < 0.05$, ** $P < 0.001$, or **** $P < 0.0001$ (One-way ANOVA followed by a Tukey's post hoc test). **(B)** Total GSH depletion by 500 µM BSO-treated HepaRG cells (gray bar) compared to untreated HepaRG cells (black bar) after 48 hr (*** $P < 0.001$, Student's t test)

2.3.9 HepaRG cells efflux inorganic and methylated arsenic species across the sinusoidal membranes.

To determine the chemical species of arsenic effluxed across the sinusoidal membrane, HepaRG cells were treated with 1 µM arsenite alone, or in the presence of 1 µM Se (selenide or selenite) for 24 hr. After 24 hr, this media was collected for analysis **(Fig 2.9A).** HepaRG cells were then washed with arsenic-free growth media, and then replaced, and cells were incubated for 1 hr at 37°C. This media was also collected for analysis by HPLC-ICP-MS **(Fig 2.9B).** Due to the instability of trivalent forms of arsenic during sample handling, storage and preparation for

analysis, arsenic species identified in culture media are simply referred to as inorganic arsenic, MMA, and DMA without valency designation.

In the culture media collected after 24 hr of treatment with arsenite, MMA was the major metabolite, accounting for 19-20% of total arsenic in media in the presence and absence of Se **(Fig 2.9A).** DMA was also detected and accounted for 4%, 2.5% and 2.6% of total arsenic in media from HepaRG cells treated with arsenite alone, arsenite + selenite, and arsenite + selenide, respectively **(Fig 2.9A).**

In the culture media collected after cell washing and efflux for 1 hr, MMA was also the major metabolite, accounting for 22-23% of total effluxed arsenic **(Fig 2.9B).** DMA was also detected and accounted for 6.2%, 3.5%, and 2.8% of total arsenic in media from HepaRG cells treated with arsenite alone, arsenite + selenite, and arsenite + selenide, respectively **(Fig 2.9B).** While there was a trend in the reduction of DMA in media in the presence of selenite and selenide after 24 hr of treatment **(Fig 2.9A)** and after 1 hr of efflux **(Fig 2.9B),** it was not significant.

Overall, these data indicate that HepaRG cells methylate arsenic and that inorganic and methylated forms are transported across sinusoidal membranes.

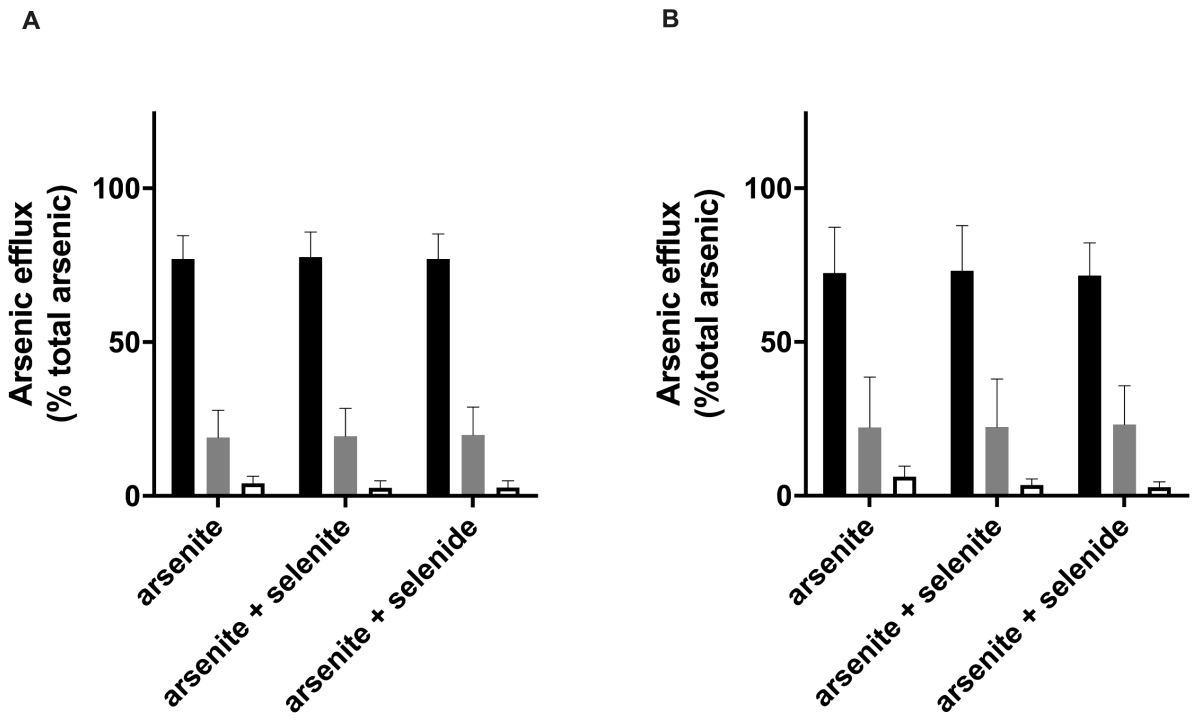

Figure 2.9: Methylation of arsenic effluxed into culture media of fully differentiated HepaRG cells treated with arsenite, arsenite + selenite, or arsenite + selenide. Arsenic species are plotted as % of total arsenic, inorganic (black bars), MMA (gray bars), and DMA (open bars). **(A)** HepaRG cells were incubated for 24 hr with 1 µM arsenite, 1 µM arsenite and 1 µM selenite, or 1 µM arsenite and 1 µM selenide. Media was collected and analyzed by HPLC-ICP-MS. **(B)** HepaRG cells were washed and treated with arsenic-free media for 1 hr at 37℃ prior to analysis by HPLC-ICP-MS. Bars represent means ± SD of four or five independent experiments.

2.3.10 *ABCC2* knockdown

HepaRG cells were stably transfected with shRNAs targeting the MRP2 gene *ABCC2* as well as a non-target control shRNA and empty vector. Three different cell clones stably expressing the *ABCC2* targeted shRNA were characterized: two independently derived clones of shRNA 9307 (9307#1 and 9307#2) as well as shRNA 9640.

2.3.10.1 HepaRG cells stably expressing *ABCC2*-targeted shRNA, empty vector, and non-target shRNA still form extensive canalicular networks.

Taurocholate is transported into canalicular networks by the bile salt export pump (BSEP/*ABCB11*) and therefore should not be influenced by reduced MRP2 levels. Thus, taurocholate efflux was evaluated to determine if canalicular networks were formed in fully differentiated HepaRG cells either parental or stably expressing empty vector, non-target or *ABCC2*-targeted shRNA (clones 9307#1, 9307#2 and 9640). There was biliary excretion of taurocholate from all HepaRG cells, suggesting the formation of canalicular networks. The BEIs for parental, empty vector, and non-target HepaRG cells and HepaRG cells stably expressing the *ABCC2*-targeted shRNA clones (9307#1, 9307#2, and 9640) were 26 ± 4%, 21 ± 2%, 24 ± 4%, 20 ± 2%, 19 ± 3% and 27 ± 3%, respectively, and not significantly different from each other **(Fig 2.10A).**

2.3.10.2 HepaRG cells stably expressing *ABCC2* targeted shRNA have reduced CDF in canalicular networks relative to controls

CDF accumulation within canalicular networks was visualized to evaluate MRP2 function in fully differentiated HepaRG cells either parental or stably expressing empty vector, non-target, or *ABCC2*-targeted shRNA. There was extensive CDF accumulation in the canalicular networks of parental, empty vector, and non-target HepaRG cells, indicating the presence of functional MRP2 **(Fig 2.10B-D).** In contrast, there was a lack of CDF accumulation in canalicular networks of HepaRG cells stably expressing the *ABCC2*-targeted shRNA (clones 9307#1, 9307#2, and 9640**) (Fig 2.10E-G),** suggesting the absence of functional MRP2 in these HepaRG cells.

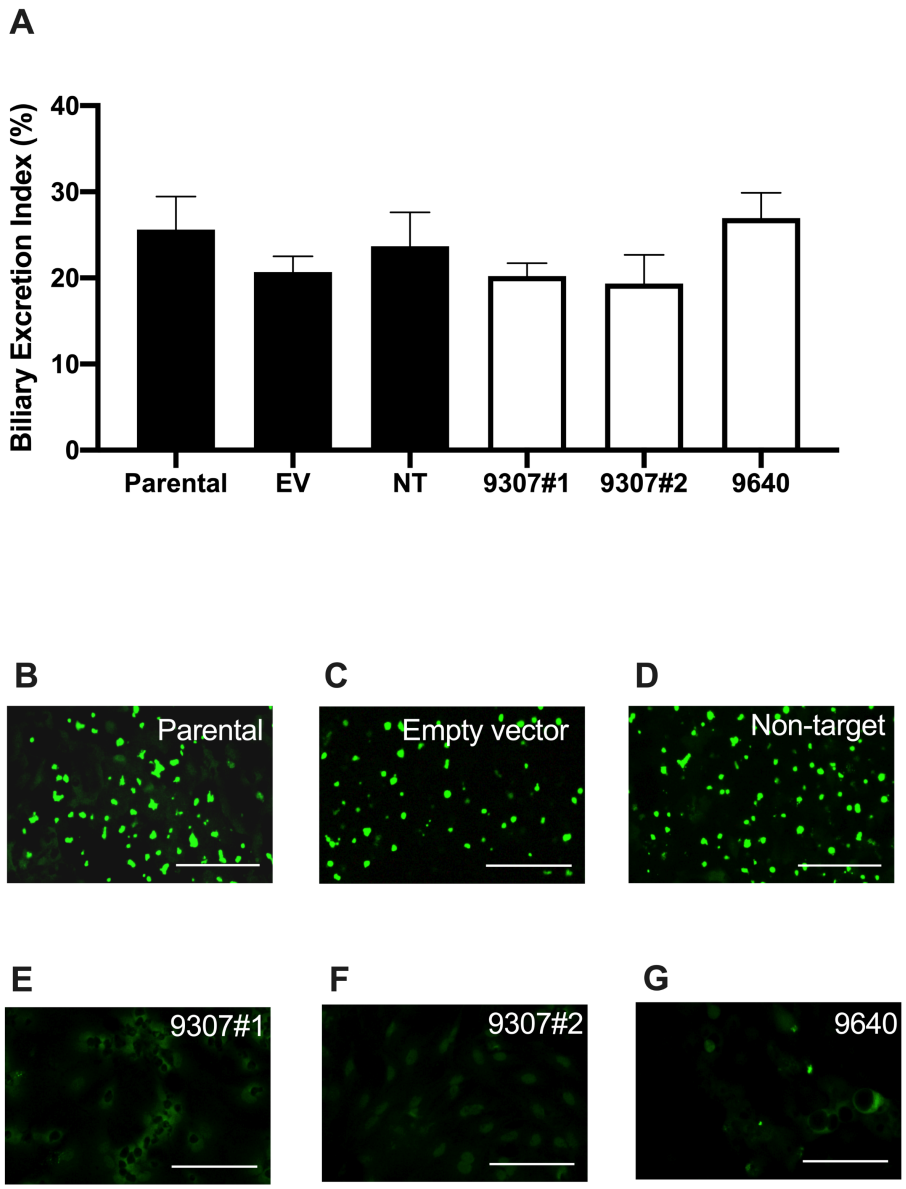

Figure 2.10: Characterization of canalicular network formation and integrity through the measurement of taurocholate biliary excretion and CDF accumulation. (A) HepaRG cells were treated with media containing ^{3}H(G)-Taurocholic acid (1 µM, 100 nCi) for 20 min. Incubation media was washed off and replaced with standard HBSS (closed bar) or Ca^{2+}/Mg^{2+}-free HBSS (with 1 mM EGTA) (open bar) at 37℃ and taurocholate efflux was measured at a 10 min time point. Bars represent means ± SD of three independent experiments. BEI values were only calculated if sinusoidal plus biliary efflux was significantly higher than sinusoidal efflux alone ($p<0.05$, Student's t test). **(B-G)** Parental HepaRG cells or HepaRG cells stably expressing empty vector, non-target, and *ABCC2*-targeted shRNA (clones 9307#1, 9307#2 and 9640) were treated with the diacetate form of CDF (2 µM) at 37℃ for 10 min. CDF accumulation in canalicular networks was viewed with a fluorescence microscope. Images are at 100X magnification and scale bars represent 100 µm.

2.3.10.3 *ABCC2* knockdown HepaRG cells stably expressing *ABCC2* targeted shRNA have reduced MRP2 levels relative to controls.

To further study the role of MRP2 in arsenic hepatobiliary transport, immunoblots of whole cell lysates were done to evaluate MRP2 levels of fully differentiated *ABCC2* knockdown HepaRG cells compared to fully differentiated parental, empty vector and non-target HepaRG cells. MRP2 was detected at similar levels in parental HepaRG cells, and HepaRG cells expressing empty vector and non-target shRNA **(Fig 2.11A & B).** The levels of MRP2 in HepaRG cells expressing *ABCC2*-targeted shRNA in clones 9307#1, 9307#2 and 9640 were 67%, 86% and 61%, respectively, lower than MRP2 levels of parental HepaRG cells **(Fig 2.11A & B).**

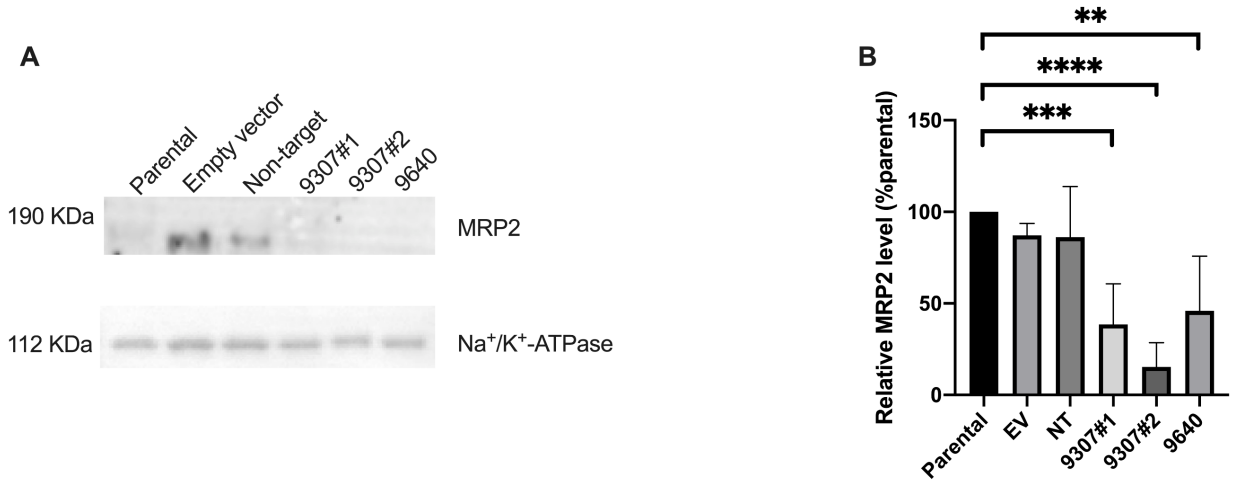

Figure 2.11: MRP2 levels in parental HepaRG cells compared to HepaRG cells expressing empty vector, non-target, or *ABCC2*-targeted shRNA (clones 9307#1, 9307#2 and 9640). Whole cell lysates were prepared and then 20 µg of protein were subjected to SDS-PAGE (6%) and transferred to a PVDF membrane. Immunoblotting was performed using the MRP2-specific mouse monoclonal antibody M_2I-4 (1:1000). The Na^+/K^+-ATPase mouse monoclonal antibody H-3 (1:30 000) was used as a loading control. Secondary antibodies labeled with horseradish peroxidase and a chemiluminescent substrate were added to enable visualization of signals. **(A)** Representative immunoblots. **(B)** Densitometry data (analyzed with ImageJ) show relative levels of MRP2 in comparison to parental HepaRGs. The means ± SD from at least three independent experiments are shown. Significant differences are indicated with ** $P < 0.01$, *** $P < 0.001$ and **** $P < 0.0001$ (One-way ANOVA followed by Dunnett's post-hoc test).

2.3.10.4 Biliary excretion of arsenic alone and in the presence of selenide was undetectable in HepaRG cells stably expressing *ABCC2*-targeted shRNA.

The extent of arsenic hepatobiliary transport was compared between fully differentiated parental HepaRG cells or stably expressing empty vector, non-target, or *ABCC2*-targeted shRNA. Export of ^{73}As-arsenic was detected across both the sinusoidal alone and canalicular + sinusoidal surfaces in parental HepaRG cells and HepaRG cells stably expressing empty vector and non-target shRNA. Data are expressed as a % of arsenic alone effluxed across the sinusoidal surface of parental HepaRG cells (3.6 ± 1 pmol/mg protein at 10 minutes) **(Fig 2.12A)**. Export of ^{73}As-arsenic across the sinusoidal + canalicular surface was significantly higher than across the sinusoidal surface alone in parental HepaRG cells and HepaRG cells stably expressing empty vector and non-target shRNA with BEIs of 19 ± 4%, 16 ± 2%, and 21 ± 1%, respectively **(Fig 2.12A).** Biliary excretion of arsenic was lost for all three HepaRG clones stably expressing *ABCC2*-targeted shRNA **(Fig 2.12Ai).**

The influence of selenium on arsenic hepatobiliary transport after *ABCC2* knockdown was also studied. As expected, in the presence of selenide, the BEI for arsenic increased by ~2-fold to 32 ± 3%, 33 ± 6% and 38 ± 3% in parental HepaRG cells and HepaRG cells stably expressing empty vector and non-target shRNA **(Fig 2.12A).** Biliary excretion of arsenic in the presence of selenide was lost for all three HepaRG clones stably expressing *ABCC2*-targeted shRNA **(Fig 2.12Aii).**

These data suggest that arsenic hepatobiliary transport in the presence and absence of selenide is MRP2-mediated.

2.3.10.5 Biliary excretion of selenium in the presence of arsenite was not detected in HepaRG cells stably expressing *ABCC2*-targeted shRNA.

To corroborate our findings from arsenic efflux studies, selenium efflux in the presence and absence of arsenite was evaluated using fully differentiated parental HepaRG cells or stably expressing empty vector, non-target, or *ABCC2*-targeted shRNA. Export of ^{75}Se-selenide was measured across the sinusoidal membrane and sinusoidal + canalicular membrane as described above. Data are expressed as a % of ^{75}Se-selenide + arsenite effluxed across the sinusoidal surface of parental HepaRG cells (1.1 ± 0.2 pmol/mg protein at 10 minutes) **(Fig 2.12B).** As expected from our results in **Figure 2.7C**, no selenide biliary excretion was detected for any of the cell lines **(Fig 2.12B).** Biliary excretion of ^{75}Se-selenide did occur in the presence of arsenite for parental, empty vector, and non-target HepaRG cells with BEIs of 22 ± 1%, 18 ± 2% and 17 ± 6%, respectively **(Fig 2.12B).** For HepaRG cells stably expressing *ABCC2*-targeted shRNA, no biliary excretion of ^{75}Se-selenide in the presence of arsenite was detected **(Fig 2.12B).** These data strongly suggest that arsenic stimulated ^{75}Se-selenide transport is MRP2-mediated.

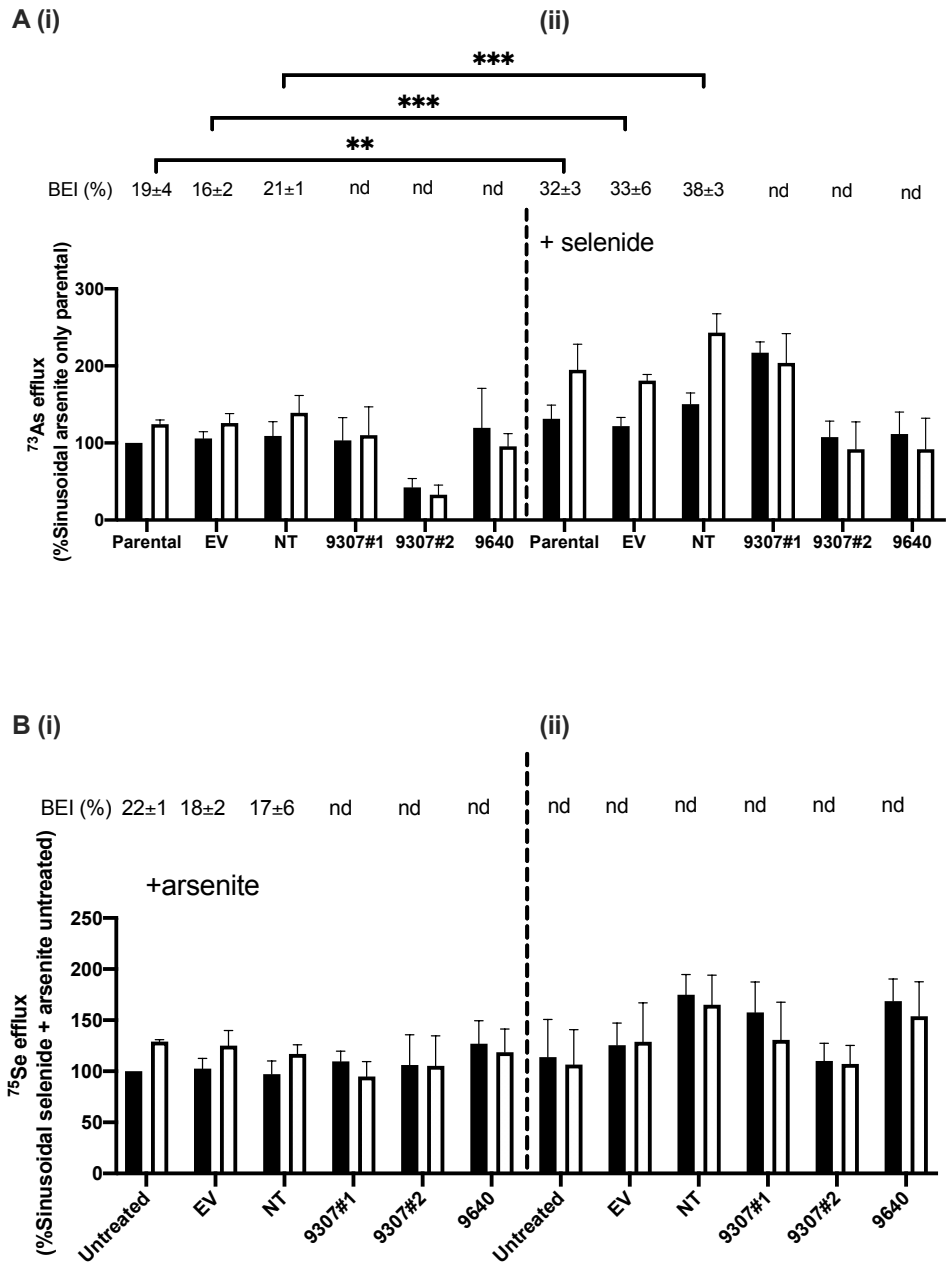

Figure 2.12: Arsenic hepatobiliary transport in parental HepaRG cells compared to HepaRG cells expressing empty vector, non-target, or *ABCC2*-targeted shRNA (clones 9307#1, 9307#2 and 9640). (A) HepaRG cells were treated with media containing ^{73}As-arsenite (1 µM, 100 nCi) ± selenide (1 µM) for 1 hr. Incubation media was replaced with standard HBSS or Ca^{2+}/Mg^{2+}-free HBSS (with 1 mM EGTA) at 37°C and arsenic efflux was measured. Black bars represent means ± SD of sinusoidal efflux and white bars represent means ± SD of sinusoidal plus biliary efflux from three independent experiments. BEI values were only calculated if sinusoidal plus biliary efflux at a 10 min time point was significantly higher than sinusoidal efflux alone ($p<0.05$, Student's t test), and significant differences in BEIs are indicated with ** $P < 0.01$ or *** $P < 0.001$. Conditions where no biliary excretion was detected are indicated with ND. **(B)** Efflux of ^{75}Se-selenide (1 µM, 100 nCi) in the presence of arsenite (1 µM) was evaluated in the same manner as for ^{73}As-arsenite with data represented in the same manner.

2.4 Discussion

Human exposure to arsenic in drinking water has been referred to as the "the largest mass poisoning of a population in history" [61]. Adverse human health effects can persist for decades following cessation of chronic arsenic exposure, thus, in addition to safer drinking water sources, therapeutic intervention strategies are needed [62–64]. After absorption across the intestine, inorganic arsenic travels via the portal circulation to the liver where it can be methylated and either exported across the sinusoidal surface of the liver for distribution to other organs or across the canalicular surface for enterohepatic cycling, with very little loss in feces [11,60,65,66]. In animal models, selenite has been shown to increase the fecal elimination of arsenic, likely through the formation and biliary excretion of $[(GS)_2AsSe]^-$ [18,19,22,23,25]. Evidence in humans suggests that in the liver, arsenic predominantly undergoes sinusoidal export (60-80% of arsenic is eliminated in urine), with some evidence of enterohepatic cycling [11,14,60,65,66]. The influence of selenium on human hepatobiliary transport is largely unknown but critical to understand due to supplementation of humans in arsenic-endemic regions. We present the first study to characterize the influence of selenium on arsenic hepatobiliary transport using a polarized human cell line capable of forming canalicular networks.

In our study, the HepaRG cell line was established as a suitable model for studying arsenic biliary excretion by demonstrating that canalicular networks were formed, MRP2 was functional and detectable, and arsenic undergoes biliary in addition to sinusoidal excretion. Consistent with the formation and biliary efflux of $[(GS)_2AsSe]^-$, selenide stimulated arsenic biliary excretion by ~2-fold and vice versa. Further characterization of arsenic (± selenide)

hepatobiliary transport suggested that this process was temperature- and GSH-dependent and mediated by MRPs. Our *ABCC2* knockdown studies strongly suggested that arsenic biliary excretion is mediated by MRP2.

Control experiments run for the HepaRG cell line were consistent with previous reports that the culture model had intact and functional canalicular networks. Taurocholate efflux had a mean BEI of 27 ± 7%, lower than what we and others have found for SCHH, but similar to the BEI of 27 ± 7 % and 29 ± 6% reported for HepaRG cells by Bachour-El Azzi et al., and Le Vee et al., respectively [14,46,55,67–70]. As expected based on Bachour-El Azzi et al., the MRP2 fluorescent substrate CDF was accumulated in canalicular networks and this was inhibited by MK571. Furthermore, reduction of MRP2 levels through shRNA knockdown of *ABCC2* resulted in a markedly reduced accumulation of CDF in canalicular networks.

Multiple approaches were taken in this study to assess the influence of arsenite and selenium compounds on the viability and integrity of the HepaRG cultures. HepaRG cells had a very comparable EC_{50} value for arsenite (**Table 2.1**, 64 μM) as previously observed in our study of HepG2 cells (61 μM), however, HepaRG cells had ~2-fold higher and 8-fold lower EC_{50} values for selenite and selenide than HepG2 cells, respectively [40]. SeMet and MeSeCys had undetectable toxicity at the concentrations tested (EC_{50} > 3 mM), consistent with low toxicity of these compounds observed in other human cell lines [71–74]. Although there was a trend towards arsenite being protective against selenide toxicity **(Table 2.1),** no significant mutual protection was observed when arsenite was dosed at equimolar concentrations with either selenide or selenite. This differed from HepG2 cells where we observed significant mutual protection between arsenite and selenide, under similar conditions [40]. The reasons for the

differences in toxicity between HepG2 and HepaRG cells and the lack of mutual detoxification between arsenic and selenide or selenite at equimolar concentrations are unknown. HepG2 and HepaRG cells likely contain different selenium and arsenic transport and metabolic pathways that could influence the toxicity of these compounds. Furthermore, HepG2 cells are a single cell type, while HepaRG cells are a mix of ~50% hepatocyte- and 50% bile duct epithelium-like cells. Differences in sensitivity between the hepatocyte- and bile duct epithelial-like cells towards arsenic and selenium likely influences the EC_{50} value.

When different concentration combinations were used, significant toxicity antagonism was observed for both the combination of arsenite plus selenite and arsenite plus selenide, with mutual antagonism being greater and at concentrations more relevant to environmental and dietary exposures, for the latter. This is consistent with our previous work in HepG2 cells, and with the higher cellular accumulation of selenide versus selenite observed by us **(Fig 2.6B** and [40]) and others [37,41,42]. Consistent with the conclusions of our HepG2 study, increased selenium (as selenide) uptake by cells appears to be protective against arsenic, presumably through the formation of $[(GS)_2AsSe]^-$.

Further to the tetrazolium salt-based MTS assay showing that arsenic and selenium concentrations were not toxic at the concentration used for transport assays (1 μM) LDH assays were run for each experiment and LDH leakage was rarely above 3%. In addition, CDF accumulation in canalicular networks were maintained in HepaRG cultures after treatment with arsenite, selenide, selenite, SeMet, and MeSeCys individually and with arsenite in combination with selenium. These data strongly support that canalicular networks and cell membranes were intact under transport assay conditions.

In our previous studies of arsenic hepatobiliary transport using SCHH, donor to donor variability existed with respect to biliary excretion of arsenic, with only 9 out of 14 SCHH preparations having detectable BEIs for arsenic [14]. HepaRG cells exhibited a modest but significant level of arsenic biliary excretion with a BEI of 14 ± 8% making it a useful model for studying hepatobiliary transport of arsenic, including biliary efflux. The addition of selenide resulted in a greater than two-fold increase in the BEI for arsenic (BEI for arsenic + selenide was 32 ± 7%) while under the conditions tested, the BEI for arsenic was no longer detectable in the presence of selenite, SeMet and MeSeCys **(Fig 2.7A).** Consistent with the formation of a complex of arsenic and selenium undergoing biliary excretion, ^{75}Se-selenide did not undergo biliary excretion by itself, but upon addition of arsenite, a BEI of 24 ± 5% was detected. Similar to selenide, ^{75}Se-selenite did not undergo biliary excretion by itself. In contrast with ^{75}Se-selenide, arsenite did not stimulate biliary excretion of ^{75}Se-selenite (consistent with selenite not stimulating biliary excretion of ^{73}As-arsenite).

Sinusoidal export of arsenic was reduced, and biliary excretion of arsenic ± selenide was lost upon GSH depletion, treatment of cells with the general MRP inhibitor MK571, and temperature reduction from 37°C to 4°C. All these data support the involvement of transporters, specifically MRPs/ABCCs in the sinusoidal and canalicular export of arsenic, and the stimulation of arsenic biliary excretion by selenide. Biliary excretion was further characterized by knocking down *ABCC2*, the gene for MRP2, the only MRP at the canalicular surface of the hepatocyte. While canalicular networks were still intact, as evidenced by similar taurocholate BEI values for control and *ABCC2* knockdown HepaRG cells, there was markedly reduced CDF accumulation in the canalicular networks of *ABCC2* knockdown cells. Furthermore,

all three independently derived HepaRG cells stably expressing the *ABCC2* knockdown shRNA, lost the biliary excretion of ^{73}As-arsenic **(Fig 2.12Ai)** and selenide stimulated ^{73}As-arsenic **(Fig 2.12Aii)**. In addition, while arsenic stimulated ^{75}Se-selenide biliary excretion occurred for control HepaRG cells, it was not detected for cells with *ABCC2* knocked down. These data strongly suggest that MRP2 is critical for the biliary excretion of arsenic, arsenic in the presence of selenide, and selenide in the presence of arsenite. These results are consistent with studies comparing Mrp2-deficient TR$^-$ Wistar rats to their WT counterparts showing that Mrp2 is responsible for >99% of total arsenic biliary excretion (in the forms $As(GS)_3$ and $MMA(GS)_2$) [11]. Rats tend to have more extensive biliary excretion than other animals [12,60,65,75], and have markedly different arsenic toxicokinetics compared to humans, thus it was critical to show this in a human model.

Multiple chemical forms of selenium have been used as supplements, including purified selenite and SeMet [76,77], as well as selenium mixtures contained in selenized yeast and selenium-enriched lentils (predominantly SeMet in combination with multiple other selenium species potentially including MeSeCys) [30,31,34,78–80]. The only chemical form of selenium that stimulated biliary excretion of arsenic from HepaRG cells was selenide. Selenide is extremely unstable and not suitable to be used as a supplement. However, all forms of selenium used in this study can ultimately be converted to selenide. Selenite is rapidly converted to selenide in the blood, and we and others have hypothesized that in an intact i*n vivo* system the hepatocyte would be exposed predominantly to albumin bound selenide [29,40,81–84]. Selenide can be released from SeMet and MeSeCys through the trans-sulfuration pathway [36,85].

This is more likely for MeSeCys than SeMet because the latter will substitute for Met and be incorporated into proteins, preventing selenide release [36,86]. The release of selenide from these selenium-containing amino acids likely takes longer than our transport assay conditions allowed.

An increased sinusoidal export of ^{73}As-arsenic in the presence of MeSeCys was observed **(Fig 2.7A).** The release of arsenic across the sinusoidal surface of the hepatocyte leads to its entry into the systemic circulation and ultimately urinary elimination of arsenic. Interestingly, results from a recent clinical trial of selenium enriched lentils, suggested that humans consuming the selenium-enriched lentils had an increased urinary (not fecal) elimination of arsenic [31]. Detailed selenium speciation data has not been published for the lentils used in this trial but could contain MeSeCys or another compound that has a similar effect. These observations warrant further investigation and strongly suggest that the chemical form of selenium consumed could influence whether biliary or sinusoidal export occurs. This thesis further explores the sinusoidal export of arsenic and the influence of MeSeCys on it in Chapter 3.

Previously, using membrane vesicle transport assays, human MRP2 was shown to mediate the ATP-dependent transport of $As(GS)_3$ and $[(GS)_2AsSe]^-$ [13]. The loss of arsenic biliary excretion by HepaRG cells upon GSH depletion or *ABCC2* knockdown provides strong support for MRP2-mediated transport of arsenic GSH conjugates. The loss of selenide-stimulated arsenite, and arsenite-stimulated selenide biliary excretion upon GSH depletion or *ABCC2* knockdown, provides indirect but strong support for the MRP2-mediated transport of $[(GS)_2AsSe]^-$. These data combined with our previous work showing that MRP2 is a high affinity,

high capacity transporter of both $As(GS)_3$ and $[(GS)_2AsSe]^-$ [13], and the fact that *ABCC2* is highly polymorphic [87–89], suggest MRP2 variants could influence selenium-dependent and -independent arsenic elimination, and ultimately carcinogenic risk. This was further investigated in Chapter 4.

Overall, this study advances our understanding of arsenic hepatobiliary transport and provides foundational knowledge for informing future selenium supplementation of humans in arsenic endemic regions.

2.5 References

[1] IARC, A review of human carcinogens – Part C: metals, arsenic, dusts, and fibres., 2012.

[2] M.F. Naujokas, B. Anderson, H. Ahsan, H. Vasken Aposhian, J.H. Graziano, C. Thompson, W.A. Suk, The broad scope of health effects from chronic arsenic exposure: Update on a worldwide public health problem, Environmental Health Perspectives. 121 (2013) 295–302. https://doi.org/10.1289/ehp.1205875.

[3] H.-J. Sun, B. Rathinasabapathi, B. Wu, J. Luo, L.-P. Pu, L.Q. Ma, Arsenic and selenium toxicity and their interactive effects in humans, Environment International. 69 (2014) 148–158. https://doi.org/https://doi.org/10.1016/j.envint.2014.04.019.

[4] J. Podgorski, M. Berg, Global threat of arsenic in groundwater, Science. 368 (2020) 845 – 850. https://doi.org/10.1126/science.aba1510.

[5] Arsenic, World Health Organization. (2018). http://www.who.int/en/news-room/fact-sheets/detail/arsenic (accessed August 9, 2018).

[6] R. Villa-Bellosta, S. V, Arsenate transport by sodium/phosphate cotransporter type IIb, Toxicology and Applied Pharmacology. 247 (2010) 36–40.

[7] R. Villa-Bellosta, V. Sorribas, Role of rat sodium/phosphate cotransporters in the cell membrane transport of arsenate, Toxicology and Applied Pharmacology. 232 (2008) 125–134. https://doi.org/10.1016/j.taap.2008.05.026.

[8] R. Mukhopadhyay, H. Bhattacharjee, B.P. Rosen, Aquaglyceroporins: generalized metalloid channels, Biochimica et Biophysica Acta. 1840 (2014) 1583–1591.

[9] W.R. Cullen, Chemical mechanism of arsenic biomethylation, Chemical Research in Toxicology. 27 (2014) 457–461. https://doi.org/10.1021/tx400441h.

[10] Z. Drobná, F.S. Walton, A.W. Harmon, D.J. Thomas, M. Stýblo, Interspecies differences in metabolism of arsenic by cultured primary hepatocytes, Toxicology and Applied Pharmacology. 245 (2010) 47–56. https://doi.org/10.1016/j.taap.2010.01.015.

[11] S. v. Kala, M.W. Neely, G. Kala, C.I. Prater, D.W. Atwood, J.S. Rice, M.W. Lieberman, The MRP2/cMOAT transporter and arsenic-glutathione complex formation are required for biliary excretion of arsenic, Journal of Biological Chemistry. 275 (2000) 33404–33408.

[12] S. v. Kala, G. Kala, C.I. Prater, A.C. Sartorelli, M.W. Lieberman, Formation and Urinary Excretion of Arsenic Triglutathione and Methylarsenic Diglutathione, Chemical Research in Toxicology. 17 (2004) 243–249.

[13] M.W. Carew, E.M. Leslie, Selenium-dependent and -independent transport of arsenic by the human multidrug resistance protein 2 (MRP2/ABCC2): Implications for the mutual detoxification of arsenic and selenium, Carcinogenesis. 31 (2010) 1450–1455.

[14] B.A. Roggenbeck, M.W. Carew, G.J. Charrois, D.N. Douglas, N.M. Kneteman, X. Lu, X. C. Le, E.M. Leslie, Characterization of arsenic hepatobiliary transport using sandwich-cultured human hepatocytes, Toxicological Sciences. 145 (2015) 307–320. https://doi.org/10.1093/toxsci/kfv051.

[15] H. Naranmandura, B.A. Roggenbeck, M.W. Carew, X.C. Le, B.D. Whitlock, M. Banerjee, E.M. Leslie, A Novel Pathway for Arsenic Elimination: Human Multidrug Resistance Protein 4 (MRP4/ABCC4) Mediates Cellular Export of Dimethylarsinic Acid (DMAV) and the Diglutathione Conjugate of Monomethylarsonous Acid (MMAIII), Molecular Pharmacology. 86 (2014) 168–179.

[16] H. Tapiero, D.M. Townsend, K.D. Tew, The antioxidant role of selenium and seleno-compounds, Biomedicine & Pharmacotherapy = Biomedecine & Pharmacotherapie. 57 (2003) 134–144. https://doi.org/10.1016/s0753-3322(03)00035-0.

[17] Institute of Medicine (US) Panel on Dietary Antioxidants and Related Compounds, Dietary Reference Intakes for Vitamin C, Vitamin E, Selenium, and Carotenoids, Washington, 2000.

[18] J. Gailer, G.N. George, I.J. Pickering, R.C. Prince, H.S. Younis, J.J. Winzerling, Biliary excretion of $[(GS)_2AsSe]^-$ after intravenous injection of rabbits with arsenite and selenate, Chemical Research in Toxicology. 15 (2002) 1466–1471. https://doi.org/10.1021/tx025538s.

[19] G.N. George, J. Gailer, O. Ponomarenko, P.F. la Porte, K. Strait, M. Alauddin, H. Ahsan, S. Ahmed, J. Spallholz, I.J. Pickering, Observation of the seleno bis-(S-glutathionyl) arsinium anion in rat bile, Journal of Inorganic Biochemistry. 158 (2016) 24–29. https://doi.org/https://doi.org/10.1016/j.jinorgbio.2016.01.022.

[20] J. Gailer, G.N. George, I.J. Pickering, R.C. Prince, S.C. Ringwald, J.E. Pemberton, R.S. Glass, H.S. Younis, D.W. DeYoung, H.V. Aposhian, A metabolic link between arsenite and selenite: The seleno-bis(S- glutathionyl) arsinium ion, Journal of the American Chemical Society. (2000).

[21] J. Gailer, S. Madden, G.A. Buttigieg, M.B. Denton, H.S. Younis, Identification of $[(GS)_2AsSe]^-$ in rabbit bile by size-exclusion chromatography and simultaneous multielement-specific detection by inductively coupled plasma atomic emission spectroscopy, Applied Organometallic Chemistry. 16 (2002) 72–75. https://doi.org/https://doi.org/10.1002/aoc.260.

[22] O.A. Levander, C.A. Baumann, Selenium metabolism. VI. Effect of arsenic on the excretion of selenium in the bile, Toxicology and Applied Pharmacology. (1966) 106–115. https://doi.org/10.1016/0041-008X(66)90035-4.

[23] O. Ponomarenko, P.F. la Porte, S.P. Singh, G. Langan, D.E.B. Fleming, J.E. Spallholz, M. Alauddin, H. Ahsan, S. Ahmed, J. Gailer, G.N. George, I.J. Pickering, Selenium-mediated arsenic excretion in mammals: A synchrotron-based study of whole-body distribution and tissue-specific chemistry, Metallomics. 9 (2017) 1585–1595.

[24] Y. Chen, M. Hall, J.H. Graziano, V. Slavkovich, A. van Geen, F. Parvez, H. Ahsan, A prospective study of blood selenium levels and the risk of arsenic-related premalignant

skin lesions, Cancer Epidemiology Biomarkers and Prevention. 16 (2007) 207–213. https://doi.org/10.1158/1055-9965.EPI-06-0581.

[25] S.A. Manley, G.N. George, I.J. Pickering, R.S. Glass, E.J. Prenner, R. Yamdagni, Q. Wu, J. Gailer, The Seleno Bis(S-glutathionyl) Arsinium Ion Is Assembled in Erythrocyte Lysate, Chemical Research in Toxicology. 19 (2006) 601–607. https://doi.org/10.1021/tx0503505.

[26] I. Csanaky, Z. Gregus, Effect of selenite on the disposition of arsenate and arsenite in rats, Toxicology. 186 (2003) 33–50. https://doi.org/https://doi.org/10.1016/S0300-483X(02)00604-2.

[27] I.S. Palmer, C.W. Bonhorst, Selenium Poisoning, Modification of Selenite Metabolism by Arsenite, Journal of Agricultural and Food Chemistry. 5 (1957) 928–930. https://doi.org/10.1021/jf60082a004.

[28] Z. Gregus, Á. Gyurasics, L. Koszorús, Interactions between selenium and group Va-metalloids (arsenic, antimony and bismuth) in the biliary excretion, Environmental Toxicology and Pharmacology. 5 (1998) 89–99. https://doi.org/https://doi.org/10.1016/S1382-6689(97)10008-4.

[29] G. Kaur, W. Javed, O. Ponomarenko, K. Shekh, D.P. Swanlund, J.R. Zhou, K.L. Summers, A. Casini, M.N. Wenzel, J.R. Casey, E. Cordat, I.J. Pickering, G.N. George, E.M. Leslie, Human red blood cell uptake and sequestration of arsenite and selenite: Evidence of seleno-bis(S-glutathionyl) arsinium ion formation in human cells, Biochemical Pharmacology. 180 (2020) 114141. https://doi.org/https://doi.org/10.1016/j.bcp.2020.114141.

[30] L. Yang, W. Wang, S. Hou, P.J. Peterson, W.P. Williams, Effects of selenium supplementation on arsenism: An intervention trial in inner Mongolia, Environmental Geochemistry and Health. 24 (2002) 359–374.

[31] J.E. Smits, R.M. Krohn, E. Akhtar, S.K. Hore, M. Yunus, A. Vandenberg, R. Raqib, Food as medicine: Selenium enriched lentils offer relief against chronic arsenic poisoning in Bangladesh, Environmental Research. 176 (2019). https://doi.org/10.1016/j.envres.2019.108561.

[32] S. Sah, A. Vandenberg, J. Smits, Treating chronic arsenic toxicity with high selenium lentil diets, Toxicology and Applied Pharmacology. 272 (2013) 256–2662. https://doi.org/10.1016/j.taap.2013.06.008.

[33] R.M. Krohn, R. Raqib, E. Akhtar, A. Vandenberg, J.E.G. Smits, A high-selenium lentil dietary intervention in Bangladesh to counteract arsenic toxicity: Study protocol for a randomized controlled trial, Trials. 17 (2016). https://doi.org/10.1186/s13063-016-1344-y.

[34] D. Thavarajah, J. Ruszkowski, A. Vandenberg, High Potential for Selenium Biofortification of Lentils (Lens culinaris L.), Journal of Agricultural and Food Chemistry. 56 (2008) 10747–10753. https://doi.org/10.1021/jf802307h.

[35] D. Thavarajah, A. Vandenberg, G.N. George, I.J. Pickering, Chemical form of selenium in naturally selenium-rich lentils (Lens culinaris L.) from Saskatchewan, Journal of Agricultural and Food Chemistry. 55 (2007) 7337–7341. https://doi.org/10.1021/jf070681i.

[36] C.M. Weekley, H.H. Harris, Which form is that? the importance of selenium speciation and metabolism in the prevention and treatment of disease, Chemical Society Reviews. 42 (2013) 8870–8894. https://doi.org/10.1039/c3cs60272a.

[37] A. Tarze, M. Dauplais, I. Grigoras, M. Lazard, N.T. Ha-Duong, F. Barbier, S. Blanquet, P. Plateau, Extracellular production of hydrogen selenide accounts for thiol-assisted toxicity of selenite against Saccharomyces cerevisiae, Journal of Biological Chemistry. 282 (2007) 8759–8767. https://doi.org/10.1074/jbc.M610078200.

[38] NCT01442727, Selenium in the Treatment of Arsenic Toxicity and Cancers, 2011.

[39] M. Alauddin, R. Cekovic, S. Alauddin, L. Bolevic, S. Saha, J.E. Spallholz, P.F. Laporte, S. Ahmed, H. Ahsan, J. Gailer, O. Ponomarenko, I.J. Pickering, S.P. Singh, G.N. George, Pharmacodynamic study of the selenium-mediated arsenic excretion in arsenicosis patients in Bangladesh, Environmental Arsenic in a ChangingWorld - 7th International Congress and Exhibition Arsenic in the Environment, 2018. 2 (2018) 391–394. https://doi.org/10.1201/9781351046633-152.

[40] G. Kaur, O. Ponomarenko, J. Zhou, D.P. Swanlund, K. Summers, N. Dolgova, O. Antipova, I.J. Pickering, G.N. George, E.M. Leslie, Studies of Selenium and Arsenic Mutual Protection in Human HepG2 Cells, Chemico-Biological Interactions. 327 (2020).

[41] S. Misra, R.W.M. Kwong, S. Niyogi, Transport of selenium across the plasma membrane of primary hepatocytes and enterocytes of rainbow trout, Journal of Experimental Biology. 215 (2012) 1491–1501. https://doi.org/10.1242/jeb.062307.

[42] D. Ganyc, W.T. Self, High affinity selenium uptake in a keratinocyte model, FEBS Letters. 582 (2008) 299–304. https://doi.org/https://doi.org/10.1016/j.febslet.2007.12.022.

[43] C. Decaens, M. Durand, B. Grosse, D. Cassio, Which in vitro models could be best used to study hepatocyte polarity?, Biology of the Cell. 100 (2008) 387–398. https://doi.org/https://doi.org/10.1042/BC20070127.

[44] P.F. Reay, C.J. Asher, Preparation and purification of 74As-labeled arsenate and arsenite for use in biological experiments, Analytical Biochemistry. 78 (1977) 557–560. https://doi.org/10.1016/0003-2697(77)90117-8.

[45] P. Gripon, S. Rumin, S. Urban, J. le Seyec, D. Glaise, I. Cannie, C. Guyomard, J. Lucas, C. Trepo, C. Guguen-Guillouzo, Infection of a human hepatoma cell line by hepatitis B virus., Proceedings of the National Academy of Sciences of the United States of America. 99 (2002) 15655–15660. https://doi.org/10.1073/pnas.232137699.

[46] P. Bachour-El Azzi, A. Sharanek, A. Burban, R. Li, R. le Guével, Z. Abdel-Razzak, B. Stieger, C. Guguen-Guillouzo, A. Guillouzo, Comparative localization and functional activity of the main hepatobiliary transporters in HepaRG cells and primary human hepatocytes, Toxicological Sciences. 145 (2015) 157–168. https://doi.org/10.1093/toxsci/kfv041.

[47] X. Liu, E.L. Lecluyse, K.R. Brouwer, R.M. Lightfoot, J.I. Lee, K.L.R. Brouwer, Use of Ca2+ modulation to evaluate biliary excretion in sandwich- cultured rat hepatocytes, Journal of Pharmacology and Experimental Therapeutics. 289 (1999) 1592–1599.

[48] I. Rahman, A. Kode, S.K. Biswas, Assay for quantitative determination of glutathione and glutathione disulfide levels using enzymatic recycling method, Nature Protocols. 1 (2007) 3159–3165. https://doi.org/10.1038/nprot.2006.378.

[49] J.K. Lee, E.M. Leslie, M.J. Zamek-Gliszczynski, K.L.R. Brouwer, Modulation of trabectedin (ET-743) hepatobiliary disposition by multidrug resistance-associated proteins (Mrps) may prevent hepatotoxicity, Toxicology and Applied Pharmacology. 228 (2008) 17–23. https://doi.org/10.1016/j.taap.2007.11.020.

[50] B. Swift, N.D. Pfeifer, K.L.R. Brouwer, Sandwich-cultured hepatocytes: An in vitro model to evaluate hepatobiliary transporter-based drug interactions and hepatotoxicity, Drug Metabolism Reviews. 42 (2010) 446–471. https://doi.org/10.3109/03602530903491881.

[51] M.J. Zamek-Gliszczynski, H. Xiong, N.J. Patel, R.Z. Turncliff, G.M. Pollack, K.L.R. Brouwer, Pharmacokinetics of 5 (and 6)-carboxy-2',7'-dichlorofluorescein and its diacetate promoiety in the liver, Journal of Pharmacology and Experimental Therapeutics. 304 (2003) 801–809. https://doi.org/10.1124/jpet.102.044107.

[52] R. Lashhab, A.C. Rumley, D. Arutyunov, M. Rizvi, C. You, H. Dimke, N. Touret, R. Zimmermann, M. Jung, X.Z. Chen, T. Alexander, E. Cordat, The kidney anion exchanger 1 affects tight junction properties via claudin-4, Scientific Reports. 9 (2019) 1–16. https://doi.org/10.1038/s41598-019-39430-9.

[53] K.C. Almquist, D.W. Loe, D.R. Hipfner, J.E. Mackie, S.P.C. Cole, R.G. Deeley, Characterization of the Mr 190,000 Multidrug Resistance Protein (MRP) in Drug-selected and Transfected Human Tumor Cells, Cancer Research. 55 (1995) 102–110.

[54] G.Y. di Veroli, C. Fornari, D. Wang, S. Mollard, J.L. Bramhall, F.M. Richards, D.I. Jodrell, Combenefit: an interactive platform for the analysis and visualization of drug combinations, Bioinformatics. 32 (2016) 2866–2868. https://doi.org/10.1093/bioinformatics/btw230.

[55] M. le Vee, E. Jigorel, D. Glaise, P. Gripon, C. Guguen-Guillouzo, O. Fardel, Functional expression of sinusoidal and canalicular hepatic drug transporters in the differentiated human hepatoma HepaRG cell line, European Journal of Pharmaceutical Sciences. 28 (2006) 109–117. https://doi.org/10.1016/j.ejps.2006.01.004.

[56] V. Gekeler, W. Ise, K.H. Sanders, W.R. Ulrich, J. Beck, The leukotriene LTD4 receptor antagonist MK571 specifically modulates MRP associated multidrug resistance,

Biochemical and Biophysical Research Communications. 208 (1995) 345–352. https://doi.org/10.1006/bbrc.1995.1344.

[57] E. Jigorel, M. le Vee, C. Boursier-Neyret, Y. Parmentier, O. Fardel, Differential Regulation of Sinusoidal and Canalicular Hepatic Drug Transporter Expression by Xenobiotics Activating Drug-Sensing Receptors in Primary Human Hepatocytes, Drug Metabolism and Disposition. 34 (2006) 1756–1763. https://doi.org/10.1124/dmd.106.010033.

[58] S. Xu, J. Weerachayaphorn, S.Y. Cai, C.J. Soroka, J.L. Boyer, Aryl hydrocarbon receptor and NF-E2-related factor 2 are key regulators of human MRP4 expression, American Journal of Physiology - Gastrointestinal and Liver Physiology. 299 (2010) G126-135. https://doi.org/10.1152/ajpgi.00522.2010.

[59] G. Kaur, Mechanistic Studies of Arsenic and Selenium Detoxification [thesis]. University of Alberta; 2020.

[60] C.G. Dietrich, R. Ottenhoff, D.R. de Waart, R.P.J. Oude Elferink, Role of MRP2 and GSH in intrahepatic cycling of toxins, Toxicology. 167 (2001) 73–81. https://doi.org/https://doi.org/10.1016/S0300-483X(01)00459-0.

[61] A.H. Smith, E.O. Lingas, M. Rahman, Contamination of drinking-water by arsenic in Bangladesh: A public health emergency, Bulletin of the World Health Organization. 78 (2000). https://doi.org/10.1590/S0042-96862000000900005.

[62] C.M. Steinmaus, C. Ferreccio, J.A. Romo, Y. Yuan, S. Cortes, G. Marshall, L.E. Moore, J.R. Balmes, J. Liaw, T. Golden, A.H. Smith, Drinking water arsenic in northern chile: High cancer risks 40 years after exposure cessation, Cancer Epidemiology Biomarkers and Prevention. 22 (2013). https://doi.org/10.1158/1055-9965.EPI-12-1190.

[63] J. Liaw, G. Marshall, Y. Yuan, C. Ferreccio, C. Steinmaus, A.H. Smith, Increased childhood liver cancer mortality and arsenic in drinking water in northern Chile, Cancer Epidemiology Biomarkers and Prevention. 17 (2008). https://doi.org/10.1158/1055-9965.EPI-07-2816.

[64] E.M. Hall, J. Acevedo, F.G. López, S. Cortés, C. Ferreccio, A.H. Smith, C.M. Steinmaus, Hypertension among adults exposed to drinking water arsenic in Northern Chile, Environmental Research. 153 (2017). https://doi.org/10.1016/j.envres.2016.11.016.

[65] X. Cui, Y. Kobayashi, T. Hayakawa, S. Hirano, Arsenic speciation in bile and urine following oral and intravenous exposure to inorganic and organic arsenics in rats, Toxicological Sciences. 82 (2004). https://doi.org/10.1093/toxsci/kfh265.

[66] N. Ishihara, T. Matsushiro, Biliary and urinary excretion of metals in humans, Archives of Environmental Health. 41 (1986). https://doi.org/10.1080/00039896.1986.9936705.

[67] G. Ghibellini, L.S. Vasist, E.M. Leslie, W.D. Heizer, R.J. Kowalsky, B.F. Calvo, K.L.R. Brouwer, In vitro-in vivo correlation of hepatobiliary drug clearance in humans, Clinical Pharmacology and Therapeutics. 81 (2007). https://doi.org/10.1038/sj.clpt.6100059.

[68] V.E. Kostrubsky, S.C. Strom, J. Hanson, E. Urda, K. Rose, J. Burliegh, P. Zocharski, H. Cai, J.F. Sinclair, J. Sahi, Evaluation of hepatotoxic potential of drugs by inhibition of bile-acid transport in cultured primary human hepatocytes and intact rats, Toxicological Sciences. 76 (2003). https://doi.org/10.1093/toxsci/kfg217.

[69] T.L. Marion, E.M. Leslie, K.L.R. Brouwer, Use of sandwich-cultured hepatocytes to evaluate impaired bile acid transport as a mechanism of drug-induced hepatotoxicity, Molecular Pharmaceutics. 4 (2007). https://doi.org/10.1021/mp0700357.

[70] S. Sharma, E.C.S. Ellis, R. Gramignoli, K. Dorko, V. Tahan, M. Hansel, D.R. Mattison, S.N. Caritis, R.N. Hines, R. Venkataramanan, S.C. Strom, Hepatobiliary disposition of 17-OHPC and taurocholate in fetal human hepatocytes: A comparison with adult human hepatocytes, Drug Metabolism and Disposition. 41 (2013). https://doi.org/10.1124/dmd.112.044891.

[71] T.A. Marschall, J. Bornhorst, D. Kuehnelt, T. Schwerdtle, Differing cytotoxicity and bioavailability of selenite, methylselenocysteine, selenomethionine, selenosugar 1 and trimethylselenonium ion and their underlying metabolic transformations in human cells, Molecular Nutrition and Food Research. 60 (2016). https://doi.org/10.1002/mnfr.201600422.

[72] I. Cordero-Herrera, S. Cuello, L. Goya, Y. Madrid, L. Bravo, C. Cámara, S. Ramos, Molecular mechanisms involved in the protective effect of selenocystine against methylmercury-induced cell death in human HepG2 cells, Food and Chemical Toxicology. 59 (2013). https://doi.org/10.1016/j.fct.2013.06.057.

[73] C.S. Hoefig, K. Renko, J. Köhrle, M. Birringer, L. Schomburg, Comparison of different selenocompounds with respect to nutritional value vs. toxicity using liver cells in culture, Journal of Nutritional Biochemistry. 22 (2011). https://doi.org/10.1016/j.jnutbio.2010.08.006.

[74] A.P. Kipp, J. Frombach, S. Deubel, R. Brigelius-Flohé, Selenoprotein W as biomarker for the efficacy of selenium compounds to act as source for selenoprotein biosynthesis, in: Methods in Enzymology, 2013. https://doi.org/10.1016/B978-0-12-405882-8.00005-2.

[75] K.T. Suzuki, T. Tomita, Y. Ogra, M. Ohmichi, Glutathione-conjugated arsenics in the potential hepato-enteric circulation in rats, Chemical Research in Toxicology. 14 (2001). https://doi.org/10.1021/tx0155496.

[76] https://clinicaltrials.gov/ct2/show/NCT01442727, n.d.

[77] https://clinicaltrials.gov/ct2/show/NCT02377635, n.d.

[78] W. Wang, L. Yang, S. Hou, J. Tan, H. Li, Prevention of endemic arsenism with selenium, Current Science. 81 (2001).

[79] https://clinicaltrials.gov/ct2/show/NCT02429921, n.d.

[80] S. Kokarnig, A. Tsirigotaki, T. Wiesenhofer, V. Lackner, K.A. Francesconi, S.A. Pergantis, D. Kuehnelt, Concurrent quantitative HPLC-mass spectrometry profiling of small selenium species in human serum and urine after ingestion of selenium supplements, Journal of Trace Elements in Medicine and Biology. 29 (2015). https://doi.org/10.1016/j.jtemb.2014.06.012.

[81] M. Sandholm, Function of Erythrocytes in Attaching Selenite-Se onto Specific Plasma Proteins, Acta Pharmacologica et Toxicologica. 36 (1975). https://doi.org/10.1111/j.1600-0773.1975.tb00799.x.

[82] M. Sandholm, The Initial Fate of a Trace Amount of Intravenously Administered Selenite, Acta Pharmacologica et Toxicologica. 33 (1973). https://doi.org/10.1111/j.1600-0773.1973.tb01500.x.

[83] K.T. Suzuki, Y. Shiobara, M. Itoh, M. Ohmichi, Selective uptake of selenite by red blood cells, in: Analyst, 1998. https://doi.org/10.1039/a706230c.

[84] Y. Shiobara, K.T. Suzuki, Binding of selenium (administered as selenite) to albumin after efflux from red blood cells, Journal of Chromatography B: Biomedical Applications. 710 (1998). https://doi.org/10.1016/S0378-4347(98)00142-X.

[85] N. Esaki, T. Nakamura, H. Tanaka, T. Suzuki, Y. Morino, K. Soda, Enzymic synthesis of selenocysteine in rat liver, Biochemistry. 20 (1981) 4492–4496. https://doi.org/10.1021/bi00518a039.

[86] R.F. Burk, K.E. Hill, Regulation of Selenium Metabolism and Transport, Annual Review of Nutrition. 35 (2015). https://doi.org/10.1146/annurev-nutr-071714-034250.

[87] S. Ito, I. Ieiri, M. Tanabe, A. Suzuki, S. Higuchi, K. Otsubo, Polymorphism of the ABC transporter genes, MDR1, MRP1 and MRP2/cMOAT, in healthy Japanese subjects, Pharmacogenetics. 11 (2001) 175–184. https://doi.org/10.1097/00008571-200103000-00008.

[88] S. Sookoian, G. Castaño, T.F. Gianotti, C. Gemma, C.J. Pirola, Polymorphisms of MRP2 (ABCC2) are associated with susceptibility to nonalcoholic fatty liver disease., The Journal of Nutritional Biochemistry. 20 (2009) 765–70. https://doi.org/10.1016/j.jnutbio.2008.07.005.

[89] M. Itoda, Y. Saito, A. Soyama, M. Saeki, N. Murayama, S. Ishida, K. Sai, M. Nagano, H. Suzuki, Y. Sugiyama, S. Ozawa, J. Sawada Ji, Polymorphisms in the ABCC2 (cMOAT/MRP2) gene found in 72 established cell lines derived from Japanese individuals: an association between single nucleotide polymorphisms in the 5'-untranslated region and exon 28., Drug Metabolism and Disposition: The Biological Fate of Chemicals. 30 (2002) 363–4.

3. Arsenic Sinusoidal Efflux is Stimulated by Methylselenocysteine and Mediated by Human Multidrug Resistance Protein 4 (MRP4/*ABCC4*)

3.1 Introduction

Chronic exposure to the Group I (proven) human carcinogen arsenic causes lung, skin, and bladder cancer [1]. In addition to causing cancer in humans, arsenic exposure also leads to a myriad of many adverse long-term health effects including cardiovascular disease, immune system dysfunction and type II diabetes [2–4]. Conservative estimates suggest between 92-220 million people worldwide are exposed to arsenic through contaminated drinking water at levels exceeding the World Health Organization guideline of 10 μg/L [5]. Although reducing arsenic-contaminated drinking water sources should be priority, humans remain susceptible to arsenic-induced diseases decades after cessation of exposure [6].

Arsenic naturally occurs in the environment as inorganic forms arsenate and arsenite. Arsenate (pKa ~2.3, 6.8 and 11.3) exists predominantly as $H_2AsO_4^-$ and $HAsO_4^{2-}$ at pH 7 and is taken up by cells through sodium-dependent phosphate transporters such as the Na^+/P_i cotransporter type IIb (gene name *SLC34A2*) [7,8]. At pH 7, arsenite (pKa ~9.2) is present in the form of $As(OH)_3$ and can permeate into cells through aquaglyceroporin channels [9–11]. There is also evidence of arsenite uptake by facilitated glucose transporters especially GLUT1 (*SLC2A1)* [10,12].

Arsenic methylation is catalyzed by a series of oxidative methylation reactions by arsenite methyltransferase (As3MT), yielding the major products: monomethylarsonic acid (MMA^V), monomethylarsonous acid (MMA^{III}), dimethylarsinic acid (DMA^V), and dimethylarsinous acid (DMA^{III}) [13]. Glutathione can form conjugates with arsenite, MMA^{III}, and DMA^{III} ($As(GS)_3$, $MMA(GS)_2$, and DMA(GS), respectively), but only $As(GS)_3$, $MMA(GS)_2$ have been identified in biological samples [14,15]. The ATP-binding cassette (ABC) transporters multidrug resistance

protein (MRP)2 (*ABCC2*) and MRP4 (*ABCC4*) are localized to the canalicular and sinusoidal surfaces of hepatocytes, respectively. There is strong evidence that these two MRPs are important for efflux of arsenic metabolites from human hepatocytes [16–18]. The focus of the current work is on hepatic sinusoidal export of arsenic. Human MRP4 is known, at least *in vitro*, to transport DMA^V and $MMA(GS)_2$ with high affinity and its localization at the sinusoidal surface of hepatocytes and apical surface of renal proximal tubule cells make it ideal for the urinary elimination of arsenic hepatic metabolites [19].

Selenium is an essential trace nutrient with a recommended dietary allowance of 55 µg/day but is toxic in excess with an upper tolerable limit of 400 µg/day [20]. Selenoproteins contain selenocysteine in their active sites and have important biological functions including redox regulation [21,22]. A mutually protective relationship between arsenic and selenium has been observed and is due, at least in part, to the formation and biliary excretion of the seleno-bis (*S*-glutathionyl) arsinium ion $[(GS)_2AsSe]^-$, which has been detected in animal models, including rats and hamsters, treated with arsenite and selenite [23–25]. When lab animals were given toxic doses of arsenite and selenite, there was less liver damage than when they were dosed with the compounds individually [26].

In arsenic-endemic regions, participants in selenium-supplementation trials have been given various forms of selenium including selenium-enriched yeast and lentils, as well as purified forms of selenium as tablets, including selenomethionine and selenite [27–33]. Although there are many selenium-supplementation trials that have been completed and some still ongoing, characterization of hepatic handling of arsenic and the influence of selenium on this has only recently been characterized in relevant human *in vitro* models [34]. While investigating the

influence of different forms of selenium on arsenic biliary excretion, we made the novel and unexpected observation that methylselenocysteine (MeSeCys), stimulated the sinusoidal export of arsenic from human HepaRG cells, an immortalized human hepatocyte cell line [31] and Chapter 2.

MeSeCys is a compound thought to have beneficial health effects including anti-cancer activity [35]. Some dietary sources that are naturally rich in MeSeCys include garlic, onions, and broccoli [36]. In contrast, grains and legumes contain substantially more selenomethionine than MeSeCys [36]. Although MeSeCys is thought to be beneficial in disease prevention, this compound has not been intentionally included in selenium-supplementation trials in arsenic-endemic regions. Selenium speciation studies using commercially available selenized yeast demonstrated that MeSeCys formed from dimethyldiselenide, a degradation product of selenomethionine, after reacting with cysteine or cystine upon heating to 150℃ [37]. Thus, dietary components high in SeMet have the potential to form MeSeCys.

These studies led us to further characterize the sinusoidal export of arsenic in HepaRG cells with the hypothesis that MeSeCys-dependent and independent arsenic transport is mediated by MRP4. Previous studies with sandwich cultured human hepatocytes and HepaRG cells suggested arsenic sinusoidal efflux was glutathione-dependent and mediated by an MRP [18,34]. Since MRP4 transports DMA^V and $MMA(GS)_2$ *in vitro*, it was a logical candidate to investigate. Arsenic sinusoidal efflux in the presence of MeSeCys in HepaRG cells was measured under various conditions to determine if this process was MRP4-mediated. Then, stable *ABCC4*-knockdown HepaRG cells were generated to further characterize sinusoidal efflux of arsenic in the presence of MeSeCys.

3.2 Materials and Methods [*]

3.2.1 Chemicals and Reagents

^{73}As-arsenate (> 5.6 Ci/mg) was purchased from Los Alamos Meson Production Facility (Los Alamos, NM)[†]. N-(2-Hydroxyethyl)piperazine-N'-(2-ethanesulfonic acid) (HEPES), polyvinylidene difluoride membranes, sodium(meta) arsenite, MeSeCys, bovine serum albumin (BSA), reduced glutathione (GSH), William's E media, dimethyl sulfoxide (DMSO), hydrocortisone 21-hemisuccinate sodium salt, fetal bovine serum (FBS), standard Hanks' balanced salt solution (HBSS), Ca^{2+}/Mg^{2+}-free HBSS, buthionine sulfoximine (BSO), sodium bicarbonate ($NaHCO_3$), Immobilon Crescendo Western HRP substrate, and puromycin dihydrochloride were purchased from MilliporeSigma (Oakville, ON, Canada). The MISSION® shRNA plasmid DNA glycerol stocks of TRC2 pLKO.5-puro empty vector control plasmid, pLKO.5-puro non-mammalian shRNA control plasmid (non-target), and *ABCC4* KD clones targeting the 3'-untranslated region and coding DNA sequence of *ABCC4* TRCN#0000005264 (NM_005845) (5264) and TRCN#0000297334 (NM_005845) (7334), respectively, were also purchased from Millipore Sigma (Oakville, ON, Canada). Triton X-100 was purchased from Fisher Scientific (Fair Lawn, NJ). GlutaMAX supplement, human recombinant insulin and Pierce™ bicinchoninic acid (BCA) protein assay reagent were purchased from Thermo Scientific (Rockford, IL). Creatine kinase, creatine phosphate, GSH reductase, NADPH, Complete Mini EDTA-free protease inhibitor

[*] This research project received ethics approval from the University of Alberta Research Ethics Board, Project Name "The role of transport proteins in toxicology", protocol number 00001646, November 28, 2009.

[†] The isotope (^{73}As) used in this research were supplied by the United States Department of Energy Office of Science by the Isotope Program in the Office of Nuclear Physics.

cocktail tablets, X-tremeGENE9 transfection reagent were purchased from Roche, Applied Sciences (Indianapolis, IN).

3.2.2 Antibodies

The MRP4-specific rat monoclonal antibody (M_4I-10) was purchased from Abcam Inc. (Cambridge, MA). The Na^+/K^+-ATPase mouse monoclonal (H-3/SC-48345) was purchased from Santa Cruz Biotechnology (Dallas, TX). The IgG (H+L) cross-adsorbed goat anti-mouse and anti-rat HRP conjugated polyclonal secondary antibodies were purchased from ThermoFisher Scientific (Waltham, MA).

3.2.3 Preparation of reagents

Arsenite and MeSeCys were freshly prepared for all experiments by dissolving in sterile phosphate buffered saline (PBS) before serial dilutions of each compound in growth media for immediate use. ^{73}As-arsenite was reduced from ^{73}As-arsenate with metabisulfite-thiosulfate reducing agent, as previously described [38].

3.2.4 HepaRG cell culture ‡

HepaRG cells were obtained from Biopredic International at passage 12 (St Gregoire, France). A working bank in liquid N_2 was then established according to the instructions provided by Biopredic International. For all experiments, HepaRG cells were used between passages 15-18. HepaRG cells were first seeded from frozen vials at a density of 2 x 10^6 cells/T-75 flasks and maintained in growth media comprised of Williams' E medium supplemented with 10% FBS, 5 µg/ml human recombinant insulin, 50 µM hydrocortisone hemisuccinate, and 200 mM

‡ The authors acknowledge Dr. Christiane Guguen-Guillouzo, Dr. Philippe Gripon, Dr. Christian Trepo, and Biopredic International© for supplying the undifferentiated cryopreserved HepaRG cells.

GlutaMAX™, as established previously [39]. After 2 weeks, HepaRG cells were seeded into 6- or 24-well plates at densities of 200 000 or 55 000 cells/well, respectively. HepaRG cells were maintained in growth media for 2 weeks, then differentiated by including 0.75% dimethylsulfoxide (DMSO) in growth media for two days, followed by 1.5% DMSO for 12 to 40 days. All experiments were performed within 4 weeks following the end of the 2-week differentiation period, as previously described [40]. HepaRG cells were maintained at 37°C in a humidified incubator with 95% air/5% CO_2 with media changes every 2-3 days.

3.2.5 Human Hepatocyte Culture

With the approval of the University of Alberta Human Ethics Review Board (protocol number 00001646), human hepatocytes were isolated from the liver of patients undergoing hepatic resection at the University of Alberta Hospital, as previously described. Hepatocytes were seeded and maintained as previously described [18].

3.2.6 Efflux studies

Fully differentiated HepaRG cells in 24-well plates or SCHH cells in 12-well plates, were incubated in fresh growth media containing ^{73}As-arsenite (1 µM, 100 nCi/well) ± MeSeCys (1 µM) for 1 or 24 hr, respectively, prior to measuring efflux across sinusoidal membranes. Cells were washed twice with standard ice-cold HBSS, then 37°C standard HBSS was added to each well. Plates were incubated at 37°C and at indicated time points, buffer was removed (50 µL from 24-well plates, 100 µL from 12-well plates) and placed in a scintillation vial. After the last time point, cells were washed twice with ice-cold HBSS buffer and lysed in 0.5% Triton X-100. ^{73}As-arsenite in efflux buffer was quantified using liquid scintillation counting with the

PerkinElmer MicroBeta^2 liquid scintillation counter. Efflux activity was normalized to total protein levels of cell lysates, determined using a BCA assay.

To evaluate the influence of GSH on arsenic efflux, HepaRG cells were treated with the GSH synthesis inhibitor, BSO (500 µM) for 48 hr prior to and during efflux experiments. Previously we have shown that these conditions depleted GSH by 70% [34]. The influence of the general MRP-inhibitor MK571 (100 µM) on arsenic efflux was evaluated by treating HepaRG cells with this compound for 1 hr prior to and for the duration of efflux. The temperature dependence of sinusoidal excretion of arsenic was evaluated by measuring arsenic efflux by HepaRG cells on ice. To determine the influence of the MRP4 inhibitor ceefourin-1 on arsenic efflux, HepaRG cells were treated with ceefourin-1 for 1 hr prior to initiation and duration of efflux.

After efflux, the release of lactate dehydrogenase (LDH) from cells was quantified using the Cytotoxicity Detection Kit (Roche, Mississauga ON), as previously described [18,34]. All efflux data had <3% LDH release at the 10 min time point indicating that efflux was being measured rather than cellular leakage due to cytotoxicity.

3.2.7 shRNA knockdown of *ABCC4* in HepaRG cells

HepaRG cells were seeded into 6-well plates at 2 x 10^5 cells/well and transfected with shRNA targeting the MRP4 gene *ABCC4* (1 µg) with DNA:XtremeGENE 9 (3 µl) as per manufacturer's instructions. HepaRG cells were also separately transfected with the empty vector pLKO.5-puro and non-target (pLKO.5-puro non-mammalian shRNA) as negative controls. Cells were selected 72 hr post-transfection and maintained as described above, with the addition of 2 µg/ml puromycin. After ~4 weeks of selection, when confluency was reached, cells were trypsinized and seeded in plates at the appropriate cell density for

proliferation/differentiation for characterization by immunoblot, and efflux studies, as described above. Cells were maintained in media containing 2 µg/ml puromycin except this was reduced to 1 µg/ml during the differentiation period and experiments.

3.2.8 Whole cell lysate preparations of HepaRG cells and immunoblotting

Fully differentiated parental HepaRG cells, as well as HepaRG cells expressing empty vector, non-target or *ABCC4*-targeted shRNA maintained in 6-well plates were lysed in 100 µL of 0.5% Triton X-100 containing protease inhibitors. Protein concentrations were determined using a BCA assay. Then 30 µg protein was subjected to SDS-PAGE (6%) and transferred to a polyvinylidene fluoride (PVDF) membrane. Immunoblotting of the PVDF membrane was performed using the MRP4-specific monoclonal rat antibody M_4I-10 (1:2000) followed by secondary HRP-conjugated anti-rat (1:5000) antibody. A Na^+/K^+-ATPase monoclonal mouse antibody (H-30) (1:10 000) was used to detect Na^+/K^+-ATPase as a sample loading control, followed by HRP-conjugated anti-mouse (1:10 000) antibody. All antibodies were prepared in 4% skim milk. PVDF membranes were imaged using ChemiDoc™ (BioRad) after addition of Immobilon Crescendo Western HRP substrate. Relative protein levels of MRP4 were quantified using ImageJ software normalized against the Na^+/K^+-ATPase signal. Levels of MRP4 are reported relative to parental HepaRG cells.

3.2.9 Data analysis and statistics

Statistical differences in ^{73}As-arsenic efflux in the presence and absence of MeSeCys over time were determined using a two-way ANOVA followed by a Sidak's post hoc-test. For all efflux studies, a one-way ANOVA followed by a Tukey's post hoc test was used to determine if there were statistical differences between ^{73}As-arsenic sinusoidal efflux and all other conditions

tested. A one-way ANOVA followed by Dunnett's post hoc test was used to determine if there were statistical differences in densitometry data. For comparisons of ^{73}As-arsenic sinusoidal efflux in the presence and absence of MeSeCys between parental, empty vector, non-target, and *ABCC4*-knockdown cells, a two-way ANOVA followed by a Sidak's post-hoc test was used to determine significance between all conditions. An alpha value of <0.05 was used to define significance for all statistical analyses performed.

3.3 Results

3.3.1 Sinusoidal arsenic efflux is stimulated by MeSeCys in HepaRG cells and SCHH

To further characterize our novel and unexpected observation that MeSeCys stimulated arsenic sinusoidal efflux by ~1.6-fold in HepaRG cells [34], time and dose dependent studies were completed. Fully differentiated HepaRG cells were treated with ^{73}As-arsenite (1 µM, 100 nCi) alone or in the presence of MeSeCys (1 µM) for 1 hr. Then, ^{73}As-arsenic efflux was measured across sinusoidal membranes at the indicated time points. Export of ^{73}As-arsenic was detected across sinusoidal surfaces with increased efflux in the presence of MeSeCys at each time point. Sinusoidal export of arsenic in the absence and presence of MeSeCys ranged from 0.64-5.11 pmol/mg protein and 1.23-6.86 pmol/mg protein, respectively. The stimulation of efflux in the presence of MeSeCys was significant at each time point and ranged from 1.2-1.9-fold **(Fig 3.1A).**

To determine if MeSeCys stimulation of arsenic sinusoidal efflux was dose dependent, fully differentiated HepaRG cells were treated with ^{73}As-arsenite (1 µM, 100 nCi) alone or in the presence of MeSeCys (1, 3 or 10 µM) for 1 hr. ^{73}As-arsenic efflux was measured across sinusoidal membranes at a 10 min time point. Data shown are a percentage of sinusoidal efflux

of arsenic alone (4.1 pmol/mg protein) **(Fig 3.1B).** In the presence of 1, 3, and 10 µM MeSeCys, sinusoidal efflux of arsenic was simulated by 1.2-, 1.5, and 1.6-fold, relative to untreated control **(Fig 3.1B).**

SCHH are considered the gold-standard for measuring hepatobiliary transport. Consistent with our observations with HepaRG cells, stimulation of sinusoidal export of ^{73}As-arsenite (1 µM, 100 nCi) by MeSeCys (1 µM), was also observed with a single preparation of SCHH. For the 5, 10, and 15 min time points there was ~1.2-fold stimulation of sinusoidal efflux of arsenic in the presence of MeSeCys **(Fig 3.1C).** Shown are data from an individual experiment with triplicate determinations, thus it was not appropriate to indicate statistical significance.

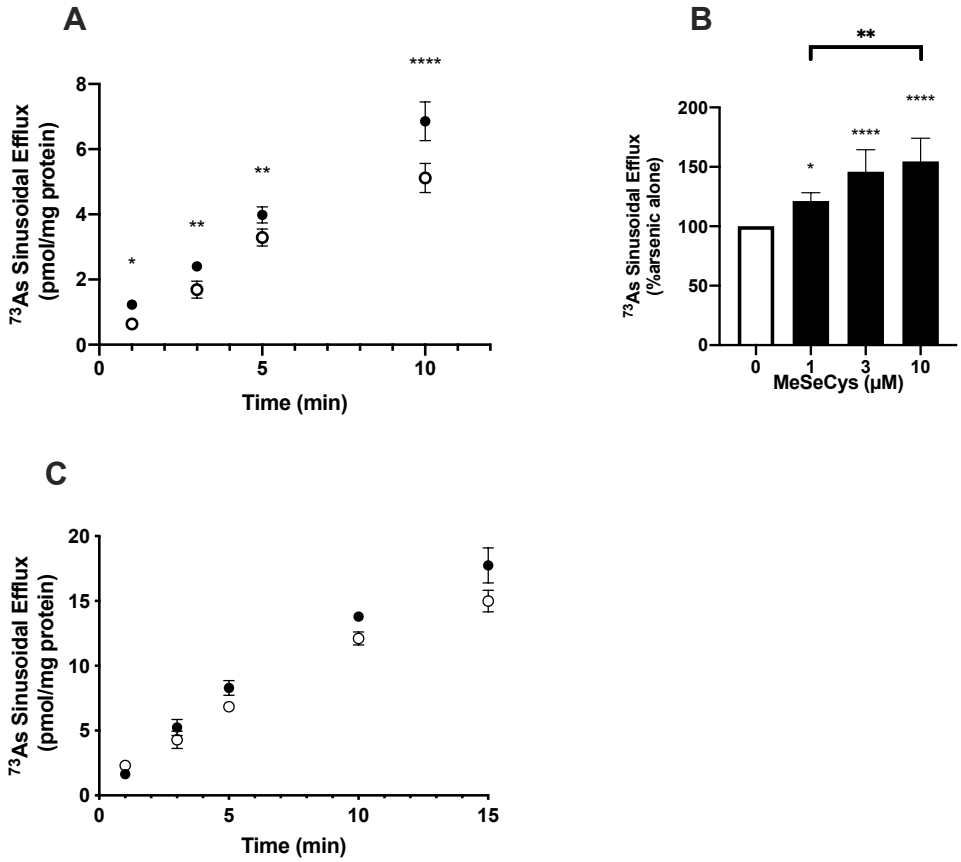

Figure 3.1: MeSeCys stimulates arsenic sinusoidal efflux [§]. **(A)** HepaRG cells were treated with media containing ^{73}As-arsenite (1 μM, 100 nCi) and MeSeCys (1 μM) for 1 hr at 37℃. Then cells were washed, and incubation media was replaced with standard HBSS at 37℃. Sinusoidal efflux of ^{73}As-arsenite was sampled at indicated time points and quantified by beta liquid scintillation counting. Each symbol represents the mean ± SD of four independent experiments with closed circles indicating ^{73}As-arsenite efflux in the presence of MeSeCys, and open circles indicating ^{73}As-arsenite efflux alone. A two-way ANOVA Sidak's multiple comparisons test was used to determine significant differences in ^{73}As-arsenite efflux between the time points with * P<0.05, ** P<0.01, and ****P<0.0001. **(B)** HepaRG cells were treated in the same manner as (A), with the exception of different concentrations of MeSeCys (0, 1, 3, or 10 μM). Sinusoidal efflux of ^{73}As-arsenite was sampled at 10 min and quantified by beta liquid scintillation counting. Data are shown as % ^{73}As-arsenite efflux without MeSeCys and bars represent the mean ± SD of three independent experiments. Significant differences between ^{73}As-arsenite sinusoidal efflux in the presence and absence of MeSeCys at each time point are indicated with * P <0.05, ** P<0.01 and ****P<0.001 (One-way ANOVA followed by Tukey's multiple comparisons test) **(C)** SCHH were treated with media containing ^{73}As-arsenite (1 μM, 100 nCi) and MeSeCys (1 μM) for 24 hr at 37℃. Sinusoidal efflux of ^{73}As-arsenite alone and in the presence of MeSeCys was measured as described for (A). Symbols represent the mean ± SD of triplicates from a single experiment with closed circles indicating ^{73}As-arsenite efflux in the presence of MeSeCys, and open circles indicated ^{73}As-arsenite efflux alone.

[§] **Fig 3.1C** experiment was conducted by Dr. Gurnit Kaur. Primary hepatocytes used in Fig 3.1C were provided by Drs Norman Kneteman and Donna Douglas.

3.3.2 Arsenic sinusoidal export is GSH- and temperature-dependent and MRP-mediated

To further characterize sinusoidal export of arsenic and its stimulation by MeSeCys, transport was measured after GSH-depletion, at 4°C, in the presence of MK571 (a general MRP inhibitor), and in the presence of ceefourin-1 (MRP4 inhibitor). Fully differentiated HepaRG cells were treated with ^{73}As-arsenite (1 µM, 100 nCi) in the presence and absence of MeSeCys (1 µM) for 1 hr and then efflux was measured at a 10 min time point. Similar to Fig 1A-C, ^{73}As-arsenic sinusoidal efflux was stimulated by MeSeCys by 1.4-fold **(Fig 3.2A).**

In previous studies using HepaRG cells and SCHH, arsenic biliary and sinusoidal export were both GSH-dependent [18,34]. Similar experiments were completed to determine if the stimulatory effect of MeSeCys on arsenic sinusoidal efflux was GSH-dependent. HepaRG cells were treated with BSO (500 µM), an inhibitor of the rate-limiting step in GSH synthesis, and this resulted in a 27% reduction of arsenic-alone export, and a complete loss of MeSeCys-stimulated arsenic export (30% reduction relative to the arsenic alone condition) **(Fig 3.2A).**

Next, temperature dependence of arsenic sinusoidal export alone and in the presence of MeSeCys was evaluated at 4℃. Arsenic-alone sinusoidal efflux was decreased by 57% at 4℃ compared to the 37℃ control, and there was a complete loss of MeSeCys-stimulated arsenic export (54% reduction relative to the arsenic alone condition) **(Fig 3.2A).** The reduced efflux of arsenic at 4℃ suggests that sinusoidal efflux of arsenic is predominantly transporter-mediated, consistent with previous findings [18,34].

MK571 is an LTD_4 receptor antagonist and general MRP inhibitor [34], previously shown to inhibit sinusoidal efflux of arsenic from SCHH and HepaRG cells [18,34]. To determine if MeSeCys-stimulated arsenic export is also inhibited, cells were treated with MK571 (100 µM).

This resulted in a 31% reduction of sinusoidal efflux of ^{73}As-arsenic from HepaRG in the arsenic alone condition, and a complete loss of MeSeCys-stimulated arsenic export (29% reduction relative to the arsenic alone condition) **(Fig 3.2A).**

MRP4 is the only MRP at the sinusoidal surface of hepatocytes with an established role in arsenic transport [17,35]. Therefore, it was the most logical candidate transporter for further characterization. Ceefourin-1 is a pharmacological inhibitor that is more selective for MRP4, than MK571 [43] and its influence on arsenic efflux from fully differentiated HepaRG cells at 20 µM was tested. Similar to the results for MK571, ceefourin-1 decreased the sinusoidal efflux of ^{73}As-arsenic alone by 35% and resulted in a complete loss of MeSeCys-stimulated arsenic export (27% reduction relative to the arsenic alone condition) **(Fig 3.2A).**

Next, the dose dependence of ceefourin-1 inhibition of arsenic sinusoidal efflux was explored. Fully differentiated HepaRG cells were treated with ceefourin-1 at increasing concentrations (0, 1, 5, 10, or 20 µM). As expected, in the absence of ceefourin-1, arsenic sinusoidal efflux was stimulated by 1.3-fold in the presence of MeSeCys **(Fig 3.2B).** When HepaRG cells were treated with 1 µM ceefourin-1, results were similar to untreated cells, and no inhibition of sinusoidal efflux of arsenic in the presence or absence of MeSeCys was observed **(Fig 3.2B).** In the presence of 5 µM ceefourin-1, sinusoidal efflux of arsenic alone was not inhibited, but the stimulatory effect of MeSeCys on arsenic efflux was diminished by 17% relative to untreated HepaRG cells **(Fig 3.2B).** When cells were treated with 10 µM ceefourin-1, sinusoidal efflux of arsenic alone and in the presence of MeSeCys was decreased by 44% and 42%, respectively **(Fig 3.2B).** The largest decrease in sinusoidal efflux of arsenic was observed after treatment with 20 µM ceefourin-1, where arsenic sinusoidal efflux alone and in the

presence of MeSeCys decreased 57% relative to untreated cells **(Fig 3.2B).** The half inhibitory concentrations for ceefourin-1 after cells were treated with arsenic alone and in the presence of MeSeCys were 7.4 ± 0.2 µM and 4.8 ± 0.2 µM, respectively **(Fig 3.2Bii).** Overall, sinusoidal efflux of arsenic alone and in the presence of MeSeCys is GSH- and temperature-dependent and likely mediated by MRP4.

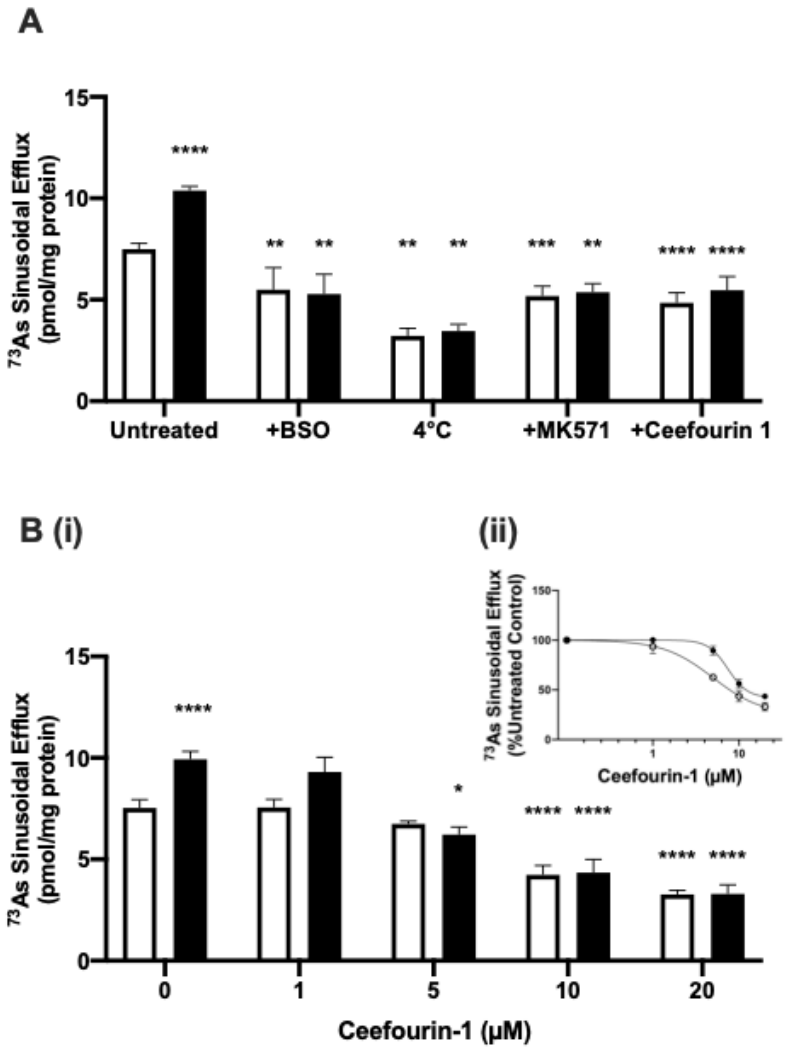

Figure 3.2: The effect of BSO, temperature, MK571 and ceefourin-1 on sinusoidal efflux of arsenic in the presence and absence of MeSeCys. (A) Efflux of ^{73}As-arsenite alone and in the presence of MeSeCys were evaluated after 48 hr pre-treatment of cells with BSO (500 µM), 30 min treatment with MK571 (100 µM) or ceefourin-1 (20 µM) before and during efflux, and at 4°C using ice-cold buffers. White bars represent means ± SD of ^{73}As-arsenite sinusoidal efflux and black bars represent means ± SD of ^{73}As-arsenite sinusoidal efflux in the presence of MeSeCys from three independent experiments. Conditions that are significantly different than untreated ^{73}As-arsenite sinusoidal efflux are indicated with ** P<0.01, ***P<0.001, and ****P<0.0001 (One-way ANOVA followed by a Tukey's post hoc test). **(B) (i)** Efflux of ^{73}As-arsenite alone and in the presence of MeSeCys were evaluated after treatment of cells with ceefourin-1 (1, 5, 10, or 20 µM) before and during efflux. White bars represent means ± SD of ^{73}As-arsenite sinusoidal efflux and black bars represent means ± SD of ^{73}As-arsenite sinusoidal efflux in the presence of MeSeCys from three independent experiments. Conditions that are significantly different than the untreated ^{73}As-arsenite sinusoidal efflux are indicated with * P<0.05, and ****P<0.0001 (One-way ANOVA followed by a Tukey's post hoc test). **(ii)** shows these data plotted as an inhibition dose response curve using the log(inhibitor) vs. response variable slope fit (GraphPad Prism 8) White circles represent means ± SD of ^{73}As-arsenite sinusoidal efflux and black circles represent means ± SD of ^{73}As-arsenite sinusoidal efflux in the presence of MeSeCys.

3.3.3 *ABCC4* knockdown studies

HepaRG cells were stably transfected with shRNAs targeting the MRP4 gene *ABCC4*. A non-mammalian target (non-target) and empty vector shRNA were included as negative controls. Two different cell clones stably expressing two different *ABCC4* targeted shRNA (clones 5264 and 7334) were established.

3.3.4 HepaRG cells expressing *ABCC4*-targeted shRNA have lower levels of MRP4 than control HepaRG cells

To evaluate the efficiency of the *ABCC4*-knockdown, whole cell lysates of fully differentiated parental, empty vector, non-target and *ABCC4* knockdown HepaRG cells were prepared and subjected to immunoblots. MRP4 was detected at similar levels in parental, empty vector, and non-target HepaRG cells **(Fig 3.3A and B).** MRP4 levels in HepaRG cells expressing *ABCC4*-targeted shRNA clones 5264 and 7334 were reduced by 65% and 71% respectively, of the parental HepaRG cells **(Fig 3.3A and B).**

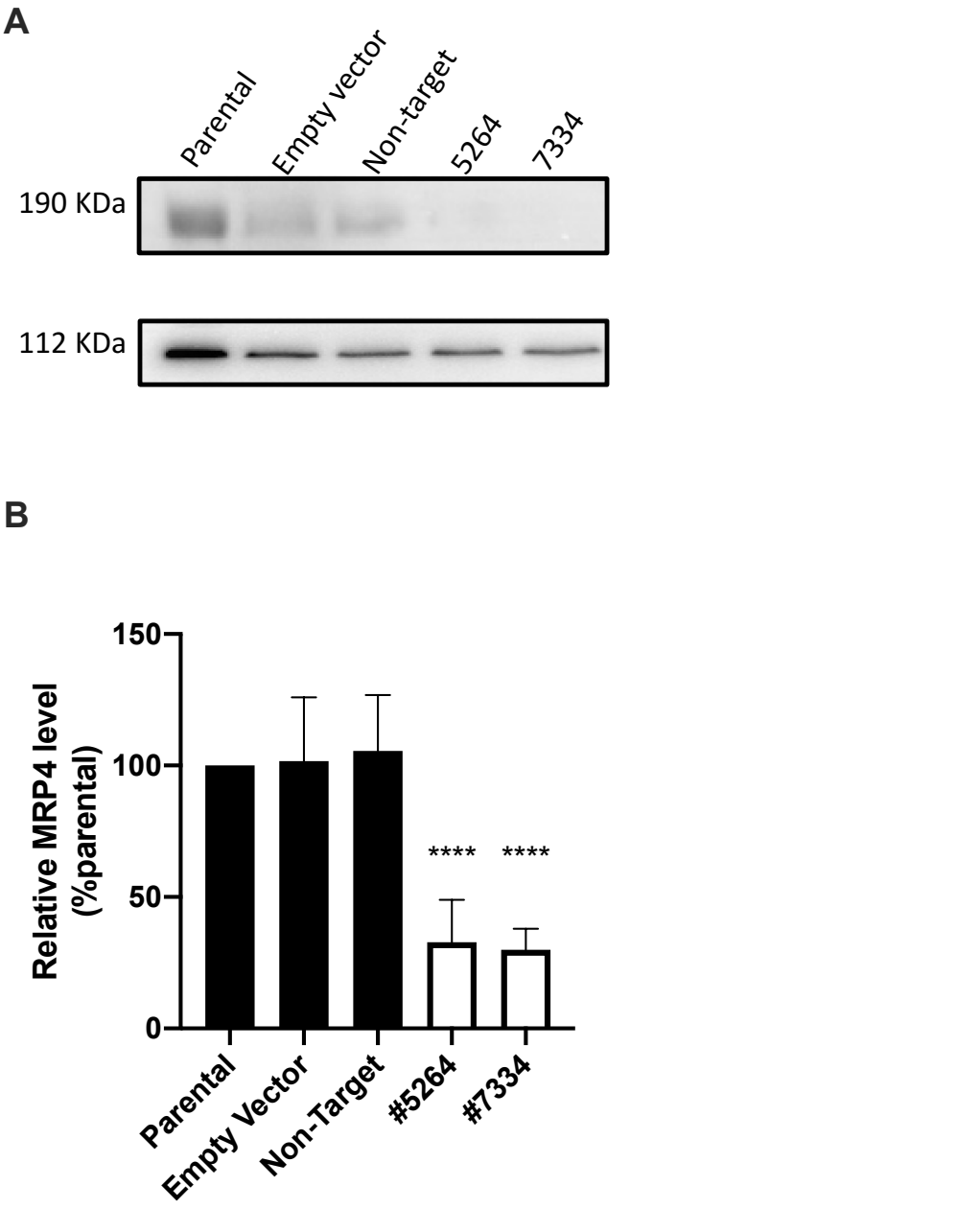

Figure 3.3: Levels of MRP4 in parental HepaRG cells compared to HepaRG cells stably expressing empty vector, non-target, and *ABCC4*-targeted shRNA (clones 5264 and 7334). Whole cell lysates were prepared, and 30 µg of protein were subjected to SDS-PAGE (6%) and transferred to a PVDF membrane. Immunoblotting was performed using the MRP4-specific rat monoclonal antibody M_4I-10 (1:2000). The Na^+/K^+-ATPase mouse monoclonal antibody (H-3) was used as a sample loading control (1:10 000). Secondary antibodies were conjugated with horseradish peroxidase and a chemiluminescent substrate was added to visualize signals. **(A)** Representative blots. **(B)** Densitometry data (analyzed with ImageJ) showing levels of MRP4 relative to parental HepaRGs and normalized to loading control. The means ± SD from five independent experiments are shown. Significant differences in MRP4 level compared to parental cells are indicated with **** $P<0.001$ (One-way ANOVA followed by Dunnett's post hoc test).

3.3.5 Sinusoidal export of arsenic alone and in the presence of MeSeCys is reduced in HepaRG cells stably expressing *ABCC4*-targeted shRNA.

The extent of arsenic sinusoidal efflux was compared between fully differentiated parental cells and HepaRG cells stably expressing empty vector, non-target, or *ABCC4*-targeted shRNA. HepaRG cells were treated with ^{73}As-arsenite (1 µM, 100 nCi) with and without MeSeCys (1 µM) for 1 hr prior to measuring efflux. Then sinusoidal efflux of arsenic was measured at a 10 min time point. Arsenic efflux across sinusoidal membranes in parental HepaRG cells was 7.2 ± 0.3 pmol/mg protein and stimulated 1.3-fold to 9.0 ± 0.3 pmol/mg protein by MeSeCys **(Fig 3.4A).** A similar extent of arsenic sinusoidal efflux in the presence and absence of MeSeCys was observed in HepaRG cells stably expressing empty vector and non-target shRNA compared with parental HepaRG cells **(Fig 3.4).** Sinusoidal efflux of arsenic alone was decreased by 29% and 27% in HepaRG cells expressing the *ABCC4*-targeted shRNA clones 5624 and 7334 respectively, compared to parental cells **(Fig 3.4).** The stimulation of arsenic sinusoidal efflux in the presence of MeSeCys was completely lost in the HepaRG cells expressing the *ABCC4*-targeted shRNA clones 5264 and 7334 **(Fig 3.4).**

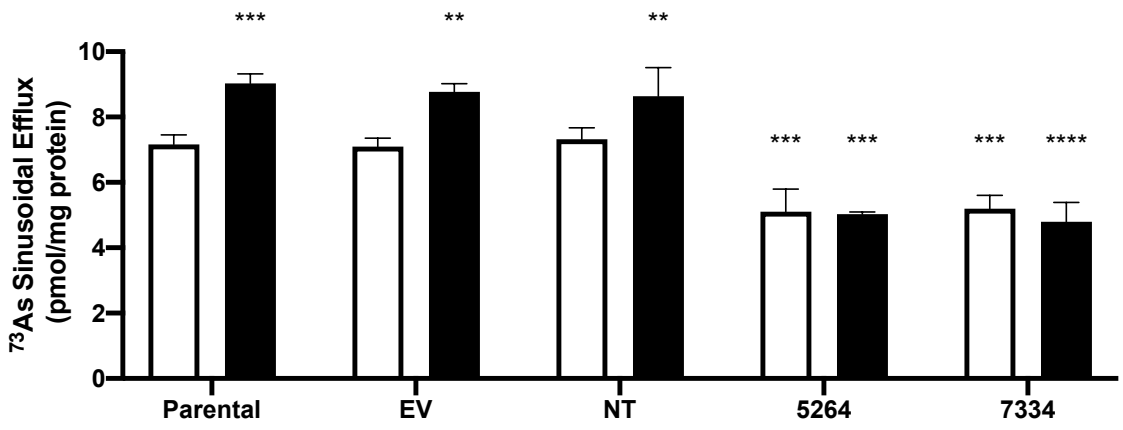

Figure 3.4: Comparison of MeSeCys-dependent and -independent ^{73}As-arsenic sinusoidal efflux in parental HepaRG cells and HepaRG cells stably expressing empty vector, non-target, and *ABCC4*-targeted shRNA (clones 5264 and 7334). Efflux of ^{73}As-arsenic alone and in the presence of MeSeCys were evaluated. White bars indicate the means ± SD of arsenic efflux alone and black bars indicate the means ± SD of ^{73}As-arsenic efflux in the presence of MeSeCys from three independent experiments. Significant differences between efflux of ^{73}As-arsenic alone in parental HepaRG cells and other conditions are indicated with **P<0.01, ***<0.001, and ****<0.0001 (Two-way ANOVA followed by Sidak's multiple comparisons post hoc test).

3.4 Discussion

Chronic exposure to arsenic through contaminated drinking water remains a concern for millions of people worldwide. In humans, ~80% of consumed arsenic is eliminated in urine, predominantly as methylated metabolites, the bulk of which are thought to form in hepatocytes. MRP4 is localized to sinusoidal membranes of hepatocytes and proximal tubules of kidney, making it an ideal candidate for urinary elimination of arsenic metabolites. Selenium-supplementation trials have been completed to try to alleviate symptoms related to chronic arsenic exposure [28–30,44]. In the present study, we examined the stimulatory effect of MeSeCys on arsenic sinusoidal transport.

We previously observed increased sinusoidal efflux of arsenic from HepaRG cells in the presence of MeSeCys [34]. This finding was observed over time and was dose dependent **(Fig**

3.1A and B). Arsenic sinusoidal efflux in the presence of MeSeCys from SCHH, the gold standard model for studying hepatic transport, was remarkably similar to HepaRG cells **(Fig 3.1A vs 3.1C)**, suggesting a reproducible stimulation of arsenic export by MeSeCys in two different models.

Arsenic sinusoidal efflux was further characterized in the presence and absence of MeSeCys using pharmacological and genetic modulation of MRP4. Sinusoidal efflux of arsenic alone was found to be GSH-dependent, temperature-sensitive, inhibited by general MRP and MRP4-specific inhibitors, and reduced when MRP4 levels were knocked down **(Figs 3.2A and 3.4A).** The stimulatory effect of arsenic sinusoidal efflux by MeSeCys was lost under the same conditions in the presence of BSO, at 4°C, and in the presence of the general MRP and specific-MRP4 inhibitors, MK571 and ceefourin-1, respectively, consistent with previous studies of arsenic export alone using SCHH and HepaRG cells [18,34]. MeSeCys did not stimulate arsenic sinusoidal efflux in the *ABCC4* knockdown HepaRG cells, but stimulation still occurred in parental and control HepaRG cells **(Fig 3.4A).** The loss of arsenic sinusoidal efflux in the presence of MeSeCys with increasing concentrations of ceefourin-1 also suggest that the stimulatory effect of MeSeCys on arsenic sinusoidal efflux is mediated by MRP4. Overall, these observations are also consistent with the involvement of transporters, specifically MRP4, for non-stimulated sinusoidal export of arsenic from human hepatocytes. While sinusoidal export of arsenic from SCHH has characteristics of being MRP4-mediated, it was not definitively shown [18]. This is the first report to show reduced sinusoidal arsenic export using an *ABCC4* knockdown model.

Although levels of MRP4 were assessed and compared in the parental, empty vector, non-target, and *ABCC4*-knockdown cells in this study, future studies should consider treating the

cells with arsenite in the presence and absence of MeSeCys prior to immunoblotting. In this study, cells were treated for 1 hr with arsenite and MeSeCys, so changes in overall MRP4 levels are unlikely to occur. However, cellular localization studies such as those included in Chapter 4 could be performed to determine if the presence of MeSeCys interferes with the trafficking or induction of MRP4 within the sinusoidal membrane.

Arsenic sinusoidal efflux was inhibited to a greater extent at cold temperature, than by MK571 and ceefourin-1, suggesting there could be another transporter or channel that contributes to arsenic sinusoidal efflux. Aquaglyceroporin 9 (AQP9) is a channel present at the sinusoidal surface of hepatocytes that allows the passage of neutral arsenic species, $As(OH)_3$ and MMA^{III} down their concentration gradients into cells [45]. AQP9 is bi-directional and can theoretically allow the passage of $As(OH)_3$ and MMA^{III} down their concentration gradients out of the cell. When arsenic efflux was measured from SCHH in the presence of phloretin, an AQP9 inhibitor, there was an 80-89% reduction in arsenic efflux across the sinusoidal membrane over a 15-min time course [18]. However, phloretin is not a specific AQP9 inhibitor, and can inhibit other transport proteins, including MRP4 [18,46,47]. Future studies could include using phloretin on *ABCC4* knockdown HepaRG cells to evaluate whether further reduction in arsenic efflux across sinusoidal membranes is observed in the presence and absence of MeSeCys. MRP3 and MRP5 are other candidates for arsenic efflux at the basolateral surface and would have been inhibited by MK571, but these two proteins did not confer resistance to inorganic or methylated arsenic species in a previous study [17]. MRP6 likely would not have been inhibited by MK571, but in a previous study using SCHH, increased levels of MRP6 were not observed with increasing levels of arsenite [18,48]. Furthermore, in MRP3-, MRP5-, and MRP6-enriched

membrane vesicles, no transport of $As(GS)_3$ was detected [42, Swanlund, Whitlock, and Leslie, unpublished].

A molecular basis for the mutually protective relationship between arsenic and selenium is the formation and biliary excretion of $[(GS)_2AsSe]^-$. Despite the expectation that any form of selenium would increase the biliary elimination of arsenic, DMA^V urinary elimination increased by 1.3-fold in humans that consumed selenium-enriched lentils (55 μg/day) compared to control lentils (1.5 μg/day) after 3 and 6 months [28]. Although selenomethionine is the predominant selenium species in lentils (accounting for >85% of total selenium), selenomethionine had no effect on arsenic export by human HepaRG cells or SCHH [34,49,50]. However, a study has demonstrated that MeSeCys can form from selenomethionine and cysteine or cysteine upon heating to 150℃ for 24 hr in sealed vials [37]. MeSeCys has also been postulated to form from the reaction between selenodiglutathione and dimethyldiselenide that has been released from selenomethionine [37]. Although the selenium-supplementation study by Smits et al., did not control how the lentils given to the participants were consumed, it is highly likely they were cooked, lentil soup, or dahl is known to be consumed on a daily basis [28]. Although lentils are an excellent source of selenomethionine (potentially converted to MeSeCys), dietary sources rich in MeSeCys without requiring chemical conversion, could be considered for future selenium supplementation trials. MeSeCys comprises up to 45% of total selenium in broccoli sprouts, broccoli florets, and as much as 80% of total selenium in onions and garlic [36]. It may be difficult to consume onions and garlic in sufficient quantities, so the use of purified MeSeCys in capsule form or selenium-enriched broccoli sprouts and florets would be a more feasible choice of supplementation. Although there have been no reports to

our knowledge of using purified MeSeCys in selenium supplementation trials, our findings suggest that MeSeCys could be beneficial to those suffering from symptoms related to chronic arsenic exposure.

3.5 References

[1] IARC, A review of human carcinogens – Part C: metals, arsenic, dusts, and fibres., 2012.

[2] R. Gera, V. Singh, S. Mitra, A.K. Sharma, A. Singh, A. Dasgupta, D. Singh, M. Kumar, P. Jagdale, S. Patnaik, D. Ghosh, Arsenic exposure impels CD4 commitment in thymus and suppress T cell cytokine secretion by increasing regulatory T cells, Scientific Reports 2017 7:1. 7 (2017) 1–13. https://doi.org/10.1038/s41598-017-07271-z.

[3] C.F. Huang, Y.W. Chen, C.Y. Yang, K.S. Tsai, R. sen Yang, S.H. Liu, Arsenic and diabetes: current perspectives, Kaohsiung J Med Sci. 27 (2011) 402–410. https://doi.org/10.1016/J.KJMS.2011.05.008.

[4] M.F. Naujokas, B. Anderson, H. Ahsan, H. Vasken Aposhian, J.H. Graziano, C. Thompson, W.A. Suk, The broad scope of health effects from chronic arsenic exposure: Update on a worldwide public health problem, Environmental Health Perspectives. 121 (2013) 295–302. https://doi.org/10.1289/ehp.1205875.

[5] J. Podgorski, M. Berg, Global threat of arsenic in groundwater, Science. 368 (2020) 845 LP – 850. https://doi.org/10.1126/science.aba1510.

[6] H.-J. Sun, B. Rathinasabapathi, B. Wu, J. Luo, L.-P. Pu, L.Q. Ma, Arsenic and selenium toxicity and their interactive effects in humans, Environment International. 69 (2014) 148–158. https://doi.org/https://doi.org/10.1016/j.envint.2014.04.019.

[7] R. Villa-Bellosta, S. V, Arsenate transport by sodium/phosphate cotransporter type IIb, Toxicology and Applied Pharmacology. 247 (2010) 36–40.

[8] R. Villa-Bellosta, V. Sorribas, Role of rat sodium/phosphate cotransporters in the cell membrane transport of arsenate, Toxicology and Applied Pharmacology. 232 (2008) 125–134. https://doi.org/10.1016/j.taap.2008.05.026.

[9] Z. Liu, M.A. Sanchez, X. Jiang, E. Boles, S.M. Landfear, B.P. Rosen, Mammalian glucose permease GLUT1 facilitates transport of arsenic trioxide and methylarsonous acid, Biochemical and Biophysical Research Communications. 351 (2006) 424–430. https://doi.org/10.1016/J.BBRC.2006.10.054.

[10] Z. Liu, E. Boles, B.P. Rosen, Arsenic Trioxide Uptake by Hexose Permeases in Saccharomyces cerevisiae, Journal of Biological Chemistry. 279 (2004) 17312–17318. https://doi.org/10.1074/JBC.M314006200.

[11] T.C. Lee, I.C. Ho, W.J. Lu, J.D. Huang, Enhanced Expression of Multidrug resistance-associated Protein 2 and Reduced Expression of Aquaglyceroporin 3 in an Arsenic-resistant Human Cell Line, Journal of Biological Chemistry. 281 (2006) 18401–18407. https://doi.org/10.1074/JBC.M601266200.

[12] M. Calatayud, J.A. Barrios, D. Vélez, V. Devesa, In Vitro Study of Transporters Involved in Intestinal Absorption of Inorganic Arsenic, Chemical Research in Toxicology. 25 (2012) 446–453. https://doi.org/10.1021/TX200491F.

[13] W.R. Cullen, Chemical mechanism of arsenic biomethylation, Chemical Research in Toxicology. 27 (2014) 457–461. https://doi.org/10.1021/tx400441h.

[14] S. v. Kala, M.W. Neely, G. Kala, C.I. Prater, D.W. Atwood, J.S. Rice, M.W. Lieberman, The MRP2/cMOAT transporter and arsenic-glutathione complex formation are required for biliary excretion of arsenic, Journal of Biological Chemistry. 275 (2000) 33404–33408.

[15] S. v. Kala, G. Kala, C.I. Prater, A.C. Sartorelli, M.W. Lieberman, Formation and Urinary Excretion of Arsenic Triglutathione and Methylarsenic Diglutathione, Chemical Research in Toxicology. 17 (2004) 243–249.

[16] M.W. Carew, E.M. Leslie, Selenium-dependent and -independent transport of arsenic by the human multidrug resistance protein 2 (MRP2/ABCC2): Implications for the mutual detoxification of arsenic and selenium, Carcinogenesis. 31 (2010) 1450–1455.

[17] M. Banerjee, M.W. Carew, B.A. Roggenbeck, B.D. Whitlock, H. Naranmandura, X.C. Le, E.M. Leslie, A Novel Pathway for Arsenic Elimination: Human Multidrug Resistance Protein 4 (MRP4/ABCC4) Mediates Cellular Export of Dimethylarsinic Acid (DMAV) and the

Diglutathione Conjugate of Monomethylarsonous Acid (MMAIII), Molecular Pharmacology. 86 (2014) 168–179.

[18] B.A. Roggenbeck, M.W. Carew, G.J. Charrois, D.N. Douglas, N.M. Kneteman, X. Lu, X. Chris Le, E.M. Leslie, Characterization of arsenic hepatobiliary transport using sandwich-cultured human hepatocytes, Toxicological Sciences. 145 (2015) 307–320. https://doi.org/10.1093/toxsci/kfv051.

[19] F.G.M. Russel, J.B. Koenderink, R. Masereeuw, Multidrug resistance protein 4 (MRP4/ABCC4): a versatile efflux transporter for drugs and signalling molecules, Trends Pharmacol Sci. 29 (2008) 200–207. https://doi.org/10.1016/J.TIPS.2008.01.006.

[20] Institute of Medicine (US) Panel on Dietary Antioxidants and Related Compounds, Dietary Reference Intakes for Vitamin C, Vitamin E, Selenium, and Carotenoids, Washington, 2000.

[21] S. Kurokawa, M.J. Berry, Selenium. Role of the essential metalloid in health, Metal Ions in Life Sciences. 13 (2013) 499–534.

[22] H. Tapiero, D.M. Townsend, K.D. Tew, The antioxidant role of selenium and seleno-compounds, Biomedicine & Pharmacotherapy = Biomedecine & Pharmacotherapie. 57 (2003) 134–144. https://doi.org/10.1016/s0753-3322(03)00035-0.

[23] J. Gailer, S. Madden, G.A. Buttigieg, M.B. Denton, H.S. Younis, Identification of [(GS)2AsSe]− in rabbit bile by size-exclusion chromatography and simultaneous multielement-specific detection by inductively coupled plasma atomic emission spectroscopy, Applied Organometallic Chemistry. 16 (2002) 72–75. https://doi.org/https://doi.org/10.1002/aoc.260.

[24] J. Gailer, G.N. George, I.J. Pickering, R.C. Prince, H.S. Younis, J.J. Winzerling, Biliary excretion of [(GS)2AsSe]- after intravenous injection of rabbits with arsenite and selenate, Chemical Research in Toxicology. 15 (2002) 1466–1471. https://doi.org/10.1021/tx025538s.

[25] O. Ponomarenko, P.F. la Porte, S.P. Singh, G. Langan, D.E.B. Fleming, J.E. Spallholz, M. Alauddin, H. Ahsan, S. Ahmed, J. Gailer, G.N. George, I.J. Pickering, Selenium-mediated

arsenic excretion in mammals: A synchrotron-based study of whole-body distribution and tissue-specific chemistry, Metallomics. 9 (2017) 1585–1595.

[26] A.L. Moxon, The effect of arsenic on the toxicity of seleniferous grains, Science (1979). 88 (1938) 81. https://doi.org/10.1126/science.88.2273.81.

[27] L. Yang, W. Wang, S. Hou, P.J. Peterson, W.P. Williams, Effects of selenium supplementation on arsenism: An intervention trial in inner Mongolia, Environmental Geochemistry and Health. 24 (2002) 359–374.

[28] J.E. Smits, R.M. Krohn, E. Akhtar, S.K. Hore, M. Yunus, A. Vandenberg, R. Raqib, Food as medicine: Selenium enriched lentils offer relief against chronic arsenic poisoning in Bangladesh, Environmental Research. 176 (2019). https://doi.org/10.1016/j.envres.2019.108561.

[29] S. Sah, A. Vandenberg, J. Smits, Treating chronic arsenic toxicity with high selenium lentil diets, Toxicology and Applied Pharmacology. 272 (2013) 256–2662. https://doi.org/10.1016/j.taap.2013.06.008.

[30] R.M. Krohn, R. Raqib, E. Akhtar, A. Vandenberg, J.E.G. Smits, A high-selenium lentil dietary intervention in Bangladesh to counteract arsenic toxicity: Study protocol for a randomized controlled trial, Trials. 17 (2016). https://doi.org/10.1186/s13063-016-1344-y.

[31] D. Thavarajah, J. Ruszkowski, A. Vandenberg, High Potential for Selenium Biofortification of Lentils (Lens culinaris L.), Journal of Agricultural and Food Chemistry. 56 (2008) 10747–10753. https://doi.org/10.1021/jf802307h.

[32] NCT01442727, Selenium in the Treatment of Arsenic Toxicity and Cancers, 2011.

[33] M. Alauddin, R. Cekovic, S. Alauddin, L. Bolevic, S. Saha, J.E. Spallholz, P.F. Laporte, S. Ahmed, H. Ahsan, J. Gailer, O. Ponomarenko, I.J. Pickering, S.P. Singh, G.N. George, Pharmacodynamic study of the selenium-mediated arsenic excretion in arsenicosis patients in Bangladesh, Environmental Arsenic in a ChangingWorld - 7th International Congress and Exhibition Arsenic in the Environment, 2018. 2 (2018) 391–394. https://doi.org/10.1201/9781351046633-152.

[34] J.R. Zhou, G. Kaur, Y. Ma, D. Arutyunov, X. Lu, X.C. Le, E.M. Leslie, Biliary excretion of arsenic by human HepaRG cells is stimulated by selenide and mediated by the multidrug

resistance protein 2 (MRP2/ABCC2), Biochemical Pharmacology. 193 (2021) 114799. https://doi.org/10.1016/j.bcp.2021.114799.

[35] C.M. Weekley, H.H. Harris, Which form is that? the importance of selenium speciation and metabolism in the prevention and treatment of disease, Chemical Society Reviews. 42 (2013) 8870–8894. https://doi.org/10.1039/c3cs60272a.

[36] M.P. Rayman, Food-chain selenium and human health: emphasis on intake, British Journal of Nutrition. 100 (2008) 254–268. https://doi.org/10.1017/S0007114508939830.

[37] P.O. Amoako, P.C. Uden, J.F. Tyson, Speciation of selenium dietary supplements; formation of S-(methylseleno)cysteine and other selenium compounds, Anal Chim Acta. 652 (2009) 315–323. https://doi.org/10.1016/J.ACA.2009.08.013.

[38] P.F. Reay, C.J. Asher, Preparation and purification of 74As-labeled arsenate and arsenite for use in biological experiments, Analytical Biochemistry. 78 (1977) 557–560. https://doi.org/10.1016/0003-2697(77)90117-8.

[39] P. Gripon, S. Rumin, S. Urban, J. le Seyec, D. Glaise, I. Cannie, C. Guyomard, J. Lucas, C. Trepo, C. Guguen-Guillouzo, Infection of a human hepatoma cell line by hepatitis B virus., Proc Natl Acad Sci U S A. 99 (2002) 15655–15660. https://doi.org/10.1073/pnas.232137699.

[40] P. Bachour-El Azzi, A. Sharanek, A. Burban, R. Li, R. le Guével, Z. Abdel-Razzak, B. Stieger, C. Guguen-Guillouzo, A. Guillouzo, Comparative localization and functional activity of the main hepatobiliary transporters in HepaRG cells and primary human hepatocytes, Toxicological Sciences. 145 (2015) 157–168. https://doi.org/10.1093/toxsci/kfv041.

[41] V. Gekeler, W. Ise, K.H. Sanders, W.R. Ulrich, J. Beck, The leukotriene LTD4 receptor antagonist MK571 specifically modulates MRP associated multidrug resistance, Biochemical and Biophysical Research Communications. 208 (1995) 345–352. https://doi.org/10.1006/bbrc.1995.1344.

[42] B.A. Roggenbeck, Hepatobiliary Transport of Arsenic, 2016.

[43] L. Cheung, C.L. Flemming, F. Watt, N. Masada, D.M.T. Yu, T. Huynh, G. Conseil, A. Tivnan, A. Polinsky, A. v. Gudkov, M.A. Munoz, A. Vishvanath, D.M.F. Cooper, M.J. Henderson, S.P.C. Cole, J.I. Fletcher, M. Haber, M.D. Norris, High-throughput screening identifies

Ceefourin 1 and Ceefourin 2 as highly selective inhibitors of multidrug resistance protein 4 (MRP4), Biochem Pharmacol. 91 (2014) 97–108. https://doi.org/10.1016/J.BCP.2014.05.023.

[44] W.J. Verret, Y. Chen, A. Ahmed, T. Islam, F. Parvez, M.G. Kibriya, J.H. Graziano, H. Ahsan, A randomized, double-blind placebo-controlled trial evaluating the effects of vitamin E and selenium on arsenic-induced skin lesions in Bangladesh, Journal of Occupational and Environmental Medicine. 47 (2005) 1026–1035.

[45] J. Lebeck, Metabolic impact of the glycerol channels AQP7 and AQP9 in adipose tissue and liver, J Mol Endocrinol. 52 (2014). https://doi.org/10.1530/JME-13-0268.

[46] Q. Wang, M.E. Morris, Flavonoids modulate monocarboxylate transporter-1-mediated transport of gamma-hydroxybutyrate in vitro and in vivo, Drug Metab Dispos. 35 (2007) 201–208. https://doi.org/10.1124/DMD.106.012369.

[47] O. Kwon, P. Eck, S. Chen, C.P. Corpe, J. Lee, M. Kruhlak, M. Levine, Inhibition of the intestinal glucose transporter GLUT2 by flavonoids, FASEB J. 21 (2007) 366–377. https://doi.org/10.1096/FJ.06-6620COM.

[48] F. Boraldi, D. Quaglino, M.A. Croce, M.I. Garcia Fernandez, R. Tiozzo, D. Gheduzzi, B. Bacchelli, I. Pasquali Ronchetti, Multidrug resistance protein-6 (MRP6) in human dermal fibroblasts. Comparison between cells from normal subjects and from Pseudoxanthoma elasticum patients, Matrix Biol. 22 (2003) 491–500. https://doi.org/10.1016/J.MATBIO.2003.09.001.

[49] G. Kaur, Mechanistic Studies of Arsenic and Selenium Detoxification, University of Alberta, 2020.

[50] D. Thavarajah, A. Vandenberg, G.N. George, I.J. Pickering, Chemical form of selenium in naturally selenium-rich lentils (Lens culinaris L.) from Saskatchewan, Journal of Agricultural and Food Chemistry. 55 (2007) 7337–7341. https://doi.org/10.1021/jf070681i.

4. Naturally Occurring Variants of MRP2/*ABCC2* Differentially Modulate the Transport of Arsenic Triglutathione ($As(GS)_3$) and the Seleno-bis (*S*-glutathionyl) Arsinium Ion ($[(GS)_2AsSe]^-$)

4.1 Introduction [*]

Arsenic is a metalloid found ubiquitously in the earth's crust and is classified as a Group I (proven) human carcinogen by the International Agency for Research on Cancer [1,2]. Millions of people worldwide are exposed to arsenic contaminated water at concentrations higher than the acceptable limit of 10 µg/L as per the World Health Organization [3]. The majority of arsenic endemic areas are in South Asian and South American countries including but not limited to Bangladesh, India, China, Indonesia, Argentina, Columbia, and Mexico [3,4]. Although developed countries including the United States and Canada are not as severely affected, arsenic contamination of drinking water remains a public health concern [5–7].

In arsenic-endemic areas, selenium supplementation trials are ongoing or completed, with the goal of alleviating symptoms related to chronic arsenic exposure [8–11]. The foundational knowledge for the basis of selenium supplementation is from animal studies as well as correlations between low blood selenium levels and adverse health effects from human arsenic exposure [12–17]. When lab animals were given toxic doses of arsenite and selenite, the ability of these compounds to cause liver damage was diminished, compared to when the compounds were given individually [18]. A molecular basis for the mutually protective relationship between arsenic and selenium is the formation and biliary excretion of the seleno-bis (*S*-glutathionyl) arsinium ion ($[(GS)_2AsSe]^-$), which was first detected in the bile of rabbits that were co-injected with arsenite and selenite [12].

[*] Dr. Gurnit Kaur included this work as an appendix in her thesis (Kaur, G. (2020) Mechanistic Studies of Arsenic and Selenium Detoxification. University of Alberta, Canada). This thesis was used as a starting point for writing this chapter.

Arsenic biotransformation occurs predominantly in the liver through a series of oxidative methylation, followed by reduction reactions, resulting in predominantly monomethylated and dimethylated trivalent and pentavalent arsenic species in humans, but trimethylated species can also form [19,20]. The trivalent arsenic species including arsenite, monomethylarsonous acid (MMA^{III}), and dimethylarsinous acid (DMA^{III}) can undergo glutathione conjugation [21]. Glutathione conjugates of MMA^{III} and arsenite have been isolated in biological samples, such as rat bile and urine of mice deficient in gamma glutamyl transpeptidase, which catabolizes glutathione and its conjugates [22,23]. Interestingly, glutathione conjugates with DMA^{III} have been synthesized *in vitro*, but have not been isolated *in vivo* [23,24].

Active transport of arsenic from cells is mediated by members of the ATP-binding cassette (ABC) transporter family, subfamily C. This family consists of 12 functional members, that include transporters involved in primary active transport of their substrates [25]. The multidrug resistance proteins (MRPs) including MRP1 (gene symbol *ABCC1*), MRP2 (*ABCC2*), and MRP4 (*ABCC4*) have established roles in the transport of arsenic metabolites [23,26–30]. Thought to be of particular importance in hepatic transport are MRP2 and MRP4, which are involved in the efflux of $As(GS)_3$ and $[(GS)_2AsSe]^-$ across canalicular membranes, and dimethylarsinic acid (DMA^V) and $MMA(GS)_2$ across sinusoidal membranes, respectively [26,29,31].

In Mrp2-deficient Wistar rats, Mrp2 is responsible for transporting >98% of arsenic into bile in the forms $As(GS)_3$ and $MMA(GS)_2$ [23,32]. Furthermore, studies with human MRP2-enriched membrane vesicles have shown, at least in vitro, that human MRP2 is a high capacity

and high affinity transporter of $As(GS)_3$ and $[(GS)_2AsSe]^-$ [26]. HepaRG cells are an immortalized, polarized human hepatic cell line that form canalicular networks. In HepaRG cells, biliary excretion of arsenic is mediated by human MRP2 as evidenced by the loss of canalicular arsenic efflux after *ABCC2* knockdown [33]. Furthermore, in HepaRG cells, arsenic biliary excretion by MRP2 is stimulated by selenide, a biologically active form of selenium [33].

The *ABCC2* gene is highly polymorphic, with greater than 1300 non-synonymous single nucleotide polymorphisms (SNPs) in the dbSNP database (https://www.ncbi.nlm.nih.gov/snp), including 44 that have been validated by the 1000 genomes project [34]. Naturally occurring MRP2 variants have been shown to influence transport of non-arsenic MRP2 substrates *in vitro* and/or in clinical settings [35]. Dubin-Johnson syndrome is a rare autosomal recessive condition characterized by a lack of functionally active MRP2 [36–38]. The aims of this study were to characterize the influence of selected MRP2 variants on cellular localization in mammalian cells and MRP2 transport of $As(GS)_3$ and $[(GS)_2SeAs]^-$. Thirteen different MRP2 variants were characterized: R353H-, R412G-, V417I-, S789F-, R1150H-, R1181L-, V1188E-, P1291L-, N1244K-, A1450T-, T1477M-, C1515Y-, and V1188E/C1515Y-MRP2 **(Fig 4.1).**

4.2 Materials and Methods

4.2.1 Materials[†]

^{73}As-arsenate (> 5.6 Ci/mg) was purchased from Los Alamos Meson Production Facility (Los Alamos, NM). ^{75}Se-selenite (0.296 Ci/mg) was obtained from the University of Missouri Research Reactor (MURR, Columbia, MO). Sodium selenite, sodium (meta)arsenite, reduced

[†] The isotopes (^{73}As and ^{75}Se) used in this research were supplied by the United States Department of Energy Office of Science by the Isotope Program in the Office of Nuclear Physics.

glutathione (GSH), Tris base, adenosine triphosphate (ATP), adenosine monophosphate (AMP), magnesium chloride ($MgCl_2$), ethylenediaminetetraacetic acid (EDTA), N-(2-Hydroxyethyl)piperazine-N'-2(2-ethanesulfonic acid) (HEPES), glycine, polyvinylidene difluoride (PVDF) membranes and Immobilon Crescendo Western HRP substrate were purchased from Millipore Sigma (Oakville, ON, Canada). Creatine kinase, creatine phosphate, GSH reductase, reduced nicotinamide adenine dinucleotide phosphate (NADPH), and Complete Mini EDTA-free protease inhibitor cocktail tablets were purchased from Roche Applied Science (Laval, QC, Canada). Sodium selenide was purchased from Alfa Aesar (Ward Hill, MA). Triton X-100 was purchased from Fisher Scientific (Fair Lawn, NJ). Pierce™ Sulfo-*N*-hydroxysuccinimide-SS-biotin, Pierce™ streptavidin-agarose beads and Pierce™ bicinchoninic acid (BCA) protein assay reagents were purchased from Thermo Scientific (Rockford, IL).

4.2.2 Antibodies

The MRP2 specific mouse monoclonal antibody (M_2I-4) was purchased from EMD Millipore (Billerica, MA). The Na^+/K^+-ATPase mouse monoclonal (H-3/SC-48345) was purchased from Santa Cruz Biotechnology (Dallas, TX). The IgG (H+L) cross-adsorbed goat anti-mouse and anti-rat HRP conjugated polyclonal secondary antibodies were purchased from ThermoFisher Scientific (Waltham, MA).

4.2.3 Cell Lines and Expression Constructs

The HEK293T cell line was from the American Type Culture Collection (ATCC) (Manassa, VA) and was maintained in Dulbecco's modified Eagle's medium containing 7.5% fetal bovine serum (FBS). Cell cultures were maintained in a humidified incubator with 95% air and 5% CO_2.

MRP2 complementary DNA in pcDNA3.1(-) was a gift from Dr. Susan P.C. Cole (Queen's University) and its construction has been previously described [39].

4.2.4 Generation of MRP2 Variants[‡]

Variants were generated using a Quikchange II XL site-directed mutagenesis kit (Stratagene, Agilent Technologies, Santa Clara, CA), using pcDNA3.1-MRP2 as the PCR template according to the manufacturer's instructions. Mutagenic primers used are listed in **Table 4.1.** All mutants were confirmed by sequencing and the entire cDNA was sequenced to confirm that only the desired mutation had been introduced (Molecular Biology Service Unit, Dept. Biological Sciences, University of Alberta).

[‡] Dr. Gurnit Kaur designed primers for and made the naturally occurring *ABCC2* variants by site-directed mutagenesis, ensured accuracy of the sequences by sending samples for sequencing, performed technical replicates of immunoblots of whole cell lysates and membrane vesicles, and the reverse mutagenesis for S789F- and A1450T-MRP2.

Table 4.1. Mutagenic primer sequences for synthesis of MRP2 variants

Amino Acid Change	Nucleotide Change	Primer Sequences (5' → 3')
R353H	1058G>A	F: GCTGATCTCCTTTGCAAGTGACCATGACACATATTTGTGGATTGG R: CCAATCCACAAATATGTGTCATGGTCACTTGCAAAGGAGATCAGC
R412G	1271A>G	F: CTATCCAATTTGGCCGGGAAGGAGTACACCG R: CGGTGTACTCCTTCCCGGCCAAGTTGGATAG
V417I	1249G>A	F: GGCCAGGAAGGAGTACACCATTGGAGAAACAGTG R: CACTGTTTCTCCAATGGTGTACTCCTTCCTGGCC
S789F	2366C>T	F: GATGACCCCCTGTTTGCAGTGGATGC R: GCATCCACTGCAAACAGGGGGTCATC
R1150H	3449G>A	F: CGCCAGCTGAGGCATCTGGACTCTGTCACC R: GGTGACAGAGTCCAGATGCCTCAGCTGGCG
R1181L	3542G>T	F: CCGTGCCTTTGAGCACCAGCAGCTATTTCTGAAACACAATGAGG R: CCTCATTGTGTTTCAGAAATAGCTGCTGGTGCTCAAAGGCACGG
V1188E	3563T>A	F: CTGAAACACAATGAGGAGAGGATTGACACCAACC R: GGTTGGTGTCAATCCTCTCCTCATTGTGTTTCAG
N1244K	3732T>G	F: GGCTTTGTTCTGTCCAAGGCACTCAATATCACACAAACCC R: GGGTTTGTGTGATATTGAGTGCCTTGGACAGAACAAAGCC
P1291L	3872C>T	F: GATAAGAGGCCTCTGCCAGATTGGCCC R: GGGCCAATCTGGCAGAGGCCTCTTATC
A1450T	4348G>A	F: CTGTGCCTGGGCAGGACTCTGCTTCGGAAATCC R: GGATTTCCGAAGCAGAGTCCTGCCCAGGCACAG
T1477M	4430C>T	F: GACAACCTCATTCAGATGACCATCCAAAACGAG R: CTCGTTTTGGATGGTCATCTGAATGAGGTTGTC
C1515Y	4544G>A	F: CGGGAAGATTATAGAGTACGGCAGCCCTGAAGAACTGC R: GCAGTTCTTCAGGGCTGCCGTACTCTATAATCTTCCCG

4.2.5 MRP2 Expression in HEK293T Cells

HEK293T cells were transfected using the calcium phosphate method, as previously described [40], with minor modifications. HEK293T cells were seeded onto 12-well tissue culture plates at a density of $1.5x10^5$ cells/well. After 24 hrs, a solution of 0.5 µg DNA was added to 4.4 µL of 250 mM $CaCl_2$, which was then added to 36 µL HEPES buffer (275 mM NaCl, 1.5 mM Na_2HPO_4, and 55 mM HEPES, pH 7.0). This DNA solution was added dropwise to cells and incubated for 24 hrs, then the cell culture media was changed. Cells to be used for cell

surface biotinylation and membrane vesicle preparation were transfected in the same manner but on a larger scale proportional to culture dish surface area (6-well tissue culture plates for cell surface biotinylation, and 150 mm tissue culture plates for membrane vesicle preparations). All experiments and preparations were performed 72 hr post-transfection.

4.2.6 Preparation of Whole Cell Lysates and Immunoblotting

HEK293T cells were washed three times in ice cold phosphate buffered saline (PBS) (137 mM NaCl, 2.7 mM KCl, 10 mM Na_2HPO_4 and 1.8 mM KH_2PO_4), and lysed in 0.5% Triton X-100 containing Complete Mini EDTA-free protease inhibitor cocktail. The lysates were centrifuged at 2800xg for 10 min and the supernatant was collected. Protein levels of the whole cell lysates were determined using a BCA assay.

For immunoblotting, 10 µg of whole cell lysate was subjected to SDS-PAGE (6%) and transferred to a PVDF membrane. Immunoblotting of the PVDF membrane was performed using the MRP2-specific mouse monoclonal antibody (M_2I-4) (1:2000). A Na^+/K^+-ATPase monoclonal mouse antibody (H-3) (1:10 000) was used to detect the Na^+/K^+-ATPase as a sample loading control. The secondary anti-mouse antibodies were HRP-conjugated (1:10 000). All antibodies were prepared in 4% skim milk. Membranes were imaged using ChemiDoc™ (BioRad) after addition of Immobilon Crescendo Western HRP substrate. Relative levels of MRP2 were quantified using ImageJ software normalized against the Na^+/K^+-ATPase signal. Levels of each variant-MRP2 were reported relative to WT-MRP2.

4.2.7 Membrane Vesicle Preparation

Plasma membrane-enriched vesicles were prepared from HEK293T cells overexpressing WT-MRP2, variant-MRP2 or empty vector control, as previously described [27]. Transfected cells

were scraped into ice cold homogenization buffer (250 mM sucrose, 50 mM Tris, 0.25 mM $CaCl_2$, pH 7.4), and washed three times by centrifugation at 500xg, 4°C for 10 min. After the last wash, cell pellets were stored at -80°C layered with homogenization buffer containing Complete Mini EDTA-free protease inhibitor cocktail tablets.

Cell pellets were thawed on ice, then cells were disrupted with nitrogen cavitation (pressurized to 200 PSI for 5 min and released to atmospheric pressure) in a 45 ml Parr cell disruption vessel. Ethylenediaminetetraacetic acid (1 mM, pH 8) as well as phenylmethylsulfonyl fluoride (PMSF) were added to the disrupted cells and then the suspensions were centrifuged at 500xg at 4°C for 10 min to remove intact cells and nuclei. The supernatant was collected and layered onto 12 mL of 35% w/w sucrose in 50 mM Tris, pH 7.4, and centrifuged at 100 000xg for 1 hr at 4°C. The interphase was collected and mixed with a dilute Tris sucrose buffer (25 mM sucrose, 50 mM Tris, pH 7.4) and centrifuged at 100 000xg for 30 min at 4°C, yielding a membrane pellet. The membrane pellet was resuspended in 1 mL Tris-sucrose buffer (250 mM sucrose, 50 mM Tris, pH 7.4) and centrifuged at 100 000xg for 20 min. The supernatant was removed, and the pellet was resuspended in an appropriate volume of Tris-sucrose buffer using a 27-gauge needle, then aliquoted and stored at -80°C. Relative levels of MRP2 in each vesicle preparation were determined by resolving 0.5 µg protein using SDS-PAGE followed by immunoblot, as described above for whole cell lysates.

4.2.8 Cell Surface Biotinylation

Cell surface biotinylation was carried out as previously described [41], with minor modifications. Cells expressing empty vector, WT-MRP2, or variant-MRP2 were incubated with the membrane impermeant EZ-link biotinylation reagent, and then washed with glycine-

containing PBS to quench the reaction. Cells were lysed as described previously [41], and total protein was measured. An aliquot of the lysate was saved (input fraction) and 450 µg of lysate was incubated with 140 µL of streptavidin beads for 1 hr on a rocker at 4°C. Following centrifugation at 800xg, the supernatant was collected (unbound/unbiotinylated fraction). Equal volumes of the input and unbound fractions were subjected to 6% SDS-PAGE followed by immunoblotting as described in Section 4.2.6. To quantify the amount of MRP2 that localizes to the cell surface, the following formula was used:

$$\%\text{MRP2 at cell surface} = \frac{\text{input} - \text{unbound}}{\text{input}} \text{ x } 100$$

4.2.9 Chemical Synthesis of $^{73}As(GS)_3$ and $[(GS)_2As^{75}Se]^-$

$^{73}As(GS)_3$ was prepared from ^{73}As-arsenite, sodium (meta)arsenite, and GSH, as described previously [24,26].

$[(GS)_2As^{75}Se]^-$ was prepared as described previously [26,42], except ^{75}Se-selenite was used as the radioactive label instead of ^{73}As-arsenite. Briefly, GSH (150 mM) was dissolved in Tris (100 mM) and the pH was adjusted to 7.5 and then incubated at 37°C for 20 min. Then, ^{75}Se-selenite (50 nCi/µl) combined with sodium selenite (50 µM) was combined with an equal volume of arsenite (50 µM). This equimolar mixture was added to GSH (150 mM) at twice the volume of this mixture, and the final pH was adjusted to 7.5.

4.2.10 $^{73}As(GS)_3$ and $[(GS)_2As^{75}Se]^-$ Transport Assays [§]

ATP-dependent transport of $^{73}As(GS)_3$ and $[(GS)_2As^{75}Se]^-$ by WT- and variant-MRP2 plasma membrane enriched vesicles was measured as described previously [26]. Briefly, membrane vesicles (20 µg) were incubated with $^{73}As(GS)_3$ or $[(GS)_2As^{75}Se]^-$ (1 µM, 100 nCi) in transport buffer (ATP or AMP (4 mM), $MgCl_2$ (10 mM), creatine phosphate (10 mM), creatine kinase (100 µg/ml), GSH reductase (5 µg/ml), NADPH (0.35 mM), GSH (3 mM), Tris (50 mM, pH 7.4), sucrose (250 mM)) at 37°C for 3 min.

To determine the linearity of $[(GS)_2As^{75}Se]^-$ uptake over time, the membrane vesicles were incubated in the transport buffer at 37°C for 1, 3, 5, and 10 minutes. Kinetic parameters of $[(GS)_2As^{75}Se]^-$ uptake were determined by measuring the initial rate of uptake at eight different concentrations (0.1 – 10 µM, 30-200 nCi) at a 3 min time point.

Transport was stopped by diluting the reaction mix with 800 µL of ice-cold Tris-sucrose buffer. Vesicles were filtered over glass fibre filters (type A/E) with three washes of Tris-sucrose buffer. For $^{73}As(GS)_3$ transport, filters were placed in scintillation vials, dissolved in scintillation fluid, and radioactivity was quantified by liquid scintillation counting using the PerkinElmer MicroBeta^2 liquid scintillation counter. For $[(GS)_2As^{75}Se]^-$ transport, filters were placed in 4.5 ml polypropylene gamma counter tubes (Sarstedt, Numbrecht, Germany) and radioactivity was quantified using the Packard Cobra II gamma counter. ATP-dependent transport was determined by subtracting transport in the presence of AMP from the transport in the presence of ATP.

[§] Dr. Gurnit Kaur performed numerous troubleshooting experiments for these assays, which are included in her thesis (Kaur, G. (2020) Mechanistic Studies of Arsenic and Selenium Detoxification. University of Alberta, Canada) as an appendix.

4.2.11 Whole Cell Accumulation Assay

^{73}As-arsenite was reduced from ^{73}As-arsenate with metabisulfite-thiosulfate reducing agent, as previously described [43]. Medium containing ^{73}As-arsenite (1 µM, 100 nCi/well) ± Se (1 µM) as selenide or selenite was added to the cells expressing EV, WT-MRP2 or variant-MRP2 for 3 hr at 37°C. For the time course study, cells expressing WT-MRP2 were treated with media containing ^{73}As-arsenite (1 µM, 100 nCi/well) at 37°C for 1, 3, 6, 9, and 24 hr. Then, the cells were washed three times using ice cold PBS and lysed in 0.5% Triton X-100. The radioactivity was quantified using the PerkinElmer MicroBeta^2 liquid scintillation counter. Arsenic accumulation was normalized to total protein levels in the lysates, which were determined using a BCA assay.

4.2.12 Selection of arsenic and selenium concentrations for experiments

Mean blood total arsenic levels resulting from chronic arsenic exposure to 10-100 µg/L of arsenic in water result in 10-100 nM and mean total blood selenium levels can range from 1.6-4 µM [17]. Arsenic and selenium were used at 1 µM, with the exception of the plasma membrane vesicle transport assays, where a higher range of concentrations were used to determine kinetic parameters.

4.2.13 Data analysis and statistics

For all densitometry statistical analyses, a one-way ANOVA followed by a Dunnett's post-hoc-test was used to determine if there were statistical differences between WT-MRP2 and variant-MRP2 levels. For plasma membrane-enriched vesicle transport of $^{73}As(GS)_3$ and $[(GS)_2As^{75}Se]^-$, a one-way ANOVA followed by a Dunnett's post-hoc test was used to determine if there was statistically significant differences between WT-MRP2 and variant-MRP2 transport

activity. For whole cell accumulation assays, statistical significance between accumulation of ^{73}As-arsenite in the absence and presence of selenium was determined using a one-way ANOVA followed by a Sidak's multiple comparisons test. A student's T-test was used to determine if there was statistical difference between accumulation of ^{73}As-arsenite in HEK293T cells expressing WT-MRP2 and T1477M-MPR2. For assessing statistical significance between WT-MRP2 and variant-MRP2 for differences in accumulating of ^{73}As-arsenite in the presence of selenide, a one-way ANOVA followed by a Dunnett's post-hoc test was used.

4.3 Results

4.3.1 Selection of *ABCC2* variants for functional studies ⊗

MRP2 variants (location indicated in **Fig 4.1** and properties summarized in **Table 4.2**) were selected for characterization based on the following: (i) a non-synonymous change, (ii) location of the amino acid change on a cytosolic loop or transmembrane domain (with one exception), and (iii) a known association with clinical toxicity to a therapeutic agent in humans or disruption of function *in vitro*. Eleven of the twelve individual mutations selected were in a transmembrane helix, or cytosolic region because these are the regions most likely to influence the binding and transport of MRP2 substrates [44]. Variants were also selected based on a minor allele frequency of at least 1%. Two additional variants, R1150H-MRP2 and T1477M-MRP2 with less than 1% allele frequency were included due to their implication in Dubin-Johnson syndrome or effects on transport activity, respectively [45,46]. With one exception, all selected variants are present in membrane spanning domains 1 and 2 and associated intracellular and cytosolic regions, including nucleotide-binding domains (NBDs). Mutations in

⊗ Dr. Gurnit Kaur selected the variants to be studied.

MSD0 (transmembrane helices 1-5) were not selected, as MSD0 is unlikely to be important for transport function but is important for the correct apical localization of MRP2 in polarized cells [47–49]. R353H-MRP2 is the only variant selected that is located in an extracellular loop, it was chosen for its prevalence (1.4-6.7% depending on the population) and previously described altered transport activity [50]. The variant, V1188E/C1551Y-MRP2 exists as a haplotype of *ABCC2* and was chosen because it contains two of the chosen variants that were previously functionally characterized [50,51].

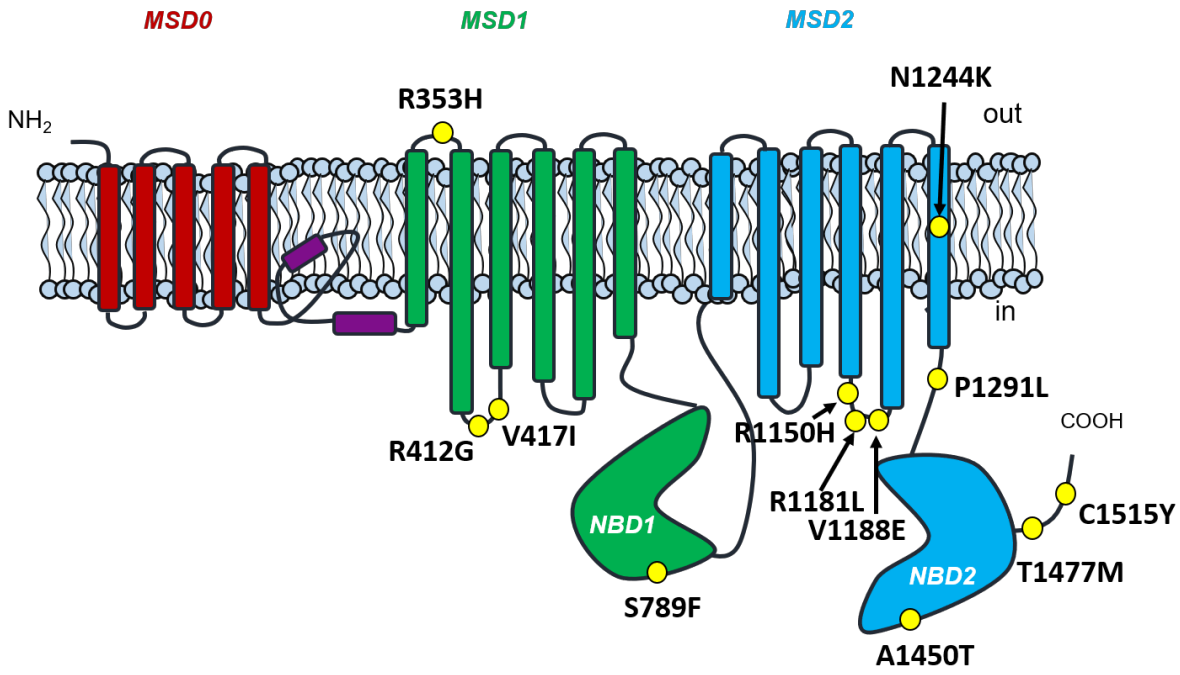

Figure 4.1: Location of the naturally occurring human MRP2 variants characterized in the current study. The figure was taken with permission and modified from [52]. Membrane spanning domain, MSD; nucleotide binding domain, NBD.

Table 4.2: Summary of selected properties of *ABCC2* non-synonymous variants characterized in this study

Amino Acid Change	Nucleotide Change	Variant ID	Minor allele frequency	PolyPhen2 Prediction[a]	SIFT Prediction[b]	Previously reported phenotype
R353H	1058G>A	rs7080681	1.4 (1000 genomes) [53] 67 (African American) [50]	Benign	Tolerated	[50]
R412G	1271A>G		Rare mutation	Benign	Affect function	[35,54]
V417I	1249G>A	rs2273697	18.7 (1000 genomes) [53]	Benign	Tolerated	[55–58]
S789F	2366C>T	rs56220353	1 (Japanese) [59]	Probably damaging	Affect function	[46,60]
R1150H	3449G>A		0.9 (Moroccan Jews) [45]	Probably damaging	Affect function	[45]
R1181L	3542G>T	rs8187692	3.3 (1000 genomes) [53]	Possibly damaging	Tolerated	[49,50]
V1188E	3563T>A	rs17222723	1 (Japanese) [61] 5.8 (African American) [50]	Benign	Tolerated	[49,62,63]
N1244K	3732T>G		1 (Japanese) [61]	Possibly damaging	Tolerated	[50]
P1291L	3872C>T	rs17216317	1 (1000 genomes) [53]	Possibly damaging	Affect function	[50]
A1450T	4348G>A		1 (Japanese) [59]	Possibly damaging	Affect function	[46,64]
T1477M	4430C>T		0.6 [65]	Benign	Affect function	[46]
C1515Y	4544G>A	rs8187710	6.7 (1000 genomes) [53] 13 (African American) [50]	Benign	Tolerated	[49,56,62,66,67]
V1188E/C1515Y	3563T>A and 4544G>A	rs17222723/ rs8187710				[50,62]

[a]Polyphen2 (Polymorphism Phenotyping v2) is a tool that predicts possible impact of an amino acid change on the structure and function of a human protein using physical considerations [68].

[b]SIFT (Sorting Intolerant from Tolerant) predicts whether an amino acid change affects protein function based on degree of conservation of amino acid residues in sequence alignments derived from closely related sequences [69].

4.3.2 S789F-, R1150H-, N1244K-, P1291L-, and A1450T-MRP2 were at lower levels in whole cell lysates than WT-MRP2.

Prior to functional characterization of the MRP2 variants, relative MRP2 levels in whole cell lysates were determined by immunoblot analysis. HEK293T cells were transfected with DNA encoding for empty vector, WT-, R353H-, R412G-, V417I-, S789F-, R1150H-, R1181L-, V1188E-, P1291L-, N1244K-, A1450T-, T1477M-, C1515Y-, or V1188E/C1515Y-MRP2. At 72 hr post-transfection, whole cell lysates were prepared, and 10 µg of protein was subjected to SDS-PAGE. Immunoblot analysis revealed levels of variant MRP2 were comparable to WT-MRP2 except for S789F-, R1150H-, N1244K-, P1291L- and A1450T-MRP2, which respectively had levels 21%, 27%, 39%, 28%, and 11% of WT-MRP2 **(Fig 4.2A and B).**

4.3.3 Variant-MRP2 levels differed from WT-MRP2 levels in plasma membrane enriched vesicles.

The levels of variant MRP2 in plasma membrane enriched vesicles from transfected HEK293T cells were also investigated. As shown in **Figure 4.2C and D**, V417I-MRP2 was detected at 180% of WT-MRP2 levels **(Fig 4.2C and 2D).** Consistent with whole cell lysate levels of R412G-, R1150H-, V1188E-, C1515Y- and V1188E/C1515Y-MRP2, levels similar to WT-MRP2 were observed in plasma membrane fractions **(Fig 4.2C and D).** Consistent with low levels in whole cell lysates, N1244K- and P1291L- were detected at 48% and 39% of WT-MRP2 levels, respectively **(Fig 4.2C and D).**

In contrast with WT-MRP2-like whole cell lysate levels, R353H-, R1181L-, and T1477M-MRP2 in plasma membrane fractions were at 40%, 60%, and 17% of WT-MRP2 levels, respectively. Also, in contrast to the low but detectable levels of S789F- and A1450T-MRP2 in whole cell lysates, these two mutants were not detected in plasma membrane enriched vesicles **(Fig 4.2C).**

To exclude the possibility that the absence of MRP2 was due to unintentional introduction of mutations other than S789F- and A1450T-MRP2, the introduced variants were reverted back to the WT-MRP2 sequence using site-directed mutagenesis, and whole cell lysates were prepared and subjected to SDS-PAGE followed by immunoblot analysis. MRP2 protein was detected in whole cell lysates expressing these revertants **(Fig 4.2E),** showing that S789F- and A1450T-MRP2 mutations were specifically responsible for the lowered protein levels. Reduced protein levels in plasma membrane enriched, relative to whole cell lysate fractions for R353H-, S789F-, R1181L-, A1450T-, and T1477M-MRP2 potentially indicates impaired trafficking to the plasma membrane.

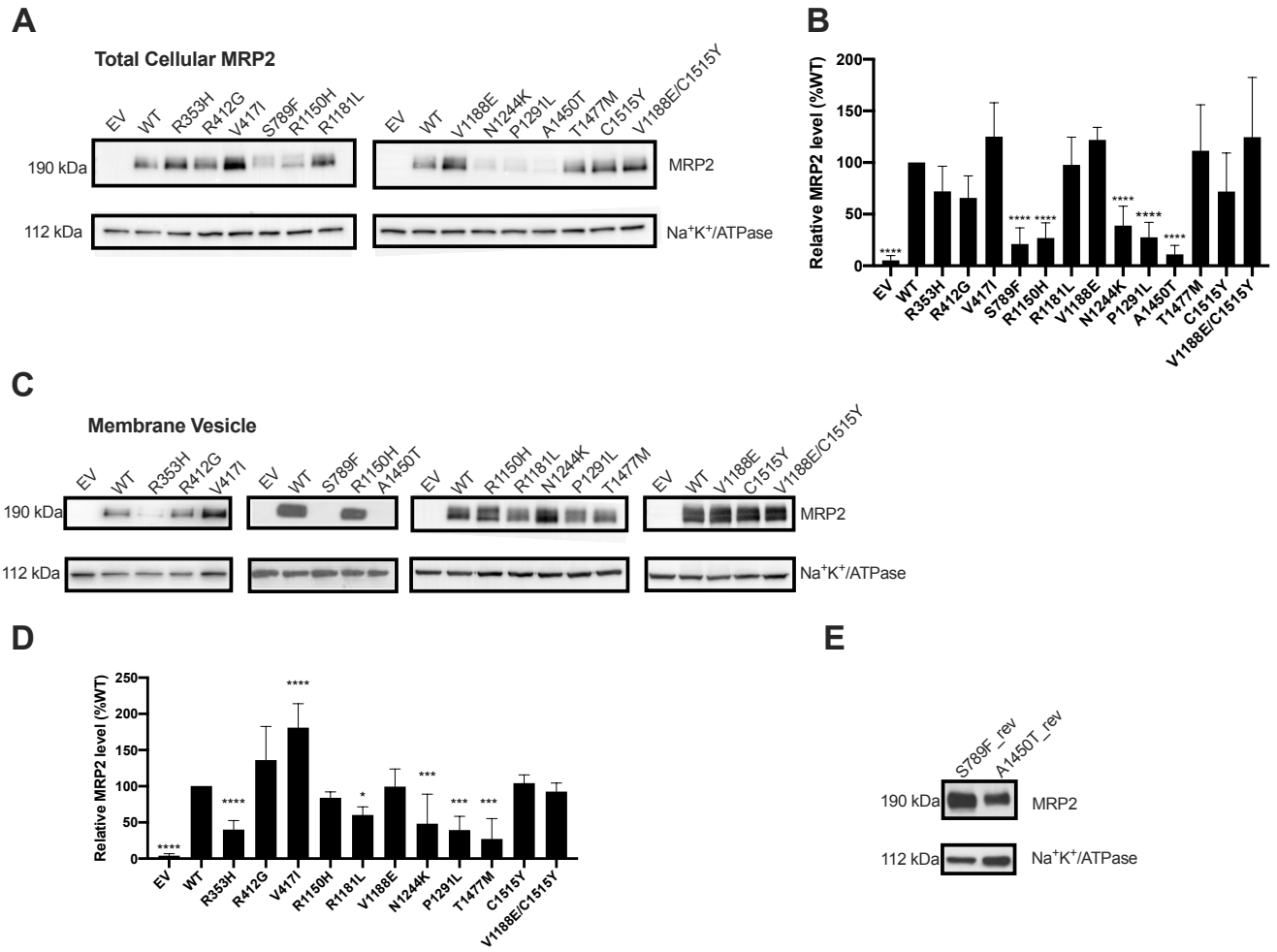

Figure 4.2: Levels of empty vector, WT-MRP2 and naturally occurring MRP2 variants in whole cell lysates and plasma membrane enriched vesicles. (A, B) Whole cell lysates (10 µg of protein) and **(C-E)** plasma membrane enriched vesicles (0.5 µg of protein) from HEK293T cells transiently transfected with empty vector, WT-MRP2 and variant-MRP2s were subjected to SDS-PAGE (6%). After transfer to a PVDF membrane, immunoblotting was performed using the MRP2-specific mouse monoclonal antibody (M_2I-4) (1:2000). The Na^+K^+/ATPase mouse monoclonal antibody H-3 (1:10 000) was used as a loading control. Secondary antibodies labeled with horseradish peroxidase and a chemiluminescent substrate were added to visualize signals. **(A)** Representative immunoblots of the whole cell lysate samples. **(B)** Densitometry data (analyzed with ImageJ) of whole cell lysate samples show levels of MRP2, which were normalized to the loading control, relative to WT-MRP2. Bars represent mean (± S.D.) determinations of at least three independent experiments. **(C)** Representative immunoblots of plasma membrane enriched vesicles with detectable levels of MRP2. **(D)** Densitometry data (analyzed with ImageJ) of plasma membrane enriched samples show levels of MRP2, which were normalized to the loading control, relative to WT-MRP2. Bars represent mean (± S.D.) determinations of at least three independent experiments. **(E)** Representative immunoblot of MRP2-S789F and -A1450T and their revertants back to WT-MRP2. Significant differences between WT-MRP2, variant-MRP2 and empty vector are indicated with *P<0.05, ***P<0.001, and ****P<0.0001 (One-way ANOVA followed by Dunnett's post-hoc test).

4.3.4 V417I-MRP2 had higher levels, and R353H-, S789F-, R1181L-, N1244K-, P1291L-, A1450T-, and T1477M-MRP2 had lower levels at the cell surface compared to WT-MRP2.

Cell surface biotinylation experiments were performed to corroborate plasma-membrane enriched fraction data and further evaluate if the naturally occurring MRP2 variants reached the cell surface to the same extent as WT-MRP2. Cell surface proteins were biotinylated with membrane-impermeable sulfo-*N*-hydroxy-succinimide-SS-biotin. The degree to which mutant- and WT-MRP2 trafficked to the cell surface was determined by measuring the input and unbiotinylated fractions to calculate the biotinylated MRP2 as described in Section 4.3.8. Representative immunoblots are shown in **Fig 4.3A.**

Cell surface expression of all variants was extremely consistent with levels observed in plasma-membrane enriched fractions **(Fig 4.2C and D versus Fig 4.3)**. Cell surface levels of R353H-, R1181L-, N1244K-, P1291L- and T1477M-MRP2 were 33%, 62%, 59%, 38% and 41% of WT-MRP2, respectively **(Fig 4.3A and B).** The level of V417I-MRP2 was 170% of WT-MRP2 at the cell surface **(Fig 4.3A and B).** The variants R412G-, R1150H-, V1188E-, C1515Y-, and V1188E/C1515Y-MRP2 had similar levels at the cell surface as WT-MRP2. The variants S789F- and A1450T-MRP2 had MRP2 levels of 8% and 4% at the cell surface, respectively **(Fig 4.3A and B).**

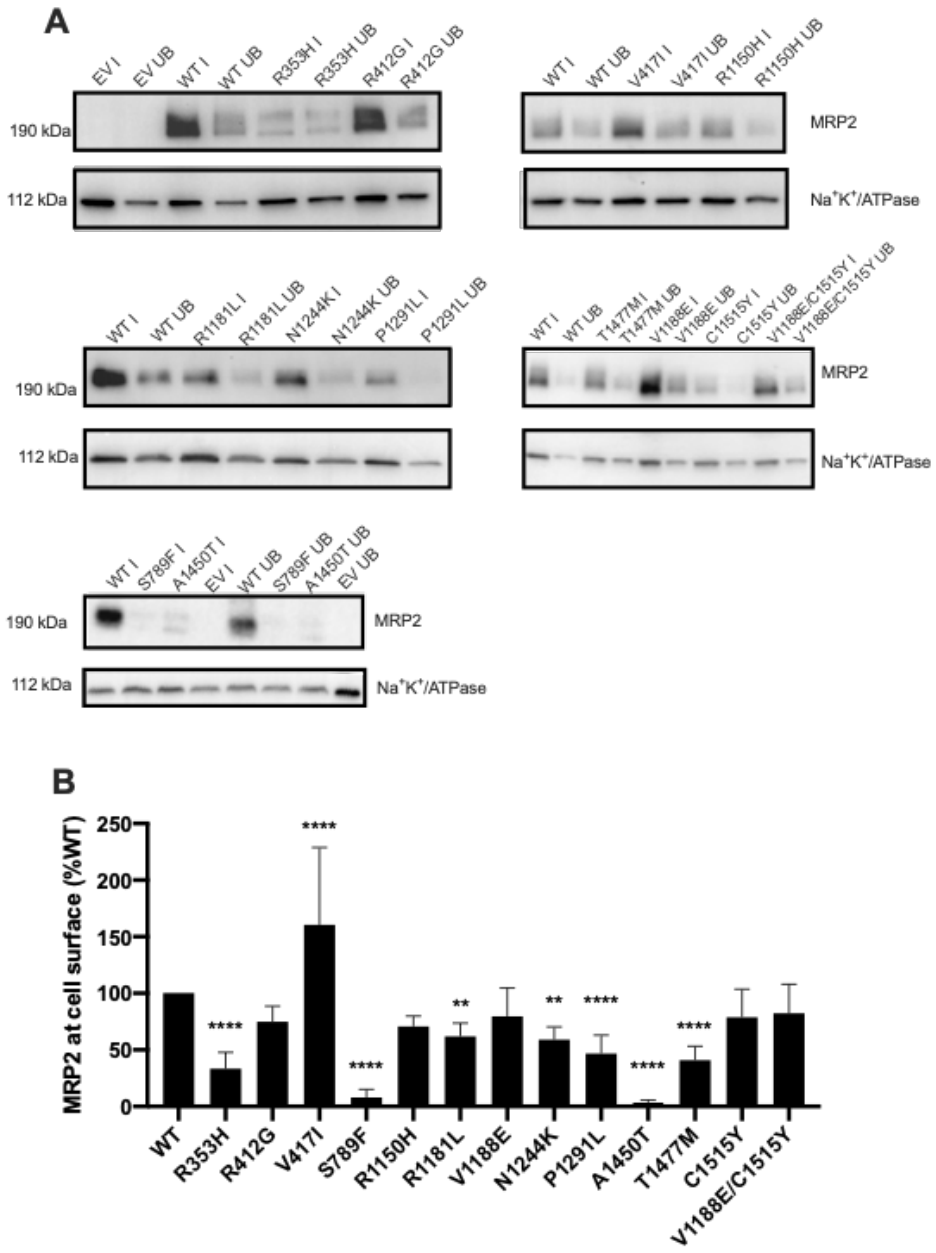

Figure 4.3: Cell surface biotinylation of HEK293T cells expressing empty vector, WT-MRP2, or variant-MRP2. HEK293T cells were transfected with empty vector, WT-MRP2, or variant-MRP2 and cell surface proteins were biotinylated. (A) The total input protein (indicated with I, 25 µL loaded) and unbiotinylated protein fractions (indicated with UB, 25 µL loaded) were resolved by 6% SDS-PAGE and immunoblotted with the MRP2-specific monoclonal antibody, M_2I-4 (1:2000). Blots were also probed using the Na^+K^+/ATPase mouse monoclonal antibody H-3 (1:10 000) as a loading control. The blots shown are from a representative experiment and similar results were obtained in at least two additional independent experiments. **(B)** Quantification (mean ± S.D. from at least three independent experiments) of the proportion of MRP2 that localizes to the cell surface based on the total (input) and unbiotinylated (UB) fractions of protein compared to WT-MRP2 are shown. Significant differences between WT- and variant-MRP2 are indicated with *P<0.05, **P<0.01, ***P<0.001, and ****P<0.0001 (One-way ANOVA followed by Dunnett's post-hoc test).

4.3.5 Variant-MRP2 had similar transport activity of $As(GS)_3$ compared to WT-MRP2.

Plasma membrane enriched vesicle transport assays with $As(GS)_3$ were used to functionally characterize MRP2 variants that were at significant levels in the plasma membrane enriched fraction and at the cell surface (all mutants except for S789F- and A1450T-MRP2) **(Fig 4.2D and 4.3B)**. $As(GS)_3$ transport by MRP2-enriched vesicles prepared from HEK293T cells has previously been characterized [26,27]. Human WT-MRP2 transported $^{73}As(GS)_3$ with a K_m of 4.2 ± 0.9 µM and a V_{max} of 134 ± 12 pmol/mg/min, with linear uptake up to 5 min [26].

Using the same methods, WT- and variant-MRP2 were characterized for $^{73}As(GS)_3$ (1 µM, 50 nCi) transport at a 3 min time point. Data are presented as a % of ATP-dependent WT-MRP2 $As(GS)_3$ transport activity, for which the average was 19.5 ± 3.8 pmol/mg/min **(Fig 4.4),** and transport activity was normalized to MRP2 levels, if levels were significantly different than WT-MRP2 in the plasma membrane-enriched vesicles. All MRP2 variants displayed similar $As(GS)_3$ transport activity compared to WT-MRP2 **(Fig 4.4A-C).** The only statistically different variant was T1477M-MRP2, which was at 60% of WT-MRP2 $As(GS)_3$ transport activity **(Fig 4.4B).**

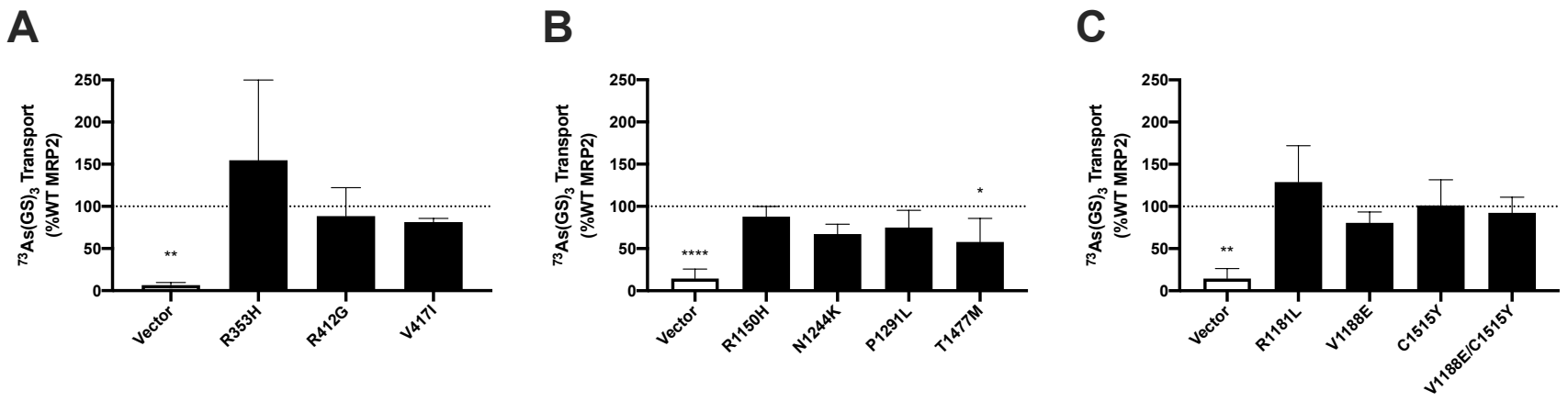

Figure 4.4: Transport of $^{73}As(GS)_3$ in plasma membrane enriched vesicles prepared from HEK293T cells transiently expressing empty vector, WT-MRP2, or variant-MRP2. Plasma membrane enriched vesicles (20 µg) were incubated for 3 min at 37°C in transport buffer with $^{73}As(GS)_3$ (1 µM, 100 nCi). The bars represent means ± SD of at least three independent experiments. Significant differences in transport activity between WT-MRP2 compared to variant-MRP2 and empty vector are shown with *P<0.05, **P<0.01 or ****P<0.0001 (One-way ANOVA followed by Dunnett's post-hoc test comparing to WT-MRP2).

4.3.6 Kinetic analysis of $[(GS)_2As^{75}Se]^-$ transport

Transport of $[(GS)_2AsSe]^-$ was previously characterized using radioactive ^{73}As-arsenite to prepare $[(GS)_2{}^{73}AsSe]^-$ [26]. In this study, the same compound was synthesized but using radioactive ^{75}Se-selenite. To ensure the transport of $[(GS)_2AsSe]^-$ with ^{75}Se in place of ^{73}As was consistent with Carew and Leslie (2010), kinetic parameters of $[(GS)_2As^{75}Se]^-$ transport by WT-MRP2 were evaluated and compared.

First, the linear range of ATP-dependent uptake of $[(GS)_2AsSe]^-$ (1 µM, 100 nCi) by WT-MRP2-enriched membrane vesicles, was measured. Transport was linear for up to 5 min with a maximum activity of 34.7 ± 4.3 pmol/mg/min, at which time it reached a plateau **(Fig 4.5A).** Kinetic analysis of MRP2-dependent transport of $[(GS)_2AsSe]^-$ was determined by measuring ATP-dependent transport of $[(GS)_2AsSe]^-$ over eight different concentrations (0.1-10 µM**) (Fig 4.5B).** Michaelis-Menten kinetic analysis (GraphPad Prism 8) revealed an apparent K_m of 1.1 ± 0.6 µM and V_{max} of 43 ± 9 pmol/mg/min **(Fig 4.5B)** for MRP2 transport of $[(GS)_2AsSe]^-$, similar to previously published values (K_m of 1.7 ± 0.8 µM and V_{max} of 45 ± 8 pmol/mg/min) [26].

4.3.7 R353H-, P1291L-, and R1181L-MRP2 have increased while V417I- and R1150H-MRP2 have decreased $[(GS)_2AsSe]^-$ transport compared to WT-MRP2.

Next, MRP2 variants that were at significant levels in the plasma membrane enriched fraction and at the cell surface **(Fig 4.2D and 3B),** were characterized for $[(GS)_2AsSe]^-$ (1 µM, 100 nCi) transport activity. Data shown for variants are normalized to relative MRP2 levels in plasma membrane enriched fractions (when necessary) and are presented as a % of ATP-dependent WT-MRP2 $[(GS)_2AsSe]^-$ transport activity, for which the average was 18.9 ± 3.0 pmol/mg/min **(Fig 4.5C-E).** Transport activity of $[(GS)_2AsSe]^-$ by variant-MRP2-enriched membrane vesicles was

at significantly increased levels for R353H-, P1291L- and R1181L-MRP2 at 156, 167, and 143% of WT-MRP2, respectively **(Fig 4.5C-E).** In contrast, $[(GS)_2AsSe]^-$ transport activity of variant-MRP2-enriched membrane vesicles was at significantly decreased levels for V417I- and R1150H-MRP2 at 60 and 27% of WT-MRP2, respectively **(Fig 4.5C and D).** Transport of $[(GS)_2AsSe]^-$ by the remaining mutants (R412G-, N1244K-, T1477M-, V1188E-, C1515Y-, and V1188E/C1515Y-MRP2) had similar transport activity as WT-MRP2 **(Fig 4.5C-E).**

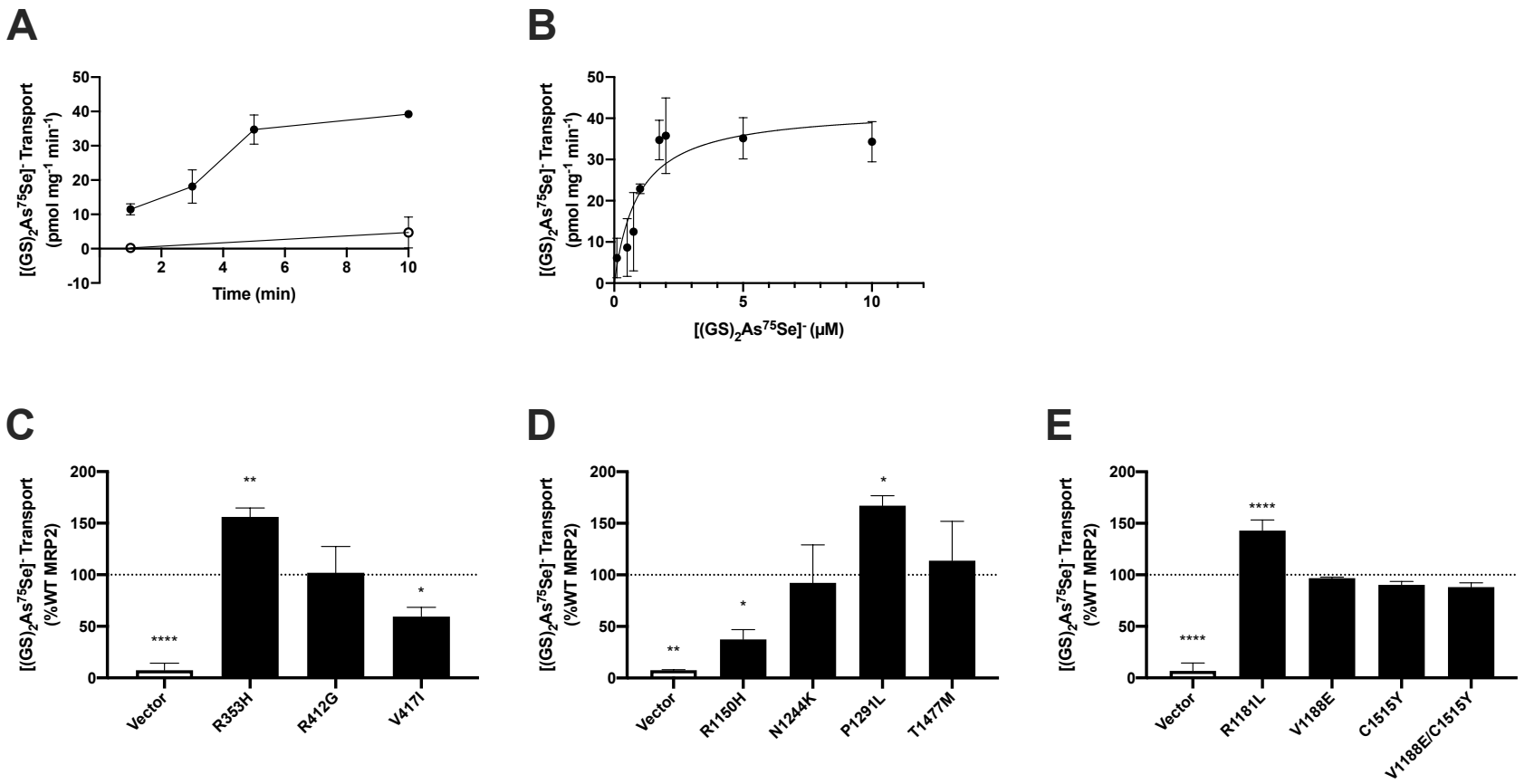

Figure 4.5: Transport of $[(GS)_2As^{75}Se]^-$ by plasma membrane enriched vesicles prepared from HEK293T cells transiently expressing empty vector, WT-MRP2, or variant-MRP2. Plasma membrane enriched vesicles (20 µg protein) were incubated at 37°C in transport buffer with $[(GS)_2As^{75}Se]^-$ (1 µM, 100 nCi, unless otherwise indicated) for a 3 min time point (unless otherwise indicated). **(A)** Time course of ATP-dependent transport of $[(GS)_2As^{75}Se]^-$ by empty vector or WT-MRP2-enriched vesicles. **(B)** Kinetic parameters of $[(GS)_2As^{75}Se]^-$ by WT-MRP2 were determined by measuring the initial rate of uptake by WT-MRP2-enriched vesicles over eight concentrations of $[(GS)_2As^{75}Se]^-$ (0.1-10 µM, 50-100 nCi), followed by data analysis with the Michaelis-Menten kinetic model (GraphPad Prism 8 software). **(C, D and E)** Transport of $[(GS)_2As^{75}Se]^-$ by empty vector, WT-MRP2, or variant-MRP2-enriched vesicles. Symbols and bars represent means ± S.D. of at least three independent experiments. Activity level was not corrected for MRP2 level. Significant differences in transport activity between WT-MRP2, variant-MRP2 and empty vector are shown with *P<0.05, **P<0.01, and ****P<0.0001 (One-way ANOVA followed by Dunnett's post-hoc test).

4.3.8 Whole cell arsenic accumulation studies with and without selenium

To supplement observations of reduced and increased transport activity of different MRP2 variants in the plasma membrane enriched fraction, a whole cell accumulation assay was completed using selected variants. The whole cell system was used to compare how HEK293T cells expressing empty vector and MRP2 variants accumulate arsenic in the presence and absence of selenium relative to WT-MRP2. Arsenic accumulation by HEK293T cells expressing WT-MRP2 was linear up to 6 hr **(Fig 4.6A),** with an average accumulation of 141 ± 4 pmol/mg protein at 24 hr. For characterization of arsenic accumulation in HEK293T cells expressing WT- and variant-MRP2, a 3 hr time point was selected and cells were treated with arsenic (1 μM, 100 nCi/well) ± selenide or selenite (1 μM).

HEK293T cells expressing empty vector or WT-MRP2 were treated with ^{73}As-arsenite (1 μM, 100 nCi/well) ± selenide (1 μM) or selenite (1 μM) for 3 hr and arsenic accumulation was quantified. As expected, cells expressing WT-MRP2 treated with arsenic, accumulated only 50% of the arsenic compared to cells expressing empty vector **(Fig 4.6B).** When cells were treated with ^{73}As-arsenite in the presence of selenite, the degree of arsenic accumulation was similar between empty vector and WT-MRP2, suggesting that export of arsenic by WT-MRP2 was inhibited **(Fig 4.6B).** When cells were treated with ^{73}As-arsenite in the presence of selenide, there was 46% less arsenic accumulation of arsenic in the cells expressing WT-MRP2 compared to empty vector, suggesting that MRP2 reduced accumulation of arsenic in the presence of selenide **(Fig 4.6B).** Although there was a trend towards the plus selenide condition reducing arsenic accumulation relative to minus selenide, there was no significant difference.

Next, the MRP2 variants with altered transport activity in **Figures 4.4** and **4.5** were further characterized using the whole cell accumulation assay. When HEK293T cells expressing WT- and T1477M-MRP2 were treated with ^{73}As-arsenite, accumulation of arsenic was 63% of WT-MRP2 in T1477M-MRP2. The decreased accumulation of arsenic by cells expressing T1477M-MRP2 suggested that in a whole cell model, there was increased efflux of arsenic from the cells. This result was unexpected because T1477M-MRP2-enriched membrane vesicles had reduced transport of $As(GS)_3$ relative to WT-MRP2 **(Fig 4.6B).** Arsenic uptake or metabolism could be altered in cells expressing T1477M-MRP2, but the differences in transport are modest and some of these differences could be attributed to variability.

The variants further investigated for accumulation of ^{73}As-arsenite in the presence of selenide were R353H-, V417I-, R1150H-, R1181L-, and P1291L-MRP2. R353H- and P1291L-MRP2 had significantly lower accumulation of ^{73}As-arsenite in the presence of selenide, which were 32 and 42% of WT-MRP2, respectively **(Fig 4.6D).** R1181L-MRP2 trended towards decreased accumulation of ^{73}As-arsenite in the presence of selenide, with arsenic accumulation that was 60% of WT-MRP2, but this trend was not significant **(Fig 4.6D).** In the presence of selenide, V417I- and R1150H-MRP2 had arsenic accumulation that was 186 and 158% of WT-MRP2, respectively **(Fig 4.6D).** Therefore, R353H-, R1181L-, and P1291L-MRP2 may have increased ability to efflux arsenic in the presence of selenide relative to WT-MRP2, and V417I- and R1150H-MRP2 may have decreased ability to efflux arsenic in the presence of selenide relative to WT-MRP2. These data are consistent with findings from membrane vesicle transport of $[(GS)_2AsSe]^-$, where R353H-, R1181L-, and P1291L-MRP2 had increased transport activity of

$[(GS)_2AsSe]^-$, and V417I- and R1150H-MRP2 had reduced ability to transport $[(GS)_2AsSe]^-$ **(Fig 4.5C-E).**

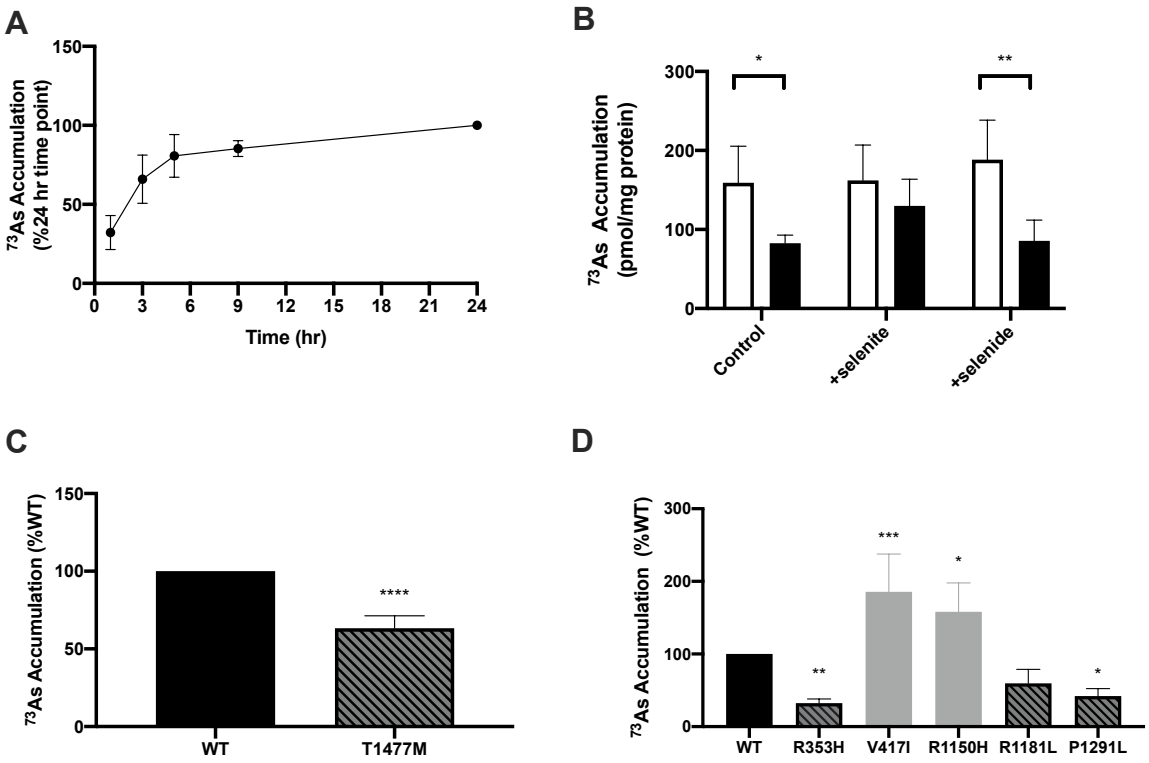

Figure 4.6: Whole cell accumulation of arsenic in the presence and absence of selenium in HEK293T cells transiently expressing empty vector, WT-MRP2, or variant-MRP2. (A) Accumulation of arsenic by HEK293T cells expressing WT-MRP2 over time. Cells were treated with media containing ^{73}As-arsenite (1 µM, 100 nCi). Then cells were washed and lysed in 0.5% Triton X-100 at indicated time points. Accumulation was quantified by beta liquid scintillation counting. **(B, C,** and **D)** were performed similarly, but cells were washed and lysed after treatment with media containing ^{73}As-arsenite (1 µM, 100 nCi) ± selenium (1 µM selenide or selenite) for 3 hr. **(B)** Accumulation of ^{73}As-arsenite alone (control), or in the presence of selenite or selenide. The white bars represent accumulation in HEK293T cells transiently expressing empty vector, and black bars represent accumulation in HEK293T cells transiently expressing WT-MRP2. The means ± S.D. of at least three independent experiments are shown. Significant differences comparing accumulation between empty vector and WT-MRP2 expressing cells are indicated with *P<0.05 and **P<0.01 (One-way ANOVA followed by Sidak's multiple comparisons test). **(C)** Accumulation of ^{73}As-arsenite in the absence of selenium. The bars represent means ± S.D. of at least three independent experiments. Significant differences in arsenic accumulation between WT-MRP2 and T1477M-MRP2 are shown with ****P<0.0001 (Student's T-test). **(D)** Accumulation of ^{73}As-arsenite in the presence of selenide. The bars represent means ± S.D. of at least three independent experiments. Significant differences between WT-MRP2, and variant-MRP2 are shown with *P<0.05, **P<0.01, or ***P<0.001 (One-way ANOVA followed by Dunnett's post-hoc test comparing to WT-MRP2).

4.4 Discussion

Twelve individual and one double non-synonymous MRP2 variants were investigated for their influence on MRP2 level, plasma membrane localization, transport of $As(GS)_3$ and $[(GS)_2AsSe]^-$ by membrane vesicles, and accumulation of arsenic alone and in the presence of selenium (selenide and selenite). The results observed for each variant have been summarized in **Table 4.3.**

Table 4.3: Summary of MRP2 variant levels in whole cell lysates and at the plasma membrane as well as transport activity relative to WT-MRP2

	MRP2 Level			Activity in plasma membrane enriched vesicles		Activity from whole cell accumulation assay	
Variant	**Whole cell lysates**	**Cell surface biotinylation**	**Plasma membrane-enriched vesicles**	**$As(GS)_3$**	**$[(GS)_2AsSe]^-$**	**Arsenite only**	**Arsenite + selenide**
R353H	WT	↓	↓	WT	↑		↑
R412G	WT	WT	WT	WT	WT		
V417I	WT	↑	↑	WT	↓		↓
S789F	↓	Not detected					
R1150H	↓	WT	WT	WT	↓		↓
R1181L	WT	↓	↓	WT	↑		↑
V1188E	WT	WT	WT	WT	WT		
N1244K	↓	↓	↓	WT	WT		↑
P1291L	↓	↓	↓	WT	↑		
A1450T	↓	Not detected					
T1477M	WT	↓	↓	↓	WT	↑	
C1515Y	WT	WT	WT	WT	WT		
V1188E/C1515Y	WT	WT	WT	WT	WT		

WT, similar to WT; ↑, increased; ↓, decreased

Three variants (R412G-, V1188E-, and C1515Y-MRP2) as well as the double variant (V1188E/C1515Y-MRP2) showed no differences from WT-MRP2 for protein levels, cell surface localization, or transport activity. In contrast, levels of S789F- and A1450T-MRP2 were markedly reduced in whole cell lysates, and not detectable in plasma membrane-enriched fractions or at the cell surface. Of the remaining variants, one had reduced $As(GS)_3$ transport (T1477M-MRP2), while three variants (R353H-, R1181L-, and P1291L-MRP2) had increased and two variants (V417I- and R1150H-MRP2) had reduced $[(GS)_2AsSe]^-$ transport. While $As(GS)_3$ is expected to undergo enterohepatic cycling, and alterations in biliary efflux may have less important consequences, biliary excretion of $[(GS)_2AsSe]^-$ is expected to increase fecal elimination of both arsenic and selenium [21,23,70,71]. Therefore, individuals expressing MRP2 variants that increase or decrease the cellular export of $[(GS)_2AsSe]^-$ may benefit more or less from selenium supplementation, respectively.

Results for the variants with similar characteristics to WT-MRP2 (R412G-, V1188E-, C1515Y-, and V1188E/C1515Y-MRP2) were reasonably consistent with previously published data and expected. Only a single previous report on the functional characterization of the rare mutation R412G-MRP2 exists using Chinese hamster ovary cells (CHO) after it was identified in a patient with impaired methotrexate elimination [35]. Although levels of R412G-MRP2 were not quantified, immunofluorescence analysis suggested that consistent with the current study, R412G-MRP2 was trafficked appropriately to the plasma membrane. Unlike our observation of WT-MRP2-like $As(GS)_3$ and $[(GS)_2AsSe]^-$ transport activity, R412G-MRP2 exported methotrexate and GS-MF from intact CHO cells with activity similar to empty vector expressing cells [35]. The small difference between the export of methotrexate and GS-MF between WT-MRP2 and

empty vector cells may suggest their accumulation assay was of lower sensitivity than our membrane vesicle assay.

Consistent with our results, cell surface levels of V1188E-, C1515Y-, and V1188E/C1515Y-MRP2 were similar to WT-MRP2 in multiple cell lines tested (Flp-In 293, HEK293, and/or Rht14-10) cells [49,50]. Cell accumulation and membrane vesicle transport of different substrates (calcein-AM, 5(6)-carboxy-2',7'-dichlorofluorescein diacetate, glutathione-methylfluorescein, and/or GS-monochlorobimane) suggested modestly reduced or unchanged transport activity for V1188E-, C1515Y-, and V1188E/C1515Y-MRP2 [49,67]. Interestingly, C1515Y-MRP2 had a ~2-fold reduction in lopinavir accumulation [67]. Consistent with the mostly modest effects of these mutations on MRP2 function, PolyPhen2 predicted that these variants are all benign, and SIFT predicted that V412G could affect function, while V1188E and C1515Y are tolerated (Table 4.2).

Low levels of S789F- and A1450T-MRP2 were detected in whole cell lysates of HEK293T cells. In plasma membrane enriched and cell surface biotinylated fractions these variants were not detected under the conditions tested. Low levels of these mutants have also been reported in LLC-PK1, Flp-In 293, and Sf9 cells, but levels were still detectable in the plasma membrane enriched fraction [46,49,60]. This led us to do the reverse mutagenesis experiment where we confirmed that MRP2 levels were rescued, and unintended mutations were not incorporated. The reason others could detect some S789F- and A1450T-MRP2 at the plasma membrane while we did not is likely related to the different cell systems. In particular, Sf9 cells are known to target proteins to the plasma membrane that do not reach the plasma membrane in mammalian cells [46]. Regardless, in all mammalian cells, these two mutants were markedly

reduced at the plasma membrane. Predictions by the Polyphen-2 and SIFT algorithm for S789F- and A1450T-MRP2 were deleterious and probably and possibly damaging, respectively (Table 2). S789F- and A1450T-MRP2 are located in the NBDs: S789F-MRP2 is located in the D-loop of NBD1, following the Walker B region and A1450T-MRP2 is located in the region between the C Signature and Walker B motifs in NBD2. The NBDs are essential for the folding and function of MRP2 as they bind ATP at their interface, and power export of solutes [72–74]. The low levels of these mutants would likely prevent the efficient export of $As(GS)_3$ and $[(GS)_2AsSe]^-$ by MRP2 into bile and humans expressing these variants would be at a disadvantage when exposed to arsenic.

Consistent with findings from Sf9 cells, T1477M- had levels similar to WT-MRP2 in whole cell lysates, but lower levels at the cell surface [46]. Even when normalized for level at the cell surface, T1477M-MRP2 had reduced transport of $As(GS)_3$, and WT-MRP2-like transport activity of $[(GS)_2AsSe]^-$. Reduced transport of $As(GS)_3$ by MRP2 into bile could lead to less hepatic glutathione depletion through enterohepatic cycling, and in the presence of selenium, individuals would still be able to export (and eliminate) $[(GS)_2AsSe]^-$ into bile, thus benefiting from selenium supplementation. In the absence of selenium, individuals with T1477M-MRP2 would potentially allow more arsenic into the systemic circulation and therefore accumulate more in peripheral tissues with more toxic effects. In addition to hepatic expression, MRP2 is found at the apical surface of the renal proximal tubular cells, and T1477M-MRP2 may reduce the urinary elimination of arsenic. Other studies of T1477M-MRP2 observed increased transport of the bile acid, tauroursodeoxycholic acid, but decreased transport of estradiol-3-

glucuronide [46]. SIFT predicted T1477M-MRP2 to affect function **(Table 4.2)**, which is consistent with this and other studies.

Individuals with R353H-, R1181L-, or P1291-MRP2 may benefit more from selenium supplementation than WT-MRP2 because these variants had increased transport of $[(GS)_2AsSe]^-$ which could ultimately increase fecal elimination. In independent studies using other cells (HEK, Flp-In 293, Rht14-10), R353H-, R1181L- and P1291L-MRP2 levels were similar to WT or moderately reduced, and the transport activity of these variants differed between substrates [49,50]. R353H-MRP2 resulted in modestly less efflux of glutathione-monochlorobimane (GS-MCB) and glutathione-methylfluorescein (GS-MF) from Rht14-10 cells [50]. R1181L- and P1291L-MRP2 resulted in modestly lower efflux of GS-MCB. R1181L-MRP2 had increased efflux of GS-MF and Calcein AM [49,50]. Consistent with how these variants altered function, they were predicted to be benign or possibly damaging by PolyPhen2 and tolerated or affect function by SIFT **(Table 4.2).**

V417I- and R1150H-MRP2 had similar transport activities of $As(GS)_3$ as WT-MRP2, but decreased transport of $[(GS)_2AsSe]^-$. This would potentially lead to depletion of GSH levels (and potentially oxidative damage) in hepatocytes via enterohepatic cycling of $As(GS)_3$ with less elimination of $[(GS)_2AsSe]^-$ relative to a person expressing WT-MRP2. Consequently, arsenic and selenium would eventually undergo export across the hepatocyte sinusoidal surface, potentially allowing more accumulation of these compounds in extrahepatic tissues. Although V417I-MRP2 levels were like WT-MRP2 in whole cell lysates, levels were increased at the cell surface, which has also been observed in human hepatocytes [56]. In contrast, V417I-MRP2 levels were WT-MRP2-like in Sf9 cells [46]. Despite lower levels of R1150H-MRP2 in whole cell lysates, we and

others observed WT-like levels at the cell surface in HEK293 cells [45]. R1150H-MRP2 also trafficked to the apical surface of HepG2 cells similarly to WT-MRP2 [64]. Consistent with our findings, V417I- and R1150H-MRP2 had a reduced ability to transport various substrates studied in Sf9 and HEK293 cells (leukotriene C_4, estradiol-3-glucuronide, and estradiol-17β-glucuronide, carboxyfluorescein) [45,46]. Therefore, selenium supplementation may not be beneficial to individuals with V417I- or R1150H-MRP2.

This study advances understanding of how inter-individual differences in selenium-independent and -dependent biliary excretion of arsenic may influence outcomes of chronic arsenic exposure in humans. Individuals with MRP2 variants that do not reach the cell surface (S789F- and A1450T-MRP2) may have an impaired ability to efflux arsenic from hepatocytes. Individuals expressing variants with a reduced ability to efflux arsenic in the presence of selenium (V417I- and R1150H-MRP2) may not benefit from selenium supplementation, so other treatments should be considered. For individuals with reduced ability to transport $As(GS)_3$ (T1477M-MRP2), or with increased ability to transport $[(GS)_2AsSe]^-$(R353H-, R1181L-, and P1291L-MRP2), selenium supplementation would be a feasible strategy for stimulating arsenic biliary excretion. However, individuals with variants that could be expressed to a lesser extent at the plasma membrane *in vivo* (R353H-, R1181L-, N1244K-, T1477M-MRP2) may still have a reduced capacity for effluxing arsenic from hepatocytes. The findings from this study could be valuable for future population studies to determine if individuals would benefit from selenium supplementation and assessing susceptibility to arsenic-induced diseases.

4.5 References

[1] J.C. Saha, A.K. Dikshit, M. Bandyopadhyay, K.C. Saha, A Review of Arsenic Poisoning and its Effects on Human Health, Critical Reviews in Environmental Science and Technology. 29 (1999). https://doi.org/10.1080/10643389991259227.

[2] IARC, A review of human carcinogens – Part C: metals, arsenic, dusts, and fibres., 2012.

[3] J. Podgorski, M. Berg, Global threat of arsenic in groundwater, Science. 368 (2020) 845 LP – 850. https://doi.org/10.1126/science.aba1510.

[4] E. Shaji, M. Santosh, K.V. Sarath, P. Prakash, V. Deepchand, B.V. Divya, Arsenic contamination of groundwater: A global synopsis with focus on the Indian Peninsula, Geoscience Frontiers. 12 (2021) 101079. https://doi.org/10.1016/j.gsf.2020.08.015.

[5] C.F. McGuigan, C.L.A. Hamula, S. Huang, S. Gabos, X.C. Le, A review on arsenic concentrations in Canadian drinking water, Environmental Reviews. (2010) 291–307. https://doi.org/10.1139/A10-012.

[6] V.D. Martinez, E.A. Vucic, S. Lam, W.L. Lam, Emerging Arsenic Threat in Canada, Science (1979). 342 (2013). https://doi.org/10.1126/science.342.6158.559-a.

[7] S. Wang, C. Mulligan, Occurance of arsenic contamination in Canada: sources, behavior and distribution, Science of the Total Environment. 366 (2006) 701–721.

[8] S. Sah, A. Vandenberg, J. Smits, Treating chronic arsenic toxicity with high selenium lentil diets, Toxicology and Applied Pharmacology. 272 (2013) 256–2662. https://doi.org/10.1016/j.taap.2013.06.008.

[9] J.E. Smits, R.M. Krohn, E. Akhtar, S.K. Hore, M. Yunus, A. Vandenberg, R. Raqib, Food as medicine: Selenium enriched lentils offer relief against chronic arsenic poisoning in Bangladesh, Environmental Research. 176 (2019). https://doi.org/10.1016/j.envres.2019.108561.

[10] R.M. Krohn, R. Raqib, E. Akhtar, A. Vandenberg, J.E.G. Smits, A high-selenium lentil dietary intervention in Bangladesh to counteract arsenic toxicity: Study protocol for a randomized controlled trial, Trials. 17 (2016). https://doi.org/10.1186/s13063-016-1344-y.

[11] W.J. Verret, Y. Chen, A. Ahmed, T. Islam, F. Parvez, M.G. Kibriya, J.H. Graziano, H. Ahsan, A randomized, double-blind placebo-controlled trial evaluating the effects of vitamin E and selenium on arsenic-induced skin lesions in Bangladesh, Journal of Occupational and Environmental Medicine. 47 (2005) 1026–1035.

[12] J. Gailer, G.N. George, I.J. Pickering, R.C. Prince, H.S. Younis, J.J. Winzerling, Biliary excretion of [(GS)2AsSe]- after intravenous injection of rabbits with arsenite and selenate, Chemical Research in Toxicology. 15 (2002) 1466–1471. https://doi.org/10.1021/tx025538s.

[13] G.N. George, J. Gailer, O. Ponomarenko, P.F. la Porte, K. Strait, M. Alauddin, H. Ahsan, S. Ahmed, J. Spallholz, I.J. Pickering, Observation of the seleno bis-(S-glutathionyl) arsinium anion in rat bile, Journal of Inorganic Biochemistry. 158 (2016) 24–29. https://doi.org/https://doi.org/10.1016/j.jinorgbio.2016.01.022.

[14] J. Gailer, G.N. George, I.J. Pickering, R.C. Prince, S.C. Ringwald, J.E. Pemberton, R.S. Glass, H.S. Younis, D.W. DeYoung, H.V. Aposhian, A metabolic link between arsenite and selenite: The seleno-bis(S- glutathionyl) arsinium ion, J Am Chem Soc. (2000).

[15] O.A. Levander, C.A. Baumann, Selenium metabolism. VI. Effect of arsenic on the excretion of selenium in the bile, Toxicology and Applied Pharmacology. (1966) 106–115. https://doi.org/10.1016/0041-008X(66)90035-4.

[16] O. Ponomarenko, P.F. la Porte, S.P. Singh, G. Langan, D.E.B. Fleming, J.E. Spallholz, M. Alauddin, H. Ahsan, S. Ahmed, J. Gailer, G.N. George, I.J. Pickering, Selenium-mediated arsenic excretion in mammals: A synchrotron-based study of whole-body distribution and tissue-specific chemistry, Metallomics. 9 (2017) 1585–1595.

[17] Y. Chen, M. Hall, J.H. Graziano, V. Slavkovich, A. van Geen, F. Parvez, H. Ahsan, A prospective study of blood selenium levels and the risk of arsenic-related premalignant skin lesions, Cancer Epidemiology Biomarkers and Prevention. 16 (2007) 207–213. https://doi.org/10.1158/1055-9965.EPI-06-0581.

[18] A.L. Moxon, The effect of arsenic on the toxicity of seleniferous grains, Science (1979). 88 (1938) 81. https://doi.org/10.1126/science.88.2273.81.

[19] F. Challenger, Biological methylation, Quarterly Reviews, Chemical Society. 9 (1955). https://doi.org/10.1039/qr9550900255.

[20] W.R. Cullen, Chemical mechanism of arsenic biomethylation, Chemical Research in Toxicology. 27 (2014) 457–461. https://doi.org/10.1021/tx400441h.

[21] E.M. Leslie, Arsenic-glutathione conjugate transport by the human multidrug resistance proteins (MRPs/ABCCs), Journal of Inorganic Biochemistry. 108 (2012) 141–149. https://doi.org/10.1016/j.jinorgbio.2011.11.009.

[22] S. v. Kala, G. Kala, C.I. Prater, A.C. Sartorelli, M.W. Lieberman, Formation and Urinary Excretion of Arsenic Triglutathione and Methylarsenic Diglutathione, Chemical Research in Toxicology. 17 (2004) 243–249.

[23] S. v. Kala, M.W. Neely, G. Kala, C.I. Prater, D.W. Atwood, J.S. Rice, M.W. Lieberman, The MRP2/cMOAT transporter and arsenic-glutathione complex formation are required for biliary excretion of arsenic, Journal of Biological Chemistry. 275 (2000) 33404–33408.

[24] M. Delnomdedieu, M.M. Basti, J.D. Otvos, D.J. Thomas, Reduction and binding of arsenate and dimethylarsinate by glutathione: a magnetic resonance study, Chemico-Biological Interactions. 90 (1994). https://doi.org/10.1016/0009-2797(94)90099-X.

[25] A.T. Nies, F. Klein, Multidrug Resistance Proteins of the ABCC Subfamily, in: G. You, M.E. Morris (Eds.), Drug Transporters: Molecular Characterization and Role in Drug Disposition, 3rd Edition, 3rd ed., John Wiley & Sons, 2022: pp. 213–233.

[26] M.W. Carew, E.M. Leslie, Selenium-dependent and -independent transport of arsenic by the human multidrug resistance protein 2 (MRP2/ABCC2): Implications for the mutual detoxification of arsenic and selenium, Carcinogenesis. 31 (2010) 1450–1455.

[27] E.M. Leslie, A. Haimeur, M.P. Waalkes, Arsenic transport by the human multidrug resistance protein 1 (MRP1/ABCC1): Evidence that a tri-glutathione conjugate is required, Journal of Biological Chemistry. 279 (2004) 32700–32708. https://doi.org/10.1074/jbc.M404912200.

[28] M.W. Carew, H. Naranmandura, C.B. Shukalek, X.C. Le, E.M. Leslie, Monomethylarsenic diglutathione transport by the human multidrug resistance protein 1 (MRP1/ABCC1),

Drug Metabolism and Disposition. 39 (2011) 2298–304. https://doi.org/10.1124/dmd.111.041673.

[29] M. Banerjee, M.W. Carew, B.A. Roggenbeck, B.D. Whitlock, H. Naranmandura, X.C. Le, E.M. Leslie, A Novel Pathway for Arsenic Elimination: Human Multidrug Resistance Protein 4 (MRP4/ABCC4) Mediates Cellular Export of Dimethylarsinic Acid (DMAV) and the Diglutathione Conjugate of Monomethylarsonous Acid (MMAIII), Molecular Pharmacology. 86 (2014) 168–179.

[30] M. Banerjee, G. Kaur, Brayden.D. Whitlock, M.W. Carew, X.C. Le, E.M. Leslie, Multidrug Resistance Protein 1 (MRP1/ABCC1)-Mediated Cellular Protection and Transport of Methylated Arsenic Metabolites Differs between Human Cell Lines, Drug Metabolism and Disposition. 46 (2018) 1096–1105.

[31] M. Banerjee, V. Marensi, G. Conseil, X.C. Le, S.P.C. Cole, E.M. Leslie, Polymorphic variants of MRP4/ABCC4 differentially modulate the transport of methylated arsenic metabolites and physiological organic anions, Biochemical Pharmacology. 120 (2016) 72–82.

[32] S. v. Kala, G. Kala, C.I. Prater, A.C. Sartorelli, M.W. Lieberman, Formation and Urinary Excretion of Arsenic Triglutathione and Methylarsenic Diglutathione, Chemical Research in Toxicology. 17 (2004). https://doi.org/10.1021/tx0342060.

[33] J.R. Zhou, G. Kaur, Y. Ma, D. Arutyunov, X. Lu, X.C. Le, E.M. Leslie, Biliary excretion of arsenic by human HepaRG cells is stimulated by selenide and mediated by the multidrug resistance protein 2 (MRP2/ABCC2), Biochemical Pharmacology. 193 (2021) 114799. https://doi.org/10.1016/j.bcp.2021.114799.

[34] A. Auton, G.R. Abecasis, D.M. Altshuler, R.M. Durbin, D.R. Bentley, A. Chakravarti, A.G. Clark, P. Donnelly, E.E. Eichler, P. Flicek, S.B. Gabriel, R.A. et al. A global reference for human genetic variation, Nature. 526 (2015) 68–74. https://doi.org/10.1038/NATURE15393.

[35] J.-S. Hulot, E. Villard, A. Maguy, V. Morel, L. Mir, I. Tostivint, D. William-Faltaos, C. Fernandez, S. Hatem, G. Deray, M. Komajda, V. Leblond, P. Lechat, A mutation in the

drug transporter gene ABCC2 associated with impaired methotrexate elimination., Pharmacogenet Genomics. 15 (2005) 277–85.

[36] N. Junge, I. Goldschmidt, J. Wiegandt, C. Leiskau, F. Mutschler, T. Laue, J. Ohlendorf, A. Stalke, B. Hartleben, J. Stindt, V. Keitel, U. Baumann, E.D. Pfister, Dubin-Johnson Syndrome as Differential Diagnosis for Neonatal Cholestasis, J Pediatr Gastroenterol Nutr. 72 (2021) e105–e111. https://doi.org/10.1097/MPG.0000000000003061.

[37] Z.J. Talaga, P.N. Vaidya, Dubin Johnson Syndrome, StatPearls. (2021). https://www.ncbi.nlm.nih.gov/books/NBK536994/ (accessed April 12, 2022).

[38] N. Memon, B.I. Weinberger, T. Hegyi, L.M. Aleksunes, Inherited Disorders of Bilirubin Clearance, Pediatr Res. 79 (2016) 378. https://doi.org/10.1038/PR.2015.247.

[39] K.I. Ito, C.J. Oleschuk, C. Westlake, M.Z. Vasa, R.G. Deeley, S.P.C. Cole, Mutation of Trp1254 in the Multispecific Organic Anion Transporter, Multidrug Resistance Protein 2 (MRP2) (ABCC2), Alters Substrate Specificity and Results in Loss of Methotrexate Transport Activity, Journal of Biological Chemistry. 276 (2001) 38108–24. https://doi.org/10.1074/jbc.M105160200.

[40] C.A. Chen, H. Okayama, Calcium phosphate-mediated gene tranfer: A highly efficient transfection system for stably transforming cells with plasmid DNA, Biotechniques. 6 (1988) 632–638.

[41] E.M. Leslie, P.B. Watkins, R.B. Kim, K.L.R. Brouwer, Differential inhibition of rat and human Na+-dependent taurocholate cotransporting polypeptide (NTCP/SLC10A1) by bosentan: A mechanism for species differences in hepatotoxicity, Journal of Pharmacology and Experimental Therapeutics. 321 (2007) 1170–1178. https://doi.org/10.1124/jpet.106.119073.

[42] J. Gailer, S. Madden, M.F. Burke, M.B. Denton, H. v Aposhian, Simultaneous multielement-specific detection of a novel glutathione–arsenic–selenium ion [(GS)2AsSe]− by ICP AES after micellar size- exclusion chromatography, Applied Organometallic Chemistry. 14 (2000) 355–363. https://doi.org/https://doi.org/10.1002/1099-0739(200007)14:7<355::AID-AOC8>3.0.CO;2-0.

[43] P.F. Reay, C.J. Asher, Preparation and purification of 74As-labeled arsenate and arsenite for use in biological experiments, Analytical Biochemistry. 78 (1977) 557–560. https://doi.org/10.1016/0003-2697(77)90117-8.

[44] K. Mease, R. Sane, L. Podila, M.E. Taub, Differential Selectivity of Efflux Transporter Inhibitors in Caco-2 and MDCK–MDR1 Monolayers: A Strategy to Assess the Interaction of a New Chemical Entity with P-gp, BCRP, and MRP2, Journal of Pharmaceutical Sciences. 101 (2012). https://doi.org/10.1002/jps.23069.

[45] R. Mor-Cohen, A. Zivelin, N. Rosenberg, M. Shani, S. Muallem, U. Seligsohn, Identification and Functional Analysis of Two Novel Mutations in the Multidrug Resistance Protein 2 Gene in Israeli Patients with Dubin-Johnson Syndrome, Journal of Biological Chemistry. 276 (2001) 36923–36930. https://doi.org/10.1074/jbc.M105047200.

[46] V. Megaraj, T. Zhao, C.M. Paumi, P.M. Gerk, R.B. Kim, M. Vore, Functional analysis of nonsynonymous single nucleotide polymorphisms of multidrug resistance-associated protein 2 (ABCC2)., Pharmacogenet Genomics. 21 (2011) 506–15. https://doi.org/10.1097/FPC.0b013e328348c786.

[47] P.E. Bandler, C.J. Westlake, C.E. Grant, S.P.C. Cole, R.G. Deeley, Identification of Regions Required for Apical Membrane Localization of Human Multidrug Resistance Protein 2, Molecular Pharmacology. 74 (2008) 9–19. https://doi.org/10.1124/mol.108.045674.

[48] S. Ryu, T. Kawabe, S. Nada, A. Yamaguchi, Identification of Basic Residues Involved in Drug Export Function of Human Multidrug Resistance-associated Protein 2, Journal of Biological Chemistry. 275 (2000) 39617–39624. https://doi.org/10.1074/jbc.M005149200.

[49] X. Wen, M.S. Joy, L.M. Aleksunes, In Vitro Transport Activity and Trafficking of MRP2/ABCC2 Polymorphic Variants, Pharmaceutical Research. 34 (2017) 1637–1647. https://doi.org/10.1007/s11095-017-2160-0.

[50] R. Arlanov, A. Porter, D. Strand, R. Brough, D. Karpova, R. Kerb, L. Wojnowski, M. Schwab, T. Lang, Functional characterization of protein variants of the human multidrug

transporter ABCC2 by a novel targeted expression system in fibrosarcoma cells., Hum Mutat. 33 (2012) 750–62. https://doi.org/10.1002/humu.22041.

[51] V.M. Pratt, B.N. Beyer, D.L. Koller, T.C. Skaar, D.A. Flockhart, K.D. Levy, G.H. Vance, Report of New Haplotype for ABCC2 Gene: rs17222723 and rs8187718 in cis, The Journal of Molecular Diagnostics : JMD. 17 (2015) 201. https://doi.org/10.1016/J.JMOLDX.2014.11.005.

[52] B.D. Whitlock, E.M. Leslie, Efflux transporters in anti-cancer drug resistance: Molecular and functional identification and characterization of multidrug resistance proteins (MRPs/ABCCs), in: Drug Efflux Pumps in Cancer Resistance Pathways: From Molecular Recognition and Characterization to Possible Inhibition Strategies in Chemotherapy, 2020: pp. 31–65. https://doi.org/10.1016/b978-0-12-816434-1.00002-4.

[53] S.T. Sherry, M. Ward, K. Sirotkin, dbSNP-database for single nucleotide polymorphisms and other classes of minor genetic variation., Genome Res. 9 (1999) 677–9. https://doi.org/10.1101/GR.9.8.677.

[54] Y. Huang, Pharmacogenetics/genomics of membrane transporters in cancer chemotherapy., Cancer Metastasis Rev. 26 (2007) 183–201. https://doi.org/10.1007/s10555-007-9050-6.

[55] E. Cecchin, M. D'Andrea, S. Lonardi, C. Zanusso, N. Pella, D. Errante, E. de Mattia, J. Polesel, F. Innocenti, G. Toffoli, A prospective validation pharmacogenomic study in the adjuvant setting of colorectal cancer patients treated with the 5-fluorouracil/leucovorin/oxaliplatin (FOLFOX4) regimen., Pharmacogenomics J. 13 (2013) 403–9. https://doi.org/10.1038/tpj.2012.31.

[56] A.K. Deo, B. Prasad, L. Balogh, Y. Lai, J.D. Unadkat, Interindividual variability in hepatic expression of the multidrug resistance-associated protein 2 (MRP2/ABCC2): quantification by liquid chromatography/tandem mass spectrometry., Drug Metab Dispos. 40 (2012) 852–5. https://doi.org/10.1124/dmd.111.043810.

[57] K. Engström, S. Ameer, L. Bernaudat, G. Drasch, J. Baeuml, S. Skerfving, S. Bose-O'Reilly, K. Broberg, Polymorphisms in genes encoding potential mercury transporters and urine

mercury concentrations in populations exposed to mercury vapor from gold mining., Environ Health Perspect. 121 (2013) 85–91. https://doi.org/10.1289/ehp.1204951.

[58] J.A. Sloan, M. de Andrade, P. Decker, J. Wampfler, C. Oswold, M. Clark, P. Yang, Genetic variations and patient-reported quality of life among patients with lung cancer., J Clin Oncol. 30 (2012) 1699–704. https://doi.org/10.1200/JCO.2010.34.5629.

[59] S. Ito, I. Ieiri, M. Tanabe, A. Suzuki, S. Higuchi, K. Otsubo, Polymorphism of the ABC transporter genes, MDR1, MRP1 and MRP2/cMOAT, in healthy Japanese subjects, Pharmacogenetics. 11 (2001) 175–184. https://doi.org/10.1097/00008571-200103000-00008.

[60] M. Hirouchi, H. Suzuki, M. Itoda, S. Ozawa, J.I. Sawada, I. Ieiri, K. Ohtsubo, Y. Sugiyama, Characterization of the cellular localization, expression level, and function of SNP variants of MRP2/ABCC2, Pharmaceutical Research. 21 (2004) 742–748. https://doi.org/10.1023/B:PHAM.0000026422.06207.33.

[61] I. Cascorbi, S. Haenisch, Pharmacogenetics of ATP-Binding Cassette Transporters and Clinical Implications, in: Humana Press, 2010: pp. 95–121. https://doi.org/10.1007/978-1-60761-416-6_6.

[62] S. Sookoian, G. Castaño, T.F. Gianotti, C. Gemma, C.J. Pirola, Polymorphisms of MRP2 (ABCC2) are associated with susceptibility to nonalcoholic fatty liver disease., J Nutr Biochem. 20 (2009) 765–70. https://doi.org/10.1016/j.jnutbio.2008.07.005.

[63] L. Wojnowski, B. Kulle, M. Schirmer, G. Schlüter, A. Schmidt, A. Rosenberger, S. Vonhof, H. Bickeböller, M.R. Toliat, E.K. Suk, M. Tzvetkov, A. Kruger, S. Seifert, M. Kloess, H. Hahn, M. Loeffler, P. Nürnberg, M. Pfreundschuh, L. Trümper, J. Brockmöller, G. Hasenfuss, NAD(P)H oxidase and multidrug resistance protein genetic polymorphisms are associated with doxorubicin-induced cardiotoxicity, Circulation. 112 (2005) 3754–3762. https://doi.org/10.1161/CIRCULATIONAHA.105.576850.

[64] V. Keitel, A.T. Nies, M. Brom, J. Hummel-Eisenbeiss, H. Spring, D. Keppler, A common Dubin-Johnson syndrome mutation impairs protein maturation and transport activity of MRP2 (ABCC2)., Am J Physiol Gastrointest Liver Physiol. 284 (2003) G165-74. https://doi.org/10.1152/ajpgi.00362.2002.

[65] A.T. Nies, D. Keppler, The apical conjugate efflux pump ABCC2 (MRP2), Pflugers Archiv European Journal of Physiology. 453 (2007) 643–659. https://doi.org/10.1007/s00424-006-0109-y.

[66] L. Elens, J.-C. Yombi, D. Lison, P. Wallemacq, B. Vandercam, V. Haufroid, Association between ABCC2 polymorphism and lopinavir accumulation in peripheral blood mononuclear cells of HIV-infected patients., Pharmacogenomics. 10 (2009) 1589–97. https://doi.org/10.2217/pgs.09.88.

[67] L. Elens, D. Tyteca, N. Panin, P. Courtoy, D. Lison, J.-B. Demoulin, V. Haufroid, Functional defect caused by the 4544G>A SNP in ABCC2: potential impact for drug cellular disposition., Pharmacogenet Genomics. 21 (2011) 884–93. https://doi.org/10.1097/FPC.0b013e32834d672b.

[68] I. Adzhubei, D.M. Jordan, S.R. Sunyaev, Predicting Functional Effect of Human Missense Mutations Using PolyPhen-2, Current Protocols in Human Genetics. 76 (2013) 7.20.1-7.20.41. https://doi.org/10.1002/0471142905.HG0720S76.

[69] P. Kumar, S. Henikoff, P.C. Ng, Predicting the effects of coding non-synonymous variants on protein function using the SIFT algorithm, Nature Protocols 2009 4:7. 4 (2009) 1073–1081. https://doi.org/10.1038/nprot.2009.86.

[70] K.T. Suzuki, T. Tomita, Y. Ogra, M. Ohmichi, Glutathione-conjugated arsenics in the potential hepato-enteric circulation in rats, Chemical Research in Toxicology. 14 (2001). https://doi.org/10.1021/tx0155496.

[71] C.G. Dietrich, R. Ottenhoff, D.R. de Waart, R.P.J. Oude Elferink, Role of MRP2 and GSH in intrahepatic cycling of toxins, Toxicology. 167 (2001) 73–81. https://doi.org/https://doi.org/10.1016/S0300-483X(01)00459-0.

[72] Z.L. Johnson, J. Chen, ATP Binding Enables Substrate Release from Multidrug Resistance Protein 1, Cell. 172 (2018) 81–89. https://doi.org/10.1016/j.cell.2017.12.005.

[73] Z.L. Johnson, J. Chen, Structural Basis of Substrate Recognition by the Multidrug Resistance Protein MRP1, Cell. 168 (2017) 1075-1085.e9. https://doi.org/10.1016/j.cell.2017.01.041.

[74] P.C. Smith, N. Karpowich, L. Millen, J.E. Moody, J. Rosen, P.J. Thomas, J.F. Hunt, ATP binding to the motor domain from an ABC transporter drives formation of a nucleotide sandwich dimer, Mol Cell. 10 (2002) 139–149. https://doi.org/10.1016/S1097-2765(02)00576-2.

5.General Discussion

In this chapter, I will summarize the main findings of my thesis and describe future directions.

Chapter 2: Biliary excretion of arsenic by human HepaRG cells is stimulated by selenide and mediated by the multidrug resistance protein 2 (MRP2/ABCC2).

It was previously demonstrated in animal models that arsenic and selenium are mutually protective via the formation and biliary excretion of $[(GS)_2AsSe]^-$. However, the influence of selenium on human arsenic hepatobiliary transport has not been studied using optimal human *in vitro* models. In this chapter, human HepaRG cells, a surrogate for primary human hepatocytes were used to investigate selenium (selenide, selenite, selenomethionine, methylselenocysteine) effects on arsenic hepatobiliary transport. When HepaRG cells were treated with arsenite and selenide, the mutual toxicity antagonism ratios were highest compared to the other selenium forms investigated. Significant levels of arsenic biliary excretion were detected with a BEI of 14%, and this was stimulated to 32% by selenide. Selenide also stimulated arsenite biliary excretion. Arsenic biliary excretion was also lost in the presence of other selenium forms. Interestingly, methylselenocysteine stimulated arsenic sinusoidal efflux by ~1.6-fold. Arsenic canalicular and sinusoidal efflux were temperature- and GSH-dependent and inhibited by the MRP-inhibitor, MK571. *ABCC2* knockdown experiments revealed that MRP2 accounted for all detectable biliary efflux of arsenic in the presence and absence of selenide.

Methylation of arsenic and selenium is important for both toxicity and elimination. Therefore, arsenic and selenium methyltransferases could also be knocked down in similar

manner to how *ABCC2* was knocked down in this chapter. Then, the role of arsenic and selenium methylation could be characterized using arsenic and selenium speciation by mass spectrometry.

Other factors influencing arsenic elimination should be studied. Inter-individual variability is a common theme in arsenic-induced toxicity. Since As3MT variants have been studied in human populations and are linked to urinary arsenic metabolites as well as arsenic-induced diseases, it would be logical to express As3MT variants in *As3MT*-knockdown cells. A plasmid containing a different antibiotic selection gene would be required to express the As3MT variant in addition to the WT-As3MT knockdown. Since minimal arsenic methylation is expected to occur, we should expect to see an increase in $As(GS)_3$ transport, and perhaps increased efflux of $[(GS)_2AsSe]^-$ in the presence of selenium. We should also see decreased efflux of methylated arsenic species from the *As3MT*-knockdown cells.

Establishing the role of arsenic uptake transporters in a human hepatic model (e.g., AQP9) would also be beneficial to future studies, which could possibility lead to studying polymorphic variants of arsenic uptake transporters.

Chapter 3: Sinusoidal efflux of arsenic by human HepaRG cells is stimulated by methylselenocysteine

In Chapter 2, methylselenocysteine (MeSeCys) unexpectedly increased sinusoidal efflux of arsenic from human HepaRG cells, which was further investigated in this chapter. We aimed to further characterize arsenic sinusoidal efflux in the presence of MeSeCys in HepaRG cells. Arsenic sinusoidal efflux was stimulated ~1.6-fold in the presence of MeSeCys, and this was also observed in sandwich-cultured human hepatocytes. Sinusoidal efflux decreased by 27%, 57%,

31% and 35% after glutathione depletion, temperature reduction, addition of MK571 (general MRP inhibitor), and ceefourin-1 (MRP4 inhibitor), respectively. Arsenic efflux from HepaRG cells stably expressing *ABCC4*-targeted shRNA was decreased by ~30% and MeSeCys was lost, relative to MRP4-replete controls. Therefore, sinusoidal efflux of arsenic was at least in part MRP4-mediated, and the stimulatory effect of MeSeCys on arsenic sinusoidal efflux was completely MRP4-mediated.

Future directions should aim to determine the species of arsenic and selenium transported by human MRP4 upon sinusoidal stimulation by MeSeCys. Some efforts have been made to address this and are summarized in Appendix 1. Establishment of an analytical method for selenium speciation to provide more insight into chemical species present after treatment with arsenite and MeSeCys would be valuable. It would also be extremely beneficial to perform selenium speciation analysis on selenium-enriched lentils that have been previously used in selenium-supplementation trials, as well as the ones that are ongoing to provide insight into which selenium species are most beneficial.

Cytotoxicity studies using *ABCC4*-knockdown HepaRG cells, as well as knockdowns of methyltransferases for arsenic and selenium metabolism could provide some insight on the influence of methylation and transport on arsenic and selenium toxicity. The parental HepaRG cells are expected to be more resistant to arsenite (higher EC_{50} value) compared to the *ABCC4*-knockdown cells. Assessing cytotoxicity in the presence of different combinations of concentrations of arsenite in the presence of MeSeCys using Combenefit will also be useful.

Lastly, inter-individual variability in susceptibility to arsenic-induced diseases can be investigated. There have been previous studies of MRP4 variants (Banerjee et al., 2016), but not

in a human hepatic cell model. *ABCC4*-knockdown HepaRG cells could potentially be used as a model for studying the effect of these previously characterized MRP4 variants on arsenic transport, and how it might be influenced by selenium. Of particular interest are C171G- and Y556C-MRP4 as they had higher transport activity of $MMA(GS)_2$ and DMA^V, respectively, relative to WT-MRP4 (Banerjee et al., 2016). Two other noteworthy variants are K304N- and G187W-MRP4, which had lower transport of $MMA(GS)_2$ and DMA^V relative to WT-MRP4 (Banerjee et al., 2016).

Chapter 4: Naturally occurring variants of MRP2/ABCC2 differentially modulate the transport of arsenic triglutathione ($As(GS)_3$) and the seleno-bis (S-glutathionyl) arsinium ion $[(GS)_2AsSe]^-$

Inorganic arsenic is a proven human carcinogen that causes lung, skin, and bladder cancer. In addition to causing cancer, chronic exposure to arsenic also leads to a myriad of adverse health effects. There is likely a genetic component in susceptibility to arsenic-induced diseases as different outcomes between individuals with similar exposure histories are observed. In this chapter, 13 non-synonymous MRP2 variants were investigated for their influence on MRP2 level, plasma membrane localization, transport of $As(GS)_3$, and $[(GS)_2AsSe]^-$ by membrane vesicles, and accumulation of arsenic alone and in the presence of selenium (selenide and selenite). The variants R412G-, V1188E-, C1515Y- and V1188E/C1515Y-MRP2 were similar to WT-MRP2 for protein levels, cell surface localization, and transport activity. S789F- and A1450T-MRP2 were not detected at the cell surface, so functional characterization was not performed.

T1477M-MRP2 had 40% less $As(GS)_3$ transport activity compared to WT-MRP2. R353H-, R1181L-, and P1291L-MRP2 had increased $[(GS)_2AsSe]^-$ transport by 160%, 145% and 170% compared to WT-MRP2, respectively. In contrast, V417I- and R1150H- had $[(GS)_2AsSe]^-$ transport that was 59% and 37% of WT-MRP2, respectively.

Future directions of this study could include generating stable cell lines so that cellular imaging studies by immunofluorescence imaging using properly polarized cell lines could be performed. Endoplasmic reticulum markers such as calnexin and Golgi apparatus markers such as giantin could be used for cellular localization studies by immunofluorescence imaging. This would give some insight to where in the cell the variants have mis-localized to. Scaffolding proteins thought to be responsible for trafficking to the plasma membrane such as NHERF1 could be probed for by immunoblotting. Alternatively, *ABCC2*-knockdown HepaRG cells could also be used as an *in vitro* model for studying these variants as they are polarized and form canalicular networks. The MRP2 variants could be expressed in the *ABCC2*-knockdown HepaRG cells using a plasmid with a different selection gene. The effect of these variants on the transport of other clinically relevant substrates such as methotrexate could be studied. Since human MRP2 transports $MMA(GS)_2$, future studies could include studying the effect of MRP2 variants on $MMA(GS)_2$ transport.

Lastly, this work should be applied to *in vivo* models. Feces, urine, and blood could be collected from humanized mice expressing MRP2 variants after treatment with selenium and arsenic to determine the effect of these variants in an *in vivo* model. Eventually, small population studies involving genotyping individuals alongside selenium-supplementation could be performed to study the effects of MRP2 variants *in vivo*.

Overall Significance

Overall, this thesis has strengthened the understanding of arsenic hepatobiliary transport by further characterizing the important roles of human MRP2 and MRP4 in arsenic efflux. The influence of selenium on arsenic hepatobiliary transport has also been further characterized. A greater understanding of how genetic variants could contribute to inter-individual variability in susceptibility to arsenic-induced disease has also been achieved.

All these components help us to better understand which form of selenium would be most efficacious when designing selenium-supplementation trials. For individuals with certain MRP2 variants, we are able to better predict whether they would benefit from selenium-supplementation as well as their susceptibility to arsenic-induced diseases.

Bibliography

Abernathy, C.O. *et al.* (1999) Arsenic: health effects, mechanisms of actions, and research issues. *Environ Health Perspect*, **107**, 593–597.

Adzhubei, I. *et al.* (2013) Predicting Functional Effect of Human Missense Mutations Using PolyPhen-2. *Current Protocols in Human Genetics*, **76**, 7.20.1-7.20.41.

Agusa, T. *et al.* (2009) Genetic polymorphisms in AS3MT and arsenic metabolism in residents of the Red River Delta, Vietnam. *Toxicol Appl Pharmacol*, **236**, 131–141.

Alauddin, M. *et al.* (2018) Pharmacodynamic study of the selenium-mediated arsenic excretion in arsenicosis patients in Bangladesh. *Environmental Arsenic in a ChangingWorld - 7th International Congress and Exhibition Arsenic in the Environment, 2018*, **2**, 391–394.

Almquist, K.C. *et al.* (1995) Characterization of the Mr 190,000 Multidrug Resistance Protein (MRP) in Drug-selected and Transfected Human Tumor Cells. *Cancer Research*, **55**, 102–110.

Amoako, P.O. *et al.* (2009) Speciation of selenium dietary supplements; formation of S-(methylseleno)cysteine and other selenium compounds. *Anal Chim Acta*, **652**, 315–323.

Annilo, T. and Dean, M. (2004) Degeneration of an ATP-binding cassette transporter gene, ABCC13, in different mammalian lineages. *Genomics*, **84**, 34–46.

Arlanov, R. *et al.* (2012) Functional characterization of protein variants of the human multidrug transporter ABCC2 by a novel targeted expression system in fibrosarcoma cells. *Hum Mutat*, **33**, 750–62.

Auton, A. *et al.* (2015) A global reference for human genetic variation. *Nature*, **526**, 68–74.

Bachour-El Azzi, P. *et al.* (2015) Comparative localization and functional activity of the main hepatobiliary transporters in HepaRG cells and primary human hepatocytes. *Toxicological Sciences*, **145**, 157–168.

Bandler, P.E. *et al.* (2008) Identification of Regions Required for Apical Membrane Localization of Human Multidrug Resistance Protein 2. *Molecular Pharmacology*, **74**, 9–19.

Banerjee, M. *et al.* (2014) A Novel Pathway for Arsenic Elimination: Human Multidrug Resistance Protein 4 (MRP4/ABCC4) Mediates Cellular Export of Dimethylarsinic Acid (DMAV) and the Diglutathione Conjugate of Monomethylarsonous Acid (MMAIII). *Molecular Pharmacology*, **86**, 168–179.

Banerjee, M. *et al.* (2018) Multidrug Resistance Protein 1 (MRP1/ABCC1)-Mediated Cellular Protection and Transport of Methylated Arsenic Metabolites Differs between Human Cell Lines. *Drug Metabolism and Disposition*, **46**, 1096–1105.

Banerjee, M. *et al.* (2016) Polymorphic variants of MRP4/ABCC4 differentially modulate the transport of methylated arsenic metabolites and physiological organic anions. *Biochemical Pharmacology*, **120**, 72–82.

Bansal, T. *et al.* (2009) Emerging significance of flavonoids as P-glycoprotein inhibitors in cancer chemotherapy. *Journal of pharmacy & pharmaceutical sciences : a publication of the Canadian Society for Pharmaceutical Sciences, Societe canadienne des sciences pharmaceutiques*, **12**, 46–78.

Bencko, V. and Foong, F.Y.L. (2017) The history of arsenical pesticides and health risks related to the use of Agent Blue. *Ann Agric Environ Med*, **24**, 312–316.

Boraldi, F. *et al.* (2003) Multidrug resistance protein-6 (MRP6) in human dermal fibroblasts. Comparison between cells from normal subjects and from Pseudoxanthoma elasticum patients. *Matrix Biol*, **22**, 491–500.

Brouwer, K.L.R. *et al.* (2013) In Vitro Methods to Support Transporter Evaluation in Drug Discovery and Development. *Clinical Pharmacology & Therapeutics*, **94**.

Bulka, C.M. *et al.* (2017) The Unintended Consequences of a Gluten-Free Diet. *Epidemiology*, **28**, e24.

Burk, R.F. and Hill, K.E. (2015) Regulation of Selenium Metabolism and Transport. *Annual Review of Nutrition*, **35**.

Bustaffa, E. *et al.* (2014) Genotoxic and epigenetic mechanisms in arsenic carcinogenicity. *Arch Toxicol*, **88**, 1043–1067.

Calatayud, M., Vázquez, M., *et al.* (2012) In Vitro Study of Intestinal Transport of Inorganic and Methylated Arsenic Species by Caco-2/HT29-MTX Cocultures. *Chemical Research in Toxicology*, **25**, 2654–2662.

Calatayud, M., Barrios, J.A., *et al.* (2012) In Vitro Study of Transporters Involved in Intestinal Absorption of Inorganic Arsenic. *Chemical Research in Toxicology*, **25**, 446–453.

Cantone, L. *et al.* (2011) Inhalable Metal-Rich Air Particles and Histone H3K4 Dimethylation and H3K9 Acetylation in a Cross-sectional Study of Steel Workers. *Environmental Health Perspectives*, **119**, 964.

Carew, M.W. *et al.* (2011) Monomethylarsenic diglutathione transport by the human multidrug resistance protein 1 (MRP1/ABCC1). *Drug Metabolism and Disposition*, **39**, 2298–304.

Carew, M.W. and Leslie, E.M. (2010) Selenium-dependent and -independent transport of arsenic by the human multidrug resistance protein 2 (MRP2/ABCC2): Implications for the mutual detoxification of arsenic and selenium. *Carcinogenesis*, **31**, 1450–1455.

Cascorbi, I. and Haenisch, S. (2010) Pharmacogenetics of ATP-Binding Cassette Transporters and Clinical Implications. Humana Press, pp. 95–121.

Caussy, D. (2003) Case studies of the impact of understanding bioavailability: arsenic. *Ecotoxicology and Environmental Safety*, **56**, 164–173.

Cecchin, E. *et al.* (2013) A prospective validation pharmacogenomic study in the adjuvant setting of colorectal cancer patients treated with the 5-fluorouracil/leucovorin/oxaliplatin (FOLFOX4) regimen. *Pharmacogenomics J*, **13**, 403–9.

Challenger, F. (1955) Biological methylation. *Quarterly Reviews, Chemical Society*, **9**.

Chan, K.W. *et al.* (2003) N-terminal transmembrane domain of the SUR controls trafficking and gating of Kir6 channel subunits. *The EMBO Journal*, **22**, 3833.

Chen, B. *et al.* (2013) JNK and STAT3 signaling pathways converge on Akt-mediated phosphorylation of EZH2 in bronchial epithelial cells induced by arsenic. *Cell Cycle*, **12**, 112.

Chen, C.A. and Okayama, H. (1988) Calcium phosphate-mediated gene tranfer: A highly efficient transfection system for stably transforming cells with plasmid DNA. *Biotechniques*, **6**, 632–638.

Chen, Y. *et al.* (2007) A prospective study of blood selenium levels and the risk of arsenic-related premalignant skin lesions. *Cancer Epidemiology Biomarkers and Prevention*, **16**, 207–213.

Chen, Z. *et al.* (2016) Mammalian drug efflux transporters of the ATP binding cassette (ABC) family in multidrug resistance: A review of the past decade. *Cancer Letters*, **370**, 153–164.

Cheung, L. *et al.* (2014) High-throughput screening identifies Ceefourin 1 and Ceefourin 2 as highly selective inhibitors of multidrug resistance protein 4 (MRP4). *Biochem Pharmacol*, **91**, 97–108.

Chung, J.-Y. *et al.* (2014) Environmental source of arsenic exposure. *Journal of preventive medicine and public health = Yebang Uihakhoe chi*, **47**, 253–257.

Cohen, S.M. *et al.* (2013) Evaluation of the carcinogenicity of inorganic arsenic. *Crit Rev Toxicol*, **43**, 711–752.

Cole, Susan P C (2014) Multidrug Resistance Protein 1 (MRP1 , ABCC1), a " Multitasking " ATP-binding Cassette (ABC). *The Journal of Biological Chemistry*, **289**, 30880–30888.

Cole, S.P.C. *et al.* (1994) Pharmacological Characterization of Multidrug Resistant MRP-transfected Human Tumor Cells. *Cancer Research*, **54**.

Cole, Susan P.C. (2014) Targeting Multidrug Resistance Protein 1 (MRP1, ABCC1): Past, Present, and Future. *http://dx.doi.org/10.1146/annurev-pharmtox-011613-135959*, **54**, 95–117.

Cordero-Herrera, I. *et al.* (2013) Molecular mechanisms involved in the protective effect of selenocystine against methylmercury-induced cell death in human HepG2 cells. *Food and Chemical Toxicology*, **59**.

Csanaky, I. and Gregus, Z. (2003) Effect of selenite on the disposition of arsenate and arsenite in rats. *Toxicology*, **186**, 33–50.

Cui, X. *et al.* (2004) Arsenic speciation in bile and urine following oral and intravenous exposure to inorganic and organic arsenics in rats. *Toxicological Sciences*, **82**.

Cullen, W.R. (2014) Chemical mechanism of arsenic biomethylation. *Chemical Research in Toxicology*, **27**, 457–461.

Davis, M.A. *et al.* (2017) Assessment of human dietary exposure to arsenic through rice. *Science of The Total Environment*, **586**, 1237–1244.

Davison, K. *et al.* (2002) Arsenic trioxide: Mechanisms of action. *Seminars in Hematology*, **39**, 3–7.

Decaens, C. *et al.* (2008) Which in vitro models could be best used to study hepatocyte polarity? *Biology of the Cell*, **100**, 387–398.

Deeley, R.G. *et al.* (2006) Transmembrane transport of endo- and xenobiotics by mammalian ATP-binding cassette multidrug resistance proteins. *Physiological Reviews*, **86**, 849–899.

Delnomdedieu, M. *et al.* (1994) Reduction and binding of arsenate and dimethylarsinate by glutathione: a magnetic resonance study. *Chemico-Biological Interactions*, **90**.

Deo, A.K. *et al.* (2012) Interindividual variability in hepatic expression of the multidrug resistance-associated protein 2 (MRP2/ABCC2): quantification by liquid chromatography/tandem mass spectrometry. *Drug Metab Dispos*, **40**, 852–5.

Dietrich, C.G. *et al.* (2001) Role of MRP2 and GSH in intrahepatic cycling of toxins. *Toxicology*, **167**, 73–81.

Drobná, Z. *et al.* (2013) Environmental exposure to arsenic, AS3MT polymorphism and prevalence of diabetes in Mexico. *J Expo Sci Environ Epidemiol*, **23**, 151.

Drobná, Z. *et al.* (2010) Interspecies differences in metabolism of arsenic by cultured primary hepatocytes. *Toxicology and Applied Pharmacology*, **245**, 47–56.

Duan, X. *et al.* (2017) Acute arsenic exposure induces inflammatory responses and CD4 + T cell subpopulations differentiation in spleen and thymus with the involvement of MAPK, NF-kB, and Nrf2. *Mol Immunol*, **81**, 160–172.

Elens, L. *et al.* (2009) Association between ABCC2 polymorphism and lopinavir accumulation in peripheral blood mononuclear cells of HIV-infected patients. *Pharmacogenomics*, **10**, 1589–97.

Elens, L. *et al.* (2011) Functional defect caused by the 4544G>A SNP in ABCC2: potential impact for drug cellular disposition. *Pharmacogenet Genomics*, **21**, 884–93.

Engström, K. *et al.* (2011) Polymorphisms in Arsenic(+III Oxidation State) Methyltransferase (AS3MT) Predict Gene Expression of AS3MT as Well as Arsenic Metabolism. *Environmental Health Perspectives*, **119**, 182.

Engström, K. *et al.* (2013) Polymorphisms in genes encoding potential mercury transporters and urine mercury concentrations in populations exposed to mercury vapor from gold mining. *Environ Health Perspect*, **121**, 85–91.

Esaki, N. *et al.* (1981) Enzymic synthesis of selenocysteine in rat liver. *Biochemistry*, **20**, 4492–4496.

Falchi, L. *et al.* (2016) The evolution of arsenic in the treatment of acute promyelocytic leukemia and other myeloid neoplasms: Moving toward an effective oral, outpatient therapy. *Cancer*, **122**, 1160–1168.

Freeman, G. (1995) Bioavailability of Arsenic in Soil and House Dust Impacted by Smelter Activities Following Oral Administration in Cynomolgus Monkeys. *Fundamental and Applied Toxicology*, **28**, 215–222.

Fukumoto, Y. *et al.* (2020) Production of a Urinary Selenium Metabolite, Trimethylselenonium, by Thiopurine S-Methyltransferase and Indolethylamine N-Methyltransferase. *Chemical Research in Toxicology*, **33**, 2467–2474.

Gailer, Jürgen *et al.* (2000) A metabolic link between arsenite and selenite: The seleno-bis(S-glutathionyl) arsinium ion. *J Am Chem Soc*.

Gailer, J., George, G.N., *et al.* (2002) Biliary excretion of [(GS)2AsSe]- after intravenous injection of rabbits with arsenite and selenate. *Chemical Research in Toxicology*, **15**, 1466–1471.

Gailer, J., Madden, S., *et al.* (2002) Identification of [(GS)2AsSe]− in rabbit bile by size-exclusion chromatography and simultaneous multielement-specific detection by inductively coupled plasma atomic emission spectroscopy. *Applied Organometallic Chemistry*, **16**, 72–75.

Gailer, J *et al.* (2000) Simultaneous multielement-specific detection of a novel glutathione–arsenic–selenium ion [(GS)2AsSe]− by ICP AES after micellar size- exclusion chromatography. *Applied Organometallic Chemistry*, **14**, 355–363.

Gammelgaard, B. *et al.* (2012) Estimating intestinal absorption of inorganic and organic selenium compounds by in vitro flux and biotransformation studies in Caco-2 cells and ICP-MS detection. *Biol Trace Elem Res*, **145**, 248–256.

Ganther, H.E. (1971) Reduction of the selenotrisulfide derivative of glutathione to a persulfide analog by gluthathione reductase. *Biochemistry*, **10**, 4089–4098.

Ganyc, D. and Self, W.T. (2008) High affinity selenium uptake in a keratinocyte model. *FEBS Letters*, **582**, 299–304.

Gao, J. *et al.* (2015) The Genetic Architecture of Arsenic Metabolism Efficiency:A SNP-Based Heritability Study of Bangladeshi Adults. *Environ Health Perspect*, **123**, 985–992.

Gebel, T.W. (2001) Genotoxicity of arsenical compounds. *Int J Hyg Environ Health*, **203**, 249–262.

Gekeler, V. *et al.* (1995) The leukotriene LTD4 receptor antagonist MK571 specifically modulates MRP associated multidrug resistance. *Biochemical and Biophysical Research Communications*, **208**, 345–352.

Geng, X. *et al.* (2017) Role of AQP9 in transport of monomethyselenic acid and selenite. *BioMetals*, **30**, 747–755.

George, G.N. *et al.* (2016) Observation of the seleno bis-(S-glutathionyl) arsinium anion in rat bile. *Journal of Inorganic Biochemistry*, **158**, 24–29.

Gera, R. *et al.* (2017) Arsenic exposure impels CD4 commitment in thymus and suppress T cell cytokine secretion by increasing regulatory T cells. *Scientific Reports 2017 7:1*, **7**, 1–13.

Ghariani, M. *et al.* (1991) Intoxication suraiguë à l'arsenic. *Annales Françaises d'Anesthésie et de Réanimation*, **10**, 304–307.

Ghibellini, G. *et al.* (2007) In vitro-in vivo correlation of hepatobiliary drug clearance in humans. *Clinical Pharmacology and Therapeutics*, **81**.

Gibaud, S. and Jaouen, G. (2010) Arsenic-Based Drugs: From Fowler's Solution to Modern Anticancer Chemotherapy., pp. 1–20.

Gong, S. *et al.* (2020) Real-world data on the dose-related effect of arsenic trioxide in the relapse of acute promyelocytic leukemia. *Molecular and Clinical Oncology*, **13**, 1–1.

Government of Canada (2021) Health Canada's Proposal to Add a Maximum Level for Inorganic Arsenic in Rice-based Foods Intended Specifically for Infants and Young Children. *https://www.canada.ca/en/health-canada/services/food-nutrition/public-involvement-partnerships/proposal-add-maximum-level-inorganic-arsenic-rice-based-foods/document.html*.

Government of Canada (2020) List of contaminants and other adulterating substances in foods. *https://www.canada.ca/en/health-canada/services/food-nutrition/food-safety/chemical-contaminants/contaminants-adulterating-substances-foods.html*.

Greenberg, C. *et al.* (1979) Acute respiratory failure following severe arsenic poisoning. *Chest*, **76**, 596–598.

Gregus, Z. *et al.* (1998) Interactions between selenium and group Va-metalloids (arsenic, antimony and bismuth) in the biliary excretion. *Environmental Toxicology and Pharmacology*, **5**, 89–99.

Gripon, P. *et al.* (2002) Infection of a human hepatoma cell line by hepatitis B virus. *Proc Natl Acad Sci U S A*, **99**, 15655–15660.

Guha Mazumder, D.N. (2005) Effect of chronic intake of arsenic-contaminated water on liver. *Toxicology and Applied Pharmacology*, **206**, 169–175.

Hall, E.M. *et al.* (2017) Hypertension among adults exposed to drinking water arsenic in Northern Chile. *Environmental Research*, **153**.

Healy, S. *et al.* (1997) Enzymatic methylation of arsenic compounds: IV. In vitro and in vivo deficiency of the methylation of arsenite and monomethylarsonic acid in the guinea pig. *Mutation Research - Genetic Toxicology and Environmental Mutagenesis*, **386**, 229–239.

Hirouchi, M. *et al.* (2004) Characterization of the cellular localization, expression level, and function of SNP variants of MRP2/ABCC2. *Pharmaceutical Research*, **21**, 742–748.

Hoefig, C.S. *et al.* (2011) Comparison of different selenocompounds with respect to nutritional value vs. toxicity using liver cells in culture. *Journal of Nutritional Biochemistry*, **22**.

https://clinicaltrials.gov/ct2/show/NCT01442727.

https://clinicaltrials.gov/ct2/show/NCT02377635.
https://clinicaltrials.gov/ct2/show/NCT02429921.
Huang, C.F. *et al.* (2011) Arsenic and diabetes: current perspectives. *Kaohsiung J Med Sci*, **27**, 402–410.
Huang, Y. (2007) Pharmacogenetics/genomics of membrane transporters in cancer chemotherapy. *Cancer Metastasis Rev*, **26**, 183–201.
Hughes, M.F. (2002) Arsenic toxicity and potential mechanisms of action. *Toxicol Lett*, **133**, 1–16.
Hulot, J.-S. *et al.* (2005) A mutation in the drug transporter gene ABCC2 associated with impaired methotrexate elimination. *Pharmacogenet Genomics*, **15**, 277–85.
IARC (2012) A review of human carcinogens – Part C: metals, arsenic, dusts, and fibres.
Inagaki, N. *et al.* (1996) A family of sulfonylurea receptors determines the pharmacological properties of ATP-sensitive K+ channels. *Neuron*, **16**, 1011–1017.
Institute of Medicine (US) Panel on Dietary Antioxidants and Related Compounds (2000) Dietary Reference Intakes for Vitamin C, Vitamin E, Selenium, and Carotenoids Washington.
Ishihara, N. and Matsushiro, T. (1986) Biliary and urinary excretion of metals in humans. *Archives of Environmental Health*, **41**.
Ito, K.I. *et al.* (2001) Mutation of Trp1254 in the Multispecific Organic Anion Transporter, Multidrug Resistance Protein 2 (MRP2) (ABCC2), Alters Substrate Specificity and Results in Loss of Methotrexate Transport Activity. *Journal of Biological Chemistry*, **276**, 38108–24.
Ito, S. *et al.* (2001) Polymorphism of the ABC transporter genes, MDR1, MRP1 and MRP2/cMOAT, in healthy Japanese subjects. *Pharmacogenetics*, **11**, 175–184.
Itoda, M. *et al.* (2002) Polymorphisms in the ABCC2 (cMOAT/MRP2) gene found in 72 established cell lines derived from Japanese individuals: an association between single nucleotide polymorphisms in the 5'-untranslated region and exon 28. *Drug Metab Dispos*, **30**, 363–4.
Jansen, R.J. *et al.* (2016) Determinants and Consequences of Arsenic Metabolism Efficiency among 4,794 Individuals: Demographics, Lifestyle, Genetics, and Toxicity. *Cancer Epidemiology and Prevention Biomarkers*, **25**, 381–390.
Jedlitschky, G. *et al.* (2006) Structure and function of the MRP2 (ABCC2) protein and its role in drug disposition. *Expert Opin Drug Metab Toxicol*, **2**, 351–366.
Jemnitz, K. *et al.* (2010) ABCC2/Abcc2: a multispecific transporter with dominant excretory functions. *http://dx.doi.org/10.3109/03602530903491741*, **42**, 402–436.
Jigorel, E. *et al.* (2006) Differential Regulation of Sinusoidal and Canalicular Hepatic Drug Transporter Expression by Xenobiotics Activating Drug-Sensing Receptors in Primary Human Hepatocytes. *Drug Metabolism and Disposition*, **34**, 1756–1763.

Johnson, Z.L. and Chen, J. (2018) ATP Binding Enables Substrate Release from Multidrug Resistance Protein 1. *Cell*, **172**, 81–89.

Johnson, Z.L. and Chen, J. (2017) Structural Basis of Substrate Recognition by the Multidrug Resistance Protein MRP1. *Cell*, **168**, 1075-1085.e9.

Jones, P.M. and George, A.M. (2014) A reciprocating twin-channel model for ABC transporters. *Quarterly Reviews of Biophysics*, **47**, 189–220.

Joya, S.A. *et al.* (2006) One solution to the arsenic problem: a return to surface (improved dug) wells. *J Health Popul Nutr*, **24**, 363–75.

Junge, N. *et al.* (2021) Dubin-Johnson Syndrome as Differential Diagnosis for Neonatal Cholestasis. *J Pediatr Gastroenterol Nutr*, **72**, e105–e111.

Kala, S. v. *et al.* (2004a) Formation and Urinary Excretion of Arsenic Triglutathione and Methylarsenic Diglutathione. *Chemical Research in Toxicology*, **17**, 243–249.

Kala, S. v. *et al.* (2004b) Formation and Urinary Excretion of Arsenic Triglutathione and Methylarsenic Diglutathione. *Chemical Research in Toxicology*, **17**.

Kala, S. v. *et al.* (2000) The MRP2/cMOAT transporter and arsenic-glutathione complex formation are required for biliary excretion of arsenic. *Journal of Biological Chemistry*, **275**, 33404–33408.

Kaur, G., Javed, W., *et al.* (2020) Human red blood cell uptake and sequestration of arsenite and selenite: Evidence of seleno-bis(S-glutathionyl) arsinium ion formation in human cells. *Biochemical Pharmacology*, **180**, 114141.

Kaur, G. (2020) Mechanistic Studies of Arsenic and Selenium Detoxification.

Kaur, G., Ponomarenko, O., *et al.* (2020) Studies of Selenium and Arsenic Mutual Protection in Human HepG2 Cells. *Chemico-Biological Interactions*, **327**.

Keitel, V. *et al.* (2003) A common Dubin-Johnson syndrome mutation impairs protein maturation and transport activity of MRP2 (ABCC2). *Am J Physiol Gastrointest Liver Physiol*, **284**, G165-74.

Kim, T.K. and Eberwine, J.H. (2010) Mammalian cell transfection: the present and the future. *Analytical and Bioanalytical Chemistry*, **397**, 3173.

Kipp, A.P. *et al.* (2013) Selenoprotein W as biomarker for the efficacy of selenium compounds to act as source for selenoprotein biosynthesis. In, *Methods in Enzymology*.

Klein, I. *et al.* (1999) An inventory of the human ABC proteins. *Biochim Biophys Acta*, **1461**, 237–262.

Kokarnig, S. *et al.* (2015) Concurrent quantitative HPLC-mass spectrometry profiling of small selenium species in human serum and urine after ingestion of selenium supplements. *Journal of Trace Elements in Medicine and Biology*, **29**.

Kostrubsky, V.E. *et al.* (2003) Evaluation of hepatotoxic potential of drugs by inhibition of bile-acid transport in cultured primary human hepatocytes and intact rats. *Toxicological Sciences*, **76**.

Krishnamohan, M. *et al.* (2007) Urinary arsenic and porphyrin profile in C57BL/6J mice chronically exposed to monomethylarsonous acid (MMAIII) for two years. *Toxicology and Applied Pharmacology*, **224**, 89–97.

Krohn, R.M. *et al.* (2016) A high-selenium lentil dietary intervention in Bangladesh to counteract arsenic toxicity: Study protocol for a randomized controlled trial. *Trials*, **17**.

Kryukov, G. v. *et al.* (2003) Characterization of Mammalian Selenoproteomes. *Science (1979)*, **300**, 1439–1443.

Kuehnelt, D. *et al.* (2007) Selenium metabolites in urine of cancer patients receiving L-selenomethionine at high doses. *Toxicol Appl Pharmacol*, **220**, 211–215.

Kumar, P. *et al.* (2009) Predicting the effects of coding non-synonymous variants on protein function using the SIFT algorithm. *Nature Protocols 2009 4:7*, **4**, 1073–1081.

Kurokawa, S. and Berry, M.J. (2013) Selenium. Role of the essential metalloid in health. *Metal Ions in Life Sciences*, **13**, 499–534.

Kwon, O. *et al.* (2007) Inhibition of the intestinal glucose transporter GLUT2 by flavonoids. *FASEB J*, **21**, 366–377.

Lashhab, R. *et al.* (2019) The kidney anion exchanger 1 affects tight junction properties via claudin-4. *Scientific Reports*, **9**, 1–16.

Le, X.C. *et al.* (2000) Speciation of Key Arsenic Metabolic Intermediates in Human Urine. *Analytical Chemistry*, **72**, 5172–5177.

Lebeck, J. (2014) Metabolic impact of the glycerol channels AQP7 and AQP9 in adipose tissue and liver. *J Mol Endocrinol*, **52**.

Lee, J.K. *et al.* (2008) Modulation of trabectedin (ET-743) hepatobiliary disposition by multidrug resistance-associated proteins (Mrps) may prevent hepatotoxicity. *Toxicology and Applied Pharmacology*, **228**, 17–23.

Lee, T.C. *et al.* (2006) Enhanced Expression of Multidrug resistance-associated Protein 2 and Reduced Expression of Aquaglyceroporin 3 in an Arsenic-resistant Human Cell Line. *Journal of Biological Chemistry*, **281**, 18401–18407.

Lerman, B.B. *et al.* (1980) Megaloblastic, dyserythropoietic anemia following arsenic ingestion. *Ann Clin Lab Sci*, **10**, 515–517.

Leslie, E.M. *et al.* (2004) Arsenic transport by the human multidrug resistance protein 1 (MRP1/ABCC1): Evidence that a tri-glutathione conjugate is required. *Journal of Biological Chemistry*, **279**, 32700–32708.

Leslie, E.M. (2012) Arsenic-glutathione conjugate transport by the human multidrug resistance proteins (MRPs/ABCCs). *Journal of Inorganic Biochemistry*, **108**, 141–149.

Leslie, E.M. *et al.* (2007) Differential inhibition of rat and human Na+-dependent taurocholate cotransporting polypeptide (NTCP/SLC10A1) by bosentan: A mechanism for species differences in hepatotoxicity. *Journal of Pharmacology and Experimental Therapeutics*, **321**, 1170–1178.

Levander, O.A. and Baumann, C.A. (1966) Selenium metabolism. VI. Effect of arsenic on the excretion of selenium in the bile. *Toxicology and Applied Pharmacology*, 106–115.

Li, G. *et al.* (1985) Keshan disease: An endemic cardiomyopathy in China. *Human Pathology*, **16**, 602–609.

Li, L. and Chen, F. (2016) Oxidative stress, epigenetics, and cancer stem cells in arsenic carcinogenesis and prevention. *Curr Pharmacol Rep*, **2**, 57.

Li, Y.F. *et al.* (2010) Direct quantitative speciation of selenium in selenium-enriched yeast and yeast-based products by X-ray absorption spectroscopy confirmed by HPLC-ICP-MS. *Journal of Analytical Atomic Spectrometry*, **25**, 426–430.

Liaw, J. *et al.* (2008) Increased childhood liver cancer mortality and arsenic in drinking water in northern Chile. *Cancer Epidemiology Biomarkers and Prevention*, **17**.

Lipinski, T. *et al.* (2013) Enhanced Immunogenicity of a Tricomponent Mannan Tetanus Toxoid Conjugate Vaccine Targeted to Dendritic Cells via Dectin-1 by Incorporating β-Glucan. *The Journal of Immunology*, **190**, 4116–4128.

Liu, S.X. *et al.* (2001) Induction of oxyradicals by arsenic: Implication for mechanism of genotoxicity. *Proceedings of the National Academy of Sciences*, **98**, 1643–1648.

Liu, X. *et al.* (1999) Use of Ca2+ modulation to evaluate biliary excretion in sandwich- cultured rat hepatocytes. *Journal of Pharmacology and Experimental Therapeutics*, **289**, 1592–1599.

Liu, Z. *et al.* (2004) Arsenic Trioxide Uptake by Hexose Permeases in Saccharomyces cerevisiae. *Journal of Biological Chemistry*, **279**, 17312–17318.

Liu, Z. *et al.* (2002) Arsenite transport by mammalian aquaglyceroporins AQP7 and AQP9. *Proc Natl Acad Sci U S A*, **99**, 6053–6058.

Liu, Z. *et al.* (2006) Mammalian glucose permease GLUT1 facilitates transport of arsenic trioxide and methylarsonous acid. *Biochemical and Biophysical Research Communications*, **351**, 424–430.

Loe, D.W., Almquist, K.C., Cole, S.P.C., *et al.* (1996) ATP-dependent 17β-Estradiol 17-(β-D-Glucuronide) Transport by Multidrug Resistance Protein (MRP). *Journal of Biological Chemistry*, **271**.

Loe, D.W., Almquist, K.C., Deeley, R.G., *et al.* (1996) Multidrug Resistance Protein (MRP)-mediated Transport of Leukotriene C4 and Chemotherapeutic Agents in Membrane Vesicles. *Journal of Biological Chemistry*, **271**.

Logemann, E. *et al.* (1990) [Suicidal administration of elemental arsenic]. *Archiv fur Kriminologie*, **185**, 80–8.

Lu, G. *et al.* (2014) Arsenic exposure is associated with DNA hypermethylation of the tumor suppressor gene p16. *J Occup Med Toxicol*, **9**.

Lu, W.J. *et al.* (2006) Organic anion transporting polypeptide-C mediates arsenic uptake in HEK-293 cells. *Journal of Biomedical Science 2006 13:4*, **13**, 525–533.

Ma, J.F. *et al.* (2008) Transporters of arsenite in rice and their role in arsenic accumulation in rice grain. *Proceedings of the National Academy of Sciences*, **105**, 9931–9935.

Mandal, B.K. *et al.* (2001) Identification of Dimethylarsinous and Monomethylarsonous Acids in Human Urine of the Arsenic-Affected Areas in West Bengal, India. *Chemical Research in Toxicology*, **14**, 371–378.

Mandal, P. (2017) Molecular insight of arsenic-induced carcinogenesis and its prevention. *Naunyn Schmiedebergs Arch Pharmacol*, **390**, 443–455.

Manley, S.A. *et al.* (2006) The Seleno Bis(S-glutathionyl) Arsinium Ion Is Assembled in Erythrocyte Lysate. *Chemical Research in Toxicology*, **19**, 601–607.

Marion, M.-J. *et al.* (2010) The HepaRG Cell Line: Biological Properties and Relevance as a Tool for Cell Biology, Drug Metabolism, and Virology Studies.

Marion, T.L. *et al.* (2007) Use of sandwich-cultured hepatocytes to evaluate impaired bile acid transport as a mechanism of drug-induced hepatotoxicity. *Molecular Pharmaceutics*, **4**.

Marschall, T.A. *et al.* (2016) Differing cytotoxicity and bioavailability of selenite, methylselenocysteine, selenomethionine, selenosugar 1 and trimethylselenonium ion and their underlying metabolic transformations in human cells. *Molecular Nutrition and Food Research*, **60**.

Martinez, V.D. *et al.* (2013) Emerging Arsenic Threat in Canada. *Science (1979)*, **342**.

Masuda, H. (2018) Arsenic cycling in the Earth's crust and hydrosphere: interaction between naturally occurring arsenic and human activities. *Progress in Earth and Planetary Science*, **5**, 1–11.

Materna, V. and Lage, H. (2003) Homozygous mutation Arg768Trp in the ABC-transporter encoding gene MRP2/cMOAT/ABCC2 causes Dubin-Johnson syndrome in a Caucasian patient. *Journal of Human Genetics 2003 48:9*, **48**, 484–486.

McConnell, K. and Cho, G. (1967) Active transport of L-selenomethionine in the intestine. *American Journal of Physiology-Legacy Content*, **213**, 150–156.

McDermott, J.R. *et al.* (2016) Zinc- and bicarbonate-dependent ZIP8 transporter mediates selenite uptake. *Oncotarget*, **7**, 35327–35340.

McGuigan, C.F. *et al.* (2010) A review on arsenic concentrations in Canadian drinking water. *Environmental Reviews*, 291–307.

Mease, K. *et al.* (2012) Differential Selectivity of Efflux Transporter Inhibitors in Caco-2 and MDCK–MDR1 Monolayers: A Strategy to Assess the Interaction of a New Chemical Entity with P-gp, BCRP, and MRP2. *Journal of Pharmaceutical Sciences*, **101**.

Megaraj, V. *et al.* (2011) Functional analysis of nonsynonymous single nucleotide polymorphisms of multidrug resistance-associated protein 2 (ABCC2). *Pharmacogenet Genomics*, **21**, 506–15.

Memon, N. *et al.* (2016) Inherited Disorders of Bilirubin Clearance. *Pediatr Res*, **79**, 378.

Messarah, M. *et al.* (2012) Hepatoprotective role and antioxidant capacity of selenium on arsenic-induced liver injury in rats. *Experimental and Toxicologic Pathology*, **64**, 167–174.

Misra, S. *et al.* (2012) Transport of selenium across the plasma membrane of primary hepatocytes and enterocytes of rainbow trout. *Journal of Experimental Biology*, **215**, 1491–1501.

Mistry, A.R. *et al.* (2003) The molecular pathogenesis of acute promyelocytic leukaemia: implications for the clinical management of the disease. *Blood Reviews*, **17**, 71–97.

Mita, S. *et al.* (2006) Vectorial transport of unconjugated and conjugated bile salts by monolayers of LLC-PK1 cells doubly transfected with human NTCP and BSEP or with rat Ntcp and Bsep. *American Journal of Physiology - Gastrointestinal and Liver Physiology*, **290**, 550–556.

Moitra, K. and Dean, M. (2011) Evolution of ABC transporters by gene duplication and their role in human disease. *Biol Chem*, **392**, 29–37.

Mor-Cohen, R. *et al.* (2001) Identification and Functional Analysis of Two Novel Mutations in the Multidrug Resistance Protein 2 Gene in Israeli Patients with Dubin-Johnson Syndrome. *Journal of Biological Chemistry*, **276**, 36923–36930.

Moxon, A.L. (1938) The effect of arsenic on the toxicity of seleniferous grains. *Science (1979)*, **88**, 81.

Mueckler, M. and Thorens, B. (2013) The SLC2 (GLUT) family of membrane transporters. *Molecular Aspects of Medicine*, **34**, 121–138.

Mukhopadhyay, R. *et al.* (2014) Aquaglyceroporins: generalized metalloid channels. *Biochimica et Biophysica Acta*, **1840**, 1583–1591.

Naujokas, M.F. *et al.* (2013) The broad scope of health effects from chronic arsenic exposure: Update on a worldwide public health problem. *Environmental Health Perspectives*, **121**, 295–302.

Navarro-Alarcon, M. and Cabrera-Vique, C. (2008) Selenium in food and the human body: A review. *Science of The Total Environment*, **400**, 115–141.

NCT01442727 (2011) Selenium in the Treatment of Arsenic Toxicity and Cancers.

Negro Silva, L.F. *et al.* (2017) Effects of inorganic arsenic, methylated arsenicals, and arsenobetaine on atherosclerosis in the apoE-/- mouse model and the role of as3mt-mediated methylation. *Environmental Health Perspectives*, **125**.

Németi, B. *et al.* (2012) Glutathione synthetase promotes the reduction of arsenate via arsenolysis of glutathione. *Biochimie*, **94**, 1327–1333.

Nies, A.T. and Keppler, D. (2007) The apical conjugate efflux pump ABCC2 (MRP2). *Pflugers Archiv European Journal of Physiology*, **453**, 643–659.

Nies, A.T. and Klein, F. (2022) Multidrug Resistance Proteins of the ABCC Subfamily. In, You,G. and Morris,M.E. (eds), *Drug Transporters: Molecular Characterization and Role in Drug Disposition, 3rd Edition*. John Wiley & Sons, pp. 213–233.

Olson, K.R. and Cihacek, L. (2020) The Fate of Agent Blue, the Arsenic Based Herbicide, Used in South Vietnam during the Vietnam War. *Open Journal of Soil Science*, **10**, 518–577.

Ono, N. *et al.* (2007) Multidrug resistance-associated protein 9 (ABCC12) is present in mouse and boar sperm. *The Biochemical Journal*, **406**, 31–40.

Oswald, C. *et al.* (2006) The motor domains of ABC-transporters. What can structures tell us? *Naunyn Schmiedebergs Arch Pharmacol*, **372**, 385–399.

Palmer, I.S. and Bonhorst, C.W. (1957) Selenium Poisoning, Modification of Selenite Metabolism by Arsenite. *Journal of Agricultural and Food Chemistry*, **5**, 928–930.

Papp, L.V. *et al.* (2007) From Selenium to Selenoproteins: Synthesis, Identity, and Their Role in Human Health. *Antioxidants & Redox Signaling*, **9**, 775–806.

Parascandola, J. (2001) History of Salvarsan (Arsphenamine). In, *eLS*. Wiley.

Pelch, K.E. *et al.* (2015) Differential DNA methylation profile of key genes in malignant prostate epithelial cells transformed by inorganic arsenic or cadmium. *Toxicol Appl Pharmacol*, **286**, 159–167.

Petrov, P.D. *et al.* (2018) Predicting drug-induced cholestasis: preclinical models. *Expert Opinion on Drug Metabolism and Toxicology*, **14**, 721–738.

Pham, D.H. *et al.* (2021) Deleterious Variants in ABCC12 are Detected in Idiopathic Chronic Cholestasis and Cause Intrahepatic Bile Duct Loss in Model Organisms. *Gastroenterology*, **161**, 287-300.e16.

Podgorski, J. and Berg, M. (2020) Global threat of arsenic in groundwater. *Science*, **368**, 845 LP – 850.

Pollutants, N.R.C. (US) C. on M. and B.E. of E. (1977) Distribution of Arsenic in the Environment.

Ponomarenko, O. *et al.* (2017) Selenium-mediated arsenic excretion in mammals: A synchrotron-based study of whole-body distribution and tissue-specific chemistry. *Metallomics*, **9**, 1585–1595.

Pratt, V.M. *et al.* (2015) Report of New Haplotype for ABCC2 Gene: rs17222723 and rs8187718 in cis. *The Journal of Molecular Diagnostics : JMD*, **17**, 201.

Rahman, I. *et al.* (2007) Assay for quantitative determination of glutathione and glutathione disulfide levels using enzymatic recycling method. *Nature Protocols*, **1**, 3159–3165.

Ratnaike, R.N. (2003) Acute and chronic arsenic toxicity. *Postgraduate Medical Journal*, **79**, 391–396.

Rayman, M.P. (2008) Food-chain selenium and human health: emphasis on intake. *British Journal of Nutrition*, **100**, 254–268.

Reay, P.F. and Asher, C.J. (1977) Preparation and purification of 74As-labeled arsenate and arsenite for use in biological experiments. *Analytical Biochemistry*, **78**, 557–560.

Rehman, K. and Naranmandura, H. (2012) Arsenic metabolism and thioarsenicals. *Metallomics*, **4**.

Rius, M. *et al.* (2003) Cotransport of reduced glutathione with bile salts by MRP4 (ABCC4) localized to the basolateral hepatocyte membrane. *Hepatology*, **38**, 374–384.

Roggenbeck, B.A. *et al.* (2015) Characterization of arsenic hepatobiliary transport using sandwich-cultured human hepatocytes. *Toxicological Sciences*, **145**, 307–320.

Roggenbeck, B.A. (2016) Hepatobiliary Transport of Arsenic.

Roman, M. *et al.* (2014) Selenium biochemistry and its role for human health. *Metallomics*, **6**, 25–54.

Rossman, T.G. and Uddin, A.N. (2004) Selenium prevents spontaneous and arsenite-induced mutagenesis. *International Congress Series*, **1275**, 173–179.

Russel, F.G.M. *et al.* (2008) Multidrug resistance protein 4 (MRP4/ABCC4): a versatile efflux transporter for drugs and signalling molecules. *Trends Pharmacol Sci*, **29**, 200–207.

Ryu, M.S. *et al.* (2012) Proteomic analysis shows the upregulation of erythrocyte dematin in zinc-restricted human subjects. *The American Journal of Clinical Nutrition*, **95**, 1096–1102.

Ryu, S. *et al.* (2000) Identification of Basic Residues Involved in Drug Export Function of Human Multidrug Resistance-associated Protein 2. *Journal of Biological Chemistry*, **275**, 39617–39624.

Sah, S. *et al.* (2013) Treating chronic arsenic toxicity with high selenium lentil diets. *Toxicology and Applied Pharmacology*, **272**, 256–2662.

Saha, J.C. *et al.* (1999) A Review of Arsenic Poisoning and its Effects on Human Health. *Critical Reviews in Environmental Science and Technology*, **29**.

Sandholm, M. (1975) Function of Erythrocytes in Attaching Selenite-Se onto Specific Plasma Proteins. *Acta Pharmacologica et Toxicologica*, **36**.

Sandholm, M. (1973) The Initial Fate of a Trace Amount of Intravenously Administered Selenite. *Acta Pharmacologica et Toxicologica*, **33**.

Saxena, R. *et al.* (2018) Nutritional Influences on One-Carbon Metabolism: Effects on Arsenic Methylation and Toxicity. *Annu Rev Nutr*, 1–29.

Sepkowitz, K.A. (2011) One Hundred Years of Salvarsan. *New England Journal of Medicine*, **365**, 291–293.

Shaji, E. *et al.* (2021) Arsenic contamination of groundwater: A global synopsis with focus on the Indian Peninsula. *Geoscience Frontiers*, **12**, 101079.

Shao, K. *et al.* (2021) Bayesian benchmark dose analysis for inorganic arsenic in drinking water associated with bladder and lung cancer using epidemiological data. *Toxicology*, **455**, 152752.

Sharma, S. *et al.* (2013) Hepatobiliary disposition of 17-OHPC and taurocholate in fetal human hepatocytes: A comparison with adult human hepatocytes. *Drug Metabolism and Disposition*, **41**.

Shen, S. *et al.* (2013) Arsenic binding to proteins. *Chemical Reviews*, **113**, 7769–7792.

Sherry, S.T. *et al.* (1999) dbSNP-database for single nucleotide polymorphisms and other classes of minor genetic variation. *Genome Res*, **9**, 677–9.

Shi, H. *et al.* (2004) Oxidative mechanism of arsenic toxicity and carcinogenesis. *Mol Cell Biochem*, **255**, 67–78.

Shiobara, Y. and Suzuki, K.T. (1998) Binding of selenium (administered as selenite) to albumin after efflux from red blood cells. *Journal of Chromatography B: Biomedical Applications*, **710**.

Shukalek, C.B. *et al.* (2016) Arsenic Triglutathione [As (GS) 3] Transport by Multidrug Resistance Protein 1 (MRP1 / ABCC1) Is Selectively Modified by Phosphorylation of Tyr920 / Ser921 and Glycosylation of Asn19 / Asn23 s. *Molecular Pharmacology*, **90**, 127–139.

Siebeneicher, H. *et al.* (2016) Identification and Optimization of the First Highly Selective GLUT1 Inhibitor BAY-876. *ChemMedChem*, **11**, 2261–2271.

Simeonova, P.P. and Luster, M.I. (2004) Arsenic and atherosclerosis. *Toxicol Appl Pharmacol*, **198**, 444–449.

Sloan, J.A. *et al.* (2012) Genetic variations and patient-reported quality of life among patients with lung cancer. *J Clin Oncol*, **30**, 1699–704.

Smith, A.H., Arroyo, A.P., *et al.* (2000) Arsenic-induced skin lesions among Atacameño people in Northern Chile despite good nutrition and centuries of exposure. *Environ Health Perspect*, **108**, 617–620.

Smith, A.H., Lingas, E.O., *et al.* (2000) Contamination of drinking-water by arsenic in Bangladesh: A public health emergency. *Bull World Health Organ*, **78**.

Smith, P.C. *et al.* (2002) ATP binding to the motor domain from an ABC transporter drives formation of a nucleotide sandwich dimer. *Mol Cell*, **10**, 139–149.

Smits, J.E. *et al.* (2019) Food as medicine: Selenium enriched lentils offer relief against chronic arsenic poisoning in Bangladesh. *Environmental Research*, **176**.

Sookoian, S. *et al.* (2009) Polymorphisms of MRP2 (ABCC2) are associated with susceptibility to nonalcoholic fatty liver disease. *J Nutr Biochem*, **20**, 765–70.

Steinmaus, C.M. *et al.* (2013) Drinking water arsenic in northern chile: High cancer risks 40 years after exposure cessation. *Cancer Epidemiology Biomarkers and Prevention*, **22**.

Styblo, M. and Thomas, D.J. (2001) Selenium modifies the metabolism and toxicity of arsenic in primary rat hepatocytes. *Toxicology and Applied Pharmacology*, **172**, 52–61.

Sun, H.-J. *et al.* (2014) Arsenic and selenium toxicity and their interactive effects in humans. *Environment International*, **69**, 148–158.

Suzuki, K.T. *et al.* (2001) Glutathione-conjugated arsenics in the potential hepato-enteric circulation in rats. *Chemical Research in Toxicology*, **14**.

Suzuki, K.T. *et al.* (1998) Selective uptake of selenite by red blood cells. In, *Analyst*.

Suzuki, Y. *et al.* (2010) Dynamic pathways of selenium metabolism and excretion in mice under different selenium nutritional statuses. *Metallomics*, **2**, 126–132.

Swift, B. *et al.* (2010) Sandwich-cultured hepatocytes: An in vitro model to evaluate hepatobiliary transporter-based drug interactions and hepatotoxicity. *Drug Metabolism Reviews*, **42**, 446–471.

Szentpétery, Z. *et al.* (2004) The Role of the Conserved Glycines of ATP-binding Cassette Signature Motifs of MRP1 in the Communication between the Substrate-binding Site and the Catalytic Centers *. *Journal of Biological Chemistry*, **279**, 41670–41678.

Talaga, Z.J. and Vaidya, P.N. (2021a) Dubin Johnson Syndrome. *StatPearls*.

Talaga, Z.J. and Vaidya, P.N. (2021b) Dubin Johnson Syndrome. *StatPearls*.

Tam, L.M. *et al.* (2020) Molecular Mechanisms of Arsenic-Induced Disruption of DNA Repair. *Chem Res Toxicol*, **33**, 709.

Tapiero, H. *et al.* (2003) The antioxidant role of selenium and seleno-compounds. *Biomedicine & pharmacotherapy = Biomedecine & pharmacotherapie*, **57**, 134–144.

Tarze, A. *et al.* (2007) Extracellular production of hydrogen selenide accounts for thiol-assisted toxicity of selenite against Saccharomyces cerevisiae. *Journal of Biological Chemistry*, **282**, 8759–8767.

Thavarajah, D. *et al.* (2007) Chemical form of selenium in naturally selenium-rich lentils (Lens culinaris L.) from Saskatchewan. *Journal of Agricultural and Food Chemistry*, **55**, 7337–7341.

Thavarajah, D. *et al.* (2008) High Potential for Selenium Biofortification of Lentils (Lens culinaris L.). *Journal of Agricultural and Food Chemistry*, **56**, 10747–10753.

Thomas, D.J. (2009) Unraveling Arsenic—Glutathione Connections. *Toxicological Sciences*, **107**, 309–311.

Tokar, E.J. *et al.* (2011) Cancer in Experimental Animals Exposed to Arsenic and Arsenic Compounds. **40**, 912–927.

Tseng, C.H. (2005) Blackfoot disease and arsenic: a never-ending story. *J Environ Sci Health C Environ Carcinog Ecotoxicol Rev*, **23**, 55–74.

Vahter, M. *et al.* (1995) Lack of methylation of inorganic arsenic in the chimpanzee. *Toxicology and Applied Pharmacology*, **133**, 262–268.

Vahter, M. (1999) Variation in Human Metabolism of Arsenic. *Arsenic Exposure and Health Effects III*, 267–279.

Vahter, M. and Marafante, E. (1985) Reduction and binding of arsenate in marmoset monkeys. *Archives of Toxicology*, **57**, 119–124.

Valko, M. *et al.* (2007) Free radicals and antioxidants in normal physiological functions and human disease. *Int J Biochem Cell Biol*, **39**, 44–84.

le Vee, M. *et al.* (2006) Functional expression of sinusoidal and canalicular hepatic drug transporters in the differentiated human hepatoma HepaRG cell line. *European Journal of Pharmaceutical Sciences*, **28**, 109–117.

di Veroli, G.Y. *et al.* (2016) Combenefit: an interactive platform for the analysis and visualization of drug combinations. *Bioinformatics*, **32**, 2866–2868.

Verret, W.J. *et al.* (2005) A randomized, double-blind placebo-controlled trial evaluating the effects of vitamin E and selenium on arsenic-induced skin lesions in Bangladesh. *Journal of Occupational and Environmental Medicine*, **47**, 1026–1035.

Villa-Bellosta, R. and Sorribas, V. (2008) Role of rat sodium/phosphate cotransporters in the cell membrane transport of arsenate. *Toxicology and Applied Pharmacology*, **232**, 125–134.

Villa-Bellosta, R. and V, S. (2010) Arsenate transport by sodium/phosphate cotransporter type IIb. *Toxicology and Applied Pharmacology*, **247**, 36–40.

Waalkes, M.P. *et al.* (2004) Animal models for arsenic carcinogenesis : inorganic arsenic is a transplacental carcinogen in mice. *Toxicology and Applied Pharmacology*, **198**, 377–384.

Waalkes, M.P. *et al.* (2014) Lung tumors in mice induced by “whole-life” inorganic arsenic exposure at human-relevant doses. *Arch Toxicol*, **88**, 1619–1629.

Wada, M. *et al.* (1998) Mutations in the canilicular multispecific organic anion transporter (cMOAT) gene, a novel ABC transporter, in patients with hyperbilirubinemia II/Dubin-Johnson syndrome. *Hum Mol Genet*, **7**, 203–207.

Walton, F.S. *et al.* (2003) Selenium compounds modulate the activity of recombinant rat AsIII-methyltransferase and the methylation of arsenite by rat and human hepatocytes. *Chemical Research in Toxicology*, **16**, 261–265.

Wang, Q. and Morris, M.E. (2007) Flavonoids modulate monocarboxylate transporter-1-mediated transport of gamma-hydroxybutyrate in vitro and in vivo. *Drug Metab Dispos*, **35**, 201–208.

Wang, S. and Mulligan, C. (2006) Occurance of arsenic contamination in Canada: sources, behavior and distribution. *Science of the total Environment*, **366**, 701–721.

Wang, W. *et al.* (2001) Prevention of endemic arsenism with selenium. *Current Science*, **81**.

Weekley, C.M. and Harris, H.H. (2013) Which form is that? the importance of selenium speciation and metabolism in the prevention and treatment of disease. *Chemical Society Reviews*, **42**, 8870–8894.

Wen, J. *et al.* (2015) The Pharmacological and Physiological Role of Multidrug-Resistant Protein 4. *J Pharmacol Exp Ther*, **354**, 358–375.

Wen, X. *et al.* (2017) In Vitro Transport Activity and Trafficking of MRP2/ABCC2 Polymorphic Variants. *Pharmaceutical Research*, **34**, 1637–1647.

Whitlock, B. (2021) Arsenic Cellular Handling by Human Multidrug Resistance Protein 1 (MRP1/ABCC1) and MRP4 (ABCC4).

Whitlock, B.D. and Leslie, E.M. (2020) Efflux transporters in anti-cancer drug resistance: Molecular and functional identification and characterization of multidrug resistance proteins (MRPs/ABCCs). In, *Drug Efflux Pumps in Cancer Resistance Pathways: From Molecular Recognition and Characterization to Possible Inhibition Strategies in Chemotherapy*., pp. 31–65.

Wiśniewski, J.R. *et al.* (2016) In-depth quantitative analysis and comparison of the human hepatocyte and hepatoma cell line HepG2 proteomes. *J Proteomics*, **136**, 234–247.

Wojnowski, L. *et al.* (2005) NAD(P)H oxidase and multidrug resistance protein genetic polymorphisms are associated with doxorubicin-induced cardiotoxicity. *Circulation*, **112**, 3754–3762.

World Health Organization (2018) Arsenic fact sheet. [Internet]. Geneva: WHO [updated 2018, accessed 2022]. Available from https://www.who.int/news-room/fact-sheets/detail/arsenic

Wrobel, J.K. *et al.* (2016) Biological activity of selenium: Revisited. *IUBMB Life*, **68**, 97–105.

Xu, S. *et al.* (2010) Aryl hydrocarbon receptor and NF-E2-related factor 2 are key regulators of human MRP4 expression. *American Journal of Physiology - Gastrointestinal and Liver Physiology*, **299**, G126-135.

Xu, Z. *et al.* (2013) Protective effects of selenium on oxidative damage and oxidative stress related gene expression in rat liver under chronic poisoning of arsenic. *Food and Chemical Toxicology*, **58**, 1–7.

Yang, L. *et al.* (2002) Effects of selenium supplementation on arsenism: An intervention trial in inner Mongolia. *Environmental Geochemistry and Health*, **24**, 359–374.

Yehiayan, L. *et al.* (2009) Speciation, formation, stability and analytical challenges of human arsenic metabolites. *Journal of Analytical Atomic Spectrometry*, **24**, 1397–1405.

Zamek-Gliszczynski, M.J. *et al.* (2003) Pharmacokinetics of 5 (and 6)-carboxy-2',7'-dichlorofluorescein and its diacetate promoiety in the liver. *Journal of Pharmacology and Experimental Therapeutics*, **304**, 801–809.

Zhang, P. *et al.* (2005) Role of Glycosylation in Trafficking of Mrp2 in Sandwich-Cultured Rat Hepatocytes. *Molecular Pharmacology*, **67**.

Zhou, J.R. *et al.* (2021) Biliary excretion of arsenic by human HepaRG cells is stimulated by selenide and mediated by the multidrug resistance protein 2 (MRP2/ABCC2). *Biochemical Pharmacology*, **193**, 114799.

Zito, C.R. *et al.* (2005) Role of a conserved glutamate residue in the Escherichia coli SecA ATPase mechanism. *Journal of Biological Chemistry*, **280**, 14611–14619.

Zwolak, I. and Zaporowska, H. (2012) Selenium interactions and toxicity: A review. *Cell Biology and Toxicology*, 31–46.

Appendix A: Determining the Species of Arsenic Transported by Human MRP4 Upon Sinusoidal Stimulation by Methylselenocysteine

Introduction

In Chapter 3, the arsenic sinusoidal efflux in the presence of methylselenocysteine (MeSeCys) was characterized. Arsenic sinusoidal efflux was stimulated by the presence of MeSeCys from both human HepaRG cells and from sandwich cultured human hepatocytes (SCHH). We demonstrated that this process is glutathione-dependent and transporter-mediated. Arsenic efflux in the presence and absence of MeSeCys, was also diminished in the presence of ceefourin-1, an MRP4 inhibitor. There was also decreased arsenic sinusoidal efflux from *ABCC4* knockdown HepaRG cells, and the stimulatory effect of MeSeCys was lost. Therefore, MeSeCys stimulated sinusoidal efflux is MRP4-mediated. The following steps of this study were initiated to determine the species of arsenic transported by MRP4 upon stimulation by MeSeCys. In this section, I describe preliminary results of membrane vesicle transport (using MRP4 over-expressed in HEK293T cells) work as well as arsenic speciation from parental and *ABCC4* knockdown HepaRG cells treated with arsenite and MeSeCys.

Materials and Methods

Materials

^{73}As-arsenate (> 5.6 Ci/mg) was purchased from Los Alamos Meson Production Facility (Los Alamos, NM). [6,7-^{3}H(N)]-estradiol-17β-glucuronide (41.4 Ci/mmol) was purchased from PerkinElmer (Woodbridge, ON). Estradiol-17β-glucuronide (E_2-17βG), N-(2-Hydroxyethyl)piperazine-N'-(2-ethanesulfonic acid) (HEPEs), polyvinylidene difluoride membranes, sodium(meta) arsenite, MeSeCys, bovine serum albumin (BSA), reduced glutathione (GSH), William's E media, dimethyl sulfoxide (DMSO), hydrocortisone 21-

hemisuccinate sodium salt, fetal bovine serum (FBS), standard Hanks' balanced salt solution (HBSS), Ca^{2+}/Mg^{2+}-free HBSS, buthionine sulfoximine (BSO), sodium bicarbonate ($NaHCO_3$), Immobilon Crescendo Western HRP substrate, and puromycin dihydrochloride were purchased from MilliporeSigma (Oakville, ON, Canada). The MISSION® shRNA plasmid DNA glycerol stocks of TRC2 pLKO.5-puro empty vector control plasmid, pLKO.5-puro non-mammalian shRNA control plasmid (non-target), and *ABCC4* KD clones targeting the coding sequence of *ABCC4* TRCN#0000005264 (NM_005845) (5264) and TRCN#0000297334 (NM_005845) (7334) were also purchased from Millipore Sigma (Oakville, ON, Canada). Triton X-100 was purchased from Fisher Scientific (Fair Lawn, NJ). GlutaMAX supplement, human recombinant insulin and Pierce™ bicinchoninic acid (BCA) protein assay reagent were purchased from Thermo Scientific (Rockford, IL). Creatine kinase, creatine phosphate, GSH reductase, NADPH, Complete Mini EDTA-free protease inhibitor cocktail tablets, X-tremeGENE9 transfection reagent were purchased from Roche, Applied Sciences (Indianapolis, IN).

Antibodies

The MRP4 specific rat monoclonal antibody (M_4I-10) was purchased from Abcam Inc. (Cambridge, MA). The Na^+/K^+-ATPase mouse monoclonal (H-3/SC-48345) was purchased from Santa Cruz Biotechnology (Dallas, TX). The IgG (H+L) cross-adsorbed goat anti-mouse and anti-rat HRP conjugated polyclonal secondary antibodies were purchased from ThermoFisher Scientific (Waltham, MA).

Preparation of reagents

Arsenite and MeSeCys were freshly prepared for all experiments by dissolving in sterile phosphate buffered saline (PBS) before serial dilutions of each compound in growth media for

immediate use. ^{73}As-arsenite was reduced from ^{73}As-arsenate with metabisulfite-thiosulfate reducing agent, as previously described [1].

Preparation of plasma membrane enriched vesicles from HEK293T cells.

The HEK293T cell line was purchased from the American Type Culture Collection (ATCC) (Manassa, VA) and maintained in Dulbecco's modified Eagle's medium containing 7.5% FBS in a humidified incubator with 95% air and 5% CO_2. The pcDNA3.1(+)-MRP4-WT was constructed as previously described using MRP4 cDNA that was a kind gift from Dr. Dietrich Keppler [2,3].

HEK293T cells were transfected using the calcium phosphate method, as previously described [4], with minor modifications. HEK293T cells were seeded onto 150 mm tissue culture plates at a density of 4.5 x 10^6 cells. After 24 hr, a solution of 18 µg of DNA (WT-MRP4 or empty vector) was added to 162 µL of $CaCl_2$, which was then added to 1.14 mL of HEPES buffer (275 mM NaCl, 1.5 mM Na_2HPO_4, and 55 mM HEPES, pH 7.0). This DNA solution was added dropwise to the cells. The cell culture media was changed 24 hr later.

Seventy-two hr post-transfection plasma membrane enriched vesicles were prepared from HEK293T cells expressing WT-MRP4 or empty vector, as previously described [5]. After preparation, membrane vesicles were stored at -80°C. An aliquot containing 0.5 µg of protein was subjected to SDS-PAGE (6%) followed by immunoblot as described (Chapter 3, section 3.3.8) to check for MRP4 levels.

Vesicular transport assays

^{3}H-E217βG vesicular transport assay

ATP-dependent transport of ^{3}H-$E_2$17βG by empty vector and WT-MRP4 plasma enriched membrane vesicles was measured as previously described [6,7]. In brief, membrane vesicles (5

μg) were incubated with ^{3}H-E$_2$17βG (1 μM, 50 nCi) in transport buffer (adenosine triphosphate (ATP) or adenosine monophosphate (AMP) (4 mM), $MgCl_2$ (10 mM), creatine phosphate (10 mM), creatine kinase (100 μg/mL), NADPH (0.35 mM), Tris (50 mM, pH 7.4), sucrose (250 mM)) at 37°C for 90 sec. Transport was stopped by diluting the reaction using 800 μL of ice-cold Tris-sucrose buffer (50 mM Tris, 250 mM sucrose, pH 7.4). Samples were filtered over glass fibre filters (type A/E) and were washed twice with 3.5 mL of Tris-sucrose buffer. Once dry, the filters were placed in scintillation vials and subjected to liquid scintillation counting using a Microbeta^2 counter (PerkinElmer). ATP-dependent transport was calculated by subtracting AMP-dependent transport from ATP-dependent transport.

Vesicular transport assays with ^{73}As-arsenite, ^{73}As(GS)$_3$, ^{73}As + MeSeCys, ^{73}As + MeSeCys + GSH, and ^{14}C-DMA^{V}.

ATP-dependent transport of ^{73}As-arsenite, ^{73}As(GS)$_3$, ^{73}As-arsenite + MeSeCys, ^{73}As-arsenite + MeSeCys + GSH by WT-MRP4 enriched vesicles were measured as previously described with modifications [5]. ^{73}As-arsenite was reduced from ^{73}As-arsenate as described in [1] and ^{73}As(GS)$_3$ was prepared as previously described [5]. For ^{73}As-arsenite + MeSeCys, 50 μM of MeSeCys was combined with ^{73}As-arsenite (50 nCi, 50 μM). For ^{73}As-arsenite + MeSeCys + GSH, ^{73}As-arsenite (50 nCi, 50 μM) was combined with MeSeCys (50 μM). Then this mixture was combined with GSH dissolved in Tris-sucrose buffer (150 mM). The ^{73}As-arsenite + MeSeCys + GSH was either used right away or was used after an hour-long incubation at room temperature.

ATP-dependent transport studies were performed as described in Chapter 4 with minor modifications. Membrane vesicles (20 μg) were incubated with the various substrates described

in the previous paragraph in transport buffer (ATP or AMP (4 mM), $MgCl_2$ (10 mM), creatine phosphate (10 mM), creatine kinase (100 μg/μL), glutathione reductase (5 μg/mL), NADPH (0.35 mM), Tris (50 mM, pH 7.4), sucrose (250 mM)) at 37℃ for 3 min. Transport was stopped and quantified as described above.

High-performance liquid chromatography-inductively coupled plasma mass spectrometry analysis of arsenic methylation in HepaRG cells

Fully differentiated HepaRG cells in 24-well plates were treated with growth media (no DMSO) containing 1 μM MeSeCys ± 1 μM arsenite for 24 hr. After 24 hr, this media was collected and stored at -80°C until analysis. The HepaRG cells were washed six times with ice cold growth media and then 37°C growth media was added. The plates were incubated for 1 hr, allowing efflux of arsenic metabolites to occur. After 1 hr, the efflux media was collected and immediately placed at -80°C until analysis.

An Agilent 1100 series high-performance liquid chromatography (HPLC) system, consisting of a pump, degasser, autosampler, column temperature control, and reverse-phased C_{18} column (ODS-3, 150 mm x 4.6 mm, 3 μM particle size; Phenomenex, Torrance, CA), was used for separation of arsenicals. The column was equilibrated with the mobile phase, consisting of 5 mM tetrabutylammonium, 5% methanol, and 3 mM malonic acid (pH 5.85), for at least 0.5 hr before sample injection. The flow rate of the mobile phase was 1.2 ml/min. The injection volume of samples and standards was 50 μL. The column temperature was maintained at 50°C. The effluent from the HPLC column was directly introduced into the nebulizer of a 7500ce inductively coupled plasma mass spectrometer (ICP-MS) (Agilent Technologies, Japan) using a PEEK tubing. The collision cell of the ICP-MS instrument was operated in helium mode.

Helium at a flow rate of 3.5 ml/min was introduced to the octopole reaction cell to reduce isobaric and polyatomic interferences. The ICP was operated at a radio-frequency power of 1550 W, and the flow rate of argon carrier gas was 0.9-1.0 L/min. Arsenic was monitored at *m/z* 75. Chromatograms from HPLC separation with ICP-MS detection were recorded and analyzed using the ChemStation software (Agilent Technologies, Santa Clara, CA). Peak areas from the analysis of samples were calibrated against those of arsenic standards to obtain concentrations of individual arsenic species in the samples. Certified reference material #18 "Human Urine" was used for quality control. The measured concentrations were in good agreement with the certified values.

Results and Discussion

To study MRP4 in an isolated system and further characterize the stimulatory effect of MeSeCys on arsenic export, plasma membrane enriched vesicles were prepared from HEK293T cells expressing empty vector and WT-MRP4. Successful over-expression of MRP4 was determined by SDS-PAGE, followed by immunoblot **(Fig A.1A).** ATP-dependent transport of the established MRP4 substrate ^{3}H-$E_2$17βG [7–9] was detected (33 ± 10 pmol/mg protein/min) for MRP4-enriched vesicles, with no significant uptake by the empty vector control **(Fig A.1B).** Therefore, the plasma membrane enriched vesicles were functional.

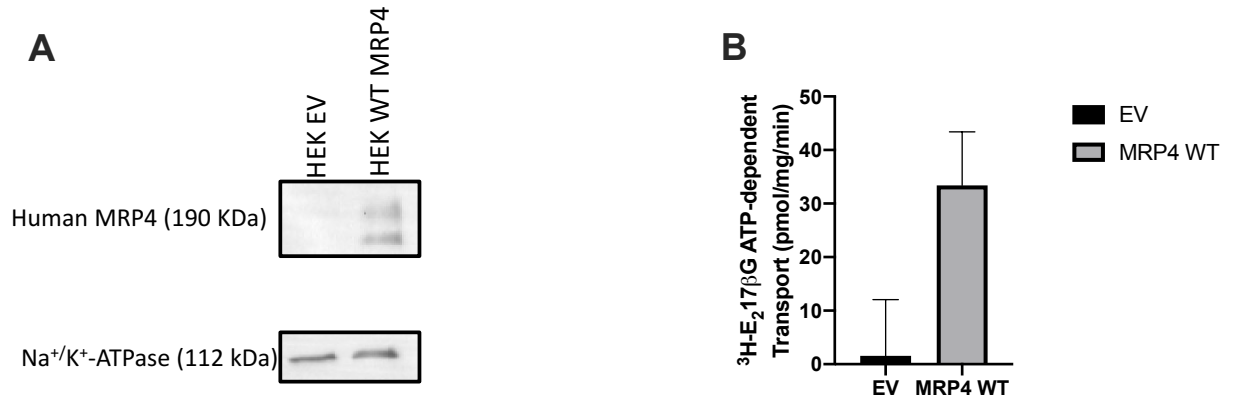

Figure A.1: **Evaluating the presence of functional MRP4 in plasma membrane enriched vesicles expressing empty vector or WT-MRP4. (A)** Membrane vesicles (0.5 µg) expressing empty vector and WT-MRP4 were subjected to SDS-PAGE (6%) and transferred to a PVDF membrane. Immunoblotting was performed using the MRP4-specific rat monoclonal antibody M_4I-10 (1:2000). The Na^+/K^+-ATPase mouse monoclonal antibody (H-3) was used as a sample loading control (1:10 000). Secondary antibodies were conjugated with horseradish peroxidase and a chemiluminescent substrate was added to visualize signals. **(B)** Vesicles (5 µg) were incubated with ^{3}H-$E_2$17βG (1 µM, 50 nCi) for 90 sec at 37 °C. Bars represent mean activity ± SD from triplicate determinations in a single experiment.

To investigate the species of arsenic being transported by MRP4, the conditions used in the HepaRG transport experiments were replicated in membrane vesicle transport experiments. Since the HepaRG cells were treated with ^{73}As-arsenite in the presence and absence of MeSeCys, it was logical to begin the investigation by treating the cells with these compounds. There was also strong evidence that MeSeCys-dependent and -independent arsenic sinusoidal efflux in HepaRG cells is GSH-dependent. Therefore, GSH was added to ^{73}As-arsenite and MeSeCys. There was no ATP-dependent transport activity detected in all of the conditions investigated (^{73}As-arsenite alone, ^{73}As-arsenite + MeSeCys, ^{73}As-arsenite + MeSeCys + GSH, ^{73}As-arsenite + MeSeCys + GSH pre-incubated, and with ^{73}As$(GS)_3$ **(Fig A.2A).** Plasma membrane vesicles expressing empty vector and WT-MRP1 were included as negative and positive controls, respectively because WT-MRP1 has been demonstrated to transport ^{73}As$(GS)_3$ [10,11].

As expected, no ATP-dependent transport activity was detected from membrane vesicles expressing empty vector. The membrane vesicles expressing WT-MRP1 transported $^{73}As(GS)_3$ with an activity of 76 ± 22 pmol/mg protein/min **(Fig A.2A).**

Since there was no ATP-dependent transport activity detected from membrane vesicles after mimicking the conditions used in efflux studies, HepaRG cells were treated in the same manner as efflux studies where ^{73}As-arsenite (1 µM, 100 nCi) in the presence and absence of MeSeCys (1 µM) were added to the cells for an hour. After the hour, this media was used for plasma membrane vesicle transport. *ABCC4***-**knockdown HepaRG cells (clone #7334) was also treated in parallel to be used as a negative control. However, no ATP-dependent transport activity was detected in any of the conditions tested **(Fig A.2B),** likely because the radioactivity was too dilute.

Previously, Banerjee et al. demonstrated that human MRP4 is a high affinity transporter of DMA^V using plasma membrane enriched vesicles expressing human MRP4 (K_m of 0.22 ± 0.15 µM, V_{max} of 32 ± 3 pmol/mg protein/min) [2,7]. Banerjee et al. used ICP-MS to detect transport activity of DMA^V, where small quantities of DMA^V could be detected [2,7]. In contrast, the specific activity of ^{14}C-DMA^V was very low, so transport needed to be performed at orders of magnitude greater than the K_m, so it is possible that saturation occurred. In the future, molar ratios of DMA^V and MeSeCys could be optimized, along with time points and including glutathione, using a more suitable method such as ICP-MS.

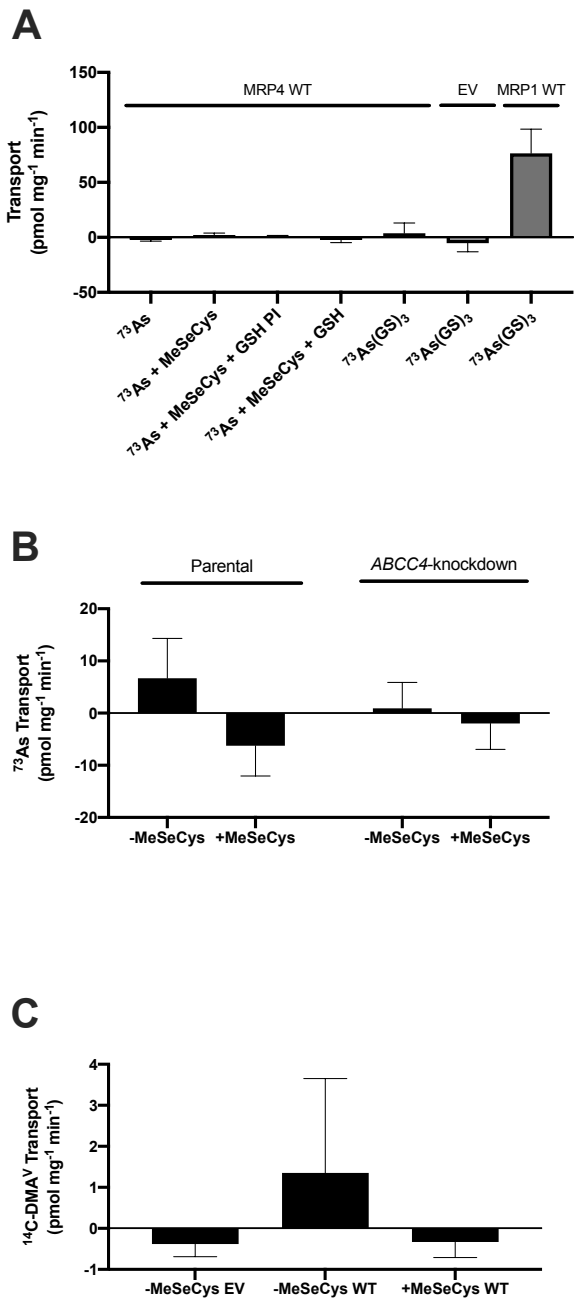

Figure A.2 Evaluating ATP-dependent of various arsenic substrates in the presence and absence of MeSeCys by WT-MRP4. Vesicles (20 µg) were incubated in transport buffer for 5 min at 37°C containing the following substrates: **(A)** 1 µM, 100 nCi of each:^{73}As, ^{73}As + MeSeCys, ^{73}As + MeSeCys + GSH pre-incubated for 1 hr, ^{73}As + MeSeCys + GSH, $^{73}As(GS)_3$. Empty vector and WT-MRP1 expressing vesicles were incubated for 1 min. Bars represent mean activity ± SD from triplicate determinations in a single experiment. **(B)** HepaRG cell efflux media from parental or *ABCC4*-knockdown cells after treatment with ^{73}As-arsenite (1 µM, 100 nCi) ± MeSeCys (1 µM) for 1 hr. **(C)** DMA^V (100 µM, 40 nCi) ± MeSeCys (10 µM).

Finally, arsenic speciation was performed after treatment of the cells with arsenite and MeSeCys in attempts to gain more insight into the arsenic species transported. HepaRG cells were treated with arsenite (1 μM) or MeSeCys (1 μM) and in combination for 24 hr. Then cells were washed with arsenic-free growth media, and then replaced, and cells were incubated for 1 hr at 37℃. This media was also collected for analysis by HPLC-ICP-MS. In the culture media collected after 24 hr of treatment with arsenite, MMA was the major metabolite in cells treated with arsenic in the presence and absence of MeSeCys, accounting for 40-60% of total arsenic **(Fig A.3A).** In the *ABCC4*-knockdown cells, MMA was also the major metabolite in cells treated with arsenite in the presence and absence of MeSeCys. However, MMA accounted for 15-30% of total arsenic **(Fig A.3A).** Less than 1% of DMA was detected after treatment of parental and *ABCC4*-knockdown cells in the presence and absence of MeSeCys **(FigA.3A).**

In the 1 hr efflux media, MMA was still the major metabolite in the parental HepaRG cells after treatment with arsenite in the presence and absence of MeSeCys. MMA accounted for about 50% of total arsenic **(Fig A.3B).** Similar findings were observed in the *ABCC4*-knockdown cells **(Fig A.3B).** Interestingly, DMA accounted for 0.6% of total arsenic in parental HepaRG cells in the presence and absence of MeSeCys but was not detected in *ABCC4*-knockdown cells **(Fig A.3B).** In all conditions, various unknown species of arsenic were detected **(Fig A.3A and B).**

Despite these modest differences in arsenic methylation, no conclusions could be drawn from this single experiment. Banerjee et al. [2] previously demonstrated that MRP4 does not transport inorganic arsenic (or in the form of $As(GS)_3$), MMA^{III}, DMA^{III}, or MMA^{V}. Therefore, we expected to see similar amounts of these species effluxed from parental and *ABCC4*-knockdown cells. Since $MMA(GS)_2$ and DMA^{V} are substrates of human MRP4, we expected more efflux of

these species from parental cells compared to *ABCC4* knockdown cells. Since stimulation of arsenic efflux by MeSeCys is MRP4-mediated, we also expected to see more efflux of $MMA(GS)_2$ and DMA^V in the presence of MeSeCys in parental HepaRG cells compared to when cells were treated with arsenite only. However, arsenic-glutathione conjugates were not detected likely due to their chemical instability in culture media and during sample handling and storage. Some of the MMA^{III} in the media could have been derived from $MMA(GS)_2$. Efflux of DMA was absent in *ABCC4* knockdown cells, which is consistent with DMA^V being a human MRP4 substrate [2]. However, due to the instability of trivalent arsenic species during sample handling, storage, and preparation for analysis, arsenic species in culture media were simply referred to as DMA, without valency designation. It is also possible that the arsenic species transported have not been previously identified as an MRP4 substrate.

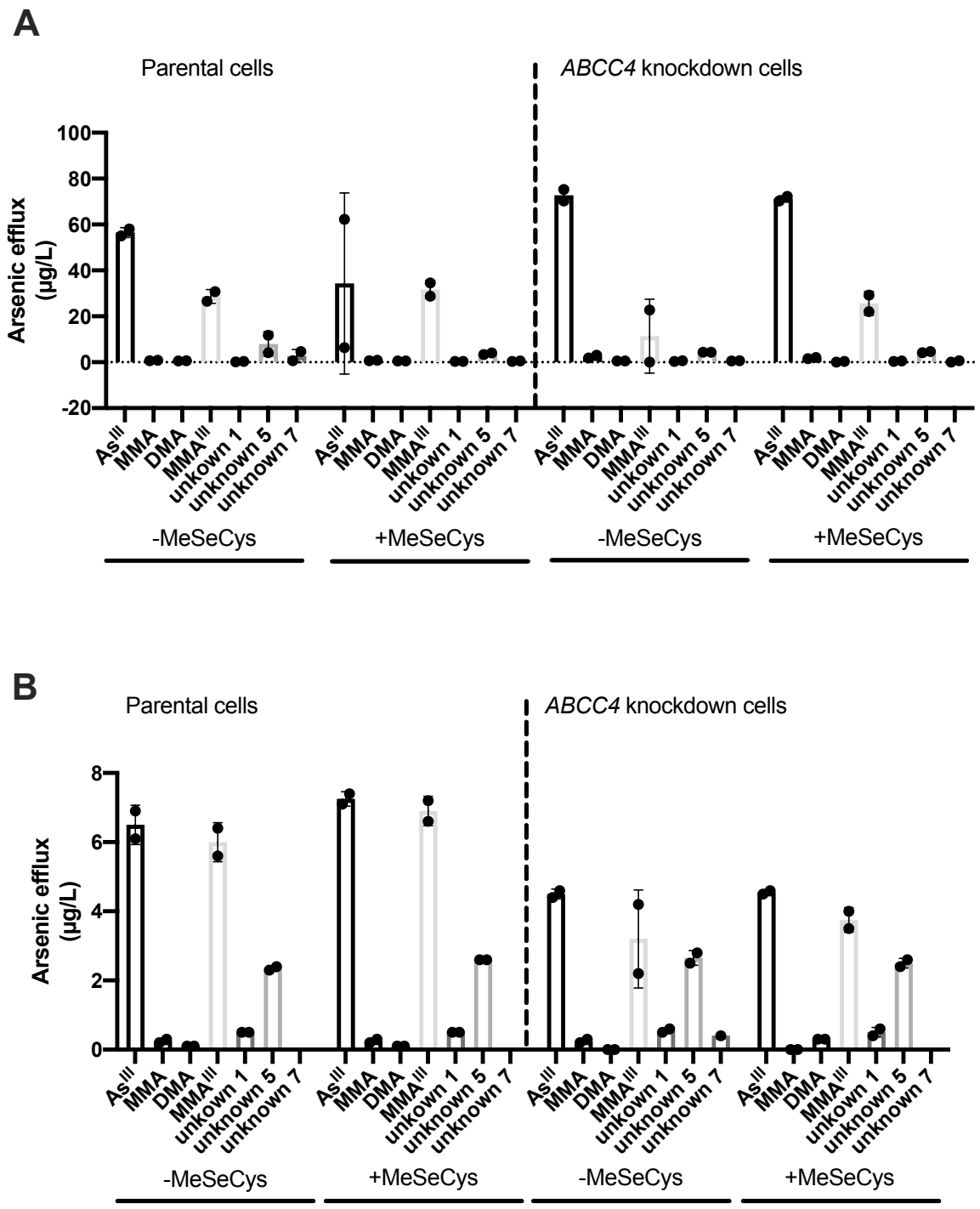

Figure A.3: Methylation of arsenic effluxed into culture media of fully differentiated parental and *ABCC4*-knockdown cells treated with arsenite (1 µM) ± MeSeCys (1 µM). Individual data points are shown. **(A)** Parental and *ABCC4*-knockdown HepaRG cells were washed and treated with arsenic-free media for 24 hr at 37℃ prior to analysis by HPLC-ICP-MS. **(B)** Parental and *ABCC4*-knockdown HepaRG cells were washed and treated with arsenic-free media for 1 hr at 37℃ prior to analysis by HPLC-ICP-MS.

References

[1] P.F. Reay, C.J. Asher, Preparation and purification of 74As-labeled arsenate and arsenite for use in biological experiments, Analytical Biochemistry. 78 (1977) 557–560. https://doi.org/10.1016/0003-2697(77)90117-8.

[2] M. Banerjee, M.W. Carew, B.A. Roggenbeck, B.D. Whitlock, H. Naranmandura, X.C. Le, E.M. Leslie, A Novel Pathway for Arsenic Elimination: Human Multidrug Resistance Protein 4 (MRP4/ABCC4) Mediates Cellular Export of Dimethylarsinic Acid (DMAV) and the Diglutathione Conjugate of Monomethylarsonous Acid (MMAIII), Molecular Pharmacology. 86 (2014) 168–179.

[3] M. Rius, A.T. Nies, J. Hummel-Eisenbeiss, G. Jedlitschky, D. Keppler, Cotransport of reduced glutathione with bile salts by MRP4 (ABCC4) localized to the basolateral hepatocyte membrane, Hepatology. 38 (2003) 374–384. https://doi.org/10.1053/jhep.2003.50331.

[4] C.A. Chen, H. Okayama, Calcium phosphate-mediated gene tranfer: A highly efficient transfection system for stably transforming cells with plasmid DNA, Biotechniques. 6 (1988) 632–638.

[5] M.W. Carew, E.M. Leslie, Selenium-dependent and -independent transport of arsenic by the human multidrug resistance protein 2 (MRP2/ABCC2): Implications for the mutual detoxification of arsenic and selenium, Carcinogenesis. 31 (2010) 1450–1455.

[6] D.W. Loe, K.C. Almquist, S.P.C. Cole, R.G. Deeley, ATP-dependent 17β-Estradiol 17-(β-D-Glucuronide) Transport by Multidrug Resistance Protein (MRP), Journal of Biological Chemistry. 271 (1996). https://doi.org/10.1074/jbc.271.16.9683.

[7] M. Banerjee, V. Marensi, G. Conseil, X.C. Le, S.P.C. Cole, E.M. Leslie, Polymorphic variants of MRP4/ABCC4 differentially modulate the transport of methylated arsenic metabolites and physiological organic anions, Biochemical Pharmacology. 120 (2016) 72–82.

[8] B. Whitlock, Arsenic Cellular Handling by Human Multidrug Resistance Protein 1 (MRP1/ABCC1) and MRP4 (ABCC4), 2021.

[9] B.D. Whitlock, E.M. Leslie, Efflux transporters in anti-cancer drug resistance: Molecular and functional identification and characterization of multidrug resistance proteins (MRPs/ABCCs), in: Drug Efflux Pumps in Cancer Resistance Pathways: From Molecular Recognition and Characterization to Possible Inhibition Strategies in Chemotherapy, 2020: pp. 31–65. https://doi.org/10.1016/b978-0-12-816434-1.00002-4.

[10] C.B. Shukalek, D.P. Swanlund, R.K. Rousseau, K.E. Weigl, V. Marensi, S.P.C. Cole, E.M. Leslie, Arsenic Triglutathione [As (GS) 3] Transport by Multidrug Resistance Protein 1 (MRP1 / ABCC1) Is Selectively Modified by Phosphorylation of Tyr920 / Ser921 and Glycosylation of Asn19 / Asn23 s, Molecular Pharmacology. 90 (2016) 127–139.

[11] E.M. Leslie, A. Haimeur, M.P. Waalkes, Arsenic transport by the human multidrug resistance protein 1 (MRP1/ABCC1): Evidence that a tri-glutathione conjugate is required, Journal of Biological Chemistry. 279 (2004) 32700–32708. https://doi.org/10.1074/jbc.M404912200.

Appendix B: Further Characterization of Localization of Naturally Occurring MRP2/*ABCC2* Variants using Immunofluorescence Imaging

Introduction

In Chapter 4, cellular localization of selected naturally occurring *ABCC2* variants were characterized using immunoblots of plasma membrane enriched vesicles as well as cell surface biotinylation. In attempts to further characterize cellular localization, immunofluorescence staining was performed on variants that had levels different than WT-MRP2 either in whole cell lysates or at the cell surface, or both. Therefore, immunofluorescence staining was performed on the following: empty vector, WT-MRP2, R353H-, R417I-, S789F-, R1150H-, R1181L-, N1244K-, P1291L-, A1450T-, and T1477M-MRP2.

Materials and Methods

Materials

The porcine kidney collecting duct cell line (LLC-PK1) was from the ATCC and was maintained in DMEM/F12 media supplemented with 4 mM L-Glutamine and 10% FBS. The rabbit anti-Calnexin polyclonal antibody (C4731) and 4'6-Diamidino-2-phenylindole (DAPI), ProLong™ Gold Anti-Fade Mountant were purchased from Millipore Sigma (Oakville, ON, Canada). The rabbit anti-giantin polyclonal antibody was from Cedarlane (Burlington, ON, Canada). The IgG (H+L) highly cross-adsorbed Alexa Fluor™ 488 conjugated goat anti-mouse and Alexa Fluor™ 594 goat anti-rabbit antibodies purchased from Invitrogen (Waltham, MA).

Expression and cellular localization of WT- and variant-MRP2 proteins in LLC-PK1 cells

LLC-PK1 cells were seeded on poly-L-lysine coated glass coverslips in 6-well plates at a density of 3 x 10^6 cells/well. Twenty-four hrs later, cells were transiently transfected with 1 µg

empty vector, WT-MRP2, or variant-MRP2 DNA using 3 µL X-tremeGENE9, as per the manufacturer's instructions. Cells were cultured for 7-9 days post-transfection, followed by washing three times with PBS and then fixation with 100% methanol at -20℃ for 20 min. Then cells were washed twice with PBS and blocked using 4% BSA/0.1% Triton-X100 for 1 hr. The coverslips were incubated with anti-human MRP2 antibody (M_2I-4) (1:250) either alone or in combination with either anti-calnexin (1:250) or anti-giantin (1:250). After this, the coverslips were washed twice with 0.4% BSA/0.1% Triton-X100. Then the coverslips were incubated for 1 hr with Alexa Fluor™ 488-conjugated anti-mouse IgG (1:500) to detect MRP2, and Alexa Fluor™ 594-conjugated anti-rabbit IgG (1:500) to detect either calnexin or giantin along with DAPI (1:500) to visualize cell nuclei. Following this incubation, coverslips with washed twice with 0.4% BSA/0.1% Triton-X100. Then the coverslips were carefully mounted on slides with mounting medium. The slides were left to dry in the dark and then placed in a -20℃ freezer until imaging.

Cells were imaged on a spinning disk confocal microscope (WaveFX, Quorum Technologies, Guelph, ON, Canada) with set up and image acquisition as previously described [1,2]. Images were acquired and visualized using Volocity (Improvision, PerkinElmer, Waltham, MA).

Results and Discussion

Cellular localization studies were performed in Chapter 4. Immunoblot analysis of whole cell lysates demonstrated that S789F-, R1150H-, N1244K-, P1291L-, and A1450T-MRP2 had lower levels than WT. In plasma membrane enriched vesicles, V417I-MRP2 had higher levels than WT-MRP2, whereas N1244K- and P1291L-MRP2 had lower levels than WT-MRP2, which was consistent with what was found in whole cell lysates. R353H-, R1181L-, and T1477M-MRP2

had reduced levels in plasma membrane enriched vesicles but levels were similar to WT-MRP2 in whole cell lysates.

In the current study, immunofluorescence staining of LLC-PK1 cells expressing empty vector, WT-MRP2 or variant MRP2 was performed. LLC-PK1 cells were chosen for their small nuclei, ability to polarize, and their use in previous studies of MRP2 [1]. First, MRP1-GFP was used to optimize the transfection method. Our transfection method was suitable because MRP1-GFP was detected **(Fig B.1).**

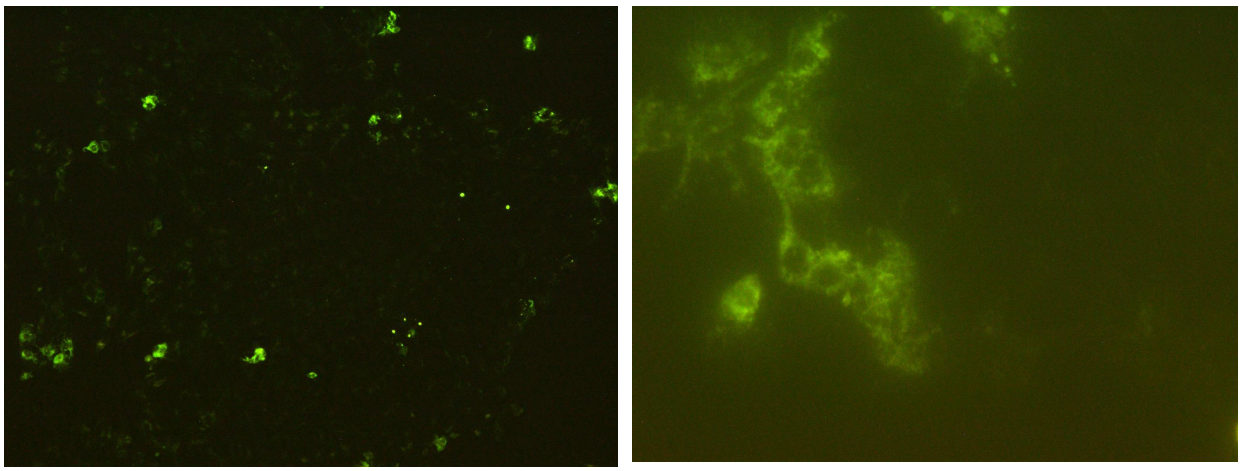

Fig B.1 Fluorescent microscopy of LLC-PK1 cells transiently expressing MRP1-GFP. LLC-PK1 cells were transfected with MRP1-GFP DNA. After 72 hr, cells were imaged using fluorescence microscopy. Images are shown at 100X magnification (left panel) and 400X magnification (right panel).

MRP2 was detected in all slides, but the staining was present co-localized with the endoplasmic reticulum and Golgi markers in the YZ planes **(Fig B.2 and Fig B.3).** The staining could have been due to lack of polarization in the cells. Similar staining patterns have been observed in other studies, such as one where the hepatic apical transporter, bile salt export pump (BSEP/*ABCB11*) was detected after expression in LLC-PK1 cells [2] .

Overall, there was less MRP2 staining in S789F-, R1150H-, R1181L-, P1291L-, A1450T- and T1477M-MRP2 variants **(Fig B.2 and Fig B.3),** which is consistent with findings in Chapter 4.

There was also expectedly no MRP2 detected in cells expressing empty vector **(Fig B.2 and Fig B.3).** Cells were also stained with calnexin, an endoplasmic reticulum marker. Calnexin was detected in all slides **(Fig B.2)**. When MRP2 and calnexin were merged, there seemed to be more co-localization between MRP2 and calnexin in S789F- and A1450T-MRP2 **(Fig B.2E & J).** These data are consistent with studies in Chapter 4, where these two variants did not appear to traffick to the plasma membrane. R417I-MRP2 stained most similarly to WT-MRP2 **(Fig B.2D).** As for the other variants, it was difficult to determine if they were co-localized with the ER marker due to low expression of the variant combined with quality of the staining. It is likely that there is some degree of co-localization between MRP2 and calnexin for the variants R353H-, R1150H-, R1181L-, and N1244K-MRP2 **(Fig B.2).**

When cells were stained with giantin, a marker for the Golgi apparatus, giantin was expectedly detected in all cells **(Fig B.3).** However, there did not seem to be any co-localization between giantin and MRP2 for any of the variants **(Fig B.3).** Therefore, none of the MRP2 variants appeared to be mislocalized to the Golgi. In a study by Hirouchi et al. using LLC-PK1 cells, V417I-MRP2 was localized to the apical surface, and S789F- and A1450T-MRP2 were localized intracellularly [1]. Wen et al. performed immunofluorescence staining to study cellular localization in Flp-In HEK293 cells and observed lower levels of S789F-MRP2 compared to WT-MRP2 [3]. However, no staining with ER or Golgi markers were performed in these studies [1,3]. Future studies using polarized cells that stably express the selected variants should be used to allow longer periods for proper polarization to occur.

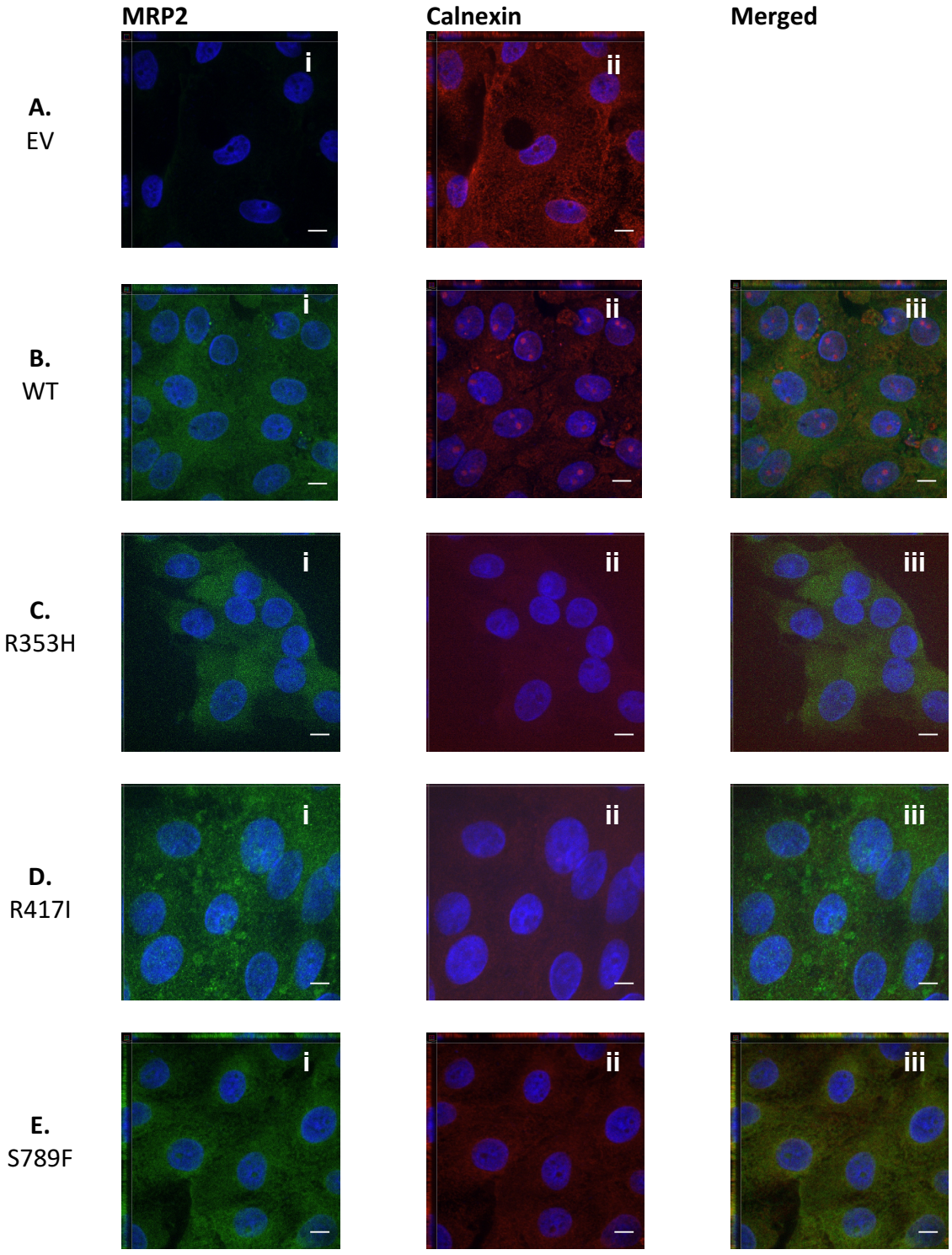
MRP2
Calnexin
Merged
A.
EV
B.
WT
C.
R353H
D.
R417I
E.
S789F
i
ii
iii

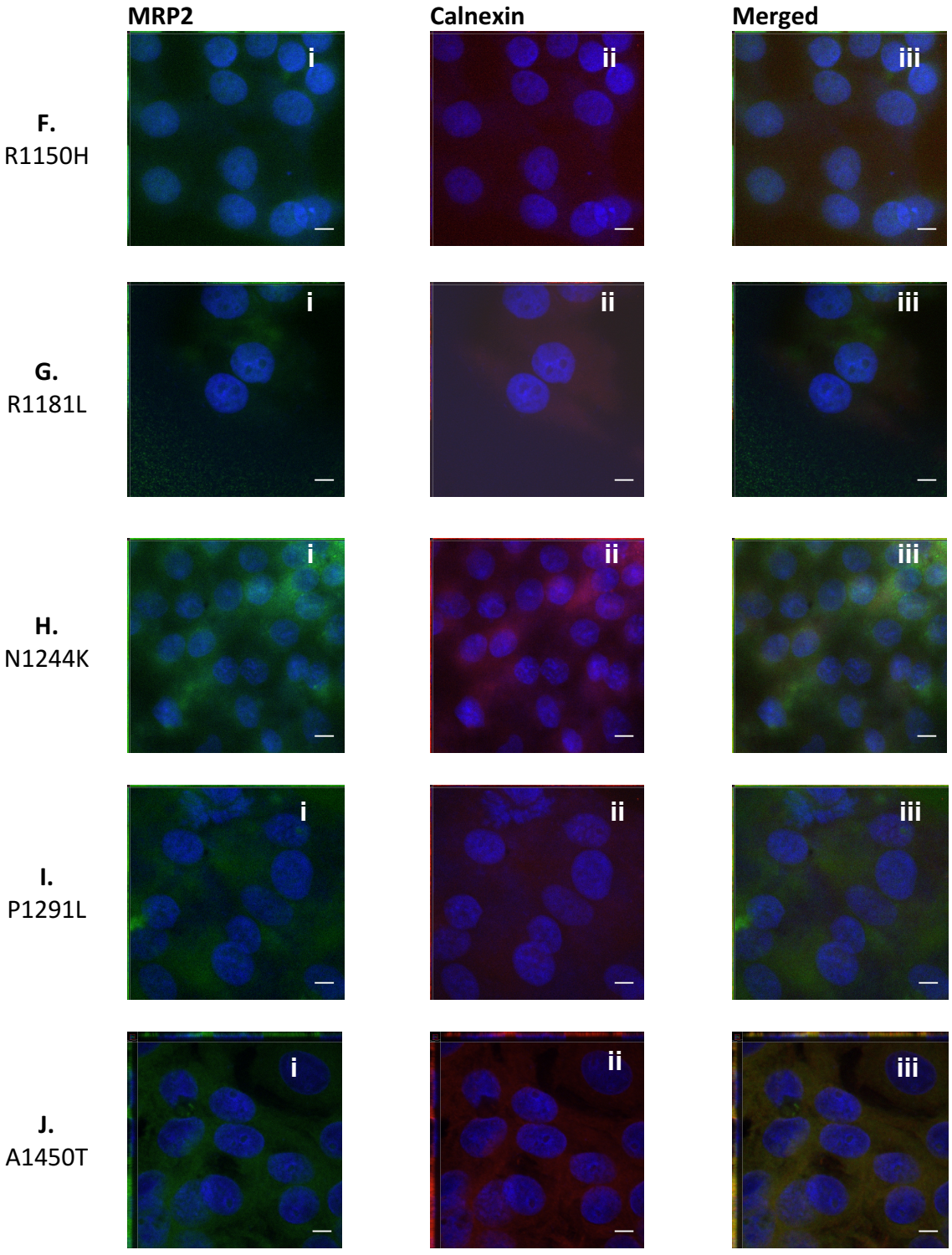
MRP2
Calnexin
Merged
F.
R1150H
G.
R1181L
H.
N1244K
I.
P1291L
J.
A1450T
i
ii
iii

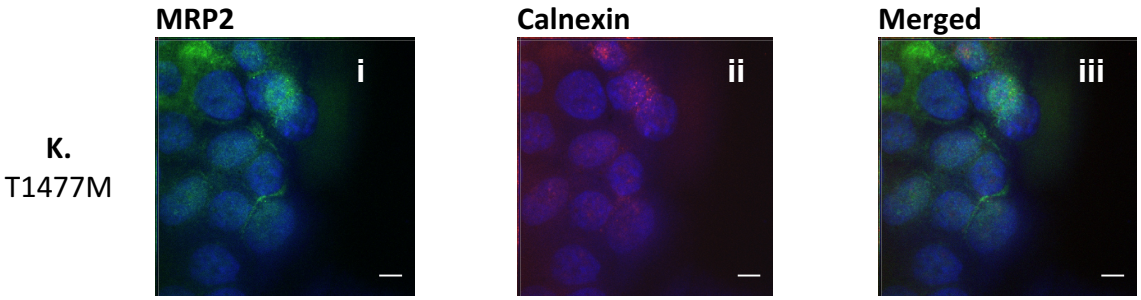

Figure B.2: Immunofluorescence confocal microscopy of LLC-PK1 cells expressing selected MRP2 variants, WT-MRP2 or empty vector stained with MRP2, calnexin, and DAPI. LLC-PK1 cells were transfected with empty vector, WT-MRP2 or selected variant-MRP2 DNA. Then 7-9 days later, cells were fixed and MRP2 was detected using mAb M_2I-4 and Alexa Fluor® 488-conjugated secondary antibody (green). Nuclei were stained with DAPI (blue). Calnexin was detected using anti-calnexin antibody followed by Alexa Fluor™ 594-conjugated secondary antibody (red). Selected fields are shown, with fields indicated with i showing MRP2, ii showing calnexin, and iii showing co-localization of MRP2 with calnexin. Scale bars represent 10 µM at 600X magnification.

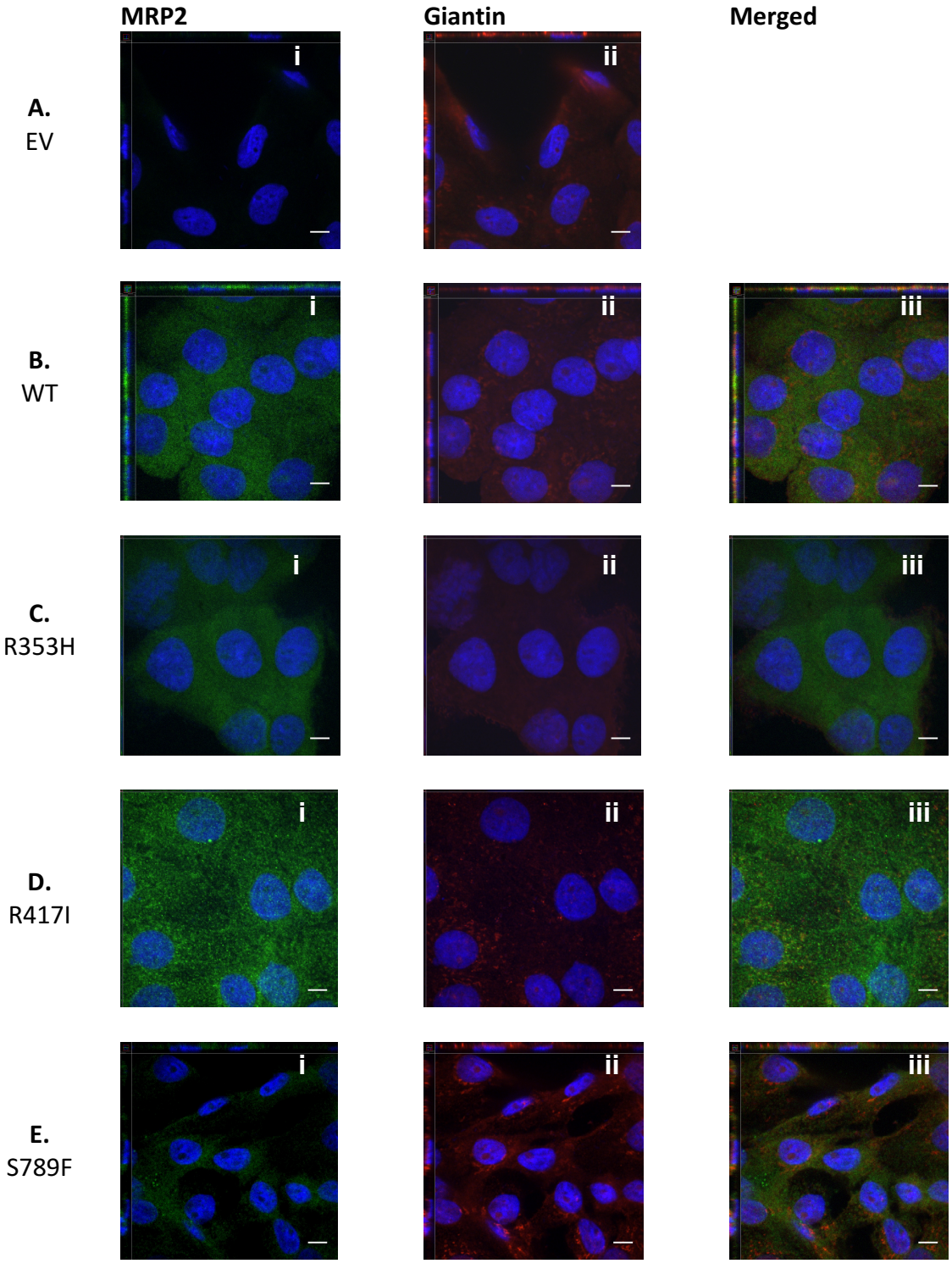
MRP2
Giantin
Merged
A.
EV
B.
WT
C.
R353H
D.
R417I
E.
S789F
i
ii
iii

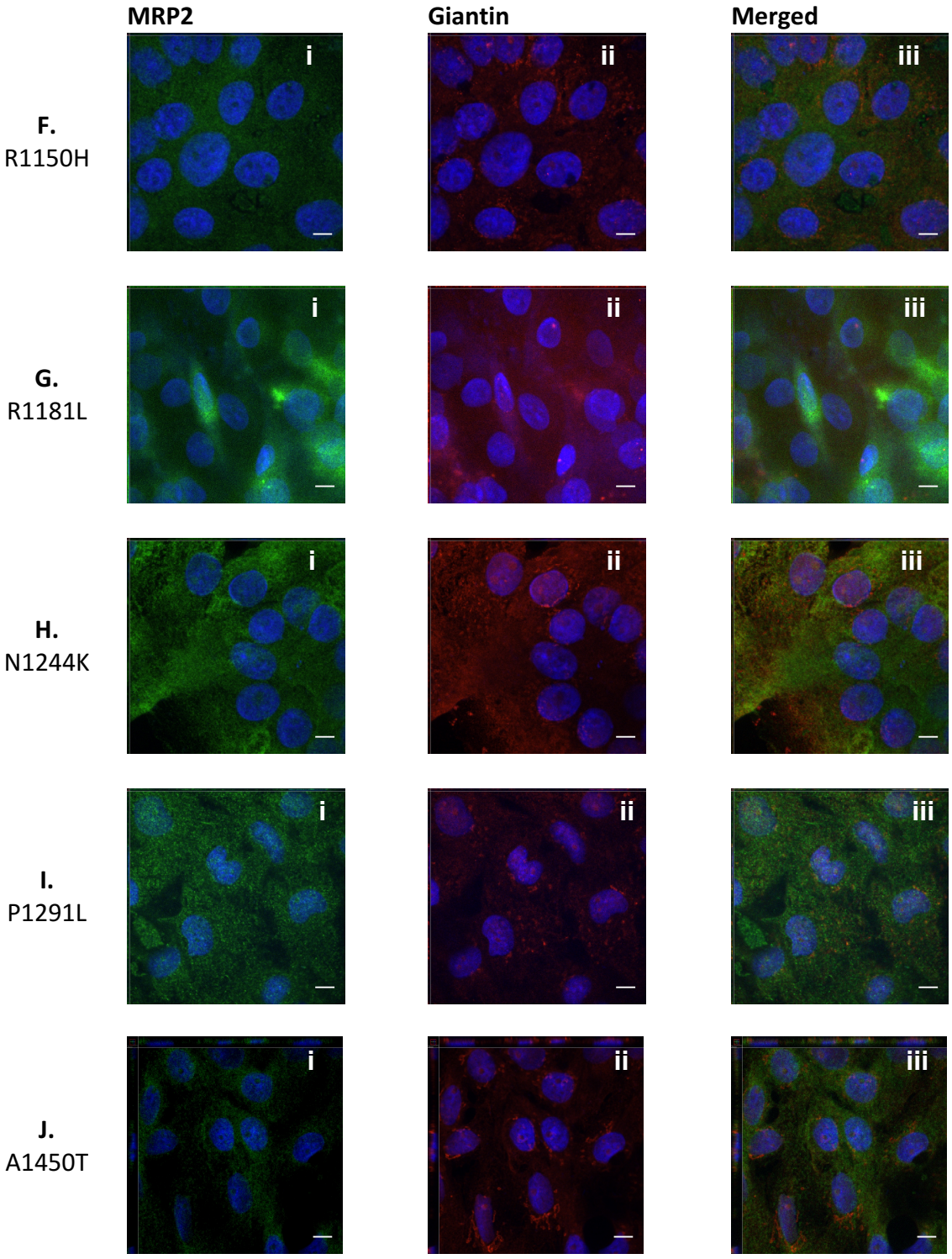
MRP2
Giantin
Merged
F.
R1150H
G.
R1181L
H.
N1244K
I.
P1291L
J.
A1450T
i
ii
iii

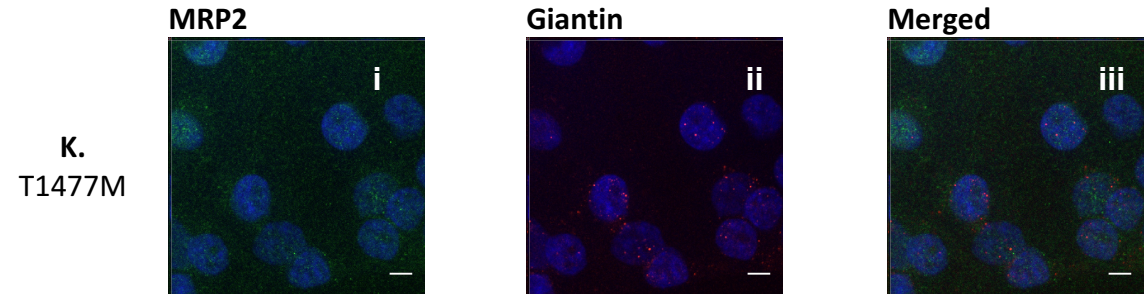

Figure B.3: Immunofluorescence confocal microscopy of LLC-PK1 cells expressing selected MRP2 variants, WT-MRP2 or empty vector stained with MRP2, giantin, and DAPI. LLC-PK1 cells were transfected with empty vector, WT-MRP2 or selected variant-MRP2 DNA. Then 7-9 days later, cells were fixed and MRP2 was detected using mAb M_2I-4 and Alexa Fluor® 488-conjugated secondary antibody (green). Nuclei were stained with DAPI (blue). Giantin was detected using anti-giantin antibody followed by Alexa Fluor™ 594-conjugated secondary antibody (red). Selected fields are shown, with fields indicated with i showing MRP2, ii showing giantin, and iii showing co-localization of MRP2 with giantin. Scale bars represent 10 μM at 600X magnification.

References

[1] M. Hirouchi, H. Suzuki, M. Itoda, S. Ozawa, J.I. Sawada, I. Ieiri, K. Ohtsubo, Y. Sugiyama, Characterization of the cellular localization, expression level, and function of SNP variants of MRP2/ABCC2, Pharmaceutical Research. 21 (2004) 742–748. https://doi.org/10.1023/B:PHAM.0000026422.06207.33.

[2] S. Mita, H. Suzuki, H. Akita, H. Hayashi, R. Onuki, A.F. Hofmann, Y. Sugiyama, Vectorial transport of unconjugated and conjugated bile salts by monolayers of LLC-PK1 cells doubly transfected with human NTCP and BSEP or with rat Ntcp and Bsep, American Journal of Physiology - Gastrointestinal and Liver Physiology. 290 (2006) 550–556. https://doi.org/10.1152/AJPGI.00364.2005/ASSET/IMAGES/LARGE/ZH30030643510008.JPEG.

[3] X. Wen, M.S. Joy, L.M. Aleksunes, In Vitro Transport Activity and Trafficking of MRP2/ABCC2 Polymorphic Variants, Pharmaceutical Research. 34 (2017) 1637–1647. https://doi.org/10.1007/s11095-017-2160-0.